Assessing the impact of ozone pollution on food security using a combined experimental and flux modelling approach

Stephanie Alice Osborne

PhD

University of York

Environment

July 2017

Abstract

Maximising global food production is a priority for the international community. Ground-level ozone (O_3) – a greenhouse gas and air pollutant – reduces yield in many important crops, and is a likely contributing factor to the global yield gap. This body of work applies experimental and modelling approaches to investigate how O_3 reduces yield in soybean and wheat, and how these responses can be represented in models.

Analysis of published dose-response data for soybean found that Indian and Chinese cultivars exhibited higher O_3 sensitivity than cultivars from the USA, and that the sensitivity of soybean cultivars to O_3 increased by 32.5% between 1960 and 2000. This temporal trend may have been driven by selective breeding strategies targeting high yield.

Exposure of European wheat to O_3 and drought in combination suggested that drought does not protect against O_3 damage, as previously hypothesised. Stomatal flux modelling indicated that 10 days of water withdrawal only reduced O_3 uptake to leaves by 3% or less, and the negative effect of drought on yield was severe (-14%), while no clear benefit of drought-induced O_3 exclusion on yield was observed. The experiment found no evidence of O_3-drought interactions not explained by stomatal behaviour, indicating that current O_3 flux modelling methods are likely to fully account for O_3-drought interactions in risk assessments.

Finally, analysis of physiological data for European wheat found no evidence of O_3 impairing the photosynthetic mechanism in unscenesced flag leaves at moderate O_3 concentrations (22 – 57 ppb 24-hour mean), indicating that accelerated senescence is likely to be the dominant O_3 effect influencing yield in agricultural environments. Ozone flux was a better predictor of physiological response to O_3 than concentration-based O_3 metrics, and flux also accounted for the difference in exposure resulting from O_3 profiles featuring acute peaks versus those characterised by a consistent background concentration.

List of contents

List of Tables

List of Figures

Acknowledgements

There are a number of people and organisations who I need to thank, without whom the completion of this thesis would definitely not have been possible.

Firstly I would like to thank the Natural Environment Research Council of the United Kingdom for funding this work, and CEH and SEI for providing me with office space.

I would like to sincerely thank my PhD supervisors, whose advice and guidance has been absolutely essential throughout. Prof. Gina Mills helped me to find my feet when I first began my PhD in Bangor, and navigated me through experimental planning, plant physiology and some tricky analysis; and Prof. Lisa Emberson was enormous help when I moved to York and began to learn how to model stomatal fluxes. Both supervisors have also reviewed and edited draft after draft of my work, shown amazing patience with all the interrupted Skype calls that we had, and have supported and believed in me over the last three years.

I also need to thank my unofficial third supervisor, Dr. Patrick Buker, for all the help he has given me over the past three years, including reviewing manuscripts, helping me to understand DO_3SE model parameters, and not forgetting a clandestine operation attempting to bring me wheat seeds from Nepal.

I am also very grateful to Professor Mike Ashmore, my TAP chair, who gave excellent advice and perspective as an external voice during TAP meetings.

Felicity Hayes, Elwyn Jones, Aled Williams, Harry Harmens, Katrina Sharps, Divya Pandey, David Cooper and David Gillies have all contributed a substantial amount of their expertise and time to helping me with various elements of my work, including experimental design and maintenance, plant physiological measurements, statistical analysis, flux modelling, and preparing manuscripts.

Finally, I would like to thank all those people who have given me non-academic support over the last three and a half years. The amazing community of colleagues and friends who I found when I joined CEH, and again when I moved to SEI, made going into the office something to look forward to. My lovely friends and family, who are spread around the various corners of the country but are nevertheless there when I need them, have helped enormously. And last but not least, I need to thank Joe, who decided to stick with me when I decided to move to the other side of the country to begin a PhD; who was oddly enthusiastic about helping with fieldwork; and who has been there for me and ready to make me laugh throughout the good times and the bad.

Author's declaration

I declare that this thesis is a presentation of original work and I am the sole author. This work has not previously been presented for an award at this, or any other, University. All sources are cited in the text and acknowledged as references.

The following research papers have been produced from this body of work and have been published, or submitted for publication, in a peer-reviewed journal:

Osborne, S.A., Mills, G., Hayes, F., Ainsworth, E.A., Büker, P., and Emberson, L. (2016). Has the sensitivity of soybean cultivars to ozone pollution increased with time? An analysis of published dose-response data. *Global Change Biology*, 22, 3097-3111. doi: 10.1111/gcb.13318

Osborne, S.A., Mills, G., Hayes, F., Gillies, D., Harmens, H., Sharps, K. and Emberson, L. (submitted). Using stomatal flux modelling to investigate ozone-drought interactions in wheat (*Triticum aestivum* L.). *Atmospheric Environment.*

Osborne, S.A., Pandey, D., Mills, G., Hayes, F., Harmens, H., Gillies, D., Büker, P. and Emberson, L. (submitted). New insights into leaf physiological responses to ozone for use in crop modelling. *Global Change Biology.*

1. Introduction

1.1 The global food challenge

Feeding the growing world population is one of the greatest challenges of our time. Demand for agricultural products is projected to be 60% higher in 2050 compared to the 2005/2007 average (FAO, 2012). This demand will need to be met in a world with little previously uncultivated land remaining for agricultural expansion (Ramankutty *et al.*, 2002), limited fresh water (Wada and Bierkens, 2014), and a changing climate (IPCC, 2013b). Analysis of yield trends has indicated that the current rate of yield improvement in the world's major crops does not match the rate of increasing food demand (Ray *et al.*, 2013) (Figure 1.1). A sustainable intensification of food systems is therefore required, to tackle hunger and malnutrition while protecting ecosystems of high ecological and social value (Rockström *et al.*, 2017).

How can this sustainable intensification take place? A concerted effort in research and innovation is required in order to increase the yield potential of crops, increase the efficiency of inputs to agriculture, reduce the environmental impact of agriculture, and close the 'yield gap' – the difference between current and attainable yields (Shiferaw *et al.*, 2013; West *et al.*, 2014). Analysis by Licker *et al.* (2010) estimated that 20% more soybean and 60% more wheat could be produced if 95% of the crops' harvested area met their current potential based on the local climate. Underlying the yield gap are factors relating to the agricultural work force, water and fertiliser management, pests and diseases, heat and drought stress, and local pollutants such as 'ground-level' ozone (O_3) (Pradhan *et al.*, 2015; Wilkinson *et al.*, 2012).

This PhD thesis has sought to increase our understanding of O_3 impacts on the growth, physiology and yield of soybean and wheat, and to develop and improve methods for modelling these responses. Both crops are of significant nutritional and economic importance globally. Wheat is the world's most widely grown cereal, contributing approximately 20% of dietary calories and protein worldwide (Shiferaw *et al.*, 2013). However, previously rapid productivity increases for this crop are now slow or static in some areas including South Asia and Western Europe (Shiferaw *et al.*, 2013), and an estimated 37% of wheat-growing areas globally are now seeing yield stagnation (Ray *et al.*, 2012). Soybean seeds are important for protein meal and vegetable oil, are one of the top-traded commodities in the world, and have long been consumed in Asia as a source of protein (Hartman *et al.*, 2011). As with wheat, this crop is also experiencing yield stagnation over approximately 23% of its global cultivated area (Ray *et al.*, 2012). In India, where a rapidly growing population means that yield increases are particularly urgent, 70% of wheat-growing areas and 51% of soybean-growing areas are experiencing yield stagnation (Ray *et al.*, 2012).

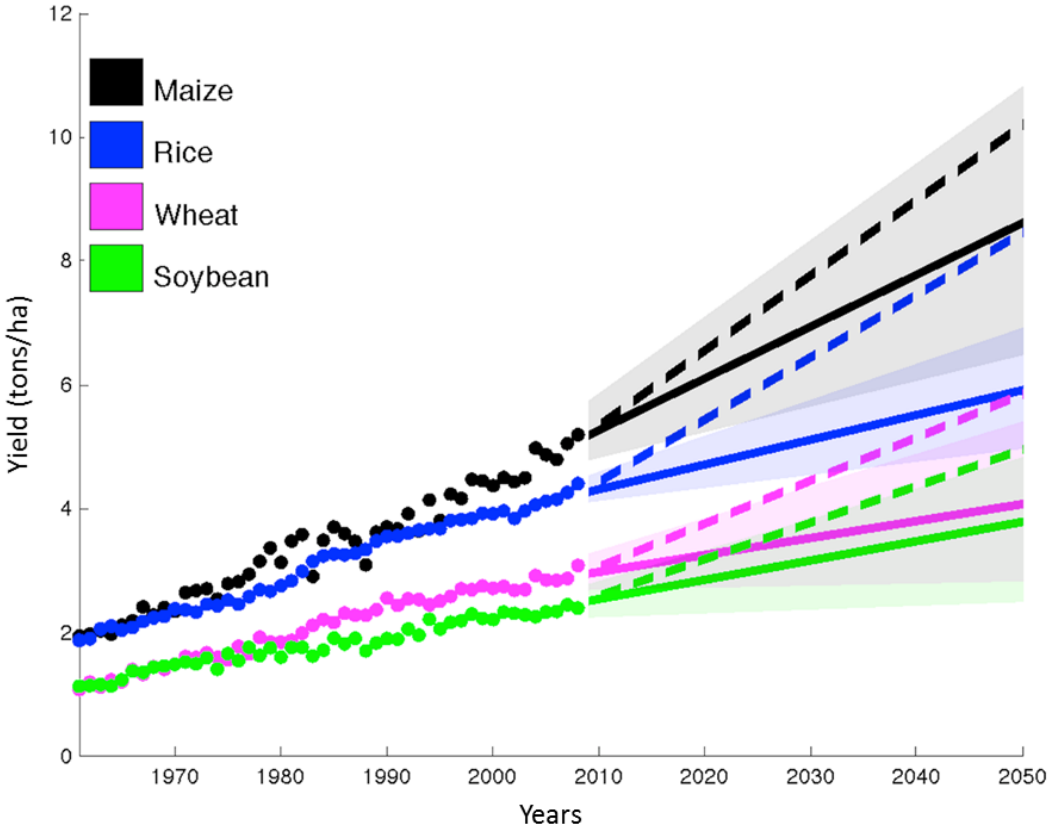

Figure 1.1. Observed weighted area global yield from 1961-2008, with predictions to 2050 for maize, rice, wheat and soybean shown as solid lines. The dashed line shows the trend of yield improvement required each year to double production of these crops by 2050 without bringing additional land under cultivation. Figure reproduced from Ray et al. (2013).

1.2 Chemistry of ground-level O_3

1.2.1 Definition of ground-level O_3

Ground-level O_3 is both an air pollutant and greenhouse gas. As well as being detrimental to crop yields, O_3 is a significant driver of premature human mortality globally (Silva *et al.*, 2013), and is also damaging to natural ecosystems, including grasslands (Mills *et al.*, 2013) and forests (Paoletti, 2007). Ozone is a natural component of the troposphere, and its concentration at a given location is a product of the combined processes of formation, transport, deposition and chemical destruction (Vingarzan, 2004). Ground-level O_3 was first discovered to be harmful in the 1950's, when O_3 concentrations in photochemical smog in central Los Angeles reached the staggering levels of 450-500 parts per billion by volume (ppb) (Finlayson-Pitts and Pitts, 1993). Such events are now known as 'peak' episodes – short periods of very high O_3 levels, spanning hours to days, resulting from warm and sunny conditions occurring together with high levels of urban emissions. As well as peak episodes, O_3 also occurs in the troposphere at a more moderate

and consistent 'background' concentration, which can vary spatially, seasonally and diurnally, and is the product of both natural and anthropogenic factors (Royal Society, 2008).

1.2.2 Ozone formation processes

Ozone is a secondary pollutant formed in the air, through a complex set of sunlight-initiated reactions of its precursors. The main O_3 precursors are the NO_X gases, comprising both nitrogen dioxide, NO_2, and nitrous oxide, NO. Volatile organic compounds (VOC's) – which include all organic molecules which react in the troposphere, including hydrocarbons, aldehydes, and alcohols – are also important in tropospheric O_3 formation reactions (Finlayson-Pitts and Pitts, 1993). NO_2 can undergo photo-dissociation in the presence of sunlight, to release an oxygen radical (equation 1.1) which then fuels the formation of O_3 (equation 1.2). The concentration of NO_x is therefore the main factor which determines the rate of O_3 production in the troposphere (Royal Society, 2008). The role of the VOC's is to oxidise NO to NO_2, thereby increasing the pool of precursor chemicals available for O_3-forming reactions. '*M'* in equation 1.2 represents any third molecule needed to stabilise the intermediate formed on the addition of O to O_2 (Finlayson-Pitts and Pitts, 1993).

1.1 $$NO_2 + hv\ (\lambda < 430nm) \rightarrow NO + O$$

1.2 $$O + O_2 \overset{M}{\rightarrow} O_3$$

The rate of photolysis – and hence the rate of O_3 formation – increases with temperature, pressure and solar intensity (Royal Society, 2008). As a result, surface O_3 concentrations are strongly influenced by meteorology, resulting in seasonal variation in concentrations, and typically a diurnal peak associated with daily peak temperature and sunlight. Seasonal peaks in O_3 levels depend on the local climate and therefore occur at different times of the calendar year in different world regions. In urban centres in the UK, surface O_3 levels peak in the summer months due to co-occurrence of precursors with high temperature and irradiance (Figure 1.2A). However, in recent decades the annual O_3 peak has been observed in the spring (March-May) at remote UK locations, due to the increasing influence of global background concentrations (Figure 1.2B) (DEFRA, 2009; Derwent and Kay, 1988). In Northern India, concentrations peak in March and April, with very high estimated levels over the agriculturally important Indo-Gangetic plain (Mittal *et al.*, 2007). The timing of the annual O_3 peak varies across the Indian sub-continent, with the coastal town of Pune experiencing a summer maximum in March, a decrease in concentration due to wind direction change in April, a monsoon minimum in August, and a post-monsoon second maximum in October (Khemani *et al.*, 1995).

Ozone occurs in the troposphere naturally at low background concentrations, due to downward movement of O_3 from the stratosphere (Derwent and Kay, 1988), and because some O_3 precursors occur in small amounts in the natural environment (Royal Society, 2008). For

example,NO_X gases are produced in lightning strikes and from soil microbial activity, while methane - a VOC – is emitted by wetlands. Carbon monoxide is formed naturally in the troposphere from the oxidation of methane (Royal Society, 2008), and biogenic VOC's emitted by trees (e.g. isoprenoids, terpenes) also contribute to O_3 formation (Calfapietra *et al.*, 2013).

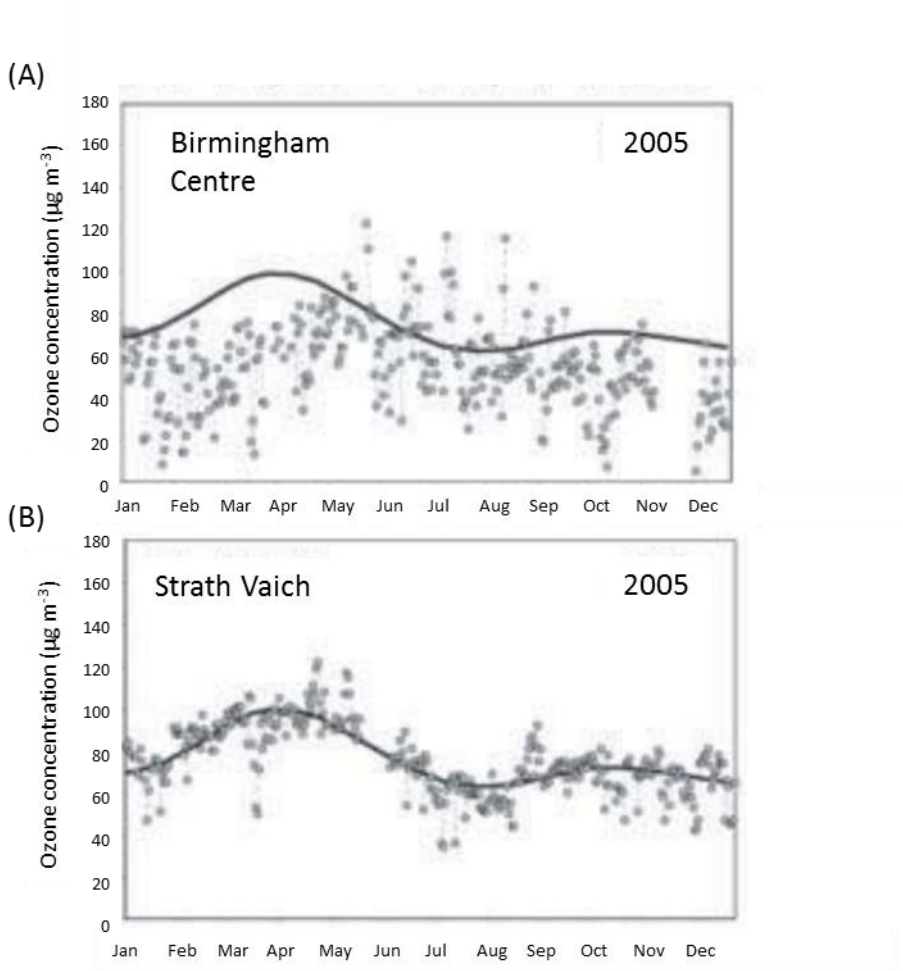

Figure 1.2. Daily maximum of the running 8-hour mean O_3 concentrations in 2005 at (A) Birmingham city centre, and (B) Strath Vaich, a remote monitoring station in Scotland. The curve in both plots is an approximate fit to the Strath Vaich data, and is reproduced in the Birmingham plot to facilitate comparison. Figure reproduced from DEFRA (2009).

1.2.3 Ozone removal processes

Ozone is removed from the troposphere either through chemical destruction, or by deposition to the earth. Approximately 1000 Tg $year^{-1}$ of O_3 is deposited onto vegetation, soil, and urban surfaces, while about 4100 Tg $year^{-1}$ is removed annually through chemical destruction (Royal Society, 2008). There are two key chemical destruction pathways for tropospheric O_3. The first involves the reaction of a halogen radical (typically iodine or bromine) with O_3 to form the corresponding halogen oxide radical, XO (Equation 1.3). Bromine and iodine-containing

species can be emitted from ocean or ice surfaces, so this mechanism of removal occurs mainly in the marine environment (Royal Society, 2008). In urban environments with elevated levels of NO_X gases, NO can react with and destroy O_3 in a process known as the NO_X titration effect (equation 1.4) (Royal Society, 2008). While this reaction can remove O_3 in the short term, it results in the production of NO_2 – the main O_3 precursor – and therefore forms part of cyclical O_3 creation and destruction reactions that can occur in polluted urban centres (Royal Society, 2008).

1.3 $$X + O_3 \rightarrow XO + O_2$$

1.4 $$NO + O_3 \rightarrow NO_2 + O_2$$

Ozone can also be removed from the troposphere through 'dry deposition', where it reacts with external surfaces of vegetation and soil or is taken up through plant stomata. Ozone is not very soluble, so the deposition velocity to water surfaces, or 'wet deposition', is approximately an order of magnitude slower (Wesely *et al.*, 1981). Deposition processes limit the maximum possible ground-level concentration (Royal Society, 2008), and also limit the lifetime of an O_3 molecule, on average 22 days long (Stevenson *et al.*, 2006). The rate of dry deposition is variable and depends on a host of factors including the amount of surface water on vegetation, wind speed and turbulence, total leaf area, and the aperture of plant stomata (Royal Society, 2008). As discussed in detail later, stomatal aperture itself is influenced by a number of variables related to the ambient environment, including solar intensity, relative humidity, temperature and soil moisture (Royal Society, 2008). The amount of dry deposition of O_3 will therefore vary seasonally with changing total leaf area, and will also be influenced by weather events. For example, hot and dry conditions across Europe during the summer of 2003 coincided with high concentrations of surface O_3. A reduction in dry deposition due to drought-induced stomatal closure is thought to have contributed significantly to the enhanced O_3 concentrations observed at the time (Solberg *et al.*, 2008).

1.2.4 Hemispheric O_3 transport

Intercontinental transport of O_3 and its precursors is an additional factor which can influence the background O_3 concentration at a given location (Hollaway *et al.*, 2012). The relatively long lifetime of the O_3 molecule and some of its precursors in the troposphere can allow them to be transported for thousands of kilometres (Royal Society, 2008). Consequently, elevated spring O_3 concentration on the west coast of North America has been linked to the trans-Pacific transport of emissions from Asia (Jaffe *et al.*, 2003). Pollution from the Asian continent has been estimated to contribute between 3 and 10 ppb to the background O_3 levels observed in the Western USA (Vingarzan, 2004). Similarly, the trans-Atlantic transport of North American NO_X emissions is thought to contribute up to ~4 ppb O_3 to background levels in Western Europe

(Derwent *et al.*, 2008). One polluting source can therefore exert influence on O_3 concentrations in distant locations, and the global O_3 budget will correlate with emission rates in source areas.

1.2.5 Historical and present-day tropospheric O_3 levels

There is a strong scientific consensus that the background O_3 concentration has increased considerably since the pre-industrial era. The oldest quantitative ambient measurements of O_3 come from the Montsouris dataset, measured in rural France between 1876 and 1910 using a poorly standardised Shönbein test paper method (Volz and Kley, 1988). Modern analysis and quality control applied to this dataset indicates that O_3 concentrations at rural monitoring stations in Europe approximately doubled between 1876-86 and 1983 (Volz and Kley, 1988). Modern-era measurements have also registered a steep rise in surface O_3 concentrations: the Arosa station in the Swiss Alps registered a doubling in mean annual O_3 concentration between 1951 and 1991 (Staehelin *et al.*, 1994), and the Radebeul-Wahnsdorf station in Germany recorded a 12 ppb rise on average between 1975 and 2010 (Weigel and Bender, 2012).

This global rise in surface O_3 concentration is thought to be the result of rising anthropogenic emissions of the O_3 precursors over the same period (Royal Society, 2008). Tropospheric abundance of NO_X and CO has been augmented over time as a result of fossil fuel and biomass combustion, while methane emissions have come from agricultural activities and coal mining (Brasseur, 2001). Consequently, the rise in surface O_3 in the 20th century has occurred alongside a five-fold increase in anthropogenic emissions of NO_X (van Aardenne *et al.*, 2001), and global annual emission rates have continued to increase over recent decades (Granier *et al.*, 2011). Between the 1940's and 1980's, the most rapid increase in emissions of NO_X from fossil fuel combustion was registered in Asia (Dignon and Hameed, 1989), and this trend has continued more recently: a 70% increase in NO_X emissions was observed over China between 1995 and 2004 (Zhang *et al.*, 2007).

Since the signing of the Gothenburg protocol in 1999 there has been a downward trend in emissions of NO_X and VOCs across Europe and North America, although there has not been a clear downward trend in O_3 indicators over the same period (Maas and Grennfelt, 2016; Maas, 2007). A recent review of tropospheric O_3 in Northern Europe reported a 'redistribution' rather than a decline, with a decrease observed in daytime summer concentrations, but a relatively stable annual mean concentration (Figure 1.3) and an increase in summer nocturnal and winter concentrations (Karlsson *et al.*, 2017; Maas and Grennfelt, 2016). This is partly due to intercontinental transport of O_3 and precursor chemicals from Asia, where precursor emissions are still increasing (Maas and Grennfelt, 2016). Over east and central China, an accelerating rate of NO_X emissions has been observed (Zhang *et al.*, 2007), and an increase in the amplitude of peak O_3 episodes was observed in the region between 1991 and 2006 (Xu *et al.*, 2008).

The seasonal and diurnal variation observed in tropospheric O_3 levels means that defining 'current' concentrations can be challenging. The review by Cooper *et al.* (2014) of *in situ* and remotely sensed O_3 observations found yearly average surface O_3 varied between ~25 and ~50 ppb at rural sites across Europe, ~30 and ~45 ppb at rural sites in the United States, and ~40 to ~60 ppb at rural sites in Japan, between 2000 and 2010. In China, annual mean concentrations as high as 74 ppb were recorded in a number of locations in early 2000's (Wang *et al.*, 2007).

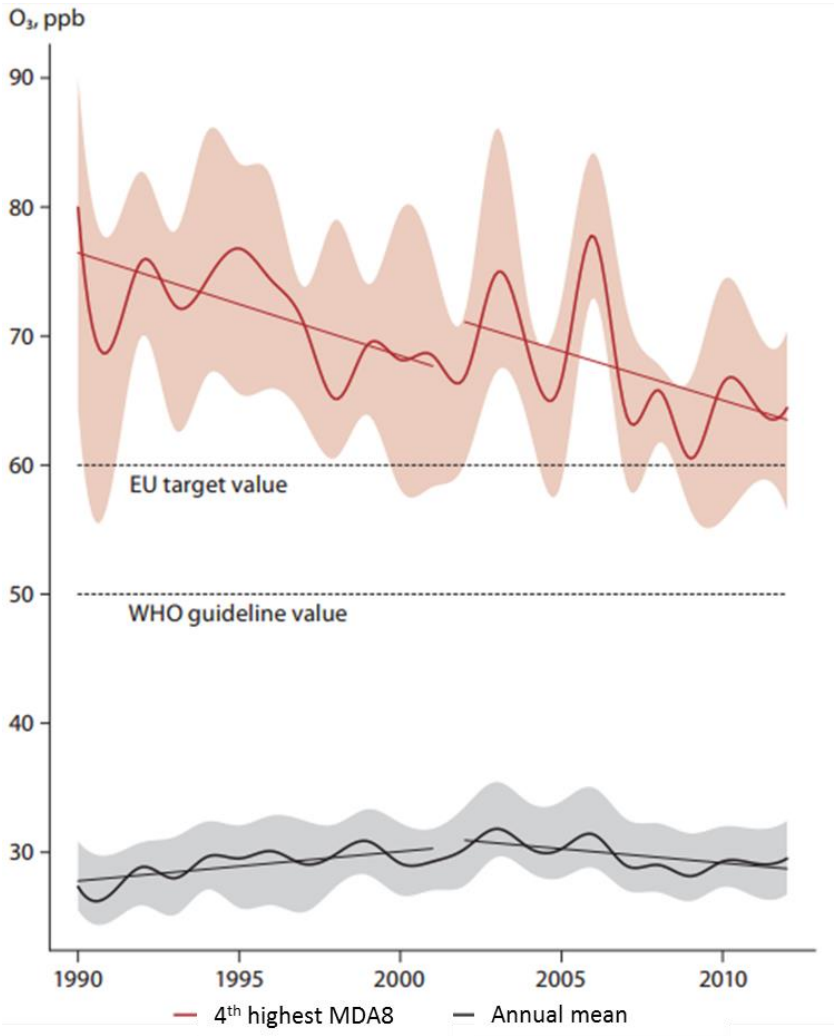

Figure 1.3. Ozone peak concentrations (4th highest daily maxima 8-hour mean O_3; MDA8) and annual mean concentrations at 54 EMEP monitoring stations in Northern Europe. Thick lines indicate the median; shaded areas the 25th and 75th percentiles. Figure reproduced from Maas and Grennfelt (2016).

1.2.6 Projections of future O_3 trends

The future distribution and concentration of surface O_3 will depend both on trends in precursor emissions, and changes in the global climate (Royal Society, 2008). Global emissions of the NO_X gases are projected to continue to increase until 2050 under all of the HTAP policy scenarios (Figure 1.4) (IPCC, 2013a). Modelled surface O_3 projections by the IPCC show large variation by region in predicted trends (Figure 1.5). Levels in Europe and North America are expected to decline under three policy scenarios, or remain approximately the same under the most pessimistic HTAP policy scenario (RCP8.5). In East Asia, concentrations are expected to remain stable or rise until 2020 under all emission scenarios and fall below current levels under the 'optimistic' RCP2.6 and RCP4.5 scenarios. South Asia is predicted to see the largest rise in O_3 concentrations in the coming decades, with steep increases to 2030 projected for the two most pessimistic scenarios, RCP6.0 and RCP8.5. These model predictions are supported by measurement station data from Delhi indicating that surface O_3 in the area is increasing at an average rate of 1.13% annually (Kumari *et al.*, 2013). The pattern of surface O_3 concentration is also expected to change over time, and to vary significantly according to global region. A number of studies have indicated that the frequency of peak O_3 episodes of short and acutely high concentrations is expected to decline in North America and Europe, but will continue to increase in developing regions until 2050 (Lei *et al.*, 2012; Paoletti *et al.*, 2014; Xu *et al.*, 2008).

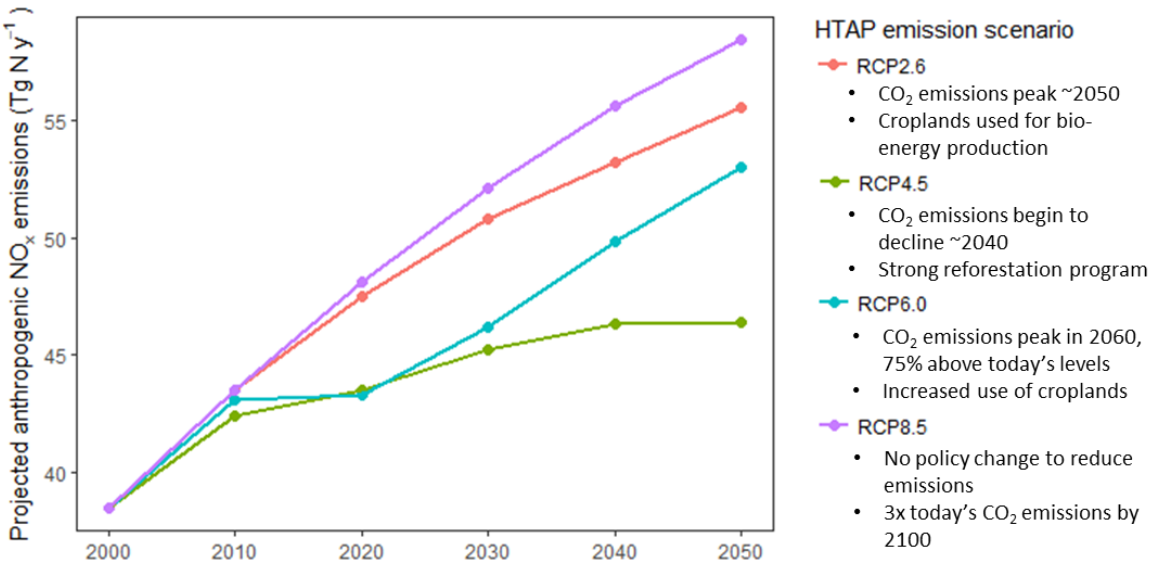

Figure 1.4. Projected global anthropogenic emissions of annual mean NO_X (sum of NO and NO_2) in Tg year^{-1} until 2050, under the four HTAP emission scenarios. Key characteristics for each emission scenario, or RCP (representative concentration pathway), are given in the figure legend. NO_x projection data extracted from IPCC (2013a). RCP definitions are from van Vuuren et al. (2011).

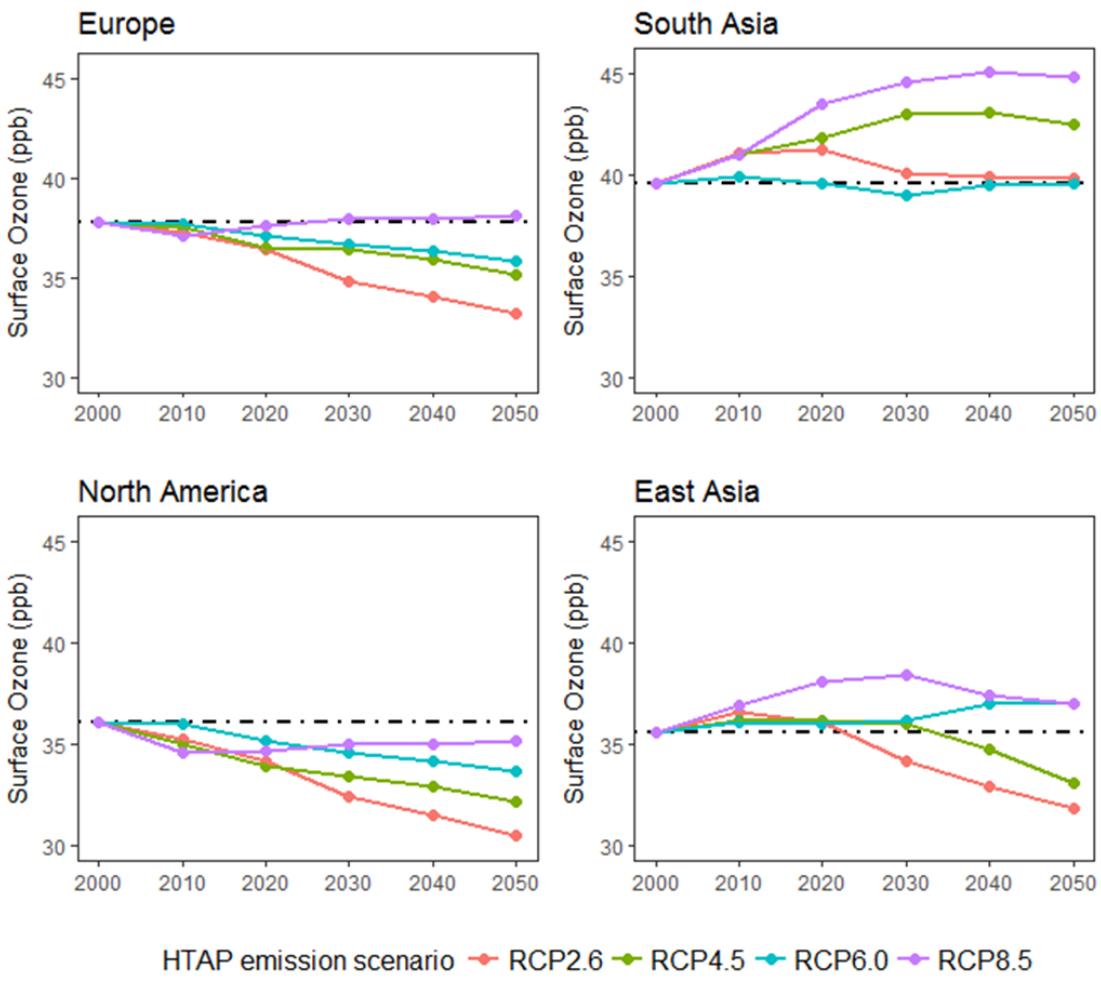

Figure 1.5. Projected surface annual mean O_3 (ppb) for HTAP regions and four HTAP emission scenarios. Data extracted from IPCC (2013a).

1.3 Physiological effect of O_3 on crop plants

1.3.1 Ozone impacts on yield

Ozone as a molecule is relatively unstable, and will readily oxidise on contact with various surfaces; it is this property which makes it a toxin for both plants and animals (Royal Society, 2008). A history of O_3 experimentation stretching back to the 1970's supports what we now know about O_3 impacts to crop yield and quality. Large-scale research programs conducted in the United States (national crop loss assessment network or NCLAN – see review by Heagle, 1989) and Europe (European crop loss assessment network or EUCLAN – see review by Jäger *et al.*, 1992) have generated and collated data from O_3 exposure experiments, allowing exposure-response relationships for different crop species to be derived. Most O_3 exposure-response experiments have been conducted under near-field conditions in open-top chambers, although more recently free-air concentration enrichment (FACE) facilities have enabled experiments to take place in full-field environments (Bernacchi *et al.*, 2006; Betzelberger *et al.*, 2010; Morgan *et al.*, 2006; Pang *et al.*, 2009).

Ozone damage to plants can be characterised as either chronic (resulting from long-term, moderate exposure) or acute (resulting from short periods of exposure to very high levels). Chronic and acute exposure lead to different manifestations in plants (Ainsworth *et al.*, 2012; Booker *et al.*, 2009; Castagna and Ranieri, 2009). As recent O_3 trends – discussed in the previous section - indicate that high background O_3 concentrations are likely to be a greater concern than peak episodes for European agriculture in the coming decades, this thesis primarily focusses on the response of soybean and wheat to *chronic* O_3 exposure (although some effects of moderate peak exposure are also considered). The state of knowledge regarding the physiological response of crops to moderate and season-long O_3 exposure will therefore be the focus of the following sections.

Chronic O_3 exposure has consistently been observed to reduce yield in a wide range of agricultural species. The meta-analysis by Feng and Kobayashi (2009) analysed dose-response data for six crops (potato, barley, wheat, rice, bean and soybean), and found that all six crops exhibited significant yield loss in response to O_3. A similar study by Mills *et al.* (2007) identified 15 agricultural and horticultural crops exhibiting a negative yield response to O_3, and ranked wheat and soybean as among the most O_3-sensitive. Commonly observed across wheat and soybean studies is a severe impact on individual seed or grain weight, with a lesser or absent effect on seed or grain number (Feng and Kobayashi, 2009; Feng *et al.*, 2008; Fuhrer *et al.*, 1989; Morgan *et al.*, 2003). Ozone has also been observed to reduce harvest index – defined as the proportion of final above-ground biomass comprising yield – in wheat and soybean (Betzelberger *et al.*, 2012; Feng *et al.*, 2008); an effect which is not fully understood but may be

related to O_3-induced impairment of carbon translocation during the grain filling stages (Grantz and Farrar, 2000).

1.3.2 Present and future yield and economic losses due to O_3

Several studies have tried to estimate the yield and economic impact of O_3 pollution on global agriculture. A commonly used method has been to combine simulated and gridded O_3 concentrations from a chemical transport model (CTM) with empirical concentration-response functions and crop production maps, to derive a regional, national or global impact estimate. Avnery *et al.* (2011a) applied this method and estimated global yield losses for the year 2000 as 9 – 14% for soybean and 4-15% for wheat, with potential additional losses for 2030 projected in the region of 1.5%-10% for wheat and 0.9-11% for soybean. The total annual financial loss to the agricultural sector from O_3 pollution in 2030 was estimated at 35 billion USD (Avnery *et al.*, 2011b). van Dingenen *et al.* (2009) applied a similar empirical methodology, and estimated that the most severe economic losses as a result of O_3-induced yield reduction in the year 2000 were taking place in India and China for wheat, and the USA and China for soybean (Figure 1.6A). They also predicted that relative yield losses as a result of O_3 would increase globally by 2030, with the greatest losses taking place in India (Figure 1.6B). A study which examined the combined impact of O_3 and climate change on future yield of wheat, rice, maize and soybean found that the likely negative impact of climate change on global production (-11%) can be either offset by O_3 pollution control measures (reducing losses to 9%), or exacerbated if the rise in O_3 is unabated (increasing losses to 15%) (Tai *et al.*, 2014). Finally, Chuwah *et al.* (2015) investigated how future unabated O_3 precursor emissions might influence future land use. They estimated that increased crop damage in 2050 could lead to a 2.5% increase in necessary crop area globally, potentially resulting in cumulative net release of 3.7 petagrams of carbon. Such assessments have acted as a powerful tool for highlighting the economic and food supply benefits that could come from further reductions in surface O_3, and have shown that tackling O_3 precursor emissions could significantly increase global yields without the potential environmental degradation associated with additional fertiliser application or land cultivation.

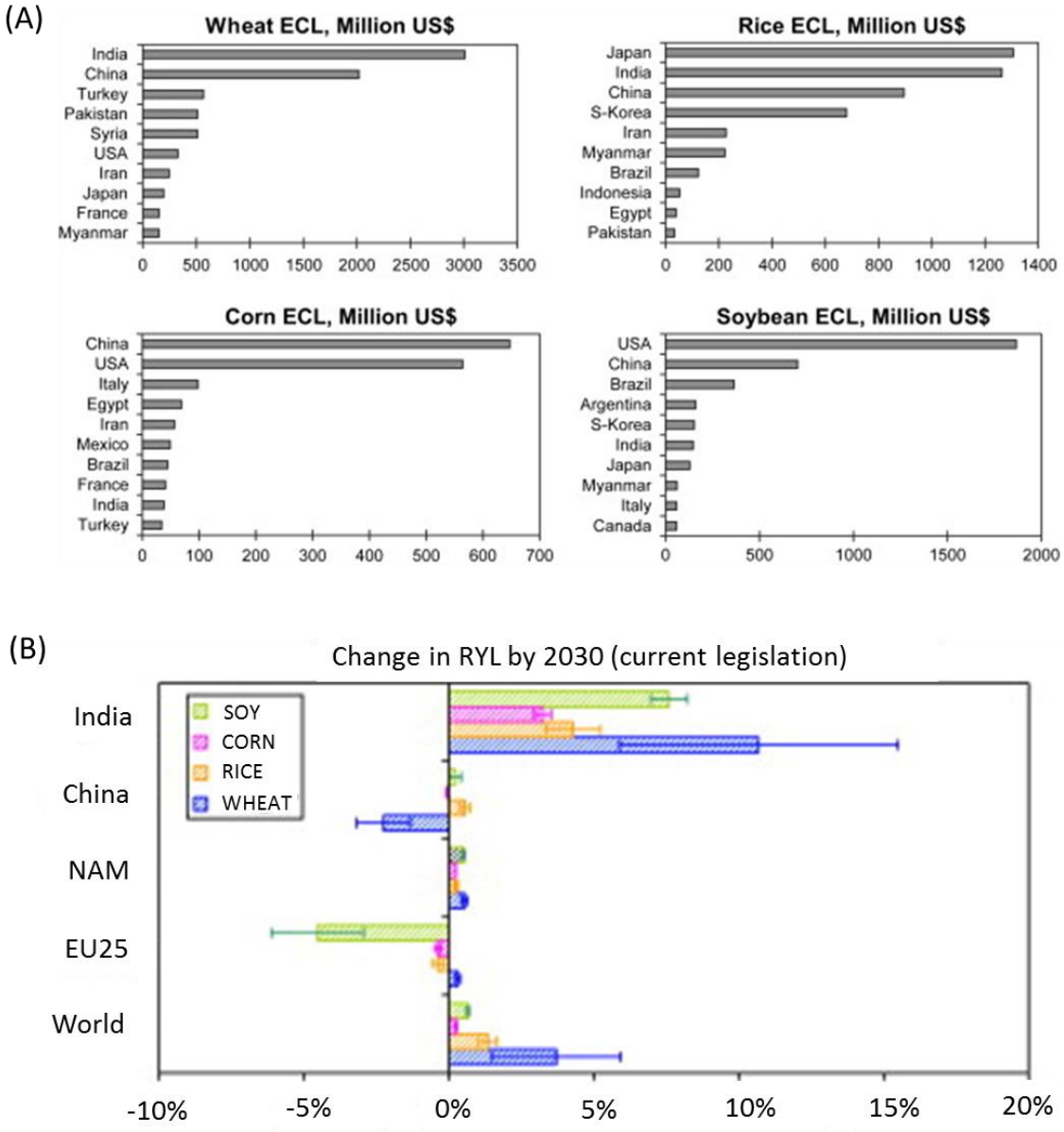

Figure 1.6. (A) Estimated economic losses (year 2000) resulting from O_3 impacts to the yields of wheat, rice, maize and soybean. Countries shown represent the top 10 countries in terms of economic loss. (B) Projected changes in relative yield loss by 2030 under the CLE scenario, which assumes that air pollution legislation in place in the year 2001 are fully implemented by 2030. In India, a worst-case scenario of non-action was assumed. Negative numbers indicate a lower loss. Both figures reproduced from van Dingenen et al. (2009).

1.3.3 Ozone uptake through stomata and initial effects

The main pathway by which O_3 causes damage to plants is via entry through stomatal pores in the leaf. Deposition to the external plant surfaces also takes place, but this causes minimal damage (Fiscus *et al.*, 2005). Once inside the apoplast, O_3 is rapidly degraded to yield reactive

oxygen species (ROS) including hydroxyl, peroxyl and superoxide radicals (Booker *et al.*, 2009). A host of plant defence mechanisms are then triggered, most notably an upregulation of activity of antioxidants (e.g. superoxide dismutase, peroxidases), which can protect against oxidative damage in the apoplast (Kangasjärvi *et al.*, 1994). Isoprene can also be produced by some plants in response to O_3 stress and is thought to be able to react with and quench O_3 before it forms ROS (Loreto and Velikova, 2001). These defence strategies are associated with a metabolic cost in the form of carbon and other substrates, and the increase in the rate of mitochondrial respiration often observed in crop species in response to O_3 is thought to be a consequence of this increase in metabolic demand (Ainsworth *et al.*, 2012).

If the defensive capacity of the apoplast is overcome, ROS can then react with and oxidise proteins and lipids in the plasma membrane, leading to membrane dysfunction (Booker *et al.*, 2009; Emberson *et al.*, submitted). Other toxic compounds with a longer half-life can be formed, and a cascade of responses can be triggered which eventually lead to the leaf and crop-level symptoms of O_3 exposure (e.g. leaf injury, impaired photosynthesis, accelerated senescence).

1.3.4 Effect on stomatal conductance (g_{sto})

A reduction in stomatal conductance (g_{sto}) in response to O_3 exposure has been observed in experiments for both wheat and soybean (Feng *et al.*, 2008; Fiscus *et al.*, 1997; Morgan *et al.*, 2003), and in other plants (Pleijel *et al.*, 2002; Wittig *et al.*, 2007). It has been hypothesised that this is a consequence of the O_3-induced reduction in photosynthetic rate, rather than a direct effect of O_3 on stomata. Stomatal conductance has long been known to be closely coupled to the rate of photosynthesis (Ball *et al.*, 1987), as a reduction in photosynthetic rate should in theory cause a build-up of CO_2 in the mesophyll, which then induces a feed-back signal to reduce g_{sto} (Reich and Amundson, 1985). This hypotheses is supported by the meta-analyses of Morgan *et al.* (2003) in soybean and Feng *et al.* (2008) in wheat, who observed similar percentage reductions on average for g_{sto} and photosynthetic rate in response to elevated O_3. In addition, Martin *et al.* (2000) found that the reduction in CO_2 assimilation rate in response to O_3 exposure could be used to successfully predict stomatal closure, also lending support to this hypothesis.

However, some experimental work has suggested that O_3 exposure can have other, more unexpected, effects on stomata. Lombardozzi *et al.* (2012) observed in an open-top chamber experiment with tulip poplar that photosynthetic rate declined at a faster rate than g_{sto} in response to O_3 exposure, and hypothesised that O_3 can induce a 'decoupling' of the two physiological processes. A similar decoupling effect has also been observed in ageing birch leaves in response to O_3 exposure (Harmens *et al.*, 2017). As some crop simulation and O_3 effect modelling techniques are based around the close association between g_{sto} and photosynthesis, a potential decoupling of the two is an important consideration for those

applying and developing modelling methods. An additional effect of O_3 on stomata that has been observed in a number of experiments is a slow or 'sluggish' response to environmental stimuli or stress (McAinsh *et al.*, 2002). Paoletti (2005) found that the stomatal response to high light intensity in the Mediterranean broadleaf tree *Arbutus unedo* was slower under chronic O_3 exposure, and a series of experiments in grassland species have reported an impaired stomatal response to drought (Mills *et al.*, 2009; Wilkinson and Davies, 2009). The loss of stomatal control under drought stress was attributed to a reduced sensitivity to the plant hormone abscisic acid (ABA), and presents a significant concern as it could severely impair the ability of plants to cope with periods of water shortage (Mills *et al.*, 2009). More research is needed in order to establish whether impaired stomatal control in response to O_3 can also be observed in crop species.

1.3.5 Effect on photosynthesis

A reduction in the rate of photosynthetic carbon assimilation in response to O_3 exposure is widely reported in the literature, across many different plant species (Dann and Pell, 1989; Farage *et al.*, 1991; Feng *et al.*, 2008; Lehnherr *et al.*, 1987; Lehnherr *et al.*, 1988). However, despite a considerable amount of research spanning several decades, the leaf-level physiological mechanisms underlying this response are still not fully understood (Emberson *et al.*, submitted; Fiscus *et al.*, 2005). One challenge for experimentalists investigating this question is separating O_3 effects on photosynthesis from other, potentially inter-related responses including a loss of leaf pigmentation, changes in g_{sto}, and accelerated plant senescence. It is generally accepted that O_3 can directly impair the photosynthetic mechanism, with the evidence largely indicating that the carbon fixation stage of photosynthesis is most sensitive (Emberson *et al.*, submitted; Kangasjärvi *et al.*, 1994). Dann and Pell (1989) observed a reduction in the quantity of the principle carbon-fixing enzyme ribulose-1,5-biphosphate carboxylase/oxygenase (rubisco) in potato leaves following O_3 exposure (60-120 ppb), and Farage *et al.* (1991) similarly observed a reduction in the efficiency of this enzyme in wheat leaves in response to 4-16 hours of relatively acute exposure (200-400 ppb). Reported reductions in mRNA transcripts for rubisco in response to O_3 indicates that inhibition of synthesis of rubisco may be the key mechanism, rather than a decrease in activity, and older leaves appear to be more susceptible than young leaves (Galmés *et al.*, 2013; Glick *et al.*, 1995; Reddy *et al.*, 1993).

However, experimental studies investigating O_3 effects on rubisco have often taken place in greenhouses or controlled environment chambers and often at high O_3 exposure concentrations (e.g. Dann and Pell, 1989; Farage et al, 1991; Glick et al, 1995; Reddy et al, 1993), meaning that the importance of this effect for crops in the field environment is still unclear. Under real-world conditions, the total O_3-induced reduction in photosynthesis observed in crops is most likely a manifestation of several different mechanisms; for example, reduced leaf chlorophyll

(Gelang *et al.*, 2000), reduced integrity of cell membranes (Biswas *et al.*, 2008), and damage to PSII centres (Guidi *et al.*, 2002) have all been observed as a response to O_3 exposure.

1.3.6 Effect on senescence

Accelerated leaf senescence in response to chronic O_3 exposure has been reported across many plant species, including wheat (Burkart *et al.*, 2013; Feng *et al.*, 2011; Gelang *et al.*, 2000; Grandjean and Fuhrer, 1989; Ojanperä *et al.*, 1998) and soybean (Kohut *et al.*, 1986; Morgan *et al.*, 2006; Reid *et al.*, 1998; Zhang *et al.*, 2014). Ozone-induced early senescence is typically characterised by a loss of total protein, leaf chlorophyll, rubisco protein, and increased leaf abscission (Miller *et al.*, 1999). Experiments investigating O_3 effects on leaf senescence have often used the leaf chlorophyll content as a proxy for leaf senescence, as chloroplasts are one of the earliest sites for catabolism during senescence, and leaf chlorophyll content can be measured non-destructively using an index (e.g. Harmens et al, 2017; Pleijel et al, 2006). The acceleration of leaf senescence – and consequent reduced leaf lifespan and grain fill duration - is likely to be a significant factor determining the magnitude of O_3-induced yield loss, but as with O_3 effects on photosynthesis, the mechanisms driving this response are not clear.

Leaf senescence is a highly regulated process, involving the degradation of proteins and lipids, and remobilisation of nutrients; and like other developmental processes it is actively regulated by differential gene expression (Smart, 1994). Experiments in the model plant species *Arabidopsis thaliana* have shown that changes in gene expression during chronic O_3 treatment are similar to the changes observed during natural senescence, with the induction of several *senescence associated genes* (SAGs), indicating that O_3 stress prematurely induces natural senescence processes (Conklin and Barth, 2004; Miller *et al.*, 1999). The mechanism of induction remains unresolved, although work in *Arabidopsis thaliana* suggests that alteration in the relative levels of certain phytohormones – e.g. salicylic acid, abscisic acid and ethylene – may play a role (Conklin and Barth, 2004). It has also been suggested that the trigger for senescence could be related to the long-term increased respiratory costs associated with detoxification and repair processes (Ewert and Porter, 2000).

1.4 Variation in O_3 sensitivity of crops and cultivars

1.4.1 How much variation?

Experimentalists have observed a considerable amount of variation among plant species and cultivars in response to chronic O_3. Mills *et al.* (2007) synthesised data from over 700 published papers to derive concentration-response functions for 19 crop species, and found that while some could be identified as O_3-sensitive (e.g. pulses, wheat, onion, soybean, tomato), others seemed to be relatively tolerant and showed no significant yield response to O_3 (e.g. strawberry, plum, barley) (Figure 1.7A). A significant level of intra-species variation has also been

observed (Barnes *et al.*, 1990; Biswas *et al.*, 2008; Butler and Tibbitts, 1979; Sawada and Kohno, 2009) (Figure 1.7B), although interestingly sensitivity to yield reduction is not always correlated to visible leaf injury (Barnes *et al.*, 1990; Sawada and Kohno, 2009). The large range of sensitivity to O_3 that exists both between and within species presents an opportunity for crop breeders, but also represents a complicating factor in efforts to model O_3 effects on yield: current modelling methods typically require parameterisation for individual cultivar or species sensitivity based on experimental data, which can often be lacking (Emberson *et al.*, submitted). Much research conducted over the last few decades has therefore focussed on establishing the physiological traits that define O_3 sensitivity, or its inverse, O_3 tolerance.

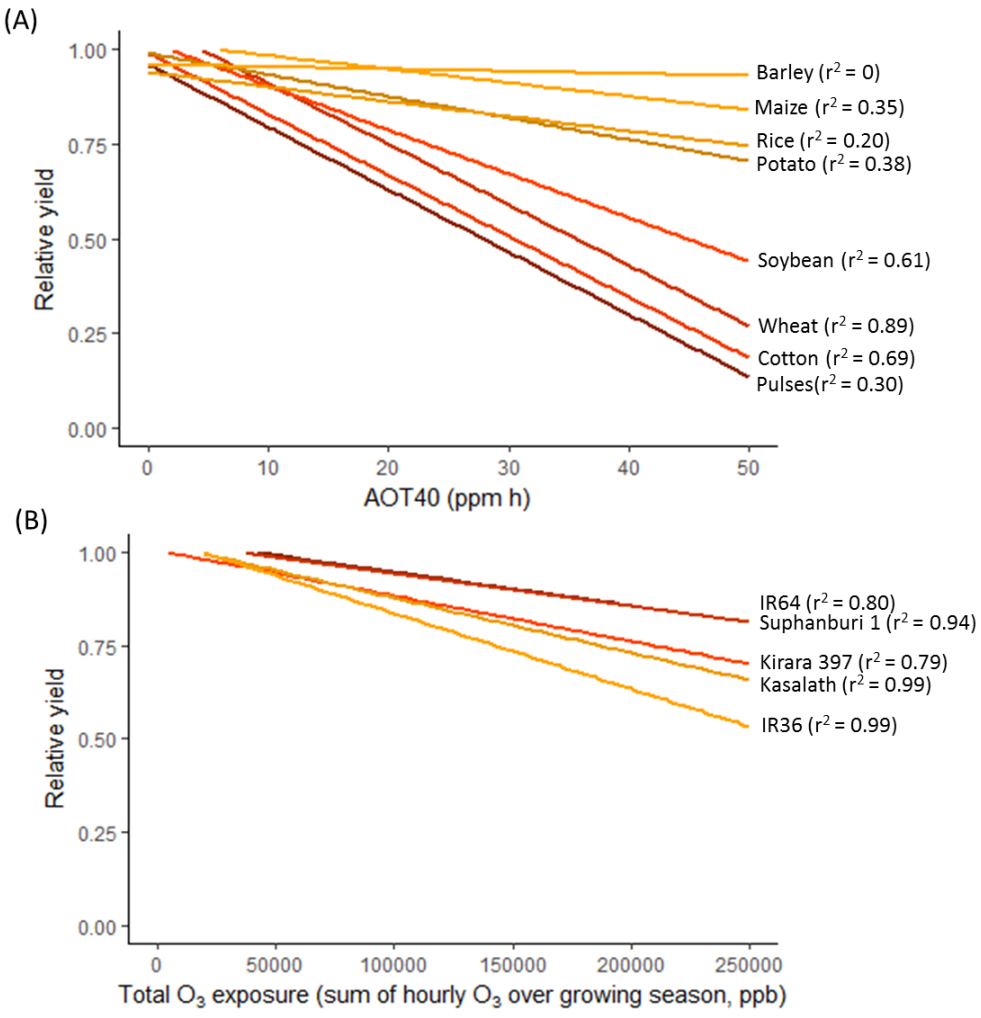

Figure 1.7. Plots demonstrating the variation in O_3 sensitivity that exists between crop species and cultivars. (A) Variation in yield-AOT40 response slope for eight crop species. Barley and maize are relatively tolerant of O_3, while soybean and wheat are amongst the most O_3-sensitive. Dose-response line equations were re-drawn from Mills et al. (2007). (B) Variation in yield-exposure slopes for five Asian cultivars of rice. Dose-response equations were re-drawn from Sawada and Kohno (2009).

1.4.2 Which plant physiological traits are associated with O_3 tolerance?

Tolerance to O_3-induced yield loss has been shown to be a heritable trait (Fiscus *et al.*, 2005), suggesting that particular genetic or physiological traits are responsible for conferring O_3 tolerance. One factor which is likely to play a role in determining the tolerance of a species or cultivar is g_{sto}; leaf conductance will directly determine the amount of O_3 uptake for a given ambient concentration and duration of exposure, and it has long been hypothesised that variation in average or maximal g_{sto} can explain at least part of the variation in O_3 sensitivity (Brosché *et al.*, 2010; Reich, 1987). Support is given to this theory by observations of amelioration of O_3 impacts when O_3 is applied in combination with environmental stresses that reduce g_{sto} (e.g. elevated CO_2, drought stress) (Biswas and Jiang, 2011; Khan and Soja, 2003; Mulholland *et al.*, 1997a). Further support comes from the findings of numerous authors that modern wheat varieties are more O_3-sensitive than older ones, and modern varieties also have higher g_{sto} (Barnes *et al.*, 1990; Biswas *et al.*, 2008; Pleijel *et al.*, 2006; Velissariou *et al.*, 1992). However, g_{sto} is unlikely to be the only factor involved in O_3 tolerance, as some cultivars with similar g_{sto} exhibit different levels of response to the same O_3 concentration (Fiscus *et al.*, 2005). The ability of a plant or cultivar to detoxify harmful ROS in the leaf tissue will also be important in determining tolerance: evidence to support this comes from the fact that the threshold exposure at which plant damage occurs is known to vary between species (Bergmann *et al.*, 1999), and by experiments which have observed a correlation between O_3 tolerance and antioxidant metabolite levels in leaves (Burkey *et al.*, 2000; Chernikova *et al.*, 2000).

1.4.3 Influence of environment and management on O_3 sensitivity

Local environmental and climatic conditions can influence the severity of plant response to O_3 exposure. For example, environmental conditions that promote a high g_{sto} (e.g. high humidity), and therefore a faster rate of O_3 uptake, are likely to be associated with more severe O_3 effects, while conditions that promote stomatal closure (e.g. high temperature and low soil moisture) may reduce the amount of O_3 damage. The close link between local meteorology and stomatal O_3 uptake means that global climate change is likely to influence the magnitude of O_3-induced yield loss, although predicting interactive effects on a large scale and across climatically heterogeneous landscapes is a significant challenge for modellers and may require significant developments in crop modelling (Challinor *et al.*, 2009). The presence of the atmospheric pollutants sulphur dioxide (SO_2) and nitrogen dioxide (NO_2) in the local environment has also been observed to alter the plant response to O_3, although the mechanism of interaction is not clear and both antagonistic and synergistic responses have been reported (Fangmeier and Bender, 2002). The ambient CO_2 concentration can also influence the response to O_3. Elevated CO_2 promotes a reduced stomatal aperture, particularly for plants that employ C3 photosynthesis such as wheat and soybean (Ainsworth and Long, 2005), and elevated CO_2 can also boost growth in some plants (Reddy *et al.*, 2010). The projected rise in atmospheric CO_2

from current levels at ca. 400 ppm to 430-720 ppm by 2100 is therefore widely expected to ameliorate some negative effects of O_3 on crop yield (IPCC, 2014a), although the question of whether CO_2 enhancement of yield observed in chamber studies will translate into the field environment is contentious and unresolved (Long *et al.*, 2006; Tubiello *et al.*, 2007).

Sowing calendars and management practises can also influence the vulnerability of a crop to O_3. Experiments with wheat and soybean have shown that O_3 exposure during grain fill typically has a more severe impact on final yield than exposure during vegetative growth (Feng *et al.*, 2008; Morgan *et al.*, 2003; Morgan *et al.*, 2004); the co-occurrence of an O_3 concentration peak with a sensitive period of plant development can therefore significantly influence the degree of final yield loss. In theory, staggering crop growing seasons to avoid the annual O_3 peak could mitigate yield losses from O_3 pollution, as long as temperature, sunlight and precipitation conditions remained favourable. Irrigation management could also potentially ameliorate O_3 impacts on yield, if watering is withdrawn before a forecast O_3 episode in order to induce stomatal closure and limit uptake. This approach would depend on the benefits of O_3 exclusion outweighing the risk of water withdrawal, and needs to be tested in a field environment.

1.5 Approaches for modelling O_3 uptake and damage

1.5.1 Metrics of O_3 exposure

The O_3 exposure that a plant experiences over a period of time can be quantified using many different approaches; for example, Paoletti *et al.* (2007) calculated and compared 17 different indices of concentration-based exposure to plants in Mediterranean Italy. In Europe, the development and improvement of O_3 exposure indices has been guided by the Convention on Long-Range Transboundary Air Pollution (LRTAP), established in 1979 as a forum for translating air pollution effects research into policy (Fuhrer *et al.*, 1997). Early O_3 experiments commonly quantified the level of exposure by calculating the mean of hourly O_3 concentration (in ppb) over a particular period of time – most often the 7-hour, 8-hour, 12-hour or 24-hour mean (Fuhrer *et al.*, 1989; Heagle *et al.*, 1986; Kohut *et al.*, 1986). During the 1990's, the LRTAP in Europe adopted the AOT40 threshold index (the accumulated amount of O_3 exceeding 40 ppb during daylight hours) for their risk assessment work, based on analysis of experimental data for wheat which showed a close linear relationship between the 3-month AOT40 and yield (Fuhrer *et al.*, 1997). In the USA around the same time, a similar metric was developed – the SUM60, defined as the sum of all hourly concentrations when those concentrations exceed 60ppb (Paoletti and Manning, 2007). These indices were introduced at the same time as the critical levels concept was being developed in Europe. The critical level was defined as the concentration or cumulative exposure of a pollutant above which direct adverse effects on vegetation may occur (CLRTAP, 2017).

However, following the adoption of these approaches within risk assessment methodology for Europe and the USA, important limitations were identified. All O_3 indices based on concentration assume that the plant exposure will be equal to the ambient concentration, but in reality the plant response is more likely to be associated with the internal O_3 concentration, which is influenced by g_{sto}. This understanding led to the development of the flux metric, designed to estimate the internal 'dose' of O_3 as modified by the influence of concurrent environmental conditions on g_{sto} (Fuhrer *et al.*, 1997). The flux approach has since been shown in a number of studies to be superior to the AOT40 approach for predicting the physiological and biomass response of plants (Karlsson *et al.*, 2007; Mills *et al.*, 2011a; Uddling *et al.*, 2004), and has been incorporated within the European Monitoring and Evaluation Programme (EMEP) photo-oxidant chemical transport model, which is used by the United Nations Economic Commission for Europe (UNECE) in their air pollution impact assessments (Simpson *et al.*, 2012). However, one limitation of the flux approach is that the calculation of flux is far more technical than the calculation of accumulated concentration, requiring some form of g_{sto} modelling; and it depends on the availability of time-series meteorological data as input. Most research and risk assessment that has applied flux as the metric of O_3 exposure to date has used the Deposition of Ozone for Stomatal Exchange (DO_3SE) model, which models both the non-stomatal and stomatal components of O_3 deposition to vegetation, and can therefore produce an estimate of O_3 flux (Emberson *et al.*, 2000b). DO_3SE is described in more detail in section 1.5.2.

Accurately capturing the variation in O_3 sensitivity that exists between species and cultivars has represented an additional challenge in the development of O_3 exposure indices. Accumulative concentration-based indices (e.g. AOT40) can theoretically be parameterised for differences in sensitivity to O_3 by varying the threshold of concentration above which accumulation takes place, with the threshold of accumulation representing the ability of the plant to detoxify O_3 and ROS. The stomatal flux component of the DO_3SE model (Emberson *et al.*, 2000b) accounts for variation by applying a species-specific maximum rate of g_{sto}, and by employing a species-specific threshold above which hourly stomatal O_3 flux is accumulated; this produces the POD_Y metric, representing the **P**hytotoxic **O**$_3$ **D**ose above the threshold *Y* in units of mmol m^{-2}. An additional approach to measuring O_3 exposure was proposed by Massman (2004), who aimed to combine the estimated O_3 uptake through stomata with the plant's ability to detoxify, to produce the 'effective ozone dose'. The limitation with this approach is the difficulty associated with modelling or estimating the detoxification capacity of a plant in a mechanistic way (Massman, 2004).

1.5.2 Models of g_{sto}

Accurate estimation of stomatal O_3 flux at the leaf level depends on a reliable method for modelling g_{sto} under a range of environmental conditions. Over the last 40 years several different approaches for modelling g_{sto} have been proposed (Damour *et al.*, 2010). One of the

simplest and most widely used methods is the multiplicative approach, which integrates the effects of multiple environmental factors on g_{sto} using empirical response relationships (Jarvis, 1976). The algorithm originally published by Jarvis (1976) is shown below:

$$g_{sto} = f_Q \times f_{Temp} \times f_{VPD} \times f_{Ca} \times f_\psi$$

Where f_Q, f_{Temp}, f_{VPD}, f_{Ca} and f_ψ each take values between 0 and 1, and represent the effect of light intensity, leaf temperature, vapour pressure deficit, ambient CO_2 concentration and leaf water potential on g_{sto} (cm s^{-1}), respectively. In this method, g_{sto} is assumed to have a defined relationship with each environmental variable, and parameters describing each function are determined by boundary line analysis (Webb, 1972) (Figure 1.8). White *et al.* (1999) built on this method by introducing a factor describing the maximal stomatal aperture (g_{max}), and Emberson *et al.* (2000a) modified it specifically for the purpose of estimating O_3 uptake and incorporated a phenology component. The DO_3SE model multiplicative algorithm is as follows:

$$g_{sto} = g_{max} \times [min(f_{phen}, f_{O3})] \times f_{light} \times max\{f_{min,}, (f_{Temp} \times f_{VPD} \times f_{SWP})\}$$

Where additional factors not previously defined are f_{phen}, f_{O3}, and f_{SWP}, representing the influence of phenology, O_3, and soil water potential on g_{sto} (mmol O_3 m^{-2}), respectively; and f_{min} represents the minimum possible g_{sto} under field conditions. Multiplicative models have been criticised for the fact that the different environmental variables are assumed to behave independently of each other – which is not always true - and because they are essentially empirical and parameterisation is therefore required for each new environmental condition and each new species or cultivar (Damour *et al.*, 2010).

Another published method for modelling g_{sto} is the optimal behaviour model, first proposed by Cowan and Farquhar (1977). This model is based around the theory that stomata will behave in the optimal way, maximising the amount of CO_2 uptake per unit of water vapour lost. The rate of transpiration (mol H_2O m^{-2} s^{-1}) and photosynthesis (mol CO_2 m^{-2} s^{-1}) will therefore fluctuate so that the marginal water cost of carbon gain, λ (mol H_2O mol^{-1} C), can be expected to remain constant:

$$\lambda = \frac{\partial E}{\partial A_n}$$

Where ∂E and ∂A_n represent the fluctuation in transpiration and net photosynthesis, respectively. This model has not yet been adequately tested at large scale, and the key parameter, λ, is difficult to estimate (Medlyn *et al.*, 2011). Some experimental evidence supports the theory that $\partial E/\partial A_n$ remains constant in a changing environment, but this evidence comes mainly from laboratory studies (Thomas *et al.*, 1999).

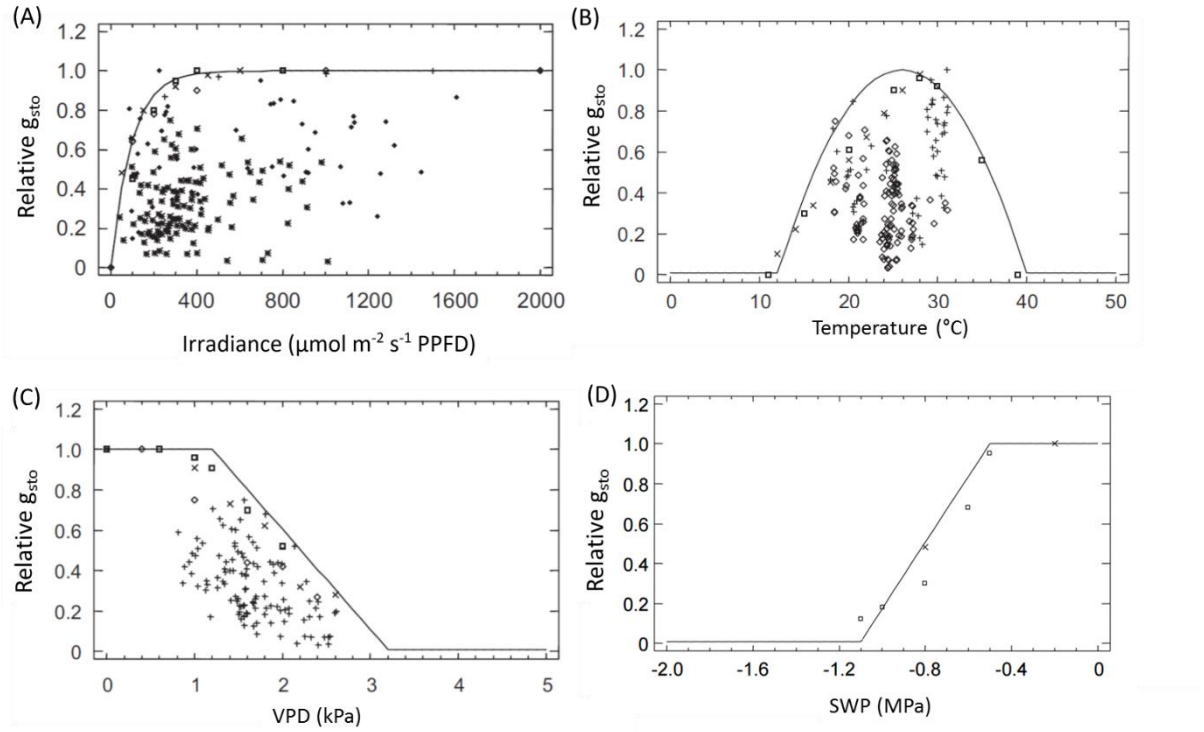

Figure 1.8. Example boundary line plots for four of the f_X functions of DO$_3$SE (Deposition of ozone for stomatal exchange) – a multiplicative g_{sto} model – to illustrate the boundary line method for deriving model parameters first described by Webb (1972). (A) Boundary line plot for f_{light}, with example data for wheat. (B) Boundary line plot for $f_{Temp,}$ with example data for wheat. (C) Boundary line plot for $f_{VPD,}$ with example data for wheat. (D) Boundary line plot for f_{SWP}, with example data for potato. All plots reproduced from CLRTAP (2017).

One of the most commonly used and influential models of g_{sto}, first published by Ball *et al.* (1987) and also known as the BWB model, is built on the association that exists between g_{sto} and photosynthetic rate. This model is often described as 'semi-empirical', as it is built on physiological hypotheses, but still uses empirical functions (Damour *et al.*, 2010). In this 'A_n-g_{sto}' model, g_{sto} responds linearly to an index calculated from the rate of photosynthesis, humidity in the air, and CO_2 concentration at the leaf surface (Figure 1.9). This model has since been modified to incorporate the CO_2 compensation point (Γ), and to better simulate the relationship between g_{sto} and water deficit in the air (Leuning, 1990, 1995). The BWB model as modified by Leuning (1995) is given below:

$$g_{sto} = g_0 + \frac{a_1 A_n}{(c_a - \Gamma)(1 + D_s/D_0)}$$

Where A_n, D_s, c_a and g_0 represent net photosynthesis (µmol m^{-2} s^{-1}), humidity deficit or VPD (kPa), CO_2 concentration at the leaf surface (ppm), and g_{sto} (mol m^{-2} s^{-1}) when A_n = 0, respectively. D_0 and a_1 are empirical coefficients (Leuning, 1995). In this model, the influence

of irradiance and temperature on photosynthesis provides the link between environment and gas exchange rate. Photosynthetic rate can either be measured directly or estimated using a photosynthesis model; the biochemical model of Farquhar *et al.* (1980) is often used to estimate A_n. A_n-g_{sto} models are considered to be relatively easy to parameterise, and are thought to represent a good compromise between ease-of-use and predictive power (Damour *et al.*, 2010).

However, a criticism levelled at A_n-g_{sto} models is that they are still essentially empirical and have not been built on a mechanistic understanding; the empirically derived parameters therefore cannot be defined in a meaningful, biological way (Medlyn *et al.*, 2011). It has been proposed that the optimal and A_n-g_{sto} approaches can be reconciled, so that the slope of the relationship between g_{sto} and the A_n index is proportional to the marginal water cost per carbon gain, λ (Medlyn *et al.*, 2011). This hypothesis has not been widely tested. Fully mechanistic models for g_{sto} do not yet exist, due to an incomplete understanding of the mechanisms that link gas exchange, photosynthesis and the environment.

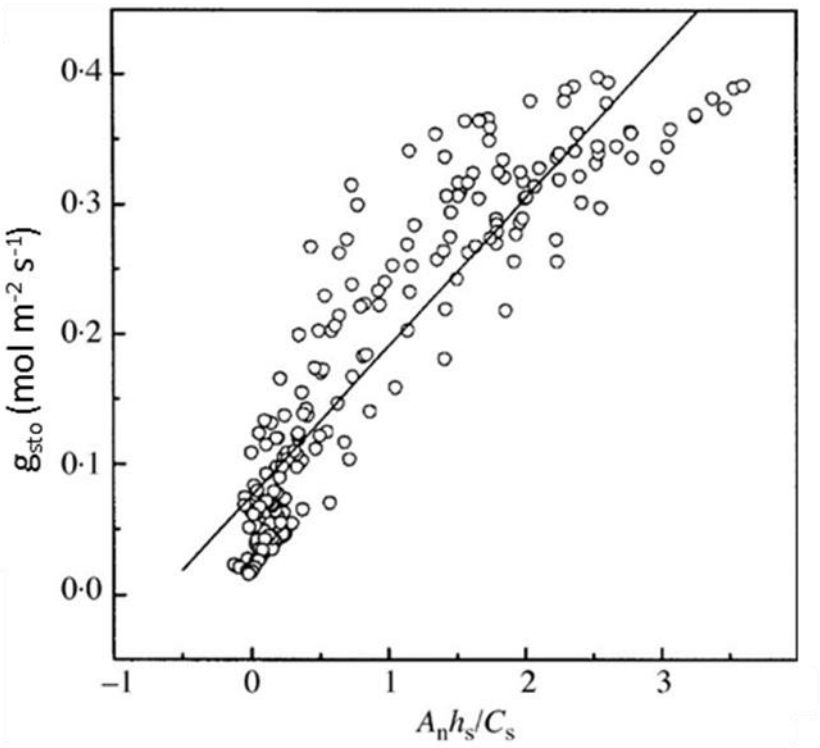

Figure 1.9. The association between g_{sto} and an index of net photosynthesis, as proposed by Ball et al. (1987), tested with data from a cultivar of winter wheat. Figure reproduced from Yu et al. (2004). A_n = net photosynthesis, h_S = relative humidity, C_S = CO_2 concentration of air at the leaf surface.

1.5.3 Potential for integrating crop simulation and O_3 effects modelling

Estimates of yield reduction under future O_3 precursor emission and climate change scenarios represent a way to quantify the potential benefits of tropospheric O_3 mitigation and adaptation strategies. However, the major estimates of future O_3-induced yield loss published to date have been based on empirical methods – chiefly, the application of concentration-based yield-response functions for converting simulated surface O_3 into predicted yield reduction (Avnery *et al.*, 2011a, b; Tai *et al.*, 2014; van Dingenen *et al.*, 2009; Wang and Mauzerall, 2004). The development of an approach built on explanatory mechanisms or processes – or at least a semi-empirical approach - could theoretically produce more robust model estimates of future yield, and could also be applied as a tool for understanding the potentially complex interactions between O_3 and future climate (Emberson *et al.*, submitted).

Crop simulation models typically calculate growth parameters at a daily or hourly time-step, and can therefore be thought of as 'dynamic', as they are able to respond to a changing environment. Many different crop models have been published – over 40 are thought to be in use for wheat – and a large diversity in model methodology exists (White *et al.*, 2011). Any crop simulation model that includes in its formulation an estimation of g_{sto} or transpiration at a daily or hourly time-step can in theory also estimate O_3 flux into the leaf, as long as the ambient O_3 concentration at the canopy or leaf surface is known or can be estimated; integrating dynamic crop modelling with O_3 flux estimation is therefore already possible using published methods.

However, accurately modelling the effect of O_3 flux on crop physiology and yield remains a challenge. For semi-empirical or process-based models, the impact of O_3 flux on leaf senescence, photosynthesis, g_{sto} and assimilate partitioning needs to be adequately replicated by mathematical functions. Some attempts have been made to model the effect of O_3 on photosynthesis and senescence at the leaf level. For example, Martin *et al.* (2000) proposed a method by which the 'instantaneous' O_3-induced impairment of photosynthetic rate can be modelled, using a function which reduces the photosynthetic parameter V_{cmax} – representing the maximum rate of carboxylation by the enzyme rubisco – linearly above a species-specific detoxification threshold of O_3 flux. This method has not been tested at the canopy or crop scale. Ewert and Porter (2000) proposed a method by which the O_3-induced acceleration of senescence could be modelled in wheat, by reducing leaf lifespan linearly with increasing O_3 flux. An alternative method for modelling the O_3 effect on leaf senescence is currently employed in DO_3SE, but could also be applied in a mechanistic or semi-mechanistic model, where senescence onset is 'triggered' when a threshold of accumulated O_3 flux is reached (Grünhage *et al.*, 2012; Pleijel *et al.*, 2007). All these potential approaches need to be tested against experimental data, and upscaling from the leaf to the canopy level brings with it many complex challenges. For example, leaves in different positions in the canopy may respond differently to

O_3 exposure; leaf age may influence the physiological response to O_3 (Hanson *et al.*, 1994); and not all leaves in the canopy are equally important for yield (Yoshida, 1972). Experimental data will be crucial in guiding and validating O_3 effect functions in models, and evidence to indicate which of the O_3 effects on plant physiology is most important for yield is also needed, in order to most effectively target model development.

1.6 Aims and objectives

The overarching aim of this PhD study is to develop understanding of how exposure to O_3, expressed both in terms of concentration and stomatal flux, induces yield reduction in two globally important crops: soybean and wheat. This will be achieved by analysing published data from the literature, and by applying a number of plant physiological measurement techniques in large-scale O_3 exposure experiments, to generate new datasets. Data generated as part of this project will be interpreted in the context of O_3-effects modelling, with the aim of aiding future efforts to integrate O_3 impacts into crop simulation modelling. The specific objectives of the project are:

- In paper 1, i) to provide an up-to date concentration-response function for soybean based on the published literature; ii) to quantify the degree of variation in O_3 sensitivity of soybean cultivars; and iii) to determine if O_3 sensitivity of cultivars is associated with release date or geographic location;
- In paper 2, i) to profile the growth and yield response of a recently released cultivar of European wheat to O_3 exposure, and ii) to determine if an interaction can be observed between O_3 and drought stress;
- In paper 3, i) to determine if a number of proposed modelling methods for simulating O_3 effects on physiology are supported by experimental data; and ii) to determine if the use of the flux metric can account for the differential impacts resulting from different patterns of O_3 exposure.

2 Has the sensitivity of soybean cultivars to ozone pollution increased with time? An analysis of published dose-response data

2.1 Abstract

The rising trend in concentrations of ground-level ozone (O_3) – a common air pollutant and phytotoxin – currently being experienced in some world regions represents a threat to agricultural yield. Soybean (*Glycine max* (L.) Merr.) is an O_3-sensitive crop species, and is experiencing increasing global demand as a dietary protein source and constituent of livestock feed. This study collates O_3 exposure-yield data for 49 soybean cultivars, from 28 experimental studies published between 1982 and 2014, to produce an updated dose-response function for soybean. Different cultivars were seen to vary considerably in their sensitivity to O_3, with estimated yield loss due to O_3 ranging from 13.3% for the least sensitive cultivar to 37.9% for the most sensitive, at a 7-hour mean O_3 concentration (M7) of 55 ppb – a level frequently observed in regions of the USA, India and China in recent years. The year of cultivar release, country of data collection and type of O_3 exposure used were all important explanatory variables in a multivariate regression model describing soybean yield response to O_3. The data show that the O_3 sensitivity of soybean cultivars increased by an average of 32.5% between 1960 and 2000, suggesting that selective breeding strategies targeting high yield and high stomatal conductance may have inadvertently selected for greater O_3 sensitivity over time. Higher sensitivity was observed in data from India and China compared to the USA, although it is difficult to determine if this effect is the result of differential cultivar physiology, or related to local environmental factors such as co-occurring pollutants. Gaining further understanding of the underlying mechanisms that govern the sensitivity of soybean cultivars to O_3 will be important in shaping future strategies for breeding O_3-tolerant cultivars.

2.2 Introduction

Ensuring that the rising global population has access to a sufficient and stable food supply is a key international priority for the 21st century. At a time when an estimated 795 million people worldwide are undernourished (FAO, 2015), agricultural productivity is being limited by several factors including, *inter alia*, rising water scarcity (Falkenmark, 2013), the limited land available for cultivation (Zabel *et al.*, 2014), widespread soil erosion and degradation (FAO, 2011), and the impacts of climate change (Parry *et al.*, 2004). A further threat to agricultural yield comes from rising concentrations of ground-level ozone (O_3) (Fuhrer, 2009) – a common air pollutant and phytotoxin (Krupa *et al.*, 2001). Ozone is a secondary pollutant formed in photochemical reactions from precursor compounds, the most important of which are nitrogen oxides (NO_x), methane (CH_4), and carbon monoxide (CO) (Royal Society, 2008). The global surface background concentration of O_3 more than doubled between the early 1900s and the end of the 20th century (Hough and Derwent, 1990; Parrish *et al.*, 2014), most likely as a result of rising anthropogenic emissions of O_3 precursor compounds from fossil fuel combustion, biomass burning and paddy-field cultivation (Brasseur, 2001). Projected changes in global surface O_3 for the period 2000-2050 range from a decrease in the 24-hour mean of 2.5 - 7.2 ppb under the optimistic emission scenarios (RCP2.6, RCP4.5, RCP6.0, B1), to an increase of 1.5 - 6.2 ppb under the more pessimistic RCP8.5 and A2 emission scenarios (IPCC, 2013a). Trends in surface O_3 are however highly variable geographically, and the most rapid increase is currently occurring in South Asia where surface O_3 concentrations are expected to continue to rise until 2050 under all but one of the emission scenarios (Beig and Singh, 2007; IPCC, 2013a). Establishing a thorough understanding of crop and cultivar responses to O_3, and the incorporation of these responses into crop production models, is therefore needed in order to quantify the potential impact of O_3 on food supply in different world regions.

Soybean (*Glycine max.* (L.) Merr.) ranks among the most O_3-sensitive agricultural crops (Mills *et al.*, 2007). It is the fifth most significant crop in terms of global production (FAO, 2012), is a key source of vegetable protein for humans (Mateos-Aparicio *et al.*, 2008), provides approximately 30% of the world's processed vegetable oil (Graham and Vance, 2003), accounts for 77% of global nitrogen fixation by crop legumes (Herridge *et al.*, 2008) and is an important feed constituent for the livestock and aquaculture industries (Hartman *et al.*, 2011). The crop holds significant economic importance for a number of world economies including the USA, Brazil, Argentina, China and India (FAO, 2014), and world soybean demand is increasing by an average of 2.2% annually (Masuda and Goldsmith, 2009). Ozone exposure reduces the photosynthetic rate, stomatal conductance (g_{sto}), leaf chlorophyll content and leaf starch concentration of soybean (Morgan *et al.*, 2003). Ground-level O_3 pollution over agricultural land has been estimated to cause an annual reduction in soybean yield ranging between 6 - 16%, and financial losses of $2.0 – 5.8 billion annually, based on analysis of year 2000 data

conducted in two separate global crop loss assessments (Avnery *et al.*, 2011a; van Dingenen *et al.*, 2009). Soybean crop yield reduction for the year 2030 as a result of O_3 is estimated to be 9.5-15% under the optimistic (B1) scenario, or 15-19% under the pessimistic (A2) emission scenario (Avnery *et al.*, 2011b).

The magnitude of O_3 damage to soybean is dependent on the timing of exposure, with greater reductions in photosynthesis and yield being observed when exposure occurs during the reproductive stages of growth (Morgan *et al.*, 2003). Co-occurrence of seasonal peaks in O_3 surface concentrations and the flowering and pod-filling stages could therefore be particularly damaging for yield. Ozone damage occurs when the gaseous pollutant enters the leaf *via* the stomatal pores, and interacts with cell membranes and walls in the apoplast to yield reactive oxygen species (ROS) (Wilkinson *et al.*, 2012); these directly damage plant tissue through protein oxidation, leading to accelerated senescence and cell death (Fiscus *et al.*, 2005). The widely observed reduction in photosynthetic rate in response to O_3 is not fully understood, but is in part the result of a reduction in the leaf concentrations of chlorophyll and rubisco (Fiscus *et al.*, 2005; Glick *et al.*, 1995). Ozone has also been observed to reduce nodulation in a range of legume species including soybean (Reinert and Weber, 1980; Tingey and Blum, 1973; Zhao *et al.*, 2012), although this effect is largely thought to be a secondary response as a result of reduced total carbon assimilation and the diversion of assimilates away from the roots (Hewitt *et al.*, 2015).

Dose-response studies for a range of crops have revealed that O_3 sensitivity is a heritable trait (Reinert and Eason, 2000), and is highly variable among species and among cultivars (Ariyaphanphitak *et al.*, 2005; Mills *et al.*, 2007; Mills and Harmens, 2011). The maximum stomatal conductance which a species or cultivar can reach (g_{max}) is thought to play a role in determining O_3 sensitivity, because greater conductance results in greater O_3 uptake. This view is supported by the observation that wheat cultivar sensitivity to O_3 is positively correlated with g_{max} (Biswas *et al.*, 2008). Furthermore, modern wheat varieties are more sensitive to O_3 than older varieties; this may be a result of selective breeding programs targeting varieties with a higher g_{sto}, as these have a higher rate of CO_2 fixation leading to higher yields (Biswas *et al.*, 2008; Roche, 2015). The detoxification and repair capacity of a plant species or variety is also thought to be important in determining sensitivity (Fiscus *et al.*, 2005): for example, O_3 tolerance of a number of plant species has been seen to positively correlate with greater apoplastic concentrations of ascorbic acid, an antioxidant (Frei, 2015; Frei *et al.*, 2010; Frei *et al.*, 2008). A thorough understanding of how O_3 sensitivity varies among cultivars of the same species – and the factors which drive these differences – is key in improving assessments of current and future O_3-induced crop losses. Previous studies in soybean investigating inter-cultivar variation in O_3 response have typically compared a relatively small number of cultivars from the same geographical region: examples include studies of USA cultivars by Betzelberger

et al. (2010, 2012), and an investigation of Chinese cultivars by Zhang *et al.* (2014). Knowledge of which cultivars are most resistant to the effects of O_3 could potentially help plant breeders to develop O_3-tolerant soybean varieties, which, if adopted by farmers, could mitigate O_3-induced crop losses.

Much of the research relating to soybean-O_3 responses conducted to date has taken place in the USA, as part of the US National Crop Loss Assessment Network (NCLAN) programme in the 1970's and 80's (Heagle, 1989), and more recently at the University of Illinois, Urbana-Champaign and USDA Agricultural Research Service SoyFACE facility in Illinois (Betzelberger *et al.*, 2010; Betzelberger *et al.*, 2012; Gillespie *et al.*, 2012; Long *et al.*, 2005). Groups in India and China have also studied O_3 responses to soybean in recent years, but these data have, to date, not been pooled to produce dose-response relationships. Response functions for soybean used in global crop loss assessments have therefore been based on experimental data collected only in the USA. Two dose-response functions for soybean have been published: one by Lesser *et al.* (1990), synthesised from the NCLAN dataset; and one by Mills *et al.* (2007), who combined some of the NCLAN data with more recent dose-response data collected in the USA to update the function. These functions have been applied in a number of different studies in order to estimate O_3-induced soybean yield reduction globally, and the associated financial loss to farmers. Producing these estimates involves combining a dose-response function for soybean with crop distribution and yield maps, growing season dates, and modelled O_3 concentrations. The Mills *et al.* (2007) function was used by Avnery *et al.* (2011a) in their global assessment of O_3-induced soybean crop losses. The Lesser *et al.* (1990) function was used by Wang and Mauzerall (2004) in their soybean yield loss assessment for East Asia, and by van Dingenen *et al.* (2009) in their global assessment. Both functions were used by Tai *et al.* (2014) in their analysis of combined O_3 and climate change effects on future soybean production. All of these assessments applied a soybean dose-response function based on data from North America to model yield impacts in Asia. However, a comparison by Emberson *et al.* (2009) of wheat and rice dose-response data from North America and Asia has shown that Asian wheat and rice cultivars appear to be more sensitive to O_3 than their North American counterparts, possibly due to locally occurring physiological traits associated with sensitivity, such as high g_{sto} and low antioxidative capacity (Emberson *et al.*, 2009). The application of North American dose-response functions in global yield loss assessments for wheat and rice may have therefore underestimated O_3-induced yield losses in Asia.

This study synthesises all existing data in the scientific literature describing soybean yield response to O_3, in order to produce a comprehensive and up-to-date dose-response function. In doing so, we update the soybean dose-response function of Mills *et al.* (2007) with data from an additional six experiments. This study also investigates inter-cultivar differences in O_3 sensitivity, allowing the most O_3-sensitive and O_3-tolerant soybean cultivars to be identified.

Additional analysis is also conducted on the dose-response dataset, to investigate potential correlations between the degree of O_3 sensitivity observed and i) the year in which the soybean cultivar was released, to identify temporal trends in sensitivity; ii) the geographical location of the dose-response experiment, to determine if sensitivity varies geographically; and iii) the method of O_3 fumigation used in experimentation, to assess whether experimental design influences the sensitivity observed.

2.3 Materials and methods

2.3.1 Literature search:

A search of the published scientific literature was performed between October 2013 and September 2014 in order to find all O_3 exposure studies conducted on soybean. The search was conducted using the Science Citation Index Expanded® (Thomson-ISI, Philadelphia, PA, USA). The criteria for inclusion were:

- Ozone exposure concentrations must have been presented as either the seasonal 7-hour (M7), 8-hour (M8), 12-hour (M12) or 24-hour (M24) means, or as the 3-month AOT40.
- The exposure experiments must have taken place in the open air, either within open-top chambers (OTC) or using free air concentration enrichment (FACE). For experiments which included one or more additional experimental variables alongside O_3 concentration (e.g. watering regime, nitrogen concentration), only the yield data from the control treatment was used.
- The duration of O_3 exposure must have spanned at least 60% of the total growing season. Soybean takes approximately 3 months (90 days) from sowing to maturity (Pedersen and Lauer, 2004). 60% of this period is equal to 7.7 weeks, which was rounded to a minimum exposure duration of 8 weeks for the purpose of this study.
- Yield must have been measured directly, as the pod or seed weight. Response parameters such as total aboveground biomass, photosynthetic rate, percentage leaf damage or the 100-seed weight were not considered to represent the yield response.

The literature search found 28 studies that met the inclusion criteria and were included in the analysis. These studies included experiments investigating 48 cultivars, and when combined produced a dataset comprising 379 data points. A list of all the experimental studies included in this analysis can be found in Table 2.1, alongside information relating to study sites, cultivars tested and experimental design. Experiments which had used pot-grown soybean were included in the analysis; this was justified given that no significant difference in the dose-response relationships exhibited by pot-grown and field-grown soybean was found (see section 2.6.1 of the supporting information).

Table 2.1. List of experimental studies included in the analysis, with information regarding the study site, experimental design and cultivars used. OTC = Open-top chamber, FACE = Free air concentration enrichment.

Reference	Study site	Exposure type used	Method of soybean cultivation	Cultivars tested	O_3 range (M7, ppb)	Calculated theoretical yield at zero O_3	Parameter used for reporting yield
Betzelberger *et al.* (2010)	Champaign, USA	FACE	Field	A3127; Clark; Dwight; Holt; HS93-4118; IA-3010; LN97-15076; Loda; NE3399; Pana	37.9 – 82.5	5048.2 – 2785.7	Seed yield, kg/ha
Betzelberger *et al.* (2012)	Champaign, USA	FACE	Field	93B15; Dwight; HS93-4118; IA-3010; LN97-15076; Loda; Pana	38.1 - 120.6	5005.3 – 3206.3	Seed yield, kg/ha
Booker *et al.* (2005)	Raleigh, USA	OTC	Pot	Essex	26.0 – 76.0	72.7 – 33.3	Seed yield, g/plant
Bou Jaoudé *et al.* (2008)	Bari, Italy	OTC	Field	Casa	31.2 - 44.7	0.58	Seed yield, kg/m^2
Chernikova *et al.* (2000)	Beltsville, USA	OTC	Field	Forest; Essex	24.2 - 62.9	491.8 – 414.3	Seed yield, g/m^2
Fiscus *et al.* (1997)	Raleigh, USA	OTC	Pot	Essex	23.7 – 94.7	212.2 – 167.4	Seed yield, g/plant
Heagle and Letchworth (1982)	Raleigh, USA	OTC	Pot	Forest; Davis; Ransom; Bragg	26.0 – 100.0	123.6 – 67.3	Seed yield, g/plant
Heagle *et al.* (1983a)	Raleigh, USA	OTC	Field	Davis	24.5 – 124.7	468.0	Seed yield, g/m of row
(Heagle *et al.*, 1983b)	Raleigh, USA	OTC	Field	Davis	25.0 – 98.0	89.8 – 67.3	Seed yield, g/plant
Heagle *et al.* (1986)	Raleigh, USA	OTC	Field	Davis	19.0 – 92.0	560.9	Seed yield, g/m of row
Heagle *et al.* (1987)	Raleigh, USA	OTC	Field	Davis	30.0 – 107.0	529.4 – 465.0	Seed yield, g/m of row
Heagle *et al.* (1991)	Raleigh, USA	OTC	Pot	Forrest; Davis; Bragg; Ransom	25.0 – 96.8	287.2 – 158.9	Seed weight, g/pot
Heagle *et al.* (1998)	Raleigh, USA	OTC	Pot	Essex; Holladay; NK 6955	21.4 – 78.4	166.4 – 123.2	Seed yield, g/plant
Heggestad *et al.* (1985)	Beltsville, USA	OTC	Field	Williams-79; Forrest; Corsoy-79	16.0 – 51.0	8140.3 – 3765.5	Seed yield, kg/ha
Heggestad *et al.* (1988)	Beltsville, USA	OTC	Field	Williams-79; Corsoy-79	19.0 – 32.0	38.4 – 30.1	Seed yield, g/plant

Heggestad and Lesser (1990)	Beltsville, USA	OTC	Field	Williams-79; Essex; Forrest; Corsoy-79	15.0 – 99.0	5867.7 – 4441.6	Seed yield, kg/ha
Kohut *et al.* (1986)	Ithaca, USA	OTC	Field	Hodgson	17.0 - 122.0	12.8	Seed yield, g/plant
Kress and Miller (1983)	Chicago, USA	OTC	Field	Corsoy	22.0 – 115.0	3097.4	Seed yield, kg/ha
Kress *et al.* (1986)	Raleigh, USA	OTC	Field	Amsoy-71; Corsoy-79	23.0 – 92.0	6.0 – 4.8	Seed yield, g/plant
Miller *et al.* (1989)	Raleigh, USA	OTC	Field	Young	15.5 – 94.7	596.2	Seed yield, g/m
Miller *et al.* (1994)	Raleigh, USA	OTC	Pot	Essex; NK 6955; S 53-34	14.4 – 94.7	200.3 – 136.0	Seed yield, g/pot
Morgan *et al.* (2006)	Champaign, USA	FACE	Field	93B15	50.0 – 75.0	800.9 – 563.9	Seed yield, g/m^2
Mulchi *et al.* (1988)	Beltsville, USA	OTC	Field	Calland; Cumberland; Pella; Williams; Miles; Sparks; Union; Ware; Bay; Essex; Forrest; York	22.7 – 67.3	564.7 – 246.0	Seed yield, g/m^2
Mulchi *et al.* (1995)	Beltsville, USA	OTC	Field	Clark	26.0 – 72.7	253.7	Seed yield, g/m^2
Robinson and Britz (2000)	Beltsville, USA	OTC	Field	Essex; Forrest	24.0 – 58.0	28.6 – 21.4	Seed yield, g/plant
Singh *et al.* (2010)	Varanasi, India	OTC	Field	PK-472; Bragg	10.0 – 61.7	6.6 – 5.3	Pod yield, g/plant
Singh and Agrawal (2011)	Varanasi, India	OTC	Field	Pusa 9712; Pusa 9814	4.0 – 74.7	8.3 – 5.2	Seed yield, g/plant
Troiano *et al.* (1983)	Ithaca, USA	OTC	Field	Beeson	8.0 – 27.0	14.9	Seed yield, g/plant
Zhang *et al.* (2014)	Harbin, China	OTC	Pot	Hefeng25; Hefeng35; Hefeng55; Heinong35; Heinong37; Heinong65; Suinong22; Suinong26; Suinong31	19.1 – 58.6	24.3 – 15.7	Seed yield, g/plant

2.3.2 Standardisation of O_3 and yield parameters:

Dose-response data in the literature were presented using a number of different concentration metrics and yield parameters, as listed above. All O_3 concentration data had to be converted into a standard metric to enable the data to be combined for analysis. The M7 was selected to act as the common O_3 metric in the analysis, because this was most frequently reported in the literature. O_3 values presented in the form of the AOT40, M12 and M24 were converted to the M7 metric using conversion functions calculated using The ICP Vegetation database (described in Figure 2.1 legend), which contains O_3 observations measured at the same time and location but using a range of different O_3 metrics. The three different conversion functions which were used to standardise data to the M7 metric, calculated from the ICP Vegetation database, are shown in Figure 2.1. For each of the separate years and measurement stations for which there were seasonal O_3 data, the 3-month M7, M12, M24, and AOT40 were calculated for the summer season (1st May – 31st August). Concentration values represented using the different O_3 metrics were then plotted against each other, and conversion functions were derived using linear regression.

During standardisation of the reported O_3 concentrations to the M7, concentrations presented as the M8 were considered to be equivalent to the M7, as the small difference between the two was considered unlikely to add significant uncertainty to the analysis. 205 O_3 concentration values were presented in the soybean dataset using the M7 or M8 metrics and did not need to be converted. 125 and 49 data points were presented using the AOT40 and M12 metrics respectively, and were converted to M7. Not all of the studies included in the analysis used a full three month O_3 exposure; for studies which had shorter exposure durations, it was assumed that the 3-month mean would not radically differ from the mean covering a shorter duration, as O_3 exposure in all studies was artificial and therefore would not follow natural seasonal patterns in O_3 concentration. No study which had used an exposure duration of less than 8 weeks (60% of the soybean growing season) was included in the analysis. Only one study - Betzelberger *et al.* (2012) - required conversion of the AOT40 to the M7, and this study used an exposure duration of 3 months. The process of conversion to the M7 metric had the potential to introduce some error into the dataset, which was tested for during statistical analysis (section 2.3.4).

As with O_3 concentration, yield was reported in the literature using a range of different metrics, and the control O_3 concentration varied considerably between the different experiments. Yield data were therefore standardised following the method described by Fuhrer *et al.* (1997). For each separate O_3 exposure experiment, linear regression was used to determine the theoretical yield at 0 ppb O_3, expressed as the M7 metric. In a second step, the theoretical yield at 0 ppb O_3 was used as the reference (relative yield of 1) for calculating relative yields. The range of theoretical yields at 0 ppb O_3 for each study is included in Table 2.1.

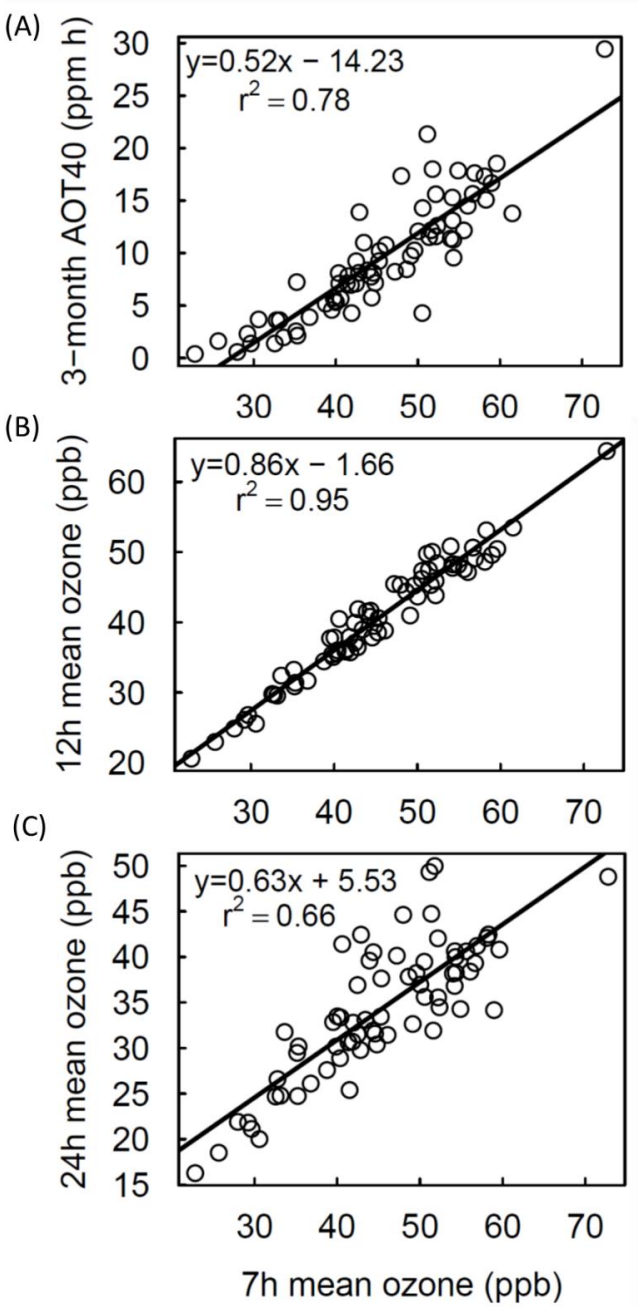

Figure 2.1. Conversion functions used to convert between (A) 3-month AOT40 and 7h mean, (B) 12h mean and 7h mean, (C) 24h mean and 7h mean O_3 concentrations. Data points represent summer season measurements of O_3 concentration at 35 stations between 2001 and 2013, recorded in the ICP Vegetation database. Measurement stations were located in Austria, Belgium, China, France, Germany, Greece, Hungary, Italy, Japan, Latvia, Poland, Portugal, Slovenia, Spain, Switzerland and the United Kingdom.

2.3.3 Derivation of species and cultivar dose-response functions*:*

All statistical analyses were carried out using R software (R Core Team, 2016). To calculate the overall dose-response function for soybean, relative yield data from all studies which met the inclusion criteria were pooled and plotted against the seasonal M7. The shape of the distribution was determined by fitting linear, quadratic and Weibull functions to the combined dose-response dataset. Goodness-of-fit of the model best-fit lines was compared by eye, and using the Akaike information criterion (AIC). The linear model was found to be the best fit to the data (AIC values for linear, quadratic and Weibull models are reported in the results section). Linear modelling was therefore chosen as the method to be used in the derivation of independent dose-response functions for individual soybean cultivars which had three or more supporting data points. A mixed model was used when deriving the overall dose-response function for soybean, and in the derivation of individual cultivar dose-response functions, with experimental study included as a random effect to account for the non-independence of data points originating from the same study. During model fitting the intercept was allowed to vary and was not forced through a relative yield value of 1. This decision was made to better allow for comparisons of the O_3 sensitivity of the different soybean cultivars based on their dose-response functions. Allowing the intercept to vary around 1 did not result in any systematic bias in the calculated slopes of the dose-response functions (see section 2.6.2 in the supporting information).

2.3.4 Analysis of the effect of cultivar release date, country of study and fumigation method on O_3 sensitivity:

Stepwise model selection was used to determine if the cultivar release date, country of data collection, and method of O_3 fumigation were important explanatory variables in the model describing the response of soybean to O_3. A fourth explanatory variable describing whether the O_3 concentration values had been reported as the M7 or had been converted was also included, to test for bias in the data introduced through standardisation to the M7 metric. A mixed-effect model structure was used to allow experimental study to act as a random effect. Model fit was assessed using Akaike's information criterion (AIC), a goodness-of-fit parameter calculated from the number of fitted parameters in a model and the maximum likelihood estimate (Symonds and Moussalli, 2011). Cultivar release dates were taken from Specht and Williams (1984), the USDA Germplasm database (USDA, 2015), and the Indian Council of Agricultural Research Oilseed report (ICAR, 2012). Data transformation of the response variable (relative yield) was carried out before analysis by taking the base-10 logarithm, to correct for non-normality observed in model residuals.

Before beginning the analysis, a diagnostic test was carried out on the dataset to test the degree of collinearity between the explanatory variables. The presence of collinearity can be a concern

in multiple regression due to difficulties differentiating the separate influence of variables that are partially correlated with each other (Belsley *et al.*, 1980). The variance inflation factor (VIF), a widely used measure of the degree collinearity of independent variables in a regression model (O'brien, 2007), was calculated for each explanatory variable (see section 2.6.3 in the supporting information). Calculated VIF values ranged from 1.1 to 6.1, falling well below the value of 10 considered to be a threshold above which it is recommended that measures are taken to counter the effects of collinearity (Mason and Perreault Jr, 1991; Smith *et al.*, 2009). The diagnostic test however reveals the presence of a certain degree of collinearity in the data, meaning that one cannot with complete certainty rank the explanatory variables in order of their relative importance. Nevertheless one is able to identify which of the candidate explanatory variables are likely to be important in describing the dose-response of soybean to O_3.

Multivariate regression analysis was step-wise and began with the simplest model (yield ~ O_3), with variables sequentially added to create a more complex model, and goodness-of-fit assessment at each step to determine if variables should be kept or removed. The order of variable addition was determined by adding each explanatory variable individually to the simplest model, to identify the single variable which gave the greatest improvement to model fit; this model was then carried forward and the process was repeated until the best model was found. A complete list of all the model configurations tested during step-wise selection is given in section 2.6.4 of the supporting information.

Candidate explanatory variables which were present in the "best" model describing the response of soybean yield to O_3 were investigated further by subsequent graph plotting and separate individual regression analyses, which also used a mixed model structure.

2.3.5 Linear regression to determine how soybean cultivar sensitivity has changed with year of cultivar release:

Soybean cultivars represented in the dataset by three or more data points (25 cultivars in total, 22 tested in USA and 3 tested in India - listed in Table 2.2) were included in a separate linear regression analysis to determine if cultivar sensitivity (represented by the slope of the dose-response function) was related to the year of cultivar release. The regression analysis was carried out twice, once on all cultivars and once excluding the cultivars from India, to ensure that any geographical differences in sensitivity were not biasing the observed relationship between sensitivity and year of release.

2.3.6 Reporting yield reductions predicted by dose-response functions:

The standardisation of reported yield data from the literature was achieved by scaling all data to yield at 0 ppb O_3. However, when reporting the yield reductions predicted by dose-response functions in the results and discussion sections of this paper, it was reasoned that it would be

more useful to express yield reductions relative to the naturally occurring background O_3 concentration. Yield reduction estimates presented in the results and discussion of this paper have therefore been calculated relative to pre-industrial O_3 levels in Europe, which are thought to have averaged around 20 ppb M24, or 23 ppb M7 (Vingarzan, 2004). The O_3 concentration used to represent present-day background levels was 55 ppb M7 – a background concentration which has been commonly exceeded in the last 20 years across different world regions (Chakraborty *et al.*, 2015; Jaffe and Ray, 2007; Wang *et al.*, 2007). Relative yield reduction at the present-day O_3 concentration relative to the pre-industrial concentration will hereafter be referred to as $RYL_{c,p}$ in this paper. A graphical representation of the method used to calculate $RYL_{c,p}$ is shown in Figure 2.2.

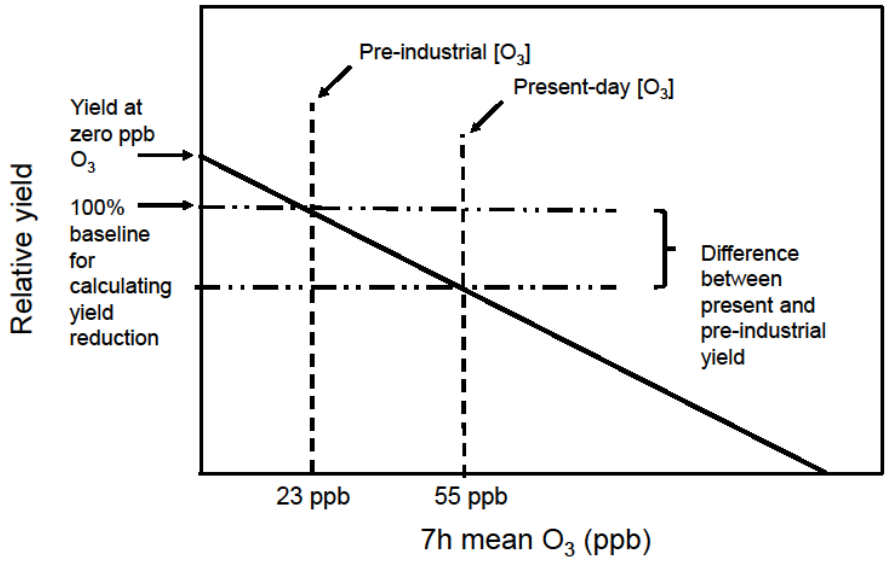

Figure 2.2. Diagram illustrating how % relative yield reduction estimates reported in the results and discussion of this paper were calculated. Pre-industrial yield, predicted by the dose-response function, was treated as the 100% baseline yield (relative yield = 1), relative to which yields at present-day O_3 concentrations were expressed.

2.4 Results

The overall yield response of soybean to O_3, combined across all cultivars, regions and exposure types, is shown in Figure 2.3A. Fitting quadratic and Weibull functions to the dataset did not improve the model goodness-of-fit, suggesting that the soybean response to O_3 was linear across the range of M7 index values examined here (linear AIC = -458, quadratic AIC = -456, Weibull AIC = -453). The combined soybean dose-response function in Figure 2.3, calculated using a mixed-effect model, estimates a $RYL_{c,p}$ of 17.3%. For comparison with earlier studies, the response function for the same dataset but using AOT40 as the O_3 metric is provided in Figure 2.3B.

Of the 49 cultivars reported in the literature, 25 had three or more data points supporting their dose-response relationship and therefore were analysed independently using linear regression. The dose-response functions for these 25 cultivars are shown in Table 2.2. 19 cultivars exhibited a statistically significant decline in yield with increasing O_3 concentration. Within those 19 cultivars, sensitivity to O_3 varied widely, with $RYL_{c,p}$ ranging from 13.3% for the least sensitive cultivar, 'Hodgson', to 37.9% for the most sensitive cultivar 'Pusa 9814'. The three most sensitive cultivars in the dataset – 'PK472', 'Pusa 9712' and 'Pusa 9814' – were from India. The most recently released USA cultivar in the dataset, 'LN97-15076' released in 2003, exhibited a $RYL_{c,p}$ of 18.8%.

The AIC values for all of the different model configurations tested in the step-wise multiple regression analysis are reported in section 2.6.4. of the supporting information. The model that performed best in describing the response of soybean to O_3 included the year of cultivar release, country of study and type of O_3 exposure as interacting variables. The AIC value for the best model shows a far greater model fit when compared to the simple model of relative yield versus O_3 concentration (delta-AIC = 42.1). It is therefore likely that the year of cultivar release, country of study, and type of exposure, all have some separate influence on the sensitivity of the response of soybean to O_3. The presence of some collinearity between the candidate explanatory variables, and the observation that many of the AIC values representing different model configurations are very similar, means that caution should be used when trying to rank the variables in order of influence. The metric conversion variable was not present in the "best" model and it is therefore likely that only minimal error was introduced to the dataset through O_3 concentration metric conversions.

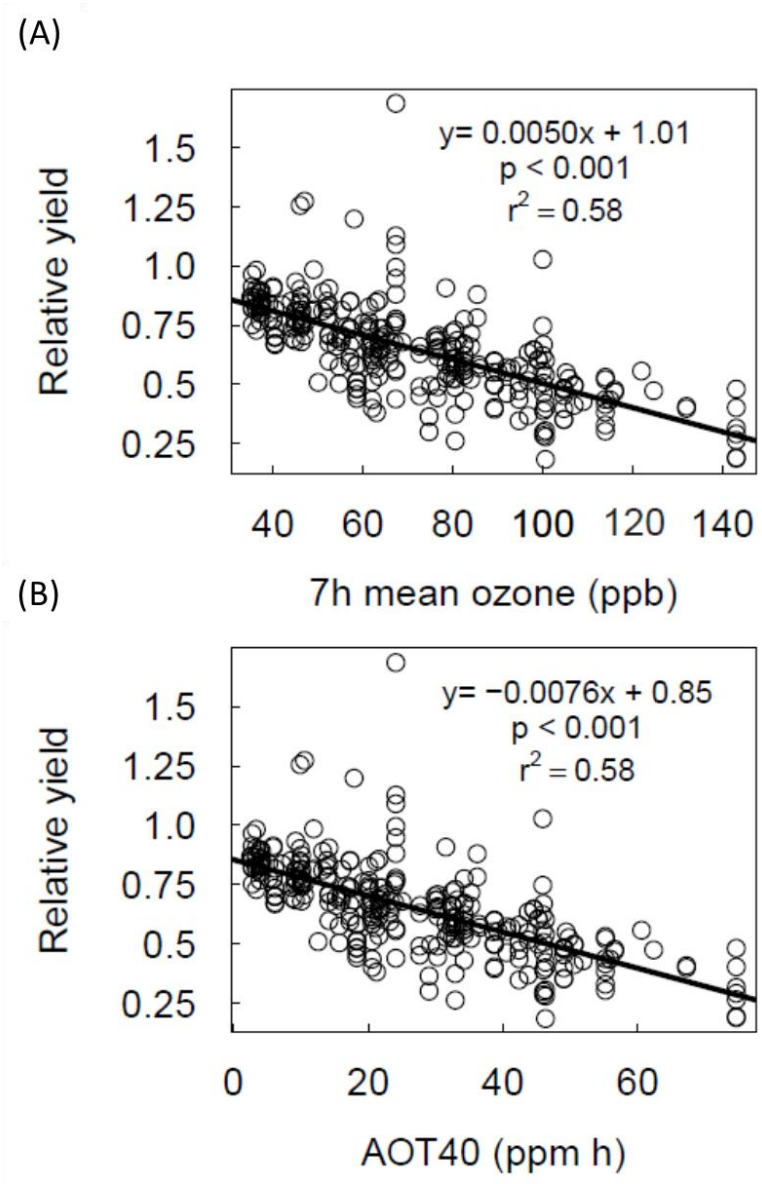

Figure 2.3. Dose-response functions for soybean and O_3, expressed using (A) 7h mean O_3 (ppb) and (B) seasonal AOT40 (ppm h). Data comprises 379 data points from 28 studies. The regression equations and p-values describing the mixed-effect models are displayed on the two plots. The r^2 values displayed on the plots are derived from simple linear regressions fitted to the same datasets; these are included here to aid in visual interpretation of model fit.

Table 2.2. Dose-response functions for individual soybean cultivars which were represented in the dataset by three or more data points. Significant p-values are highlighted in bold. Study reference, type of O_3 fumigation used, country in which data was collected, release year and growth habit (D = determinate, I = indeterminate, U = unknown) of each cultivar are also shown. Growth habit information for the soybean cultivars were derived either from the respective dose-response papers, or from the USDA Germplasm database (USDA, 2015).

Cultivar	Dose-response function	P-value	# refs	# data points	O_3 exposure type	Country of study	Year of release	Growth habit	References
93B15	Y = -0.0053x + 0.91	**<0.001**	2	22	FACE	USA	2000	I	Morgan et al (2006); Betzelberger et al (2012)
Amsoy-71	Y = -0.0046x + 0.99	**< 0.05**	1	4	OTC	USA	1972	I	Kress et al (1986)
Bragg	Y = -0.0022x + 0.97	0.21	3	7	OTC	USA and India	1964	D	Singh et al (2010); Heagle et al (1991); Heagle and Letchworth (1982)
Clark	Y = -0.0052x + 1.02	**< 0.01**	2	5	OTC and FACE	USA	1952	I	Betzelberger et al (2010); Mulchi et al (1995); Mulchi et al (1992)
NK 9655	Y = -0.0038x + 1.03	0.17	2	9	OTC	USA	1989	D	Miller et al (1994); Heagle et al (1998)
Corsoy	Y = -0.0049x + 1.00	**<0.001**	1	5	OTC	USA	1970	I	Kress and Miller (1983)
Corsoy-79	Y = -0.0052x + 1.04	**<0.001**	3	11	OTC	USA	1975	I	Kress et al (1986); Heggestad et al (1985); Heggestad et al (1988)
Davis	Y = -0.0045x + 0.99	**<0.001**	6	36	OTC	USA	1966	D	Heagle et al (1986); Heagle et al (1991); Heagle et al (1983a); Heagle and Letchworth (1982); Heagle et al (1983b) Heagle et al (1987)
Dwight	Y = -0.0049x + 1.00	**<0.001**	2	22	FACE	USA	1997	I	Betzelberger et al (2010); Betzelberger et al (2012);

Essex	Y = -0.0043x + 1.05	**<0.001**	8	36	OTC	USA	1972	D	Mulchi et al (1988); Fiscus et al (1997); Booker et al (2005); Chernikova et al (2000); Robinson and Britz (2000); Miller et al (1994); Heagle et al (1998); Heggestad and Lesser (1990)
Forrest	Y = -0.0046x + 1.02	**<0.01**	7	17	OTC	USA	1972	D	Mulchi et al (1988); Chernikova et al (2000); Heggestad et al (1985); Robinson and Britz (2000); Heagle et al (1991); Heggestad and Lesser (1990); Heagle and Letchworth (1982)
Hodgson	Y = -0.0038x + 1.00	**<0.001**	1	5	OTC	USA	1973	I	Kohut et al (1986)
Holladay	Y = -0.0054x + 0.99	0.11	1	3	OTC	USA	1993	D	Heagle et al (1998)
HS93-4118	Y = -0.0057x + 1.05	**<0.001**	2	22	FACE	USA	2000	I	Betzelberger et al (2010); Betzelberger et al (2012)
IA-3010	Y = -0.0045x + 0.97	**<0.001**	2	21	FACE	USA	1998	U	Betzelberger et al (2010); Betzelberger et al (2012)
LN97-15076	Y = -0.0054x + 1.04	**<0.001**	2	22	FACE	USA	2003	I	Betzelberger et al (2010); Betzelberger et al (2012)
Loda	Y = -0.0059x + 1.04	**<0.001**	2	23	FACE	USA	2000	I	Betzelberger et al (2010); Betzelberger et al (2012)
Pana	Y = -0.0059x + 1.03	**<0.001**	2	21	FACE	USA	1997	I	Betzelberger et al (2010); Betzelberger et al (2012)
PK472	Y = -0.0065x + 1.00	0.068	1	3	OTC	India	1986	D	Singh et al (2010)
Pusa 9712	Y = -0.0083x + 1.00	0.051	1	3	OTC	India	2005	D	Singh and Agrawal (2011)
Pusa 9814	Y = -0.0093x + 1.00	**<0.05**	1	3	OTC	India	2006	D	Singh and Agrawal (2011)

Ransom	Y = -0.0036x + 1.00	0.19	2	4	OTC	USA	1973	D	Heagle et al (1991); Heagle and Letchworth (1982)
S53-34	Y = -0.0054x + 0.96	**<0.001**	1	6	OTC	USA	1980	D	Miller et al (1994)
Williams-79	Y = -0.0047x + 1.01	**<0.001**	3	18	OTC	USA	1978	I	Heggestad et al (1985); Heggestad et al (1988); Heggestad and Lesser (1990)
Young	Y = -0.0044x + 1.00	**<0.05**	1	5	OTC	USA	1987	D	Miller et al (1989)

The effect of country of study on soybean sensitivity to O_3 was investigated further by fitting separate regression lines to the combined dose-response dataset according to country. Dose-response data from Indian and Chinese studies were seen to exhibit a steeper decline in yield with increasing O_3 concentration than the data from the USA (Figure 2.4A). The response function based on USA data alone predicts a $RYL_{c,p}$ of 16.5%, relative to pre-industrial levels. The Indian and Chinese functions predict a $RYL_{c,p}$ of 30.3% and 33.3%, respectively. The interaction between O_3 concentration and country was highly statistically significant in a separate regression analysis carried out to investigate the individual country effect ($p = 0.0015$, $F = 6.625$, d.f. = 348). There was no significant difference between the dose-response functions for India and China ($p = 0.79$ when the India-O_3 and China-O_3 interactions are compared). Their data was therefore combined to produce a more robust 'Asia' function based on more data points (Figure 2.4B).

The individual effect of exposure method on the observed sensitivity of soybean to O_3 was also investigated. Data from FACE experiments were seen to exhibit a steeper dose-response relationship than data collected in OTC's (Figure 2.5). A linear regression analysis to investigate the individual effect of exposure type found the interaction of exposure type and O_3 concentration to be of borderline statistical significance ($p = 0.048$, $F = 3.93$, d.f. = 364.17).

Figure 2.6A distinguishes the data points in the combined soybean dose-response dataset by the decade of cultivar release. Modern cultivars, represented on the plot by darker hues, tend to represent the steeper side of the dose-response distribution. A separate linear regression analysis on the 25 soybean cultivars with three or more supporting data points showed that cultivar sensitivity to O_3 has increased over time (Figure 2.6B). The regression analysis was carried out twice, once with and once without the Indian cultivars. The sensitivity-time function comprising data exclusively from the USA is the one that avoids the possibility of bias due to geographic differences in sensitivity. This function estimates that the average slope of the soybean dose-response relationship would have been -0.0040 in 1960 and -0.0053 in 2000, representing an increase in the dose-response slope of 32.5%, over a period of 40 years.

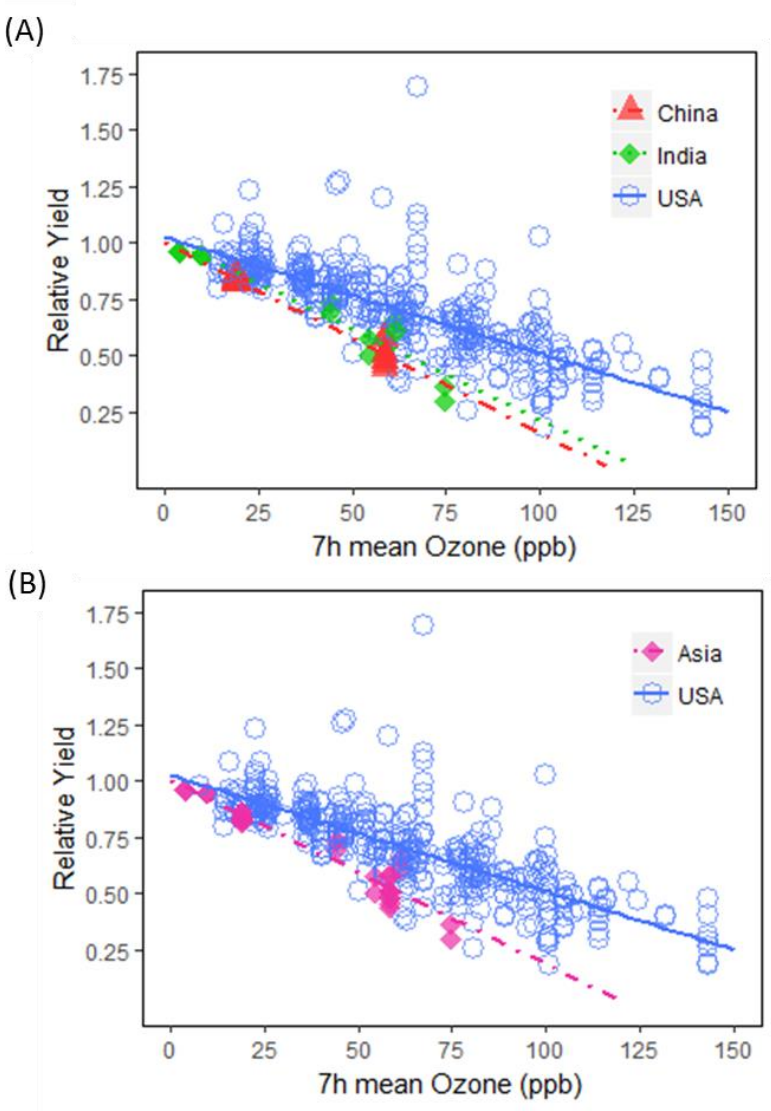

Figure 2.4. (A) Subdivision of soybean dose-response data by the country in which data collection took place, and (B) with the data for China and India combined into one dose-response function ('Asia'). Dose-response functions are: USA, y= -0.0047x + 1.020 (df=323, p<0.001). India, y= -0.0079x + 1.015 (df=9, p<0.001). China, y= -0.0084x + 1.00 (df=16, p<0.001). Asia, y= -0.0081x + 1.01 (df=26, p<0.001).

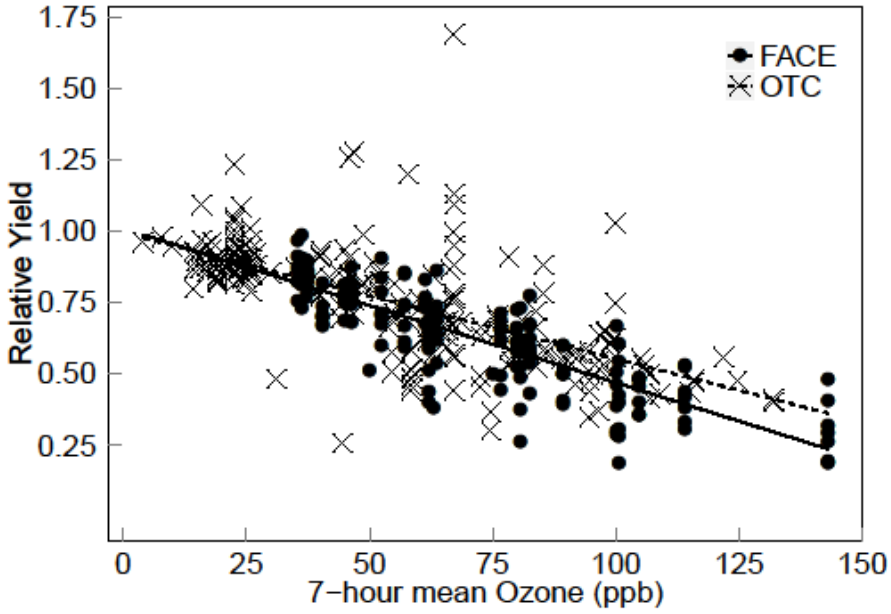

Figure 2.5. Plot showing regression lines when data is subdivided by the exposure method. Dose-response functions are: OTC, y = -0.0045x + 1.00. FACE, y = -0.0053x + 0.97.

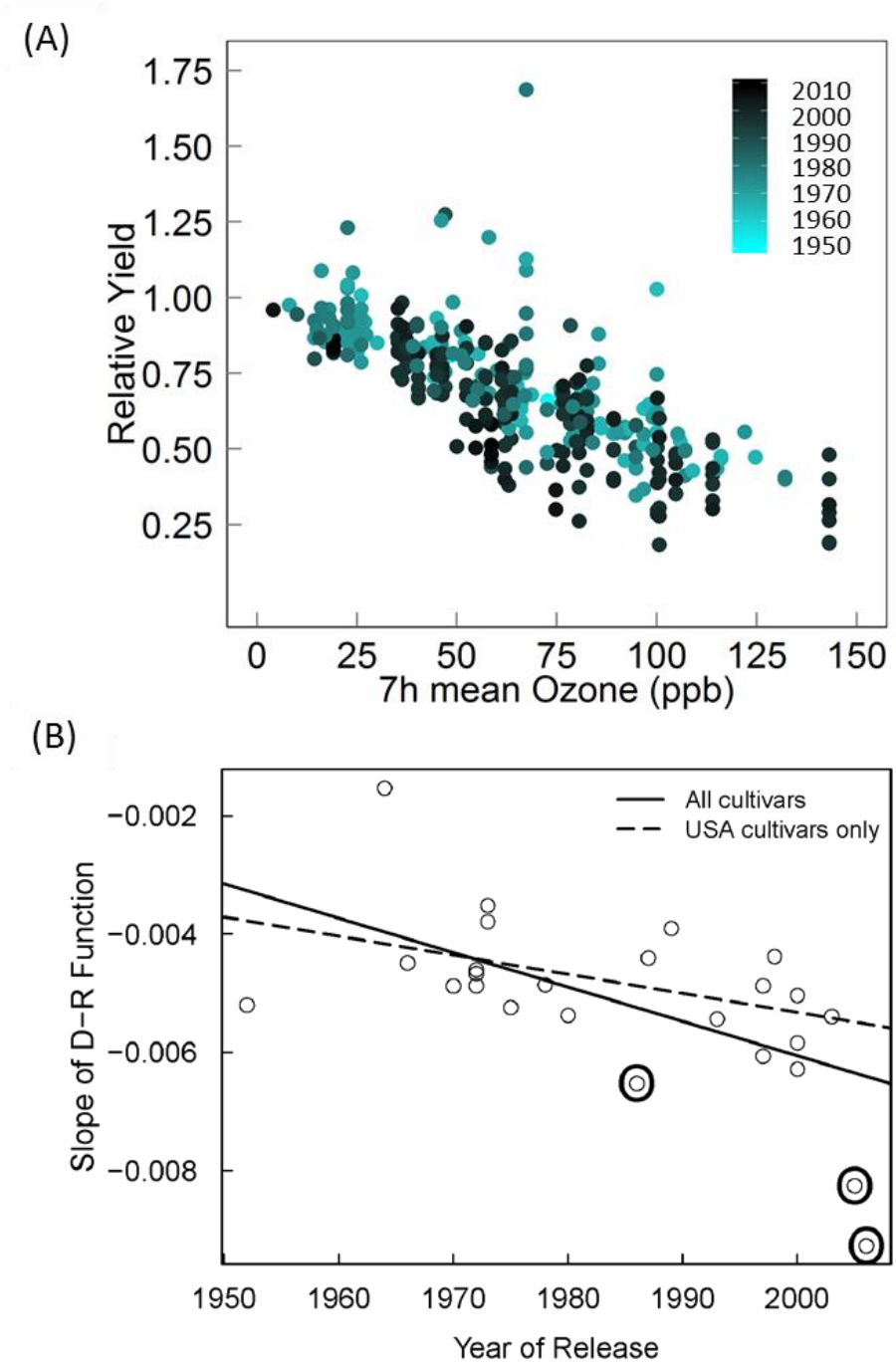

Figure 2.6. (A) Gradient plot showing the time of release of cultivars in the combined dataset. (B) Dose-response slope of 25 soybean cultivars expressed using the M7 metric, plotted against the year in which they were released to market. Two regression lines are shown; one which has been fitted to all cultivars (d.f.=23, p=0.0019, r^2=0.32), and one which has been fitted to cultivars tested in the USA only (d.f.=20, p=0.0271, r^2=0.18), excluding the data for Indian cultivars which are circled. Linear equation for all cultivars: y = -0.000058x + 0.11. USA-only linear equation: y = -0.000032x + 0.06.

2.5 Discussion

The combined dose-response function for soybean in Figure 2.3 predicts similar yield reductions at current O_3 levels as previously published functions. $RYL_{c,p}$ is estimated to be 17.2% using the function presented in this study, compared to 16.2% and 18.9% predicted by the functions of Mills *et al.* (2007) and Lesser *et al.* (1990), respectively. However, the dose-response relationship presented in this paper is linear, with 100% relative yield occurring at a theoretical background O_3 M7 value of zero. This is in contrast to the Mills *et al.* (2007) function which is based on the AOT40 metric and therefore assumes that O_3 concentrations below 40 ppb are not contributing to effects . The dose-response function for soybean published by Lesser *et al.* (1990) is in Weibull form and is therefore non-linear, although the curve is very slight and much closer to a linear model when compared to other crop dose-response functions calculated from the NCLAN experiments (Wang and Mauzerall, 2004). Both of the previously published soybean dose-response functions are based only on data from the USA, and do not include any data published after 1998. The dose-response function shown here is therefore the most comprehensive published to date, and predicts that some soybean yield reduction will occur even at low concentrations of ambient O_3, consistent with the previously published Weibull function for soybean (Lesser *et al.*, 1990)

The critical level for soybean – defined as the O_3 concentration threshold at which statistically significant yield reduction (5%) can be observed (Mills *et al.*, 2007) - is predicted using the dose-response function presented here to be 32.3 ppb M7, when calculated relative to pre-industrial O_3 levels (M7 of 23 ppb). This is in line with the 32.4 ppb M7 critical level estimated by the function of Lesser *et al.* (1990) but a lower estimate than the 40.3 ppb M7 level predicted by the function in Mills *et al.* (2007), when both are converted to the M7 metric using the conversion functions presented in Figure 2.1. The dose-response functions presented in this paper for India and China predict slightly lower critical levels of 28.3 ppb and 27.8 ppb M7, respectively.

Further analysis of cultivar sensitivity within the dose-response dataset has revealed several important trends. The first is the significant positive correlation observed between soybean cultivar sensitivity and the year of release. Based on sensitivity-time relationship calculated from the USA cultivars only, O_3-induced $RYL_{c,p}$ is estimated to be on average 14.1% for cultivars released in 1960, compared to 19.3% for cultivars released in 2000. This change in cultivar sensitivity is considered to be a conservative estimate. The sensitivity-time relationship which includes the Indian cultivars estimates a greater change in cultivar sensitivity over time, with $RYL_{c,p}$ increasing from 13.1% in 1960 to 22.6% in 2000. However, this steeper sensitivity-time function incorporating the Asian cultivars could be artificially steep if differences in sensitivity due to geographical location are also influencing the values. The trend that has been identified in cultivar sensitivity to O_3 over time is in line with the results of a number of studies

conducted for wheat, which found modern wheat cultivars to have greater O_3-sensitivity than older ones (Barnes *et al.*, 1990; Biswas *et al.*, 2008; Pleijel *et al.*, 2006; Velissariou *et al.*, 1992), although this study is to our knowledge the first evidence of this phenomenon in soybean.

The mechanism underlying this temporal trend in sensitivity is unclear, although it may be linked to varietal improvement strategies. Selective breeding across different world regions has transformed the agronomic characteristics of soybean cultivars over the last half century (Agarwal *et al.*, 2013; Jin *et al.*, 2010; Koester *et al.*, 2014; Morrison *et al.*, 2000; Rincker *et al.*, 2014). As well as having dramatically higher seed yield, modern varieties also have higher net photosynthetic rate, chlorophyll content, and transpiration rate; and have lower leaf area index and shorter maturation periods compared to older varieties (Liu *et al.*, 2012; Miladinović *et al.*, 2015). It is possible that agronomic traits which have been targeted by crop breeders are mechanistically linked to physiological traits associated with O_3 sensitivity, such as a low antioxidative capacity and high g_{max} (Biswas *et al.*, 2008; Fiscus *et al.*, 2005). For example, selection for high yield could have simultaneously targeted a high g_{max} to facilitate greater CO_2 fixation (Roche, 2015). This hypothesis is supported by results from a study on 24 soybean cultivars with release dates spanning 1923 to 2007, which observed an increase in g_{sto} with year of release in cultivars which also exhibited increasing instantaneous rates of carbon uptake with year of release (Koester *et al.*, 2014). The g_{sto} of wheat cultivars has also been reported to progressively increase with their year of release and correlates positively with O_3 sensitivity (Biswas *et al.*, 2008). Breeding for a high harvest index and rapid maturation over recent decades (Jin *et al.*, 2010; Morrison *et al.*, 2000) may have also played a role in the greater O_3 sensitivity of modern cultivars of soybean, by selecting for a trade-off which prioritises vegetative and reproductive growth over antioxidant synthesis, which could be associated with a metabolic cost under O_3 enriched conditions (Frei, 2015; Huot *et al.*, 2014).

A net increase in the yield of soybean cultivars has taken place over recent decades despite their increasing sensitivity to O_3. The heterogeneity of O_3 concentrations temporally and geographically may explain the lack of sufficient natural selection pressure for O_3 tolerance at cultivar breeding sites (Ainsworth *et al.*, 2008). Cultivar breeding programs focussing on enhancing the ability of varieties to detoxify O_3 would increase tolerance and improve yield further (Frei, 2015). Another approach for breeding O_3 tolerance would be to select for reduced g_{max} to reduce the rate of O_3 flux into the plant, and faster stomatal dynamics to allow leaves to close their stomata more rapidly in response to O_3 stress (Morgan *et al.*, 2003). While the reduction in photosynthetic gas exchange associated with excluding O_3 could result in a small yield penalty during less polluted years, cultivars with reduced g_{max} would likely perform better during years with high levels of air pollution, perhaps resulting in an average yield gain over time. A similar strategy in soybean with drought tolerant traits has shown early signs of success,

with a 50-year simulation based on US weather data showing a significant improvement in average yields, despite some of the traits being detrimental in wet years (Sinclair *et al.*, 2010).

A second important pattern identified in the data analysis relates to the observed geographical variation in O_3 sensitivity. A steeper decline in soybean yield with increasing O_3 was observed in experimental data collected in India and China, compared to data from the USA. Unfortunately, a limited amount of dose-response data was available for the Asian region: two studies from India and one from China met the inclusion criteria for analysis, with Asian cultivars comprising 12 of the 49 cultivars and 30 of the 379 data points included in the complete dataset. Despite the small number of data points representing the Asian region in the analysis, the interaction between O_3 concentration and country of data collection exhibited a high level of statistical significance in the individual regression describing the variation in soybean yield response to O_3 ($p = 0.0015$), and country of study emerged as an important variable in the step-wise multiple regression.

The greater sensitivity observed in the Asian data suggests that the use of region-specific dose-response functions could potentially improve the accuracy of modelled crop loss estimates. It also highlights the urgent need for more O_3 exposure studies in India and China, which are currently significantly underrepresented in the dose-response literature compared to the USA. Historical and contemporary O_3 trends in India and China are not well documented (Cooper *et al.*, 2014), but both countries have seen a rapid increase in emissions of O_3 precursors as a result of rapid urbanisation and industrialisation (Granier *et al.*, 2011), and are likely to experience significant increases in surface O_3 concentrations by 2050 (Fiore *et al.*, 2012). Ozone modelling in South Asia by Engardt (2008) based on emissions for the year 2000 estimated surface O_3 concentrations during the soybean growing season (September-November) to be 40-45 ppb M7 over large areas of the state of Maharashtra, which produces over 30% of India's total soybean crop (DAC, 2014). The dose-response function combined across all regions predicts relative yield reduction at this O_3 concentration to be 9.2-11.9% relative to pre-industrial levels, while the India-specific response function estimates yield reduction to be 16.2-20.9% - a large discrepancy of estimation. Over large areas of the agriculturally important Indo-Gangetic plain where soybean is also grown (Singh, 2006), modelled surface O_3 exceeds 49 ppb M7, with soybean yield reduction here estimated to be 24.8% using the Indian response function presented in this paper. Accurate estimates of potential O_3 effects on crop yield is arguably particularly important for the South Asian region, where 21% of the population are currently undernourished, an estimated 51% of soybean cropland is reported to be experiencing stagnating or declining yields (Ray *et al.*, 2012), and average soybean yield per hectare is less than half that in the USA (Panthee, 2010).

The mechanism underlying the differential sensitivity observed in North American and Asian dose-response data is unclear. Interestingly, greater O_3 sensitivity of Asian cultivars compared

to North American ones has been previously observed in wheat and rice (Emberson *et al.*, 2009). Differences between the climate and environment of the different geographical regions could be one factor driving the observed difference in sensitivity. Large areas of China and India experience a humid subtropical climate (Rubel and Kottek, 2010), which facilitates high g_{sto} and therefore high O_3 flux. Similarly, warm temperatures correlate with high g_{sto} up to a species-specific optimum temperature, above which conductance falls (Emberson *et al.*, 2000d). The co-occurrence of O_3 concentration peaks with periods of high humidity and optimum temperature - which follow seasonal and diurnal patterns specific to geographical regions – could therefore be a significant factor in determining the degree of crop loss. Unfortunately, the wide range of study locations, open-air experimental designs, and seasonal duration of experiments included in this analysis meant that humidity and temperature could not be investigated when synthesising the data.

Another important factor which must be considered when interpreting the Asia data is the possibility of interactions between O_3 and other ambient air pollutants. There is some evidence that the simultaneous or sequential occurrence of O_3 with SO_2, NO_2 and NH_3 can have a greater-than additive effect on the yield of crops (Bender and Weigel, 2011; Fangmeier and Bender, 2002). Two of the three experimental studies included in this analysis which took place in Asia added O_3 to non-filtered air, and concentrations of other ambient air pollutants were not recorded during these experiments. The potential for O_3 interactions with other pollutants means that the higher sensitivity of soybean observed in the Asian studies should be interpreted with some caution. However, all of the data points collected in Asia – including those from the experiment which added O_3 to carbon-filtered air (Singh *et al.*, 2010) and therefore removed other ambient pollutants – lie below the dose-response line fitted to USA-only data (Figure 2.10), suggesting that multi-pollutant interactions are not the sole driver of the greater sensitivity of Asian dose-response data.

As discussed earlier in relation to temporal trends, crop breeding strategies may be partly driving the observed regional differences in O_3 sensitivity. Crop breeding strategies in the USA, China and India over the last half century have shared the common aim of increasing yield and harvest index (Jin *et al.*, 2010; Karmakar and Bhatnagar, 1996; Morrison *et al.*, 2000), but other breeding targets are likely to have varied by region. For example, the high sensitivity of soybean to day-length means that maturation periods are highly tailored for different latitudes (Agarwal *et al.*, 2013). In addition, region-specific efforts to breed resistance to local diseases or pests could have increased the capacity of cultivars to upregulate antioxidants, potentially increasing their tolerance to O_3 (Bowler *et al.*, 1992).

The third key result from the data analysis is that the sensitivity of soybean cultivars to O_3 varies widely, and varieties introduced at a similar time and from the same geographic region also exhibit a certain degree of variation in sensitivity. For example, 'Corsoy-79' and 'Hodgson'

– both released in the USA in the same decade (1970s) – are predicted using the functions calculated in this study to experience a $RYL_{c,p}$ of 18.1% and 13.3% respectively, relative to pre-industrial O_3. A wide range of within-species variation in O_3 sensitivity has been observed before in other crop species. Quarrie *et al.* (2007) studied 95 wheat cultivars and observed yield reduction ranging from 0% to 56% following season-long O_3 exposure at an M7 of 91 ppb. Further evidence of differential cultivar sensitivity in wheat has come from studies on Chinese (Biswas *et al.*, 2008) and Bangladeshi (Saitanis *et al.*, 2014) varieties. A similar range of sensitivity has also been observed in Thai rice cultivars (Ariyaphanphitak *et al.*, 2005). The variation in O_3 sensitivity among cultivars observed in this study suggests that there is substantial scope for breeding O_3-tolerant soybean varieties.

The difference in the yield response observed in FACE and OTC's should be interpreted with caution, due to the marginal p-value in the individual regression ($p = 0.048$), and the presence of some collinearity. FACE data exhibited a marginally steeper dose-response slope compared to data collected in OTC's. This result indicates that both methods of exposure produce dose-response data that is comparable, and that the impact of the 'chamber effect' – the alteration of the growth environment in OTC's which can lead to heightened temperatures, altered air flow and greater vapour pressure deficit (Long *et al.*, 2005; Sanders *et al.*, 1991) – on the soybean yield response to O_3 is only small, if it exists. More work is needed in order to confirm or reject the possibility that exposure method impacts the yield response of crops in O_3 exposure studies.

In conclusion, this study has revealed a large degree of inter-cultivar variation in soybean O_3 sensitivity, and has also identified temporal and geographical patterns in sensitivity. These patterns are relevant to efforts in breeding O_3-tolerant crop cultivars, and also to those carrying out global modelling assessments of O_3 impacts on crop yield. This paper has discussed potential factors which might be playing a role in driving these patterns, but they are not yet fully understood. The derivation of flux-based dose-response relationships for soybean, which estimate O_3 exposure based on known relationships between climatic conditions and g_{sto} (Emberson *et al.*, 2000d), could shed light on the hypothesis that local climatic factors and particular physiological traits related to gas exchange are driving the observed regional and temporal patterns in sensitivity.

2.6 Supporting Information

2.6.1 Analysis of the effect of pot-grown soybean on the O_3 dose-response relationship

Of the 378 data points included in the combined analysis of soybean dose-response data, 78 points from 7 studies were derived from pot-based experiments. Mixed effect model fitting in R software was used to determine if there was a significant difference in the O_3 response of pot-grown and field-grown soybean. Study was included in the model as a random effect, to account for the non-independence of data points derived from the same study. Model goodness-of-fit

was assessed by comparing the Akaike information criterion (AIC). The model which did not include a categorical variable describing the method of soybean cultivation was the best fit to the data, showing that there was no significant effect of pot-grown soybean on the slope of the dose-response relationship (Figure 2.7). The AIC values from model fitting are reported in the legend of Figure 2.7.

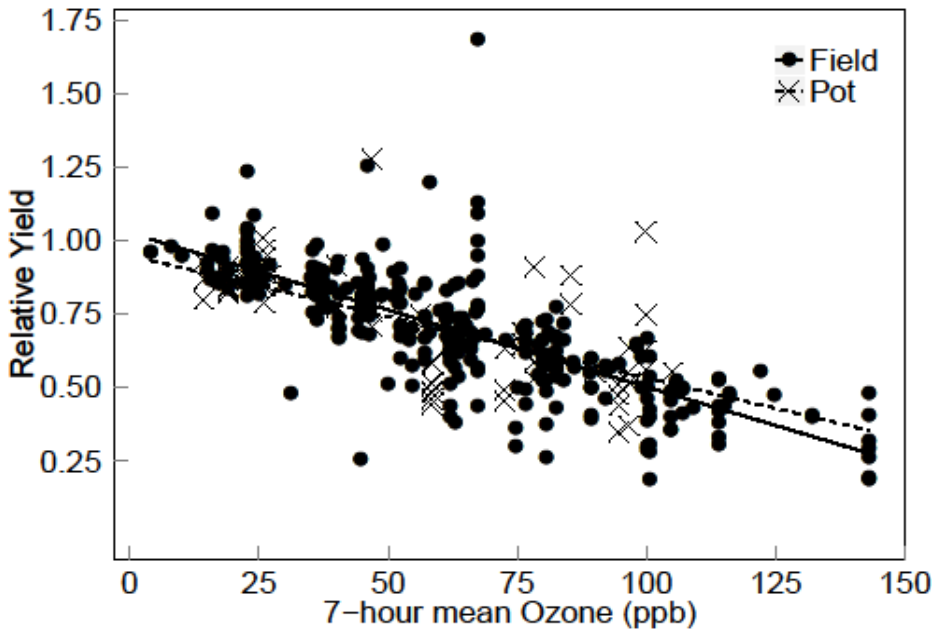

*Figure 2.7. Plot showing the whole dose-response dataset subdivided by the method of soybean cultivation, with the regression lines for each cultivation method overlain. AIC values for models fitted: Ozone only = -514, Ozone*Pot vs Field = -510, Ozone+Pot vs Field = -512.*

2.6.2 Comparison of cultivar dose-response slopes when calculated with a free intercept, and when intercept is fixed to 1:

In order to determine if the method applied in this study of deriving dose-response functions without an explicit intercept of 1 had resulted in systematic bias of the calculated dose-response slopes, individual linear regressions for the different soybean cultivars were repeated with the intercept fixed to 1. The dose-response slope values fitted using the two different methods were then plotted against each other, and linear regression was carried out in order to determine how closely the results of the two methods aligned with each other. The two datasets were significantly correlated at level $p < 0.001$, and the r-squared of the best-fit-line was 0.915. No systematic bias in estimation was visible on the regression plot, either above or below the line (Figure 2.8).

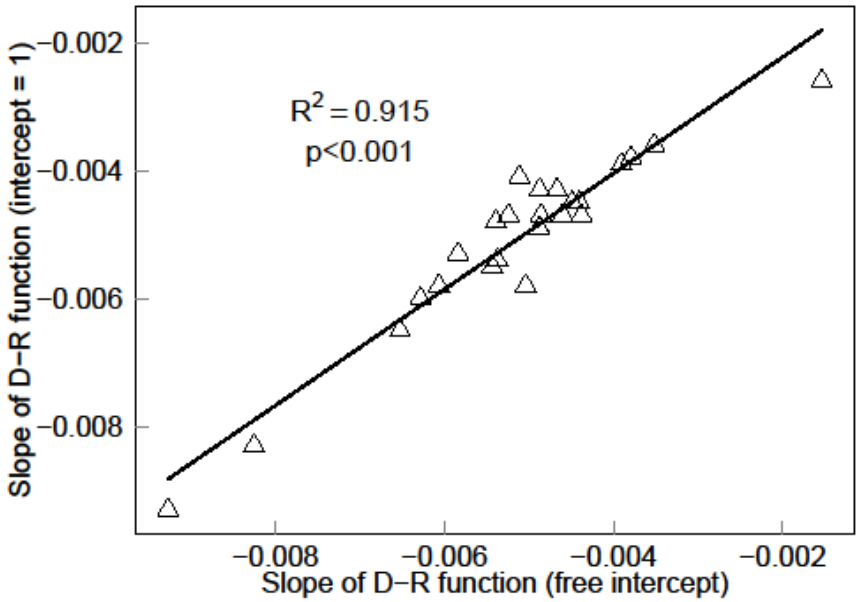

Figure 2.8. Slopes of the dose-response functions of the different soybean cultivars, calculated with and without an explicit intercept, plotted against each other. The regression line fit to the data has been overlain. The p-value and r^2 from the linear regression are displayed on the plot.

2.6.3 Diagnostic test for collinearity of variables in multiple regression

Table 2.3. Generalised variance inflation factors (VIF) for each of the five candidate explanatory variables included in the step-wise model selection analysis. The VIF measures how much variance in the estimated regression coefficients are inflated as compared to when the explanatory variables are not linearly related. VIF values were calculated using the "car" package in R software (Fox and Weisberg, 2011).

Explanatory Variable	Degrees of Freedom	Generalised variable inflation factor
Ozone concentration (M7)	1	1.1175
Country of study	2	2.0902
Fumigation type	1	6.0805
Year of release	1	4.3277
Metric conversion variable	2	3.7917

2.6.4 Model configurations tested during step-wise model selection

Table 2.4. Table showing complete list of all the model configurations tested during step-wise model selection. More negative AIC values indicate better model fit, and a delta-AIC of 1 or more signifies a significant difference in model fit. The symbol "" in the table denotes that a factor is able to interact (i.e. vary both the slope and the position of the intercept of the regression model). Variables in model configurations are referred to as: RY = relative yield, Metric = metric conversion factor, Year = year of cultivar release, Country = country in which data collection took place, Exp = Type of O_3 exposure used. Model selection began with the simplest model (model 1), and each of the candidate explanatory variables was then added in turn to identify which single variable improved model fit by the greatest amount. This model was then carried forward and the process was repeated until the best model was found. The model with the "best" fit to the data (model 17) is highlighted in bold.*

Model number	Num. of explanatory variables in model	Change from previous model	Model configuration	Model AIC
1	1	Simplest model	RY ~ M7	-800.96
2	2	metric variable added (main effect)	RY ~ M7 + Metric	-797.58
3	2	metric variable added (interaction)	RY ~ (M7*Metric)	-817.49
4	2	Year variable added (main effect)	RY ~ M7 + Year	-805.19
5	2	Year variable added (interaction)	RY ~ (M7*Year)	-832.10
6	2	Country variable added (main effect)	RY ~ M7 + Country	-810.73
7	2	Country variable added (interaction)	RY ~ (M7*Country)	-816.48
8	2	Exposure type variable added (main effect)	RY ~ M7 + Exp	-801.31
9	2	Exposure type variable added (interaction)	RY ~ (M7*Exp)	-821.62
10	3	metric variable added (main effect)	RY ~ (M7*Year) + Metric	-828.33

11	3	metric variable added (interaction)	RY ~ (M7*Year) + (M7*Metric)	-825.33
12	3	Country variable added (main effect)	RY ~ (M7*Year) + Country	-840.05
13	3	Country variable added (interaction)	RY ~ (M7*Year) + (M7*Country)	-841.69
14	3	Exposure type variable added (main effect)	RY ~ (M7*Year) + Exp	-830.17
15	3	Exposure type variable added (interaction)	RY ~ (M7*Year) + (M7*Exp)	-828.50
16	4	Exposure type variable added (main effect)	RY ~ (M7*Year) + (M7*Country) + Exp	-841.54
17	**4**	**Exposure type variable added (interaction)**	**RY ~ (M7*Year) + (M7*Country) + (M7*Exp)**	**-843.06**
18	4	Metric variable added (main effect)	RY ~ (M7*Year) + (M7*Country) + Metric	-838.22
19	4	Metric variable added (interaction)	RY ~ (M7*Year) + (M7*Country) + (M7*Metric)	-838.60
20	5	Metric variable added (main effect)	RY ~ (M7*Year) + (M7*Country) + (M7*Exp) + Metric	-839.906
21	5	Metric variable added (interaction)	RY ~ (M7*Year) + (M7*Country) + (M7*Exp) + (M7*Metric)	-837.8161

2.6.5 Comparison of data originally reported as different O_3 metrics

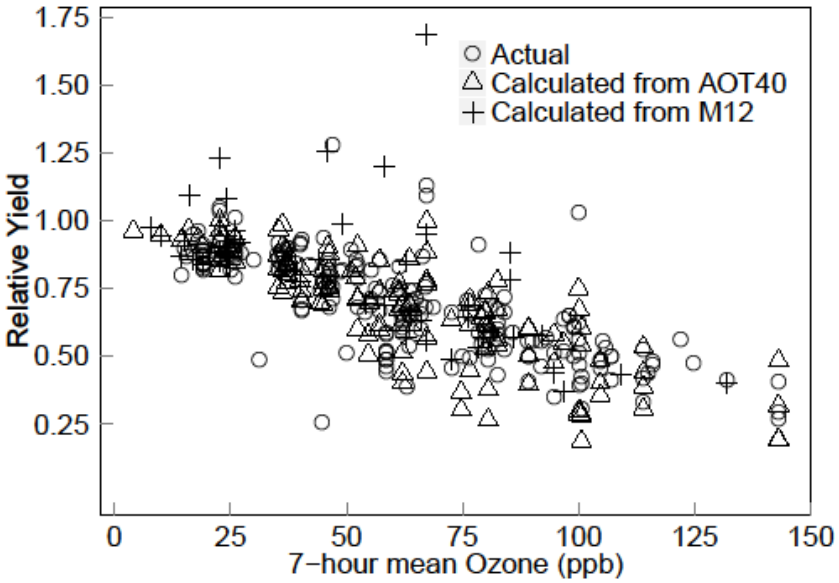

*Figure 2.9. Plot showing all data points used in the analysis, symbol-coded to show values which were reported in experimental studies as the M7 or M8 ('Actual'); values which had to be converted to M7 from M12 ('Calculated from M12'); and values which had to be converted to M7 from AOT40 ('Calculated from AOT40'). AIC values for models fitted: Ozone only = -521, Ozone*metric factor = -517, Ozone+metric factor = -517.*

2.6.6 Dose-response data points from Asian studies compared to USA-only dose-response data regression line

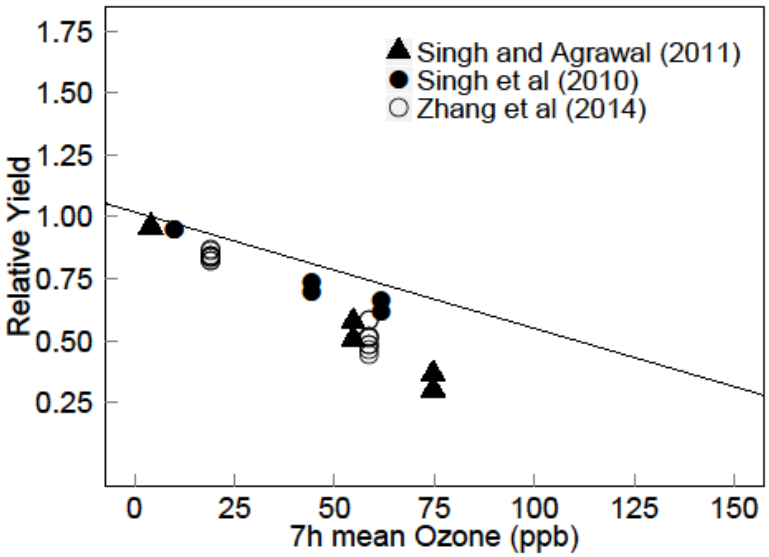

Figure 2.10. Plot showing all dose-response data points collected in experimental studies which took place in Asia. The study by Singh et al (2010) added O_3 to carbon-filtered air; the other two studies added O_3 to ambient air. All of the data points collected in Asia lie below the dose-response line representing exclusively US soybean data, represented on the plot by the straight black line.

3 Using stomatal flux modelling to investigate ozone-drought interactions in wheat (*Triticum aestivum* L.)

3.1 Abstract

Wheat provides 20% of calories consumed worldwide, and is sensitive to yield reduction from ground level ozone (O_3) pollution. The question of how O_3 exposure and drought interact to influence crop yield is unresolved in the O_3 effects community, with some reports that drought can protect against O_3, and other reports of greater-than additive damage when the two stresses co-occur. In this study a modern cultivar of European wheat (*Triticum aestivum* L., cv. 'Mulika') was exposed to precision-controlled O_3 in hemispherical glass domes for three months. Plants were either well-watered or subjected to an early-season or late-season 10-day drought event. Ozone treatments ranged from a 24-hour mean of 27 to 57 ppb, and varied in the profile of exposure with some treatments characterised by daily peaks in concentration, and others characterised by a consistent background level. Ozone flux to the flag leaf was modelled using a bespoke parameterisation of the DO$_3$SE stomatal conductance (g_{sto}) model, allowing comparison of O_3 uptake during drought and non-drought periods. Ozone exposure resulted in significant yield reduction (-32.9% in highest O_3 treatment relative to lowest). Early-season and late-season drought stress resulted in an equivalent degree of yield loss (-14.1% on average across all O_3 treatments in early-drought plants, -13.8% in late-drought plants). Model output indicated that early-season drought limited g_{sto} and total O_3 uptake substantially more than late-season drought. However, positive effects of reduced O_3 uptake due to drought were far outweighed by negative impacts of drought on final yield. Ozone therefore did not protect against drought in this experiment. The results also show no evidence of additional O_3-drought interactions taking place that are not explained by stomatal behaviour. The flux-based approach to calculating O_3 exposure is therefore likely to account for O_3-drought interactions in O_3 risk assessments for European wheat.

3.2 Introduction

Agricultural production in the 21st century must feed a growing global population (FAO, 2012) amid a changing climate (IPCC, 2014b). High surface concentrations of the phytotoxin ozone (O_3) are widely accepted as being a significant threat to agricultural yield (Long *et al.*, 2005). Ground-level O_3 concentrations have approximately doubled globally since the 1950's (Vingarzan, 2004), driven by anthropogenic emissions of hydrocarbons and nitrogen oxides which react photochemically to form O_3 (Derwent *et al.*, 2003). Future O_3 projections differ between geographical regions and will depend on future emission pathways (IPCC, 2013a; Lei *et al.*, 2012). In South Asia, surface O_3 concentrations are expected to increase until 2050 in all except the RCP6.0 scenario, with mean concentrations for 2050 expected to range from 39 – 45 ppb (IPCC, 2013a). Peak O_3 'episodes' – short periods of acute surface O_3 concentration, typically 100 ppb or above – are also expected to become more frequent in the South Asia region (Lei *et al.*, 2012). In North America and Europe O_3 concentrations are likely to remain stable or decline, with a reduction in the frequency of peak episodes and a mean surface concentration in the range of 34-42 ppb projected for 2050 (Paoletti *et al.*, 2014). Conditions favouring O_3 formation – namely hot, dry and stable weather – are also associated with drought events, which are projected to become more frequent with global climate change (Dai, 2011; IPCC, 2014b). Co-occurrence of drought and O_3 is therefore likely to become increasingly common in the coming decades. Understanding how O_3 and drought act separately and in combination to influence yield is therefore necessary in order to estimate the crop response to future changes in air quality and climate.

Wheat is the world's most widely grown cereal, comprising approximately 20% of global calorie and protein consumption by humans (Shiferaw *et al.*, 2013). It is also one of the most sensitive of the staple crops to O_3-induced yield reduction (Mills *et al.*, 2007). A comprehensive picture of wheat response to O_3 has been established over the previous four decades due to experiments conducted as part of the European open-top chamber network (EOTCN) (Finnan *et al.*, 1997), the National crop loss assessment network (NCLAN) in the USA (Heagle, 1989; Lesser *et al.*, 1990), and numerous more recent studies (Biswas and Jiang, 2011; Biswas *et al.*, 2008; Burkart *et al.*, 2013; Danielsson *et al.*, 2003; Saitanis *et al.*, 2014). The majority of O_3 damage occurs following entry through stomata, where it can react with cell walls or membranes, or break down to produce reactive oxygen species (ROS) (Fiscus *et al.*, 2005). This oxidative stress eventually leads to accelerated senescence, damage to photosynthetic machinery, and foliar lesions (Fiscus *et al.*, 2005; Krupa *et al.*, 2001). A recent study estimated global wheat yield losses based on modelled O_3 (MOZART-2 model) as ranging from 4 - 15% in the year 2000, with projected losses for 2030 ranging from 6 - 26% under the A2 emission scenario (Avnery *et al.*, 2011a, b).

The physiological effects of drought in wheat bears some similarity to O_3 effects, as both stresses induce oxidative stress and influence stomatal behaviour (Matyssek *et al.*, 2006). Blum (1996) describes how a crop plant experiencing water withdrawal undergoes three phases of response. In the first phase transpiration and assimilation proceed normally, with the plant meeting evapotranspiration demand by reducing leaf water potential through osmotic regulation; this can cause reduced cell expansion and division, and death of apical leaf parts before there is an effect on stomatal conductance (g_{sto}). In phase two transpiration and assimilation are reduced below the potential level, and in phase three stomata are fully closed (Blum, 1996). Under drought stress, ROS can be generated if thermal dissipation and use of light in photosynthesis or photorespiration is not sufficient to cope with excess energy in the leaf (Chaves *et al.*, 2003). As a result, enhanced activity of antioxidant enzymes is a common response to drought (Chaves *et al.*, 2003) – a response which is also seen in some plants following O_3 exposure in response to O_3-induced ROS (Rao *et al.*, 1995; Rao *et al.*, 1996). This has led to suggestions that co-occurring drought stress may influence the response to O_3 stress or *vice versa*, either in a protective way – with heightened antioxidant activity from acclimation to one stress 'hardening' against the other – or in negative way, if the oxidative stress induced by one exceeds the ability to react to both stresses (Matyssek *et al.*, 2006). Observations that drought enhances O_3 damage in birch (Pääkkönen *et al.*, 1998), and that O_3 exposure reduces the ability of Aleppo pine to withstand drought stress (Alonso *et al.*, 2001) support the latter hypothesis. Unfortunately, evidence relating to non-stomatal O_3-drought interactions largely comes from studies in trees (Chappelka and Freer-Smith, 1995; Matyssek *et al.*, 2006), with relatively little evidence from crops.

Interactions between drought and O_3 stress mediated by stomatal behaviour has been more widely studied in crop species, but the experimental evidence has created a contradictory picture. Drought stress induces stomatal closure, and should theoretically be able to ameliorate O_3 impacts by reducing flux through stomata (Fiscus *et al.*, 1997). In experiments with wheat, drought-mediated protection from O_3 has been reported by some authors (Biswas and Jiang, 2011; Khan and Soja, 2003), but other experiments have failed to show this effect (Biswas and Jiang, 2011; Fangmeier *et al.*, 1994a; Fangmeier *et al.*, 1994b). In addition, O_3 has been observed to impair stomatal closure during drought stress in two grassland species, suggesting that the physiological response of plants to drought stress may not function as expected in the presence of O_3 (Mills *et al.*, 2009); however, this effect has not yet been observed in a crop species. More experimental evidence relating to crop species under combined O_3 and drought stress is needed in order to develop the level of understanding required to predict the yield outcome when O_3 and drought co-occur.

In this study a flux modelling approach is applied to a combined O_3-drought exposure experiment in European wheat, in order to compare O_3 uptake through stomata under drought

and non-drought conditions. Flux modelling for estimating O_3 dose has been applied by the Convention on Long-Range Transboundary Air Pollution (CLRTAP) since 2004, in its work developing methods for mapping O_3 impacts on vegetation under current and future concentrations to inform air pollution policy (CLRTAP, 2017; Fuhrer *et al.*, 1997). The flux approach is based on the principle that plant response to O_3 is more closely related to instantaneous stomatal flux of O_3 than to the ambient concentration (Emberson *et al.*, 2000d). Flux is a product of the leaf-level O_3 concentration and the instantaneous g_{sto}, which responds to environmental variation (Jarvis, 1976) and plant phenology (Uddling and Pleijel, 2006). The Deposition of Ozone for Stomatal Exchange (DO_3SE) model has been developed over the last 15 years, based on the multiplicative method of modelling g_{sto} developed by Jarvis (1976), to calculate seasonal O_3 flux to leaves as a function of O_3 concentration, meteorology, phenology and soil water potential (SWP) (Büker *et al.*, 2012; Emberson *et al.*, 2000d). The calculation of O_3 flux within exposure experiments enables the construction of flux-response relationships, which take into account the effect of soil moisture – and hence, drought – on the in-leaf O_3 dose. Comparison of flux-response functions under different drought treatments therefore provides some indication of whether additional interactions between O_3 and drought – not explained by stomatal behaviour – are likely to be taking place (e.g. parallel flux-response functions under different drought regimes indicates that drought-induced stomatal closure is the only key interaction mechanism).

This study combines experimental measurements with flux modelling, in order to i) assess the separate effects of O_3 exposure, early drought, and late drought on development and yield of a modern wheat cultivar; ii) compare the effect of early-season and late-season drought on the amount of O_3 taken up into leaves; and iii) test whether O_3 stress interacts with drought stress – either in a positive or negative way - by comparing flux-yield relationships for different drought treatments.

3.3 Materials and Methods

3.3.1 Experimental facility and treatments

The O_3 exposure experiment was conducted during March-August 2015 at the Centre for Ecology and Hydrology (CEH) air pollution facility in Abergwyngregyn, North Wales (53.2°N, 4.0°W). Wheat seeds (*Triticum aestivum* L., cv. Mulika) were planted in 25-litre rectangular containers (height = 40cm, width = 35cm, length = 38cm) filled with John Innes No.3 compost in late March. Seeds were sown in rows 7cm apart with 40 seeds per container, resulting in a seedling density of approximately 260 seedlings per m^2, which aligns with the recommended field seedling density (AHDB, 2015). Four containers per O_3 treatment were planted, resulting in a canopy of ~144 seedling per treatment. Containers were inoculated with soil microbial communities from a nearby wheat field using a soil slurry applied shortly after sowing. Ozone exposure in eight ventilated hemispherical glasshouses known as 'solardomes', described previously (Hayes *et al.*, 2015; Mills *et al.*, 2009), began on the 15th of May and lasted for 82 days. Air entering solardomes was carbon-filtered to remove ambient O_3, before a precision-controlled quantity was added. Ozone was supplied by an O_3 generator (Dryden Aqua G11, Edinburgh, UK) and injection concentrations were regulated by a computer-controlled O_3 injection system (Lab VIEW, version 8.6, National Instruments, Texas, US). Solardomes were ventilated at two air changes per minute, and O_3 concentration within all domes was monitored on a 30-minute cycle using two O_3 analysers of matched calibration (Envirotech API 400A, St Albans, UK).

The eight O_3 concentrations varied from a 24-hour mean of 27 ppb in the lowest treatment to 57 ppb in the highest, spanning a range including contemporary concentrations in Europe (Cooper *et al.*, 2014; Paoletti *et al.*, 2014), and future projected concentrations in South and East Asia (IPCC, 2013a). The O_3 treatments applied in this experiment are presented in Figure 3.1. Treatments varied in their exposure pattern, with four treatments characterised by high daily peaks (36-115 ppb) and low night-time concentrations (28-32 ppb) – classified as 'peak profile' treatments – and the other four characterised by a consistent, moderate background concentration (25-59 ppb) and small daily peaks (32-65 ppb) – classified as 'background profile' treatments. Treatment profiles followed a weekly cycle, with five 'full treatment days' and two 'low treatment' days per week. Although each O_3 treatment was not replicated in this experiment, the use of eight different O_3 treatments enables the construction of exposure-response relationships, and numerous studies published previously have demonstrated the statistical validity of un-replicated experiments at the solardome facility (Hayes *et al.*, 2012; Hewitt *et al.*, 2014; Mills *et al.*, 2009). Previous work has shown that no significant difference in air or leaf temperature is detectable between the different solardomes (Hewitt *et al.*, 2016), but as an additional precaution treatments were allocated at random to the different solardomes.

Potential impacts of pseudoreplication on the output of the statistical analysis was countered through the use of mixed models, described in more detail in section 3.3.5.

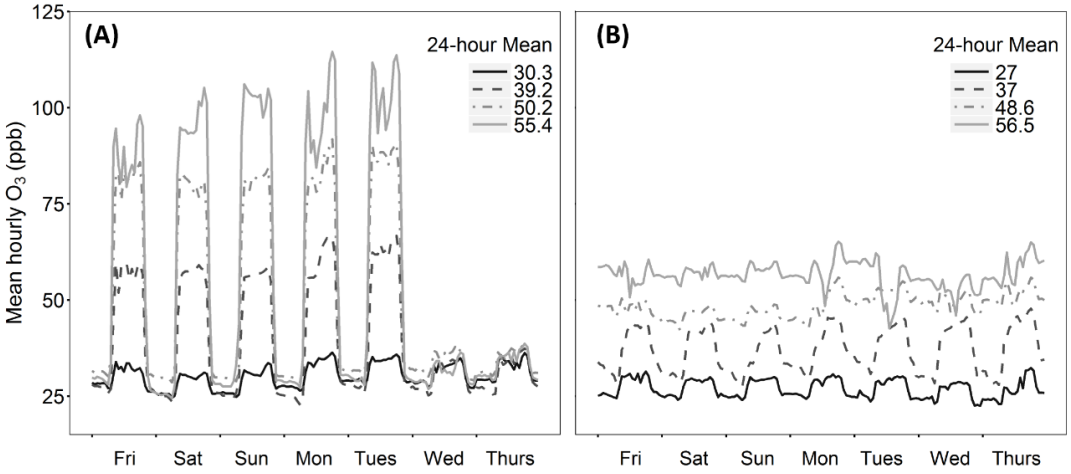

Figure 3.1. Weekly O_3 exposure profiles for (A) the four 'peak profile' treatments, and (B) the four 'background profile' treatments applied in the 2015 experiment. The seasonal 24-hour mean O_3 concentration (ppb) calculated for each treatment is provided in the figure keys.

During the experiment, wheat plants were subjected to one of three watering regimes: i) well-watered, ii) early-season drought, or iii) late-season drought. Drought events comprised 10 days of watering withdrawal, with a small amount of watering half-way through each drought to prevent plant death. Early drought was applied pre-anthesis during booting and flag leaf sheath extension (growth stages 40 to 46), while late drought was applied post-anthesis during late milk and early dough development (growth stages 78 to 84). Soil water content (SWC %) was measured continuously using soil moisture probes (ML2 ThetaProbe, Delta-T, Cambridge, UK) connected to a DL2 data logger (Delta-T, Cambridge, UK), inserted to a depth of 10cm in the three watering treatments. Hourly air temperature, photosynthetically active radiation (PAR) and relative humidity – required as input data for stomatal flux modelling – were monitored in one solardome using an automatic weather station (Skye Instruments Ltd, Llandridod Wells, UK). Fungicide was applied once ("Unix", Cyprodnil, 1.6 kg/ha) before the beginning of O_3 exposure to treat powdery mildew. Insecticide was applied three times (pyrethrum, 1ml/litre) throughout the growing season to treat aphids. Fertiliser was applied once in the mid-season (ammonium nitrate, total product rate equivalent to 80kg/ha).

3.3.2 Measurements of growth stage development, leaf chlorophyll and g_{sto}

Growth stage assessments based on the Tottman (1987) system were conducted on four days distributed across the growing season (9th June, 30th June, 14th July, 27th July). During each

growth stage assessment, four non-edge wheat plants were selected at random from each of the four containers within each O_3 treatment, and their decimal growth stage was recorded; the mean decimal growth stage for that day was then calculated for each O_3 treatment.

Leaf chlorophyll content was measured non-destructively as an index (chlorophyll content index or CCI) using CCM-200 and CCM-200+ instruments (Opti-sciences, Hudson, USA). A regression line fit to paired measurements was used to standardise observations made using the two instruments. 523 CCI measurements were made on 28 separate days ranging from early May to late July. Measurements were made in the most recent fully expanded leaf (represented by the flag leaf from the 28th May onwards) of randomly selected non-edge plants.

A total of 318 measurements of g_{sto} were gathered across 9 days spanning the 27th of May to the 22nd of July; as with CCI, g_{sto} was measured on randomly selected non-edge plants, in the most recently fully expanded leaf (represented by the flag leaf from the 28th of May onwards), during physiologically active daytime hours (10am-4pm). g_{sto} was measured using an AP4 leaf porometer (Delta-T, Cambridge, UK), and measurements were paired with simultaneous measurements of SWC (ML2 Thetaprobe, Cambridge, UK) and CCI. Measurements were intentionally made across a range of meteorological conditions to allow for model parameterisation at a later stage.

3.3.3 Biomass and yield measurements

Harvest was conducted in early August, when wheat plants in all O_3 treatments were considered to be fully mature. All non-edge plants from each container were harvested. Ears were threshed and grains were weighed. The weight of 100 grains per container was also measured, to determine the 100-grain weight in each O_3 treatment. Relative yield reduction in each O_3 treatment was calculated using the method described by Fuhrer *et al.* (1997): absolute yield per O_3 treatment was divided by the y-axis intercept of the regression line of absolute yield versus O_3 exposure.

3.3.4 Ozone flux modelling using bespoke parameterisation of DO$_3$SE model

A bespoke parameterisation of the DO$_3$SE g_{sto} model (Emberson *et al.*, 2000d) was used to calculate O_3 flux for each of the O_3 and watering treatment combinations. DO$_3$SE uses a multiplicative approach (Jarvis, 1976) to estimate hourly g_{sto} to O_3 over a projected leaf area (PLA) using the following algorithm, which modifies an empirically derived species or cultivar-specific maximum g_{sto} value (g_{max}) according to the concurrent environment:

$$g_{sto\_O3} = g_{max} * [\min(f_{phen}, f_{O3})] * f_{light} * \max\{f_{min}, (f_{temp} * f_{VPD} * f_{SWP})$$

where g_{sto_O3} represents g_{sto} to O_3 (mmol O_3 m^{-2} PLA, s^{-1}); g_{max} is the maximum g_{sto_O3}; f_{phen}, f_{O3}, f_{light}, f_{temp}, f_{VPD} and f_{SWP} represent the influence of phenology, O_3, photosynthetically active radiation (PAR), air temperature, vapour pressure deficit (VPD) and soil water potential on g_{max},

respectively; and f_{min} represents the minimum g_{sto}. A detailed description of how the parameters relating to each of the DO_3SE *f*-functions are derived can be found in CLRTAP (2017).

The hourly mean instantaneous stomatal flux of O_3, F_{st} (nmol m^{-2} PLA s^{-1}), is calculated in the model following the assumption that the O_3 concentration at the top of the canopy represents a reasonable estimate of the concentration at the upper surface of the laminar layer of the flag leaf. F_{st} is calculated using the following equation:

$$F_{st} = c(z_i) * g_{sto\_O3} * r_c/(r_b + r_c)$$

Where $c(z_i)$ is the concentration of O_3 at the top of the canopy of height *i* (m), and r_c and r_b represent leaf surface and quasi-laminar resistances, respectively. Equations used to derive r_c and r_b based on leaf dimension and prevailing wind speed are described in detail in CLRTAP (2017). Calculated hourly values of F_{st} are then accumulated over a species or cultivar-specific accumulation period according to the following equation:

$$POD_YSPEC = \Sigma[(F_{st} - Y) * (3600/10^6)$$

Where POD_YSPEC (previously known as POD_Y) represents the species-specific 'phytotoxic ozone dose' above the threshold flux value of *Y* (mmol m^{-2} PLA), and the term $(3600/10^6)$ converts to hourly fluxes and to mmol m^{-2} PLA. The threshold value *Y* can be varied to account for the ability of plants to detoxify a certain amount of O_3 entering through stomata. A *Y* value of six was applied when calculating the POD_6SPEC, as previous analysis carried out on data from 13 separate wheat exposure experiments found that a threshold flux of six produced the closest correlation between O_3 flux and yield (Pleijel *et al.*, 2007). This threshold has since routinely been used in studies which have applied the DO_3SE model to wheat (González-Fernández *et al.*, 2013; Klingberg *et al.*, 2011), and in pan-European risk assessments of wheat yield loss due to O_3 (CLRTAP, 2017).

A parameterisation of DO_3SE for European wheat, derived from a pooled dataset comprising multiple experiments and cultivars, has been published previously (CLRTAP, 2017; Grünhage *et al.*, 2012). The g_{sto} dataset for 'Mulika' gathered in this experiment allowed us to modify this parameterisation for cultivar specificity. The bespoke parameterisation applied i) an empirically derived, cultivar-specific value of g_{max}; ii) a cultivar-specific flux accumulation period, defined by the recorded dates for flag leaf emergence, mid-anthesis and leaf senescence observed in the experiment; and iii) cultivar-specific parameters for the f_{SWP} and f_{O3} functions within the DO_3SE algorithm, derived using the dataset of measured g_{sto} values for Mulika. All other model parameters were unchanged from the CLRTAP (2017) parameterisation. Parameters applied in the bespoke parameterisation for Mulika are reported in Table 3.1, alongside the published CLRTAP (2017) parameters for European wheat.

Table 3.1. Multiplicative DO$_3$SE parameter values and definitions for i) CLRTAP (2017) wheat parameterisation, and ii) the bespoke 'Mulika' parameterisation applied in this study. Effects of soil water on g_{sto} are modelled in the CLRTAP (2017) parameterisation using f_{PAW} (i.e. based on the empirical relationship between g_{sto} and plant available water), and in the bespoke parameterisation using f_{SWP} (i.e. based on the empirical relationship between g_{sto} and soil water potential).

Function	Parameter	Units	Parameter description	CLRTAP (2017)	Bespoke, 'Mulika'
g_{max}	g_{max}	mmol O_3 m^{-2} PLA s^{-1}	maximum rate of g_{sto_O3}	500	383
f_{min}	f_{min}	Fraction	Fraction of g_{max} at minimum g_{sto_O3}	0.01	0.01
f_{phen}	*SGS*	DOY	Plant emergence	70°C days following sowing date, which is estimated based on climatic region	95
	A_{start}	DOY	Beginning of flux accumulation (flag leaf emergence)	163 (200°C days backwards from mid-anthesis)	148
	A_{end}/*EGS*	DOY	End of flux accumulation (flag leaf senescence)	208 (700°C days from mid-anthesis)	208
	f_{phen_a}	Fraction	Proportional fall in g_{sto_O3} between f_{phen_g} and f_{phen_h}	0.3	0.3
	f_{phen_b}	Fraction	Fraction of g_{max} that g_{sto_O3} takes at the beginning of flag leaf senescence	0.7	0.7
	f_{phen_e}	°C days	Temperature sum at A_{start}	-200	-490
	f_{phen_f}	°C days	Temperature sum at mid-anthesis	0	0
	f_{phen_g}	°C days	Temperature sum at end of	100	100

			maximum g_{sto_O3} following mid-anthesis		
	f_{phen_h}	°C days	Temperature sum at start of flag leaf senescence	525	525
	f_{phen_i}	°C days	Temperature sum at A_{end}	700	749
f_{light}	*light_a*	constant	The rate of saturation of g_{sto_O3} in response to PAR	0.0105	0.0105
f_{temp}	T_{min}	°C	Temperature below T_{opt} where g_{sto_O3} reaches f_{min}	12	12
	T_{opt}	°C	Optimum temperature for g_{sto_O3}	26	26
	T_{max}	°C	Temperature above T_{opt} where g_{sto_O3} reached f_{min}	40	40
f_{VPD}	VPD_{max}	kPa	Value where VPD begins to limit g_{sto_O3}	1.2	1.2
	VPD_{min}	kPa	Value of VPD where f_{min} is reached	3.2	3.2
	ΣVPD_{crit}	kPa	Sum of hourly VPD values after sunrise above which afternoon stomatal reopening will not occur	8.0	8.0
f_{PAW}	PAW_t	%	Minimum non-limiting percentage of soil water	50	N/A
f_{SWP}	SWP_{max}	MPa	Maximum SWP below which	N/A	-0.08

			g_{sto_O3} will start to decline		
	SWP_{min}	MPa	SWP at which g_{sto_O3} reaches f_{min}	N/A	-3.25
f_{O3}	POD_0SPEC *threshold*	mmol m^{-2}	Threshold POD_0SPEC at which O_3-induced senescence begins	14	28
	exponent	constant	Rate of g_{sto_O3} decline with increasing flux accumulation	8	25

The cultivar-specific g_{max} parameter was calculated as the 95th percentile of all flag leaf measurements made during physiologically active daytime hours, before leaf senescence, and in non-limiting environmental conditions (PAR > 500, ambient temperature >18°C). A total of 113 g_{sto} data points for Mulika met these criteria. Before the calculation of g_{max}, raw observations of g_{sto} to water (H_2O) were transformed to g_{sto_O3} using the ratio of molecular diffusivity between O_3 and H_2O in air (0.663) (Massman, 1998). As all g_{sto} measurements were made on the adaxial leaf surface, these were normalised on a projected leaf area basis by multiplying adaxial g_{sto_O3} by the cultivar-specific ratio of average leaf g_{sto} and adaxial g_{sto}: this was found to be 0.78 based on 53 paired abaxial and adaxial g_{sto} measurements. The Mulika g_{max} parameter was calculated as 383 mmol O_3 m^{-2} PLA s^{-1} (100th percentile value = 645, 90th percentile value = 330).

The beginning of flux accumulation in the bespoke parameterisation was defined as the observed date of flag leaf emergence (28th May). The cultivar-specific observed date of mid-anthesis (23rd June) was used as the parameter f_{phen_f} in the phenological function of DO_3SE (f_{phen}). f_{phen_f} is used in the f_{phen} function as a reference point for calculating the likely onset and completion of natural leaf senescence. A thermal time interval of 525°C from f_{phen_f} onwards was used to define the onset of leaf senescence, following the parameterisation of CLRTAP (2017). A slightly modified thermal time interval of 749°C from f_{phen_f} onwards was used to define the completion of leaf senescence; this thermal time interval was calibrated so that completion of senescence (and therefore the end of the flux accumulation period) aligned approximately with observed completion of leaf senescence in the lowest O_3 treatments (26th July). The shape of the f_{phen} function used in DO_3SE is described in full in Grünhage *et al.* (2012).

Hourly measurements of soil water potential (SWP) were input to DO_3SE to simulate drought effects on flux. The observed soil water content at permanent wilting point (~6-8%), and water content at field capacity (~16-20%), for the John Innes No. 3 compost matched well with that

predicted by the soil water release curve for a general silt loam soil (Tuzet *et al.*, 2003); this generalised release curve was therefore used to convert measured soil water content (SWC %) to SWP. Six days of missing SWC data at the beginning of the flux accumulation period (DOY 148-153) were interpolated (method described in section 3.7.1 of the supporting information). Model parameters for the f_{SWP} function were derived by applying a boundary line approach to the data cloud, following the procedure outlined in the mapping manual of the CLRTAP (2017) and applied in a number of studies which have employed the DO_3SE model (González-Fernández *et al.*, 2013; Pleijel *et al.*, 2007) (Figure 3.2).

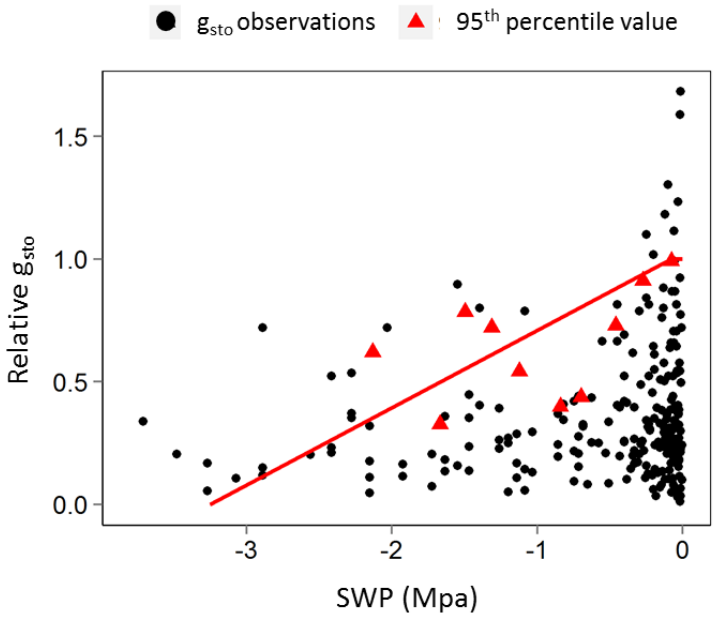

Figure 3.2. Stomatal conductance (g_{sto}) measurements for wheat cultivar 'Mulika', expressed relative to the species-specific maximum g_{sto} value (g_{max}) and plotted against the soil water potential (SWP) at the time of measurement. Triangular data points represent the 95th percentile g_{sto} observation within SWP bins of equal width. The red line represents the boundary line fitted to the data cloud.

A cultivar-specific parameterisation of the f_{O3} function in DO_3SE, which models O_3-induced accelerated senescence, was calibrated by assessing flag leaf CCI observations from the highest and lowest O_3 treatments. Chlorophyll content has commonly been used as a proxy for leaf senescence (Gelang *et al.*, 2000; Grandjean and Fuhrer, 1989; Pleijel *et al.*, 1997), as catabolism of chlorophyll occurs progressively throughout the senescence process (Lim *et al.*, 2007). Total loss of chlorophyll from the flag leaf was observed approximately two weeks earlier in the highest O_3 treatment compared to the lowest. The parameters of the f_{O3} function were therefore adjusted so that the end of flux accumulation in the highest and lowest O_3 treatments coincided with the observed total loss of chlorophyll from flag leaves in these treatments (Figure 3.3A). When the cultivar-specific f_{O3} function derived in this study is overlain on the data cloud of Mulika g_{sto} observations versus the accumulated flux at the moment of measurement, the

bespoke f_{O3} function performs better than the CLRTAP (2017) f_{O3} parameterisation (Figure 3.3B).

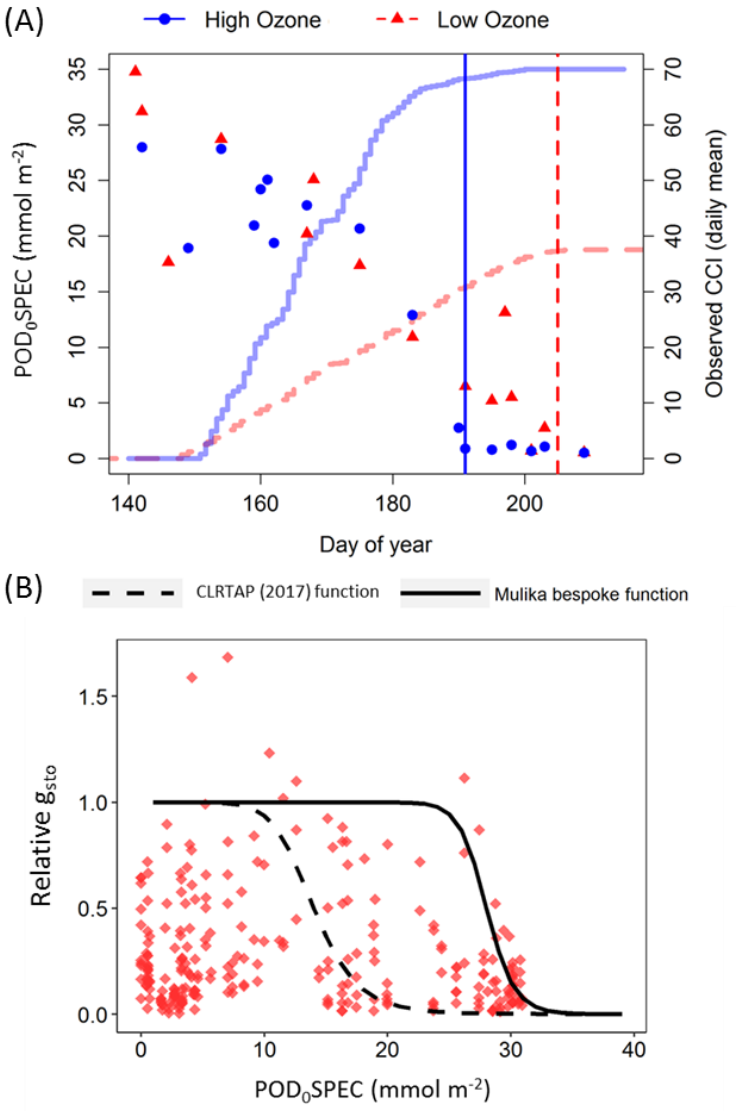

Figure 3.3. (A) Change in mean chlorophyll content index (shown as data points on the plot) over time in the highest and lowest O_3 treatments. The profiles of modelled flux accumulation over time in the highest and lowest O_3 treatments, as produced by the bespoke DO_3SE parameterisation, have been overlain. Vertical lines on the plot indicate the approximate date of total flag leaf senescence. Total loss of CCI, indicative of total senescence, aligns with the end of modelled flux accumulation in both high and low O_3 treatments. (B) Observations of g_{sto} for Mulika plotted against the accumulated O_3 flux at the time of measurement. The f_{O3} functions from the bespoke Mulika parameterisation, and from the CLRTAP (2017) parameterisation, have been overlain. The f_{O3} function was parameterised using POD_0SPEC (phytotoxic O_3 dose accumulated above no flux threshold) as the O_3 flux metric, following the parameterisation methodology of Pleijel et al. (2007) and Grünhage et al. (2012).

Seasonal O_3 flux (POD_6SPEC) was modelled using both the cultivar-specific bespoke parameterisation, and the CLRTAP (2017) parameterisation, to allow comparison of flux-response functions produced by both parameterisations. The CLRTAP (2017) parameterisation ordinarily estimates wheat sowing date based on latitude, and then uses fixed thermal time intervals to estimate mid-anthesis relative to sowing date. As daily temperature data was only available for the O_3 exposure period (15th May onwards), and not for the sowing or seedling emergence period (early April), mid-anthesis could not be calculated from thermal time, and therefore the actual observed data of mid-anthesis was applied within the CLRTAP (2017) parameterisation; all other CLRTAP (2017) parameters were as listed in Table 3.1.

3.3.5 Statistical analysis

All statistical analysis was carried out in R version 3.3.2 (R Core Team, 2016). Mixed model multivariate regression was carried out using package 'nlme' (Pinheiro *et al.*, 2015) to test for main effects of O_3 and drought on harvest variables, and to test for a significant interaction between O_3 and drought. Ozone flux (POD_6SPEC) and watering treatment were explanatory variables in models, and solardome ID was included as a random effect to account for non-independence of measurements made within each solardome. A quadratic term was included in model selection to test for non-linear responses to O_3 flux, and three further variables were tested during model selection: i) a variable describing plant density in containers, to account for the effect that varying germination success could have on calculated yield per unit area; ii) a variable describing presence or absence of aphids during a July outbreak, and iii) a variable describing whether O_3 was administered as a peak or high background profile. The same method as above was applied in the analysis of O_3 and drought effects on CCI, growth stage, and in analysis of yield response to AOT40 (a concentration-based metric of O_3 exposure calculated as the sum of $O_3 > 40$ ppb during daylight hours). Analysis of weekly average CCI included container ID as an additional random effect to account for repeat measurements made from the same container, and a Tukey post-hoc test was applied to identify which treatments differed significantly from one another.

Model assumptions of normality and even spread of residuals were tested using residual plots, and transformation was carried out where necessary. The 'best' model was identified using the Akaike Information Criterion (AIC), a goodness-of-fit parameter calculated from the number of model parameters and the maximum likelihood estimate (Burnham and Anderson, 2002). The model with the lowest AIC was considered optimal, and models differing in < 2 AIC units from the best model were defined as having little empirical support (Burnham and Anderson, 2002). P-values were obtained for terms in the optimal models using the R package lmerTest, v2.0-33 (Kuznetsova *et al.*, 2016).

3.4 Results

3.4.1 Ozone exposure in the different O_3 and drought treatments

Table 3.2 compares AOT40, 24h mean and seasonal accumulated flux (POD_6SPEC) for each of the treatment combinations. The table shows that the O_3 metrics that employ a threshold for damage – AOT40 and POD_6SPEC – indicate a much higher level of exposure in peak profile treatments compared to background profile treatments. Conversely, the mean concentration index (24h mean) suggests an equivalent level of exposure across paired peak and background treatments. The early and late drought events reduced seasonal POD_6SPEC by 3.01% and 0.3%, respectively (% average across all treatments). The parameterisation of DO_3SE using the observed dates of flag leaf emergence, mid-anthesis and leaf senescence from this experiment resulted in a total flux accumulation period of 60 days, substantially longer than the accumulation period of 45 produced by the CLRTAP (2017) parameterisation.

Table 3.2. Ozone exposure in experimental treatments during the life of the flag leaf (28th May – 28th July), expressed using concentration-based metrics (24h mean and AOT40) and modelled accumulated O_3 flux (POD_6SPEC). POD_6SPEC values presented in this table have been derived using the bespoke 'Mulika' parameterisation.

Solardome number	Ozone profile	Measured 24 h mean O_3 (ppb – season average)	AOT40 (ppm h)	POD_6SPEC (well-watered)	POD_6SPEC (early drought treatment)	POD_6SPEC (late drought treatment)
6	Background	27.0	0.0031	3.28	2.97	3.25
4	Peak	30.3	0.024	4.36	4.00	4.32
1	Background	37.0	3.65	8.66	8.04	8.60
5	Peak	39.2	11.10	12.78	12.39	12.73
7	Background	48.6	13.24	13.14	12.80	13.09
8	Peak	50.2	21.42	15.80	15.55	15.77
2	Background	56.5	21.10	14.95	14.72	14.91
3	Peak	55.4	30.50	18.08	17.83	18.07

Modelled f_{SWP} across the growing season for the early and late drought treatments are shown in Figure 3.4A and 3.4B, respectively. Modelled f_{SWP} represents the degree by which the model is simulating soil water limitation of g_{sto}, with a value of 1 indicating no limitation and a value of 0.01 (equivalent to f_{min}) indicating complete limitation. To assess performance of the f_{SWP} function, daily maximum (95th percentile) observed g_{sto} values have been overlain on the plots. Observed g_{sto} values have been calculated as relative to g_{max}, and the g_{max} value has been scaled

according to the f_{O3} and f_{phen} value on each day. Although this process involves applying model assumptions to observed data, it was thought to be necessary to modify the g_{max} 'baseline' to account for phenological and O_3-induced decline in g_{sto} in the late-season when assessing model performance. Figure 3.4A shows that substantial limitation of g_{sto} was simulated during the early-season drought, which is supported by observations of low maximum g_{sto} from that time, and substantial soil drying which was observed in the SWC record (daily mean SWC versus time is shown below the f_{SWP} plots in Figure 3.4). In contrast, very little soil water-induced limitation of g_{sto} was simulated during the late drought, which can be explained by the fact that the soil SWP minima during the late drought (-0.28 MPa, equal to 12.3% SWC) was only slightly lower than SWP_{max} - the SWP threshold below which g_{sto} limitation is modelled in DO_3SE (SWP_{max} = -0.08 MPa, equal to 16% SWC). The model simulation of very little drought-induced g_{sto} limitation during the late drought is supported by g_{sto} observations from that time, which show daily maximum g_{sto} values close to g_{max} (Figure 3.4B).

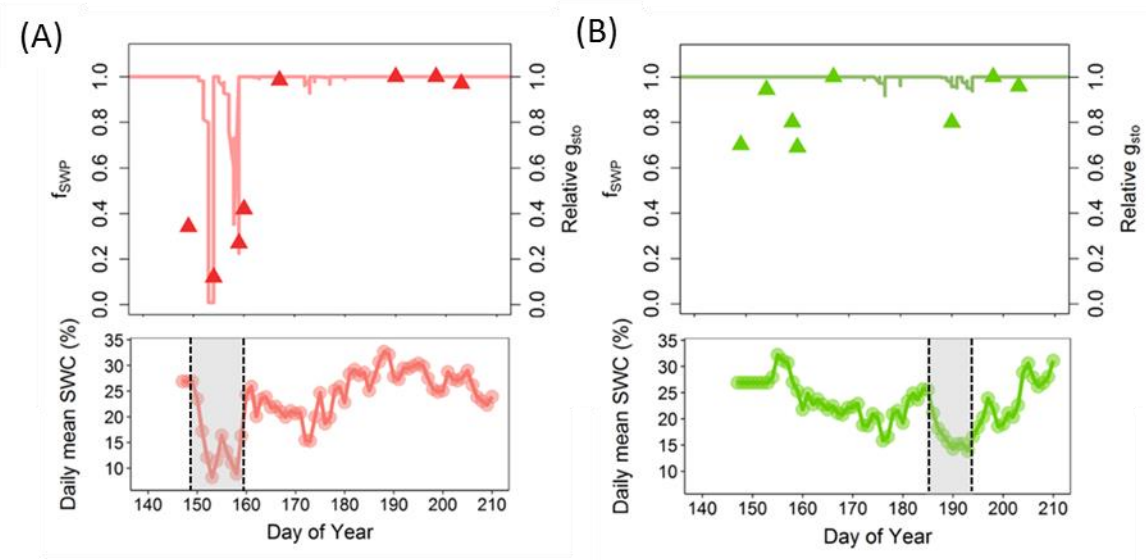

Figure 3.4. Modelled f_{SWP} profile over time in (A) the early drought treatment and (B) the late drought treatment. g_{sto} observations expressed relative to g_{max} – with g_{max} scaled using f_{O3} and f_{phen} model parameters to account for O_3 and phenology effects on maximal g_{sto} - have been overlain (right-hand y-axis). The daily mean soil water content (%) measured to a depth of 10cm in the two treatments are shown below the plots. Drought periods are shown on the SWC plots as shaded regions marked out by vertical dashed lines (early drought 29th May – 8th June; late drought 4th July – 13th July).

3.4.2 Effect of O_3 and drought on yield parameters and growth stage development

Figure 3.5 shows the results of the post-anthesis growth stage assessments, carried out on the 30th June, 14th July and 27th July. There were no significant effects of drought or O_3 in pre-anthesis growth stage assessments (data not shown). Drought effects on growth stage progression were apparent at the final assessment on the 27th July (9 days before harvest): at this time late drought plants were significantly advanced by 2.7 growth stages ($p < 0.0001$) and early drought plants behind by 1.1 growth stages ($p < 0.05$) relative to well-watered. There was no significant O_3 effect on growth stage at any time-point, although accelerated development at high POD_6SPEC was apparent at the final assessment ($p = 0.06$). Wheat plants were undergoing whole-plant senescence in late July, and therefore accelerated development at this time can be interpreted as accelerated senescence. Ozone exposure and late-season drought therefore accelerated leaf senescence, while early-season drought slightly delayed it. Statistical analysis of CCI data indicates significantly lower CCI in flag leaves in the high O_3 compared to the low O_3 treatment during the week of the 13th-19th July ($p < 0.001$), and CCI divergence between O_3 treatments was visible from the week beginning the 6th July (see section 3.7.2 of the supporting information).

The response of four harvest variables to O_3 flux and drought is shown in Figure 3.6. The outcome of statistical analyses conducted on these data is reported in full in section 3.7.3 of the supporting information. Ozone caused significant yield reduction, with yield in the highest treatment (55 ppb 24h mean) 33% lower relative to the lowest O_3 treatment (27 ppb 24h mean). Early drought and late drought both significantly reduced yield (early drought = 14.1% reduction on average across all O_3 treatments, late drought = 13.8% reduction on average across all O_3 treatments). The mechanism of yield loss differed depending on drought timing: both significantly reduced individual grain weight, but early drought also severely reduced the number of ears per plant. Early-season drought also led to a significant increase in the number of grains per ear. There was no significant interaction between O_3 and drought for any of the harvest variables.

Figure 3.7 shows O_3 exposure-yield functions for the different watering treatments expressed according to relative yield. Yield is plotted against POD_6SPEC in Figure 3.7A and AOT40 in Figure 3.7B. Conversion to relative yield was conducted separately for each watering treatment to account for drought effects on yield and to allow for comparison of the exposure-response slopes only. Flux-response slopes for the watering treatments do not differ significantly (Δ-AIC of 7.2 between model omitting the drought variable, and model containing drought-O_3 interaction variable). There is therefore no evidence of an O_3-drought interaction taking place that is not explained by changes in g_{sto}. The exposure-response slopes constructed using a concentration-based metric – the AOT40 – are marginally less steep in the two drought treatments compared to the well-watered treatment, but these differences in slope are not

statistically significant (Δ-AIC of 7.3 between best and second-best model). Drought-induced reduction in O_3 uptake therefore did not significantly ameliorate O_3 effects on yield.

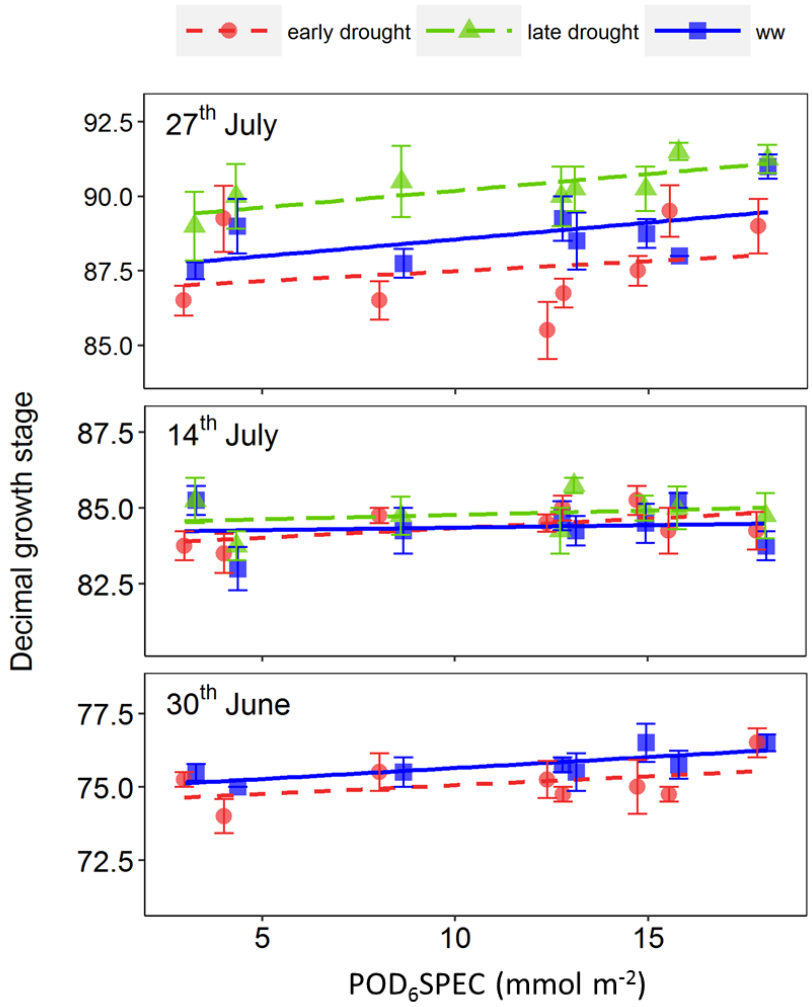

Figure 3.5. Data from post-anthesis growth stage assessments made on the 30/06/2015, 14/07/2015 and 27/07/2015. Watering regime was a significant factor in the 'best' model at the final assessment on the 27th July (Δ-AIC = 6.3 between best and next-best model, variable significance = $p < 0.001$). On the 27th July, both the early drought and late drought line intercept differed significantly from the well-watered line intercept (early drought vs well-watered = $p < 0.05$, late drought vs well-watered = $p < 0.0001$). Error bars represent +/- one standard error.

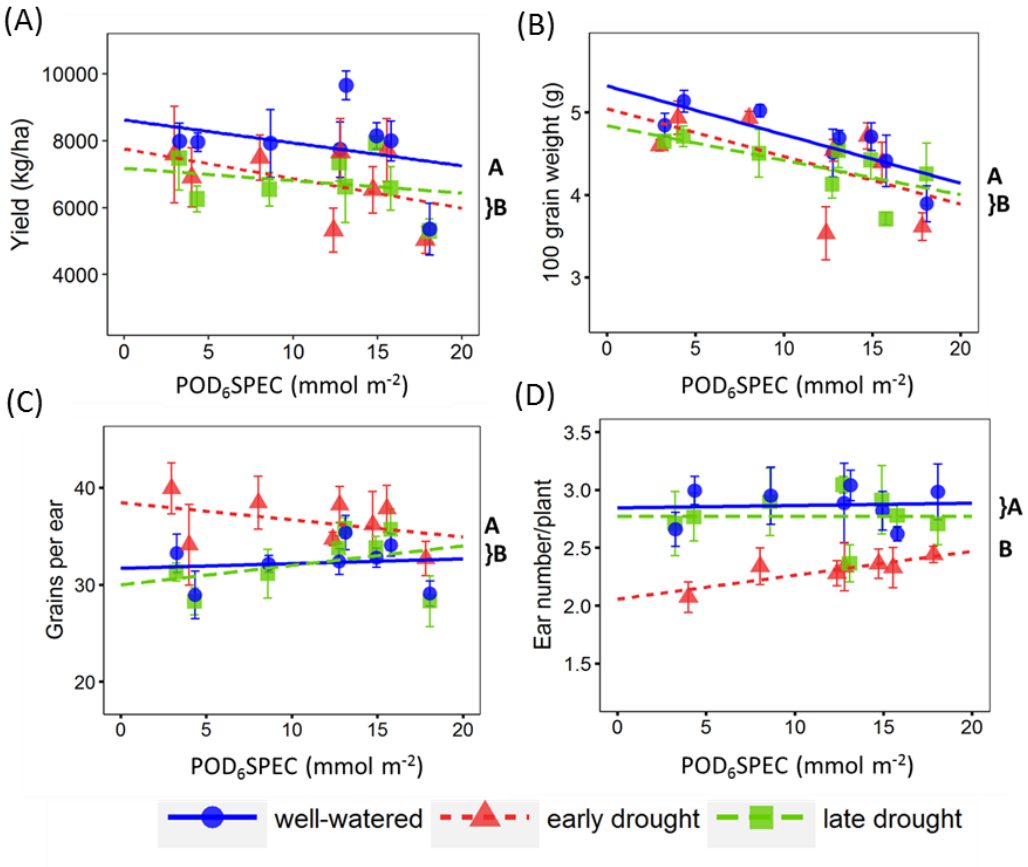

Figure 3.6. Flux-response relationships for (A) yield, B) 100 grain weight, C) number of grains per ear and D) number of ears per plant. The outcome of pairwise comparisons (Tukey post-hoc test) between watering treatments is shown as letters on the right of each plot; lines which share the same letter do not differ significantly from one another at level $p < 0.05$. Error bars represent +/- one standard error.

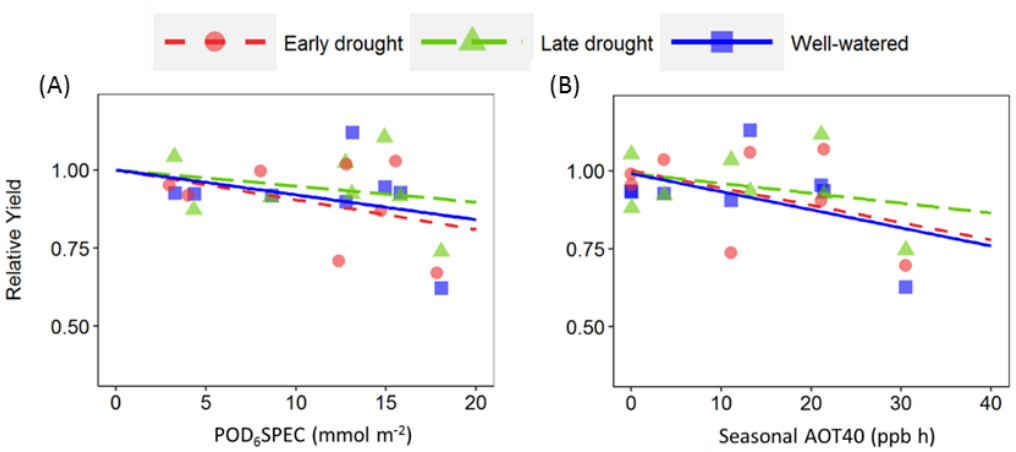

Figure 3.7. Flux-response relationships for well-watered, early drought and late drought plants, expressed according to relative yield and using (A) POD_6SPEC, and (B) AOT40 as the O_3 exposure metric. As with POD_6SPEC, the AOT40 accumulation period was defined by the life of the flag leaf (28th May – 28th July).

3.4.3 Comparison of flux-response functions for wheat from different data sources and DO_3SE parameterisations

Figure 3.8 compares three flux-response functions for wheat: the bespoke 'Mulika' function derived in this study; the 'Mulika' function derived using the CLRTAP (2017) DO_3SE parameterisation; and a function based on data from five wheat cultivars and the CLRTAP (2017) DO_3SE parameterisation, derived by Grünhage *et al.* (2012). The yield data for 'Mulika' largely aligns with the Grünhage *et al.* (2012) pooled data function, when the same DO_3SE parameterisation is used to calculate POD_6SPEC (no significant difference between the two function slopes, $p = 0.4$). The shallower slope of the Mulika flux-response function derived using the CLRTAP (2017) DO_3SE parameterisation compared to the Grünhage *et al.* (2012) function indicates that Mulika is relatively O_3-tolerant, compared to the wheat cultivars used to construct the Grünhage *et al.* (2012) function. The flux-response function for Mulika derived using the bespoke, cultivar-specific parameterisation derived in this study is significantly less steep than the Grünhage *et al.* (2012) function.

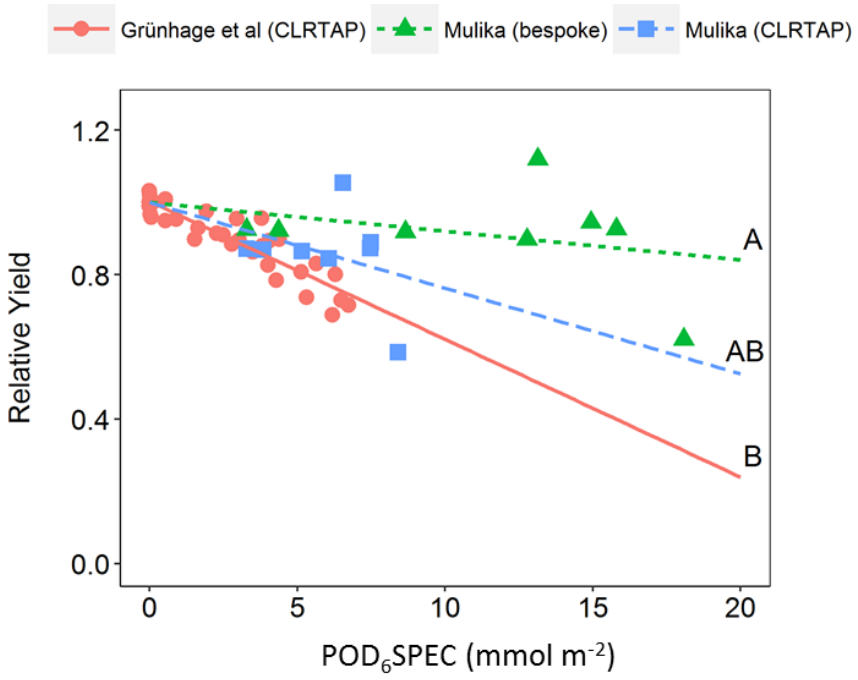

Figure 3.8. Comparison of wheat flux-response functions from different data sources and DO_3SE parameterisations. Solid line: function based on data published in Grünhage et al. (2012) from five European wheat cultivars, with flux derived using the CLRTAP (2017) parameterisation. Dashed line: 'Mulika' function derived using the CLRTAP (2017) parameterisation. Dotted line: 'Mulika' function derived using the bespoke parameterisation. Dose-response function type was important in the model as an interacting variable (Δ-AIC of 22 between best and next-best model). The outcome of pairwise comparisons (Tukey post-hoc test) between the regression lines is shown on the plot as letters; lines that do not differ significantly at level $p < 0.05$ share the same letter.

3.5 Discussion

The O_3-induced yield reduction in 'Mulika' supports results from previous experiments with wheat, which observed yield reduction in response to O_3 exposure (Feng *et al.*, 2008; Finnan *et al.*, 1997; Heagle, 1989). A 33% reduction in yield (kg ha^{-1}) was observed in the highest O_3 treatment (55 ppb 24h mean) relative to the lowest (27 ppb 24h mean). Ozone-induced yield reduction in 'Mulika' was primarily driven by reduced individual grain weight, with no effect on grain number. A similar pattern of effect was described in a meta-analysis of O_3 effects in wheat (Feng *et al.*, 2008), which found that reduced grain weight was substantially more important than changes in grain number in explaining O_3-induced yield reduction. Comparison of the 'Mulika' flux-response slope with the previously published function based on five European cultivars (Grünhage *et al.*, 2012), when the same DO_3SE parameterisation is applied, indicates that 'Mulika' is less O_3-sensitive than the cultivar average (Figure 3.8). The g_{max} value for 'Mulika' of 383 mmol O_3 m^{-2} PLA s^{-1} falls within the lowest decile of the observed range of g_{max} recorded for 17 European wheat cultivars (Grünhage *et al.*, 2012), and this may explain the relative O_3 tolerance of 'Mulika'. High g_{max} has previously been associated with high O_3 sensitivity in wheat (Biswas *et al.*, 2008; Pleijel *et al.*, 2006; Velissariou *et al.*, 1992) and other plants (Brosché *et al.*, 2010), as entry through stomata is the principal pathway for O_3 damage (Booker *et al.*, 2009).

In addition to O_3 effects, the results presented in this study indicate that a short period of drought during either booting or grain fill can significantly reduce yield in wheat. Early and late drought led to average yield losses relative to well-watered of 14.1% and 13.8%, respectively. The observation that pre-anthesis drought can cause equal or greater yield reduction than drought during grain filling is supported by a field study in wheat, which observed 33% lower grain yield when watering was withdrawn during the period preceding anthesis, compared to post-anthesis water withdrawal (Estrada-Campuzano *et al.*, 2012). The yield consequences of drought relate to whether stress coincides with a number of sensitive developmental stages, the most sensitive of which in wheat is thought to be the meiosis phase of early grain initiation (Saini and Westgate, 1999). The early drought event in this study significantly reduced the total number of ears, possibly as a result of the common drought adaptation strategy of actively degenerating tissue to reduce total leaf area and control water balance (Blum, 1996). Early drought reduced individual grain weight, but also led to a compensatory effect which saw an increased number of grains per ear; compensation responses following stress are thought to be an important developmental mechanism for reconstructing yield in grain crops (Blum, 1996; Eck, 1986). The primary mechanism by which late drought reduced yield was a reduction in individual grain weight (Figure 3.6), most likely driven by the reduced grain filling duration due to accelerated leaf senescence (Figure 3.5), and reduced capacity to fill grains due to physiological stress (Saini and Westgate, 1999). Saini and Westgate (1999) describe a gradual

decline in drought stress sensitivity of crops following grain initiation, suggesting that the late drought event in this experiment would have had a more severe effect if it had occurred earlier in the grain fill period.

A key result from this study is the lack of a significant interaction between co-occurring O_3 and drought. The slope of the flux-response (POD_6SPEC) and concentration-response (AOT40) functions for Mulika did not vary significantly by drought treatment (Figure 3.7). As the flux-based metric (POD_6SPEC) can be assumed to account for the effect of drought on the in-leaf O_3 dose, the lack of a significant O_3-drought interaction when this metric is used indicates that no further interaction at the leaf level – not explained by stomatal behaviour – was taking place. There is therefore no evidence that O_3 exposure predisposed plants to drought stress, nor 'hardened' them against it. The lack of a significant O_3-drought interaction in the AOT40-yield response functions is perhaps more surprising, as this contradicts the notion that drought can protect against O_3 damage by reducing g_{sto} and moderating uptake. This study joins a contradictory literature on the subject, with some authors reporting drought protecting crop plants against O_3 damage by inducing stomatal closure (Fagnano *et al.*, 2009; Heagle *et al.*, 1988; Khan and Soja, 2003), and others failing to observe such an interaction (Fangmeier *et al.*, 1994a; Temple, 1986). In the experiment presented here, the lack of drought-induced protection against O_3 was most likely due to the relatively small impact which the drought treatments had on O_3 flux: early and late drought reduced accumulated POD_6SPEC by 3.0% and 0.3%, respectively. Early drought reduced flux by a greater amount than late drought, because faster soil drying was observed during the early drought event (early drought SMC minima = 6.3%, late drought SMC minima = 12.3%) (Figure 3.4). This differential soil drying could be a consequence of different rates of whole-plant conductance in the early and late season, as g_{sto} in wheat declines towards the end of the life-cycle (Uddling and Pleijel, 2006). Despite the apparently small effect which both droughts - in particular, the late drought - had on the whole-season g_{sto}, both resulted in substantial end-season yield reductions.

The results therefore indicate that short periods of drought are unlikely to provide significant protection against O_3 pollution, particularly in environments where O_3 exposure is moderate and chronic. Both droughts in this experiment were associated with a significant yield penalty, and the review by Blum (1996) describes how the first plant response to water stress is a cessation of cell division and expansion, well before there is a reduction in g_{sto}. Drought-induced impairment of growth and function is therefore likely to occur before protective effects against O_3 can take place. An experiment with spring wheat which applied a simple flux modelling method found that water stress did not significantly reduce O_3 flux to leaves, but did result in severe yield reductions (Fangmeier *et al.*, 1994a). Similarly, the late drought treatment led to only minor soil drying and almost no limitation of g_{sto} (Figure 3.4B), but substantially reduced final yield. The results suggest that mild drought which induces stress but not stomatal closure,

and drought which occurs late in the season when g_{sto} is typically lower (Uddling and Pleijel, 2006), is unlikely to offer protection against O_3. Conversely, severe drought in the early and mid-season may offer protective effects, but the yield consequences of drought stress may outweigh the benefits. The ratio of cost to benefit will be more favourable if only a short period of water stress is required to protect against a large quantity of flux: conceivably this circumstance could arise in agricultural landscapes which experience O_3 peaks of high concentration and short duration. The withdrawal of water just before a forecasted O_3 episode could therefore be an effective strategy for protecting wheat yield, but is likely to be detrimental in landscapes experiencing a more consistent O_3 concentration.

The findings of this study are relevant to efforts to simulate crop yields under present and future climate and emission scenarios. Interactions between multiple environmental variables - including O_3, elevated CO_2, temperature, rainfall, and humidity – are a key source of uncertainty in crop yield modelling (Challinor *et al.*, 2009). Flux-based dose-response relationships are preferable to concentration-based ones for integration of O_3 effects into crop models, because they are assumed to account for the influence of temperature, VPD, radiation, soil water, phenology and ambient O_3 on O_3 uptake (Harmens *et al.*, 2007). The lack of observed non-stomatal interactions between O_3 and drought in this experiment suggests that flux-based dose-response functions are able to fully account for interactive effects of O_3 and water stress in wheat. However, some caution should be applied when extrapolating the results presented here to other wheat cultivars and environments. The contradictory results observed by previous O_3-drought exposure experiments is suggestive of a wide variety in response to these two stresses in combination, which may be in part linked to the large degree of variation in drought and O_3 tolerance that is known to exist between and within crop species (López-Castañeda and Richards, 1994; Mills *et al.*, 2007; Richards *et al.*, 2002). Furthermore, a key limitation of this experiment is the fact that wheat plants were grown in containers and not directly in the soil. Although large containers were deliberately chosen for this experiment to maximise rooting depth, and previous comparisons of response to O_3 exposure have shown no significant difference between pot and field-grown crops (Feng and Kobayashi, 2009; Osborne *et al.*, 2016), it is still possible that soil drying during the drought events may have taken place faster in containers than it would have in the full-field environment. More experimental data – particularly data from field experiments – is needed in order to build a fully comprehensive picture of how O_3-drought interactions influence crop yield.

An interesting result from the analysis presented in this paper is the difference between the 'Mulika' flux-response slope derived using the bespoke DO_3SE parameterisation, and using the CLRTAP (2017) parameterisation. The bespoke function predicts yield loss of 8% for 'Mulika' relative to zero O_3 at a POD_6SPEC of 10, compared to yield loss of 24% predicted using the CLRTAP (2017) function at the same POD_6SPEC exposure. This discrepancy between

parameterisations appears to stem from the much larger range of POD_6SPEC values modelled by the bespoke parameterisation (3.3 - 18.1 mmol m^{-2}) compared to the CLRTAP (2017) parameterisation (3.3 - 8.4 mmol m^{-2}), producing a flux-response function which is elongated and therefore less steep. A key factor underlying the higher flux values produced by the bespoke parameterisation was the accumulation period, which began 15 days earlier than the CLRTAP (2017) accumulation period, allowing 15 additional days of flux accumulation unlimited by phenology (f_{phen}) or O_3 (f_{O3}) effects. The CLRTAP (2017) parameterisation calculates the date of flag leaf emergence using a thermal time (base 0°C) interval of 200°C days before mid-anthesis. However, the observed dates of flag leaf emergence and mid-anthesis for 'Mulika' exhibited a thermal time interval of 490°C days. The rate of development with temperature accumulation in 'Mulika' therefore appears to differ substantially from the cultivar average. Potential reasons for this include inter-cultivar variation in development rate, and the potential additional influence of photoperiod on phenological development which is not currently accounted for in the stomatal flux methodology (Miglietta, 1989; Slafer and Rawson, 1995). The wheat crop growth model AFRCWHEAT2 uses a phenological modelling framework based on 'developmental time' accumulation, where developmental time is calculated by integrating thermal time with additional photoperiod and vernalisation factors, which can take a value between zero and 1 (Jamieson *et al.*, 2007). Incorporation into the stomatal flux methodology of a similar phenological modelling method incorporating both temperature and day-length could potentially increase the accuracy of flux modelling applied across multiple wheat cultivars and regions.

3.6 Conclusions

This study identified the modern wheat cultivar 'Mulika' to be comparatively O_3-tolerant relative to other cultivars, but nevertheless confirms the vulnerability of wheat to O_3-induced yield reduction. Flux modelling indicated that 10-day drought events in the early and late season only led to a small reduction in total O_3 dose (POD_6SPEC) accumulated over the season. In this experiment, the negative impacts of a 10-day period of water withdrawal on yield considerably outweighed the benefits of O_3 exclusion. This study therefore suggests that short periods of drought are unlikely to protect against O_3 damage, particularly in environments where O_3 exposure is moderate and chronic. There was no evidence of O_3-drought interactions not explained by stomatal behaviour, indicating that O_3 flux modelling - which incorporates drought impacts on g_{sto} – is likely to fully account for O_3-drought interactions in crop yield modelling.

3.7 Supporting Information

3.7.1 Interpolation method for soil moisture data

A gap in the soil moisture data record had to be interpolated to allow soil moisture to be used as input data to DO_3SE. The data gap spanned six days within the flux accumulation period, from the 28th of May (DOY 148) to the 4rd of June. This comprised the first five days of the early drought event.

Figure 3.9 shows the interpolated segment of the soil water content (SWC) (%) profiles, alongside the measured data record. Interpolation for the well-watered and late drought watering treatments, which both received full watering in the early-season, was done by taking the average across both treatments of all hourly SWC values recorded in the two-week period following the data gap. This value was also used as the starting SWC value in the early drought treatment, before the beginning of the drought on the 29th of May. A SWC minima of 6.3% was recorded at the beginning of the data record on the 4th of June, before early drought plants were given a small amount of supplementary water; a decline was therefore assumed between the starting SWC on the 29th of May and the recorded minima on the 4th of June. The shape of the SWC decline used to interpolate this gap replicated the observed polynomial shape of soil drying observed in the early drought plants following supplementary water addition, observed in the data record from the afternoon of the 4th of June to the 8th of June.

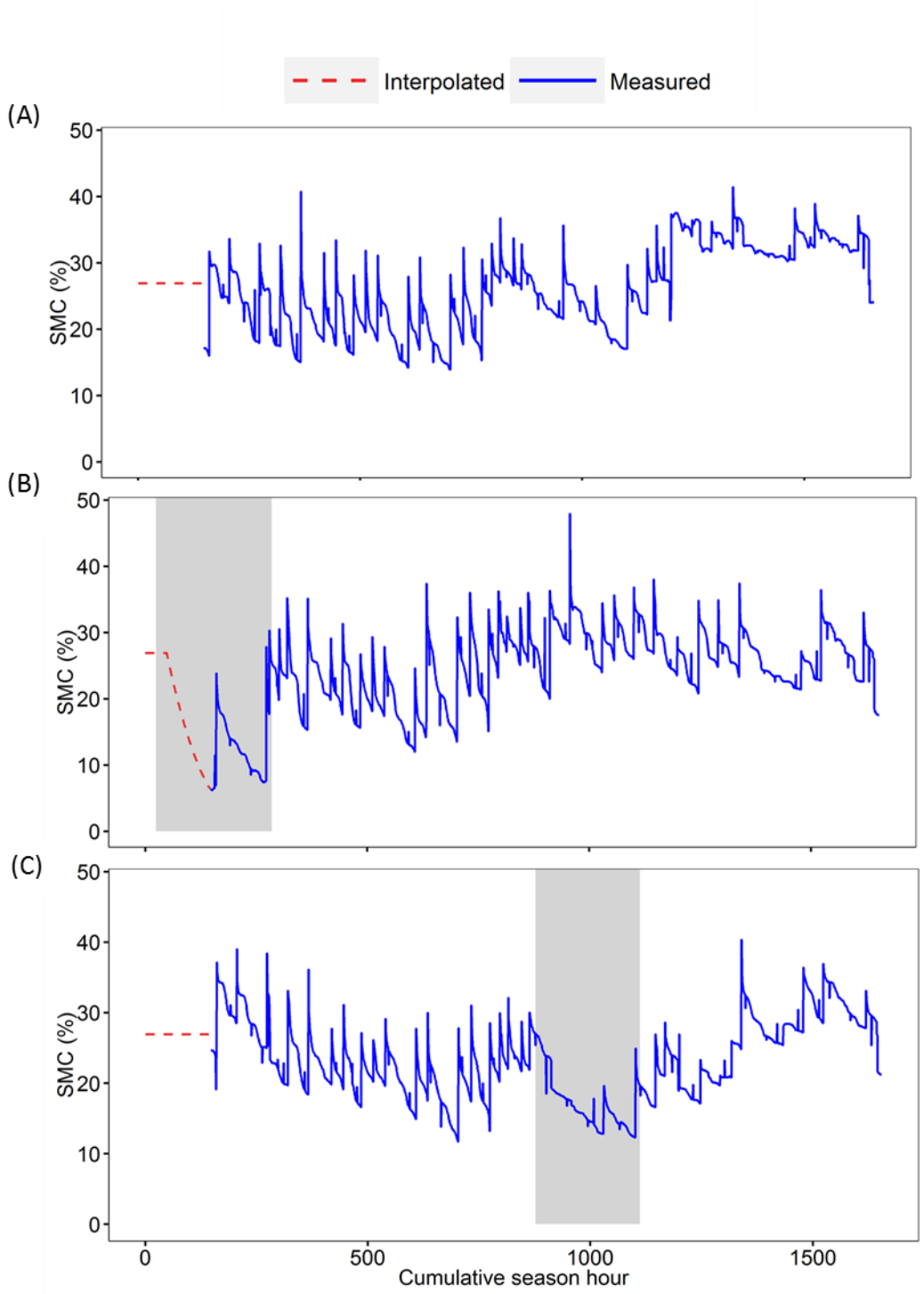

Figure 3.9. Soil moisture content (SMC, %) at 10cm depth for (A) the well-watered treatment, (B) the early drought treatment (29th May – 8th June), and (C) the late drought treatment (4th July – 13th July). Interpolated data is indicated by the dashed line, with measured data represented by the solid line. The two drought events have been identified as grey shaded regions overlaid on the plots.

3.7.2 Profile of chlorophyll content index in highest and lowest O_3 treatments

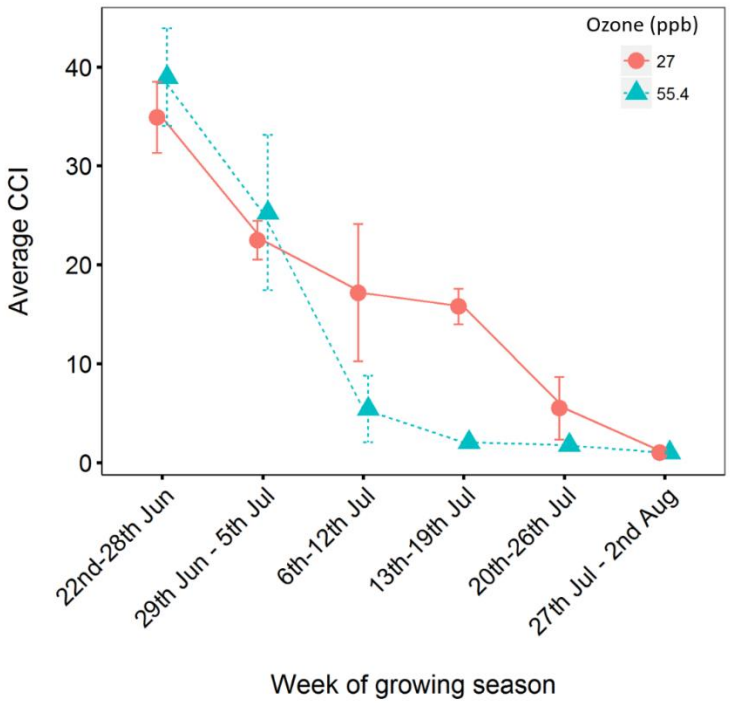

Figure 3.10. Weekly average CCI in the highest and lowest O_3 treatments, for the post-anthesis period. Ozone treatment was a significant interacting variable in the model describing CCI change over time (Δ-AIC of 41.8 between best and next-best model). A Tukey post-hoc test indicated a significant difference in leaf CCI content between O_3 treatments for the week of the 13^{th}-19^{th} of July ($p < 0.001$). Average leaf CCI did not significantly differ between O_3 treatments for the other weeks. Error bars represent +/- one standard error.

3.7.3 Summary of statistical analysis investigating O_3 and drought effects on harvest variables

Table 3.3. Delta-AIC between the best and second-best models describing four harvest variables, alongside p-values for the explanatory variables tested during model selection. The statistical outcome of pair-wise comparisons between watering treatments is also given in the right-hand segment of the table, separated by a vertical line. Statistically significant p-values ($p < 0.05$) have been highlighted in bold and underlined. In all cases O_3 and drought stress reduced the value of the harvest variable, with the exception of the early drought effect on the number of grains per ear, which was positive.

Harvest variable	Best model ΔAIC	Plant density	Aphids	Peak/ background profile	POD_6S PEC	Watering regime	O_3/drought interaction	WW vs. ED	WW vs. LD	ED vs. LD
Yield (kg ha^{-1})	7.6	**p ≤ 0.001**	**p ≤ 0.01**	N/R	**p ≤ 0.05**	**p < 0.0001**	N/R	**p ≤ 0.001**	**p ≤ 0.01**	p = 0.5
100 grain weight (g)	2.0	N/R	**p <0.01**	p <0.1	**p ≤ 0.0001**	**p < 0.05**	N/R	**p ≤ 0.05**	**p ≤ 0.001**	p = 0.8
Grains per ear	7.7	N/R	N/R	N/R	N/R	**p < 0.0001**	N/R	**p ≤ 0.0001**	p = 1.0	**P ≤ 0.0001**
Ears per plant	1.5	N/R	N/R	N/R	N/R	**p < 0.001**	N/R	**p ≤ 0.0001**	p = 0.3	**P ≤ 0.0001**

4 New insights into leaf physiological responses to ozone for use in crop modelling

4.1 Abstract

Accurate estimates of food production under future air pollutant emission and climate scenarios depends on the phytotoxic effect of ozone (O_3) on growth and yield being accurately represented in models. This study tests a number of assumptions that form part of published approaches for modelling the effects of O_3 on photosynthesis and leaf duration against experimental data for two modern cultivars of wheat, from two exposure experiments. In 2015 and 2016, wheat plants were exposed in eight hemispherical glasshouses to precision-controlled O_3 concentrations ranging from 22 to 57 ppb (24h mean), with profiles ranging from increased background to high peak treatments. The stomatal ozone flux (Phytotoxic Ozone Dose, POD) to the flag leaf in different O_3 treatments was modelled using a Jarvis-type multiplicative model of stomatal conductance. Both cultivars exhibited accelerated loss of leaf chlorophyll and early loss of photosynthetic capacity at high O_3 flux. Leaf senescence onset and completion occurred earlier as average POD increased, according to a linear relationship, regardless of the shape of the O_3 profile. Timing of senescence onset and rate of senescence were both cultivar-specific, and therefore both need to be able to vary according to cultivar or species in O_3 senescence model functions. Negative effects of O_3 on photosynthesis were only observed with O_3-induced leaf senescence, suggesting that O_3 does not impair photosynthesis in un-senesced young flag leaves at the realistic O_3 exposure concentrations applied here. It is hypothesised that accelerated senescence is therefore likely to be the dominant O_3 effect influencing final yield in most agricultural environments. The phytotoxic O_3 dose was better than 24-hour mean concentration and AOT40 at predicting the response of five physiological variables - Chlorophyll content index (CCI), Light-saturated photosynthetic rate (A_{sat}), maximum carboxylation capacity (V_{cmax}), maximum rate of electron transport (J_{max}), and stomatal conductance - to O_3, and the use of POD also successfully accounted for the greater amount of O_3 exposure resulting from peak-dominated treatments and those featuring a consistent background concentration.

4.2 Introduction

The phytotoxic air pollutant ozone (O_3) reduces yield in many crop species including wheat, rice and soybean (Feng and Kobayashi, 2009; Mills *et al.*, 2007). Ground-level O_3 forms from precursor gases – chiefly NO_x and volatile organic compounds (VOC's) – in chemical reactions catalysed by sunlight and heat (Finlayson-Pitts and Pitts, 1993). Concentrations over much of the Earth's land surface have approximately doubled since the pre-industrial era as a result of anthropogenic emissions from vehicle use, industry and agriculture (Royal Society, 2008; Vingarzan, 2004; Volz and Kley, 1988). Annual mean surface O_3 concentrations have largely stabilised in Europe since 2000 as a result of emission control policies (Cooper *et al.*, 2014; Parrish *et al.*, 2012), but a continued increase until 2050 is likely across South and East Asia (IPCC, 2013a; Lei *et al.*, 2012). The pattern of O_3 exposure in different regions is also expected to change over coming decades: short, acute peak 'episodes' of very high concentration are predicted to become more frequent in India and China (Lei *et al.*, 2012; Xu *et al.*, 2008), while in Europe and North America the background O_3 level is expected to remain relatively high but with fewer peak episodes (Paoletti *et al.*, 2014).

Model-based estimates of yield loss under future climate and air pollution scenarios represent a powerful way of highlighting the yield benefits that could come from further reductions in surface O_3 (Avnery *et al.*, 2011a, b; van Dingenen *et al.*, 2009; Wang and Mauzerall, 2004). Global O_3-induced wheat yield loss for the year 2000 has been estimated as ranging from 5% to 26%, with potential additional losses of 1.5% to 10% predicted for 2030 (Avnery *et al.*, 2011b; van Dingenen *et al.*, 2009). However, all large-scale assessments of O_3-induced yield loss for wheat published to date have followed an empirical approach, where surface O_3 concentration is simulated spatially using a chemical transport model (CTM), concentration is linked to yield loss using published concentration-response functions, and response is scaled up using crop production maps and agricultural statistics (Avnery *et al.*, 2011a; Tai *et al.*, 2014; van Dingenen *et al.*, 2009). A more mechanistic or process-based approach could potentially produce more robust estimates of future yield, as empirical assessments do not account for potential interactive effects between future O_3, CO_2 and climate change (Emberson *et al.*, submitted).

The development over the last twenty years of methods for modelling O_3 flux into leaves (Büker *et al.*, 2012; Emberson *et al.*, 2000a; Emberson *et al.*, 2000d; Simpson *et al.*, 2012) – which provide an hourly estimate of O_3 dose reaching sites of damage in the leaf – has created potential for O_3 effects to be integrated into crop simulation models in a dynamic way. Studies applying O_3 flux modelling have generally either used a multiplicative stomatal conductance (g_{sto}) algorithm (Danielsson *et al.*, 2003; Emberson *et al.*, 2000c; González-Fernández *et al.*, 2013) first developed by Jarvis (1976), or followed a semi-mechanistic approach first proposed by Ball *et al.* (1987) where g_{sto} is estimated empirically from photosynthetic rate, which in turn is modelled using the biochemical photosynthesis model of Farquhar *et al.* (1980) (Ewert and

Porter, 2000; Leuning, 1990). Since most crop models simulate growth responses at daily or hourly time-steps and can therefore respond to a changing environment (Boote *et al.*, 2013), integration of O_3 effects into crop models is feasible, as long as plant response to O_3 can be represented reasonably well in the model formulation. Some attempts have been made to integrate O_3 effects with crop modelling (Ewert and Porter, 2000; Martin *et al.*, 2000), but no estimate of O_3-induced yield loss in croplands using a dynamic or process-based approach has been published to date. Reasons for slow progress in this field include the challenges associated with upscaling responses from the leaf to the canopy level; the need for species and cultivar-specific model parameterisation; and incomplete understanding of the physiological mechanisms underlying O_3-induced yield reduction (Emberson *et al.*, submitted).

A substantial body of experimental work has established without doubt that O_3 exposure reduces yield in wheat (see reviews by Heagle, 1989; Jäger et al, 1992; Feng et al 2008). Ozone-induced yield loss results from a combination of foliar injury, impaired photosynthesis, altered carbon translocation, and accelerated leaf senescence (Booker *et al.*, 2009; Fiscus *et al.*, 2005). However, the processes that link O_3 uptake through stomata to these responses are not fully understood, and it is unclear which are most important for determining final yield loss. The O_3-induced reduction in photosynthetic rate has been widely reported (Feng *et al.*, 2008; Lehnherr *et al.*, 1987; Lehnherr *et al.*, 1988), but quantifying in experiments the extent by which this represents a direct effect of O_3 on the photosynthetic mechanism, or an indirect effect via changes in leaf pigmentation or g_{sto}, has represented a challenge for experimentalists. Disentangling short-term O_3 impacts on photosynthesis from the long-term accelerated senescence response is also difficult. Some studies have observed reduced activity of the carbon-fixing enzyme ribulose-1,5-biphosphate carboxylase/oxygenase (rubisco) in response to O_3 (Dann and Pell, 1989; Farage and Long, 1995; Farage *et al.*, 1991), leading to the hypothesis that 'instantaneous' effects of O_3 on photosynthesis are largely a consequence of effects on this enzyme. The physiological mechanism underpinning the often-observed accelerated leaf senescence response to O_3 (Burkart *et al.*, 2013; Feng *et al.*, 2011; Gelang *et al.*, 2000; Grandjean and Fuhrer, 1989; Ojanperä *et al.*, 1998) is also unknown, although it has been hypothesised that it could be related to the long-term increased respiratory costs associated with detoxification and repair processes (Ewert and Porter, 2000).

Several approaches for modelling O_3 effects on photosynthesis and senescence in wheat have been published. A function for modelling 'instantaneous' O_3 suppression of photosynthesis was proposed by Martin *et al.* (2000), who simulated a linear reduction in the carboxylation capacity of rubisco (the parameter V_{cmax} in the biochemical model of Farquhar *et al.*, 1980), above a threshold value of hourly flux representative of the species or cultivar-specific detoxification capacity. Ewert and Porter (2000) applied a version of this 'short-term' function alongside a 'long-term' algorithm for modelling O_3-induced senescence, and assumed that instantaneous

suppression of photosynthesis by O_3 takes place throughout the leaf lifespan. The senescence function described by Ewert and Porter (2000) assumes a linear reduction in total leaf lifespan as accumulated O_3 flux increases, and leaf senescence makes up the final third of the leaf lifespan, during which time V_{cmax} is assumed to decline linearly. In this function, the onset and completion of leaf senescence therefore move progressively earlier and closer together as seasonal O_3 flux increases. An alternative approach for modelling O_3-induced senescence is currently used in the multiplicative version of DO_3SE (Deposition of ozone for stomatal exchange), a g_{sto} model which estimates accumulated O_3 flux – known as the Phytotoxic Ozone Dose (POD) - to vegetation (Büker *et al.*, 2012; Emberson *et al.*, 2000b; Emberson *et al.*, 2000d; Simpson *et al.*, 2012). In the f_{O3} function of this model, leaf senescence is 'triggered' by a threshold value of POD, which induces a curvilinear decline in leaf g_{sto} of fixed shape but variable decline rate (Danielsson *et al.*, 2003; Grünhage *et al.*, 2012; Pleijel *et al.*, 2007). The flux or POD 'trigger' can be parameterised according to the sensitivity of the cultivar or species.

The integration of O_3 damage functions such as those described above into crop simulation models could improve yield estimates under O_3 stress. Model development must however be guided by experimental evidence to inform parameterisation, show the likely degree of error, and indicate the relative importance of different damage mechanisms. Modelling approaches must also be able to replicate the physiological response to differing patterns of O_3 exposure: for example, acute peaks in concentration have been reported to induce greater physiological stress compared to consistent, moderate levels with the same 24-hour mean exposure (Meyer *et al.*, 2000), and modelling methods need to be able to capture these nuances. This study combines data from two O_3 exposure experiments with European wheat, mimicking current and potential future O_3 scenarios, and analyses the response of leaf chlorophyll, g_{sto} and photosynthesis, in order to test some key assumptions of published O_3 effect model functions.

Firstly, with regards to the O_3 effect on leaf senescence, this study i) examines whether inter-cultivar differences in response are captured by current senescence functions, and ii) whether senescence onset occurs at an accumulated O_3 flux 'trigger' value. Secondly, it examines whether V_{cmax} is significantly reduced by O_3 before, and therefore independent of, O_3-induced leaf senescence. Thirdly, it investigates if O_3 flux – both with and without a threshold flux for accumulation - is a better predictor of the physiological response to O_3 compared to concentration-based metrics, and whether flux can account for the difference in O_3 exposure resulting from O_3 profiles dominated by acute peaks, versus a consistent background concentration.

4.3 Materials and Methods

4.3.1 Experimental site and treatments

Both experiments that provided data for this study took place at the Centre for Ecology and Hydrology (CEH) air pollution exposure facility in Abergwyngregyn, North Wales (53.2°N, 4.0°W). In 2015 two European wheat cultivars (*Triticum aestivum* L., 'Mulika' and 'Skyfall') were exposed to O_3 for 82 days. In 2016, the cultivar which had exhibited the highest O_3 sensitivity - 'Skyfall' - was exposed to O_3 for another season (92 days), to allow for the collection of further physiological data relating to the response to O_3. Timelines for sowing, emergence, O_3 exposure and harvest in both experiments are presented in section 4.7.2 of the supporting information. In both experiments, plants were grown in 25-litre containers (40 x 35 x 38cm) filled with John Innes No.3 compost, and soil was inoculated shortly after sowing with microbial communities using a soil slurry taken from a nearby wheat field. Seeds were sown in rows 7cm apart at a density of ~260 seedling per square metre, which aligns with recommended seedling density for field conditions (AHDB, 2015). Four containers per cultivar and treatment were planted and placed next to each other, producing a canopy of ~144 plants per cultivar and O_3 treatment. In both years, ammonium nitrate fertiliser was applied once mid-season (80kg/ha). In 2015, fungicide ('Unix', Cyprodnil, 1.6 kg/ha) was applied once and insecticide (pyrethrum, 1ml/litre) was applied three times. In 2016, fungicide was applied twice (1st application: trifloxystrobin, 0.12g/litre; tebuconazole, 0.125g/litre. 2nd application: cypodinil, 2.25g/litre) and insecticide was applied once (thiachloprid, 0.15g/litre).

Ozone exposure took place within 'solardomes', hemispherical glass domes three metres in diameter and two metres in height, described previously (Hayes *et al.*, 2015; Mills *et al.*, 2009). Air entering the domes was carbon-filtered to remove O_3 before a precision-controlled quantity supplied by an O_3 generator (Dryden Aqua G11, Edinburgh, UK) linked to an oxygen concentrator (Sequal 10, Pure O2, UK), was added. Concentrations for injection were determined by a computer-controlled O_3 injection system (Lab VIEW, version 8.6, National Instruments, Texas, US). Air within domes was circulated at a rate of two air changes per minute, and the O_3 concentration within each dome was recorded on a 30-minute cycle using two O_3 analysers of matched calibration (Envirotech API 400A, St Albans, UK). Weekly O_3 profiles for each treatment are presented in Figure 4.1. Treatments spanned a wide range of seasonal mean concentrations, and also represented different O_3 exposure patterns, representing potential future profiles of increasing background or decreasing peak O_3. In 2015 four treatments consisted of a relatively low night-time background level, with high peaks during the day – classified as 'peak' treatments – while the other four comprised consistent concentrations with only small peaks – classified as 'background' treatments. 'Peak' and 'background' treatments were paired to give similar 24-hour mean O_3 concentration over a 7 day period (Table 4.1). In 2016, all elevated treatments were 'peak' in profile. Treatments were categorised

according to their 24-hour mean concentration and exposure profile, as 'low background' (LB), 'low peak' (LP), 'medium background' (MB), 'medium peak' (MP), 'high background' (HB), 'high peak' (HP), 'very high background, (VHB), and 'very high peak' (VHP). Although O_3 treatments were not replicated, numerous studies have established the statistical validity of conducting unreplicated experiments using the solardome facility (Hayes *et al.*, 2012; Hewitt *et al.*, 2014; Mills *et al.*, 2009), and previous work has shown that no solardome effect on air or leaf temperature is detectable (Hewitt *et al.*, 2016).

Climatic conditions fluctuated naturally in the solardomes according to ambient conditions. Air temperature, photosynthetically active radiation (PAR), relative humidity and wind speed were monitored in one solardome during both experiments using an automatic weather station (Skye instruments Ltd, Llandridod Wells, UK), to obtain data for stomatal flux modelling. Plants were well-watered throughout, and soil moisture content was continuously monitored in selected plant containers to a depth of 10 cm using Theta Probes (Delta-T Devices Ltd., Cambridge, UK).

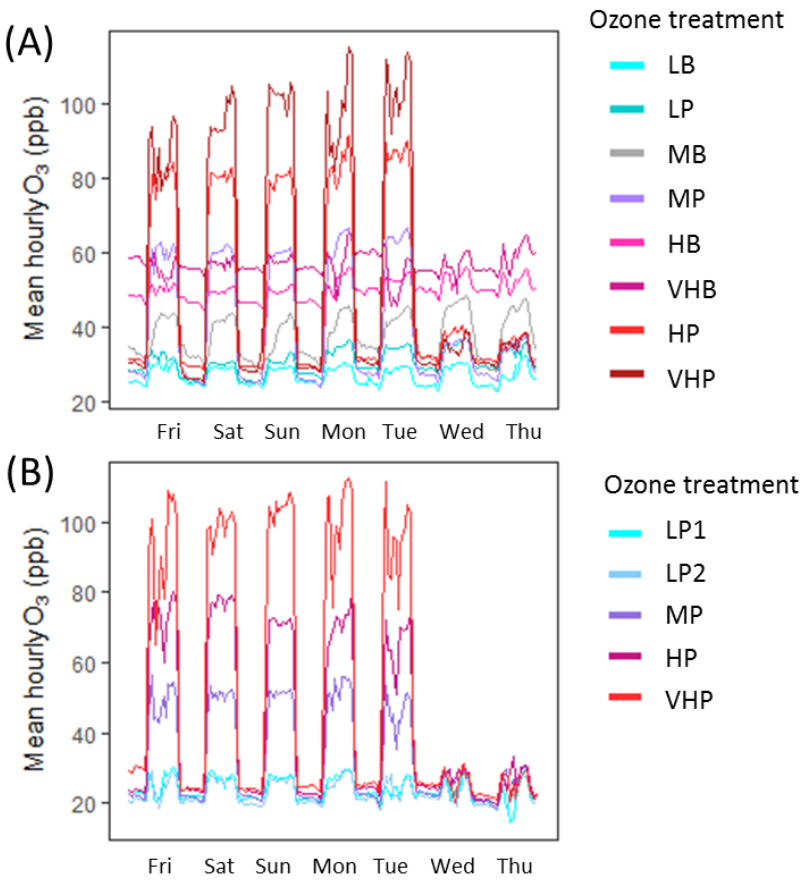

Figure 4.1. Average hourly O_3 exposure concentrations in (A) 2015, and (B) 2016. Values are shown for a one-week period, averaged over the whole of each growing season. Each treatment has been categorised based on the 24-hour mean exposure (Low, Medium, High, Very high) and the characteristic profile of exposure (peak or background). Treatments were applied five days out of seven to mimic real-world O_3 exposure.

4.3.2 Leaf chlorophyll and gas exchange measurements

Chlorophyll content was measured non-destructively as an index (chlorophyll content index, CCI) using CCM-200 and CCM-200+ instruments (Opti-sciences, Hudson, USA). A regression line fit to paired measurements was used to standardise observations made using the two instruments. In 2015, 684 measurements were made over 70 days; in 2016, 105 measurements were made over 22 days.

To assess the effect of O_3 on photosynthetic capacity and g_{sto}, response curves of net photosynthetic rate (A) to intercellular CO_2 concentration (C_i) – i.e. A-C_i curves - were constructed using a portable infrared gas analyser (Li-Cor 6400XT; LI-COR Biosciences, Lincoln, US). In 2015, measurements were made in the two lowest O_3 treatments at the beginning of exposure (20th-26th May). Further measurements in the two lowest treatments (LB and LP) and two high O_3 treatments (VHB and VHP) were made in the mid-season (8th-17th June) and late-season (16th-24th July). Measurements were made in the youngest fully expanded leaf of randomly selected plants (represented by the flag leaf from 28th May onwards). In 2016, four sets of A-C_i curve measurements were made at approximate two-weekly intervals spanning 6th June – 29th July. Measurements in 2016 were made in all treatments at each of the time intervals, except for the final measurement set in late July, when plants in HP and VHP treatments were too senesced for measurements to take place. All 2016 measurements were made in the flag leaf. For both years, four A-C_i measurements were made per treatment and per cultivar at each time-point, and leaves were tagged following measurement so that the same leaf could be measured throughout the season.

All response curve measurements were conducted at light saturation (minimum photosynthetic photon flux density = 1500 µmol m^{-2} s^{-1}; LED light source), and sample chamber relative humidity was maintained between 50 and 80%. Photosynthetic rate and g_{sto} were allowed to stabilise in the leaf chamber at ambient CO_2 (400 µmol mol^{-1}). The A-C_i curve was constructed by measuring A at a minimum of nine air CO_2 concentrations, ranging from ca. 50 to 2000 µmol mol^{-1}. A_{sat} and associated g_{sto} values were determined from the ambient CO_2 measurements (400 µmol mol^{-1}) from each A-C_i curve.

Additional measurements of A_{sat} and associated g_{sto} were made in 2016 over six days (16th June; 1st July; 8th July; 14th July; 20th July; 26th July). Measurements were made at ambient CO_2 concentration (400 µmol mol^{-1}) under the same light and relative humidity conditions as described above.

4.3.3 Derivation of V_{cmax} and J_{max}

Maximum rate of carboxylation (V_{cmax}) and maximum rate of electron transport (J_{max}) were derived from A-C_i curves using the estimating utility and methodology described by Sharkey *et*

al. (2007). Leaf temperature and atmospheric pressure, which were measured using the Licor 6400XT simultaneously with all photosynthesis measurements, were input parameters. V_{cmax} and J_{max} values calculated from curves were adjusted to 25°C.

The V_{cmax} dataset was extended by applying the 'one-point method' of deriving V_{cmax} from A_{sat} as described in De Kauwe *et al.* (2016). Estimation of V_{cmax} when only A_{sat} is known using the one-point method relies on the assumption that photosynthetic rate at ambient CO_2 is rubisco-limited (De Kauwe *et al.*, 2016). As the measurements of A at 400 µmol mol^{-1} CO_2 in the measured A-C_i curves typically fell within the rubisco-limited section of the curve (i.e. before the transition point), this assumption was thought to be likely to hold true for the two cultivars used in this study. The one-point method also assumes, in the absence of a known daytime respiration rate (R_{day}), that R_{day} can be estimated as 1.5% of V_{cmax}. V_{cmax} was calculated from A_{sat} using the following equation:

$$(1) \quad V_{cmax} = A_{sat} * \left(\frac{C_i + K_m}{C_i - \Gamma*} - 0.015\right)$$

Where K_m is the Michaelis-Menten constant, given by:

$$(2) \quad K_m = K_c * \left(1 + \frac{O_i}{K_O}\right)$$

The parameters K_c (Michaelis-Menten constant for CO_2), K_O (Michaelis-Menten constant for O_2) and Γ* (CO_2 compensation point in the absence of mitochondrial respiration) were estimated at 25°C following the equations and constants published in Bernacchi *et al.* (2001) describing their temperature dependence in the model species tobacco (*Nicotiana tabacum,* L.). Equations and constants used to derive these three parameters are listed in section 4.6.5 of the supporting information. O_i represents the intercellular concentration of O_2 (210 mmol mol^{-1}) (De Kauwe *et al.*, 2016).

The robustness of the one-point method was evaluated by comparing V_{cmax} values calculated from a subset of the measured A-C_i curves with the V_{cmax} values calculated from each corresponding A_{sat} value (i.e. the 400 µmol mol^{-1} CO_2 value from each A-C_i curve). V_{cmax} values derived using both methods were adjusted to 25°C. A very close association was observed between V_{cmax} values derived using the two methods (Figure 4.2, adjusted $r^2 = 0.95$, $p < 0.001$), indicating that the one-point method is robust for the cultivars used in this study. V_{cmax} values derived using the one-point method were therefore pooled with A-C_i-derived V_{cmax} values for analysis, and the potential error introduced through the use of two different derivation methods was accounted for in the statistical analysis by including in model selection an explanatory variable describing the derivation method (explained in more detail in section 4.3.7).

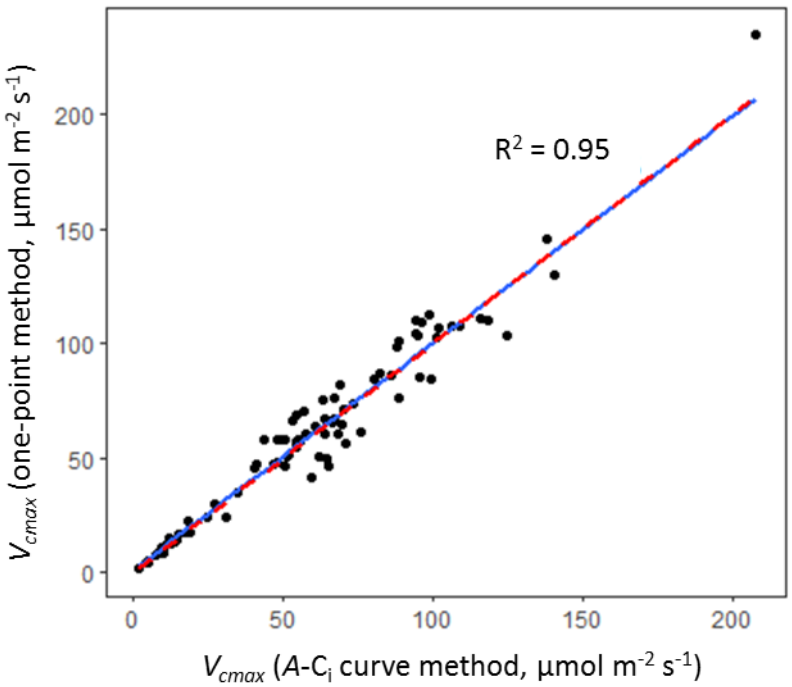

Figure 4.2. Plot of V_{cmax} values derived from A-C_i curves versus V_{cmax} values calculated using the one-point method (De Kauwe et al., 2016) from the corresponding A_{sat} value extracted from each curve (A at 400 µmol mol^{-1} CO_2). The blue line represents the linear regression model fit ($p < 0.001$, adjusted $r^2 = 0.95$, line equation: $y = 0.99x + 1.33$). The red dashed line represents the line of x=y. Data for this comparison comprise a subset of the A-C_i curve dataset used in this study.

4.3.4 Modelling O_3 flux

Stomatal O_3 flux to the flag leaf was modelled in each treatment and for both years, to derive a measure of exposure that accounted for the environmental influence on O_3 uptake, and that could be tracked over time. Flux was modelled using the multiplicative g_{sto} module of the DO_3SE model (Emberson *et al.*, 2000a; Emberson *et al.*, 2000d; Simpson *et al.*, 2012), which has a published parameterisation for European wheat (CLRTAP, 2017; Grünhage *et al.*, 2012; Pleijel *et al.*, 2007) and has been applied previously to model O_3 flux to this crop (González-Fernández *et al.*, 2013; Klingberg *et al.*, 2011). A summary of the DO_3SE algorithms and parameters used in this study are presented in section 4.7.1 of the supporting information.

Ozone flux for wheat is accumulated above a detoxification threshold of six in the DO_3SE methodology (producing the POD_6SPEC flux metric – species-specific phytotoxic O_3 dose above a threshold of 6, mmol m^{-2} PLA s^{-1}, previously known as the POD_6, with "SPEC" referring to the species-specific version of the DO_3SE model) (CLRTAP, 2017), as this threshold has produced the closest correlation between POD and wheat yield in previous experiments (Pleijel *et al.*, 2007). However, as thresholds of physiological effect in wheat have

been far less studied, the POD_0SPEC (where no threshold for accumulation is applied, previously known as the POD_0) was also calculated, in order to avoid assuming a threshold of effect. Modelled POD_0SPEC and POD_6SPEC for 2015 and 2016 O_3 treatments are shown in Figure 4.3.

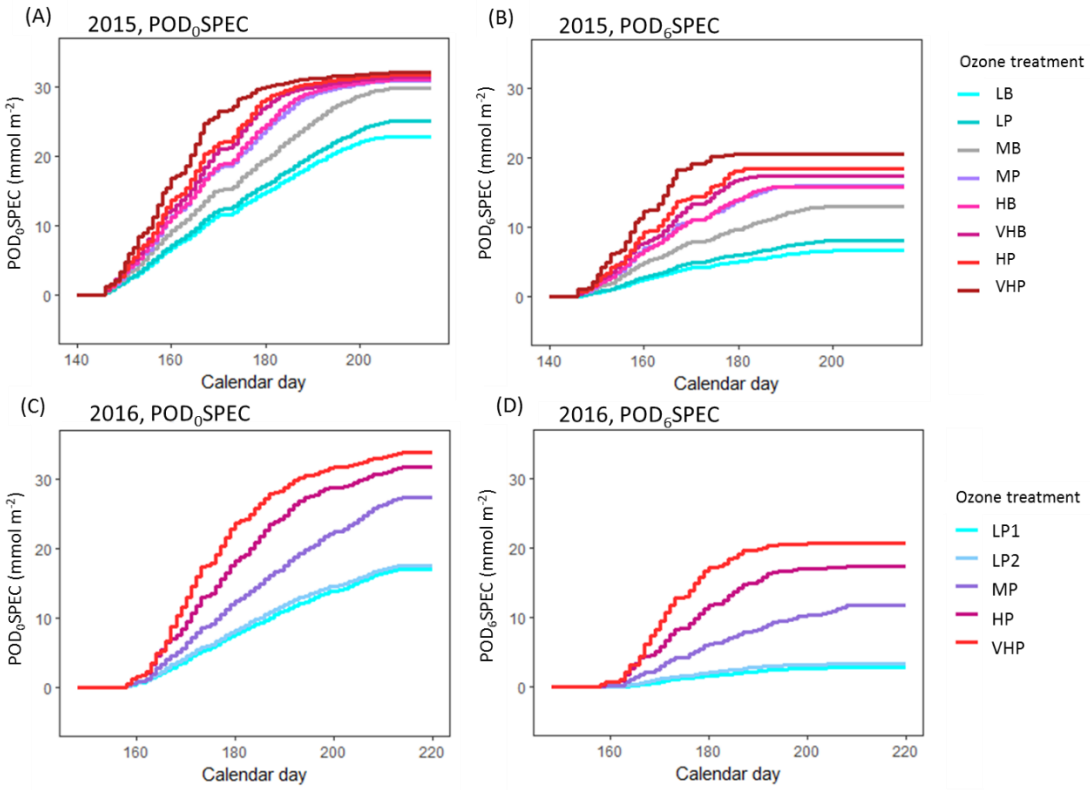

Figure 4.3. Modelled O_3 flux over time in the different O_3 treatments. (A) POD_0SPEC in 2015; (B) POD_6SPEC in 2015; (C) POD_0SPEC in 2016; (D) POD_6SPEC in 2016. Each O_3 treatment in both years was categorised based on the 24-hour mean exposure (L =low, M = medium, H = high, VH = very high) and the characteristic profile of exposure (P = peak, B = background).

4.3.5. Alignment of physiological observations with O_3 flux, and calculation of mean flux exposure (mean daily POD_0SPEC)

Each physiological observation (CCI, A_{sat}, V_{cmax}, J_{max}, g_{sto}) was aligned with the treatment-specific accumulated POD_0SPEC and POD_6SPEC on the day of measurement, and at the exact time of measurement wherever this data was available (referred to hereafter in this paper as 'accumulated POD_0SPEC' and 'accumulated POD_6SPEC'). This was done to allow the impact of real-time O_3 flux exposure on physiology to be analysed. The mean daily POD_0SPEC (i.e. the average accumulation of flux per day, mmol m^{-2} PLA day^{-1},) was also calculated for each O_3 treatment, to act as a metric of mean exposure intensity. Mean daily POD_0SPEC values for each O_3 treatment are presented in the results section in Table 4.1. Mean daily POD_0SPEC was

calculated as the average of daily POD_0SPEC accumulation, from A_{start} until the modelled onset of senescence.

4.3.6. Data standardisation

The two experiments had different sowing and harvest calendars; time was therefore standardised by calculating thermal time from plant emergence onwards (daily mean temperature sum > 0 °C). Physiological data was also standardised, by conversion from raw to relative values. This was done to account for differences in instrument calibration between years, and to account for differences in beginning of season 'baseline' physiology between cultivars. Relative values for the physiological observations were calculated by deriving a reference value for each parameter (CCI, A_{sat}, V_{cmax}, J_{max}, g_{sto}) and each cultivar-year combination (i.e. Mulika in 2015, Skyfall in 2015, Skyfall in 2016). The reference value - calculated as the 90th percentile value of all observations, spanning the whole season and all treatments - was considered as optimal physiological performance and was used as the baseline for calculating relative change. Skyfall CCI data from 2016 comprised too few data points for the derivation of an individual reference value; 2016 and 2015 CCI data for Skyfall was therefore combined to produce a single reference value for Skyfall, as CCI data for Skyfall was found to not significantly differ by year ($p = 0.06$ in regression model). A comparison of CCI data for Skyfall measured in 2015 and 2016 can be found in section 4.7.3 of the supporting information.

4.3.7 Statistical analysis

Statistical analysis was conducted in R version 3.3.2 (R Core Team, 2016), and either involved linear regression or linear mixed models (LMMs) using the package lme4 (v1.17, Bates *et al.*, 2015). Model selection was by AIC (Akaike Information Criterion). The model with the lowest AIC was considered the 'best' model of those fitted, and models differing in < 2 AIC units from the best model were defined as having little empirical support (Burnham and Anderson, 2002). Wherever relevant, a random factor describing solardome number was included in models to account for multiple measurements made within domes, and unique pot ID was a random factor when analysis involved multiple measurements made from the same pot. P-values were obtained for terms in the optimal models using the R package lmerTest, v2.0-33 (Kuznetsova *et al.*, 2016). Assumptions of normality and even spread of residuals were checked using residual plots, and data were transformed where necessary. Four key analyses were conducted as part of this study, and are described in more detail below.

4.3.7.1 Identification of O_3 treatments with significantly accelerated senescence:

Flag leaf CCI data was analysed in all O_3 treatments to test for accelerated senescence. Each elevated O_3 treatment was paired in turn with the control treatment for that experiment, and the

significance of the thermal time/mean daily POD_0SPEC interaction term was tested using LMMs. Control treatments were defined as the lowest in terms of mean daily POD_0SPEC, and comprised treatment LB for the 2015 experiment and treatment LP2 for the 2016 experiment.

4.3.7.2 Analysis of O_3 effect on the timing of senescence onset and completion:

The impact of O_3 on leaf senescence onset and completion was examined using regression models, fitted to each of the 2015 O_3 treatments (separately for the two cultivars). It was not possible to conduct this analysis for 2016, as 2016 CCI measurements only spanned 22 days. Regression models comprised relative CCI as the dependent and thermal time as the independent variable, and the shape of response was determined by comparing linear, quadratic and cubic models. The best model for each O_3 treatment was then used to determine i) thermal time at leaf senescence onset, ii) thermal time at senescence completion, and iii) the post-anthesis curve integral (i.e. area under the curve), as shown in Figure 4.4. Thermal time at senescence onset was aligned with the accumulated POD_0SPEC at that time for each O_3 treatment, to identify the accumulated flux 'trigger' values for senescence onset.

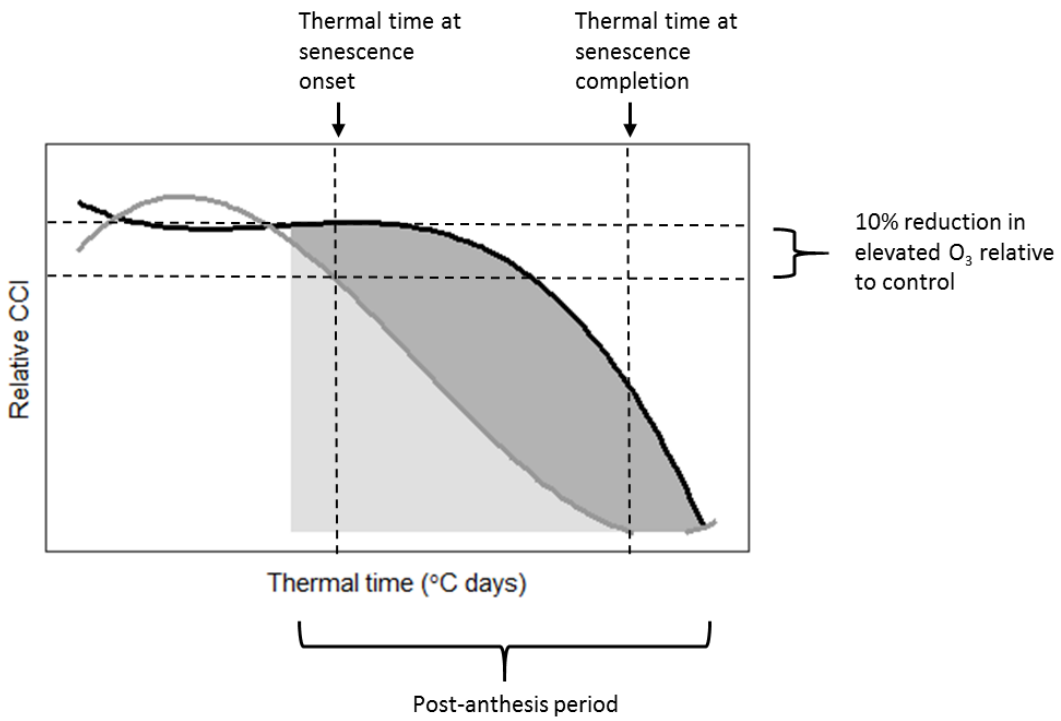

Figure 4.4. Summary of methods used to derive i) thermal time at leaf senescence onset, defined as a 10% reduction in relative CCI in the elevated treatment (grey line) relative to the control (black line); ii) thermal time at senescence completion, defined by the x-abscissa of the treatment regression line; iii) the post-anthesis integral of the regression curve, indicated on the plot as shaded regions (Post-anthesis period in 2015 = 1142 °C days onwards). Diagram not to scale.

4.3.7.3 Analysis of relative timing of O_3 effects on different aspects of physiology:

The effect of accumulated POD_0SPEC on CCI, A_{sat}, V_{cmax}, J_{max}, and g_{sto} during successive periods of the growing season was analysed, to identify when O_3 began to influence physiology. The range of thermal time spanned by flag leaf physiological measurements was divided into six thermal time bins of equal width. The effect of accumulated POD_0SPEC on each parameter, within each time-bin and for each cultivar-year combination, was analysed by comparing model fit with and without accumulated POD_0SPEC as an explanatory variable. An additional explanatory variable was included in model selection for V_{cmax}, describing the derivation method (i.e. A-Ci curve or one-point method).

4.3.7.4 Comparison of flux and concentration-based O_3 exposure metrics for predicting physiological response:

Accumulated POD_0SPEC, accumulated POD_6SPEC, 24-hour mean concentration and AOT40 (accumulated O_3 > 40ppb during daylight hours) were compared in their ability to predict the response of CCI, A_{sat}, V_{cmax}, J_{max}, and g_{sto} during the 5th thermal time bin. The 5th time bin was selected for this analysis as most physiological parameters exhibited a response to O_3 exposure during this time. For each physiological parameter, LMMs constructed with each of the metrics of O_3 exposure were compared for model fit. An explanatory variable describing whether O_3 had been administered as a 'peak' or 'background' profile was also included in model selection, to test whether the O_3 metric that produced the best model fit also accounted for different patterns of exposure.

4.4 Results

4.4.1 Ozone exposure in 2015 and 2016

Table 4.1 summarises the O_3 treatments administered in 2015 and 2016 using a number of exposure indices including the 24-hour mean (ppb), the seasonal AOT40 (ppm h), and the mean daily POD_0SPEC (mmol m^{-2} PLA day^{-1}). Treatments with a 'peak' style profile in 2015 resulted in a higher AOT40 and mean daily POD_0SPEC, compared to the paired 'background' treatment with a matched 24-hour mean. For example, the VHB and VHP treatments in 2015 shared a similar 24-hour mean (56.8 ppb and 55.7 ppb), but the VHP treatment had a far higher mean daily POD_0SPEC (1.07 mmol m^{-2} day^{-1}) compared to the VHB treatment (0.78 mmol m^{-2} day^{-1}).

Table 4.1. Summary of O_3 treatments administered in the 2015 and 2016 experiments, using a range of concentration-based and flux-based metrics. 24-hour mean, AOT40 and mean daily peak O_3 have been calculated over the full O_3 exposure period, whereas the mean POD_0SPEC, POD_0SPEC and POD_6SPEC quantifies exposure in the flag leaf only (i.e. calculated over the period following flag leaf emergence).

Season	Ozone treatment	24-hour mean (ppb)	AOT40 (ppm h)	Mean daily peak O_3 (ppb)**	Mean daily POD_0SPEC (mmol m^{-2} PLA day^{-1})	POD_0SPEC (mmol m^{-2} PLA)	POD_6SPEC (mmol m^{-2} PLA)
2015	LB	26.94	0.002	33.21	0.43	22.87	6.64
	LP	30.39	0.02	36.44	0.46	25.19	8.17
	MB	37.42	4.19	47.74	0.57	29.91	13.03
	MP	40.39	14.51	67.59	0.69	30.99	15.95
	HB	50.06	12.49	56.73	0.71	31.10	15.8
	HP	50.14	28.56	91.90	0.82	31.79	18.48
	VHB	56.81	19.45	66.28	0.78	31.42	17.36
	VHP	55.73	40.03	116.55	1.07	32.16	20.55
2016	LP1	23.42	0.01	31.44	0.36	17.66	3.47
	LP2	22.05	0.03	30.73	0.34	17.11	2.93
	MP	30.41	6.003	55.75	0.54	27.36	11.90
	HP	39.72	21.25	81.04	0.78	31.87	17.39
	VHP	50.14	37.54	113.93	1.04	33.91	20.72

**** Mean daily peak O_3 has been calculated only from the 'full treatment' days (i.e. days when full elevated O_3 was applied, five days per week).**

4.4.2 Response of CCI over time and in elevated O_3

Relative CCI declined over the course of the growing seasons in all cultivar-year combinations, and O_3 accelerated this senescence (Figure 4.5). A substantial difference in the senescence response of the two cultivars was observed. In the 2015 experiment, cv. Mulika exhibited O_3-induced early senescence only in the highest treatment (VHP) (Figure 4.5A), whereas for cv. Skyfall in the same year, all treatments exhibited accelerated senescence relative to the control (Figure 4.5B). In 2016 for Skyfall, the three highest O_3 treatments exhibited accelerated senescence (Figure 4.5C). A statistical summary of this analysis is reported in Table 4.6, in section 4.7.6 of the supporting information.

Analysis conducted within the different thermal time groupings indicated that a significant negative effect of O_3 on CCI was observed substantially earlier in the season for Skyfall compared to Mulika. For Skyfall In 2015, accumulated POD_0SPEC was significantly negatively associated with flag leaf CCI from the third thermal time group onwards (1109 – 1337 °C days), after 25-36 days of O_3 exposure. For Mulika in 2015, accumulated POD_0SPEC was significantly negatively associated with CCI only at the fifth thermal time group (1568 – 1796 °C days), after 49-59 days of O_3 exposure. The limited CCI data for Skyfall in 2016 supports the 2015 results, with a significant negative association between accumulated POD_0SPEC and CCI observed in the 3rd and 4th thermal time-bins. A significant positive association between accumulated POD_0SPEC and CCI was observed for Skyfall in 2015, in thermal time group one (649-879 °C

days) spanning the first 14 days of O_3 exposure. A statistical summary of the time-bin analysis is presented in Table 4.7, in section 4.7.6 of the supporting information.

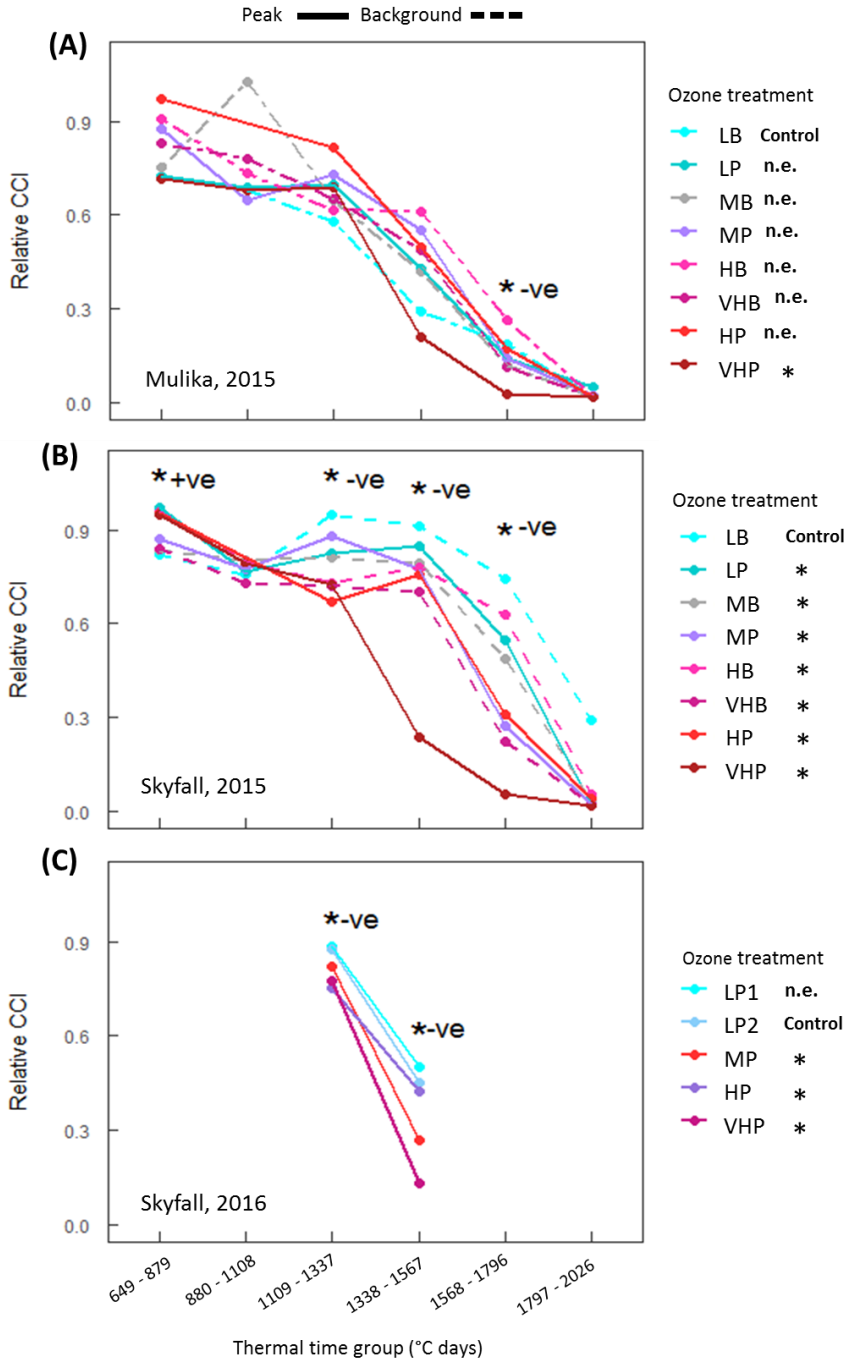

Figure 4.5. Average relative chlorophyll content index (CCI) of flag leaves for six thermal time groups, for (A) cv. Mulika in 2015, (B) cv. Skyfall in 2015 and (C) cv. Skyfall in 2016. Time-bins where a statistically significant association between CCI and accumulated POD_0SPEC was observed are marked with an asterisk (*). The direction of O_3 effect - i.e. positive (+ve) or negative (–ve) effect on CCI - is also shown. Ozone treatments which exhibited a significant early decline in CCI relative to the control treatments are marked in the figure keys with asterisks (*), and those which showed no effect are marked as n.e. (no effect).

4.4.3 Effect of O_3 on senescence onset and completion

The timing of leaf senescence onset and completion was influenced by O_3 exposure. For both cultivars in 2015, leaf senescence onset occurred earlier in O_3 treatments with higher mean daily POD_0SPEC, although this trend was only statistically significant for Mulika (Figure 4.6A). On average, O_3-induced senescence onset occurred later in the season for Mulika (1725 °C days) compared to Skyfall (1216 °C days). Senescence completion also occurred earlier in O_3 treatments with a higher mean daily POD_0SPEC, according to a linear relationship exhibited by both cultivars (Figure 4.6B). Completion of senescence occurred at a similar thermal time on average for both cultivars (Mulika = 1841 °C days; Skyfall = 1867 °C days). The total duration of the O_3-induced senescence period was therefore longer on average for Skyfall relative to Mulika.

Skyfall also exhibited a linear reduction in the CCI-thermal time curve integral as the mean daily POD_0SPEC increased (Figure 4.6C). This indicates that Skyfall exhibited reduced CCI in the flag leaf throughout the post-anthesis period in elevated O_3. No significant association between mean exposure and curve integral was found for Mulika, although the highest treatment in terms of mean flux exposure (VHP) did exhibit a reduced integral compared to the other treatments.

4.4.4 Ozone flux at onset of early senescence

Accumulated O_3 flux at the onset of leaf senescence, for all of the treatments in 2015 which exhibited significant accelerated senescence, is shown in Table 4.2. In the highest O_3 treatment (VHP), senescence onset occurred at a substantially lower accumulated POD_0SPEC for the cultivar Skyfall (25.7 mmol m^{-2}) compared with Mulika (30.1 mmol m^{-2}). When accumulated POD_0SPEC and POD_6SPEC at senescence onset are compared across the different O_3 treatments for the cultivar Skyfall, senescence onset was observed to occur across a fairly wide range of accumulated flux (15.3 – 25.7 mmol m^{-2} POD_0SPEC; 6.5 – 18.6 mmol m^{-2} POD_6SPEC). The range of flux at senescence onset was more narrow when flux was calculated without a detoxification threshold (POD_0SPEC flux range = 10.4 mmol m^{-2}; POD_6SPEC flux range = 12.1 mmol m^{-2}), and considerably more narrow when only the five highest O_3 treatments – which exhibited the strongest accelerated senescence response – are considered (POD_0SPEC flux range of five highest treatments = 3.7 mmol m^{-2}; POD_6SPEC flux range of five highest treatments = 5.7 mmol m^{-2}).

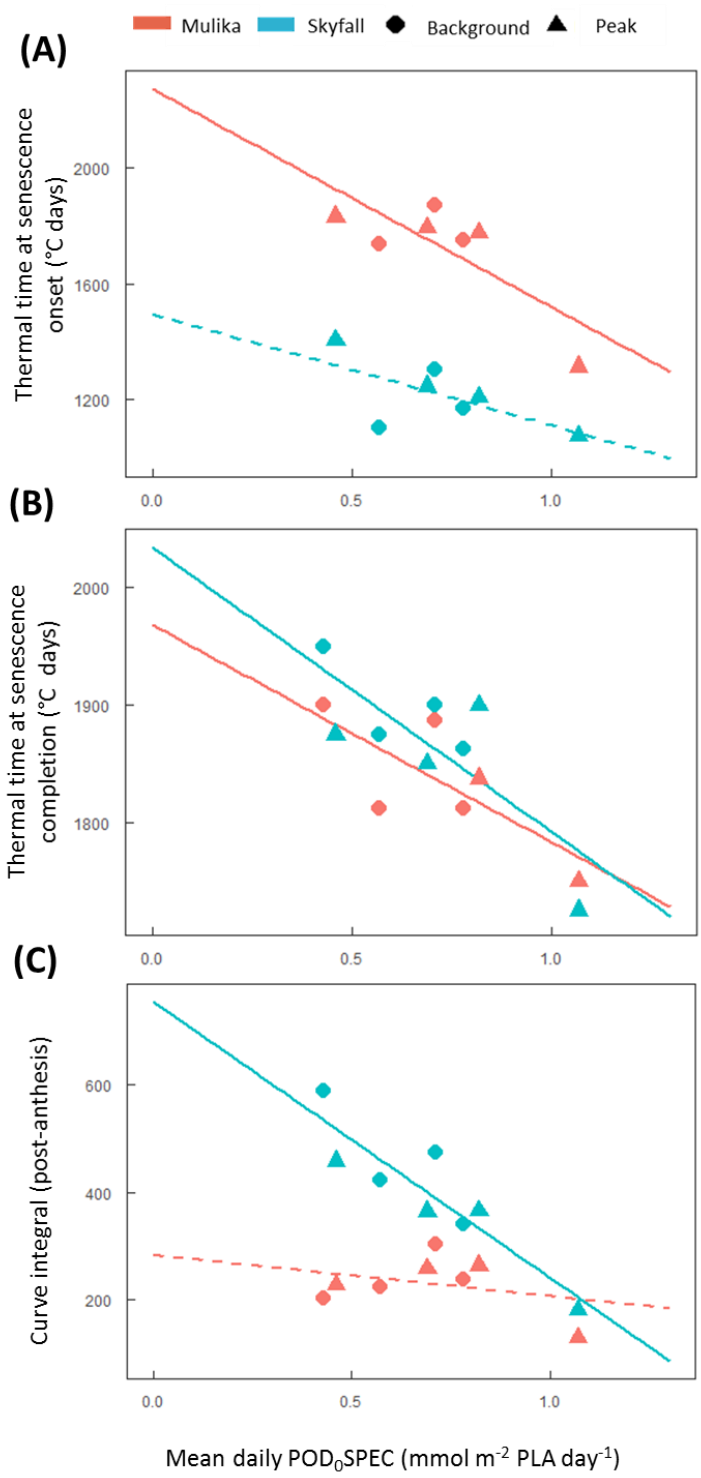

Figure 4.6. Effect of O_3 on the onset and completion of leaf senescence in 2015. (A) Thermal time at senescence onset versus the mean daily POD_0SPEC in each treatment (B) Thermal time at senescence completion versus mean daily POD_0SPEC in each treatment. (C) Area under the post-anthesis section of the CCI-thermal time curve versus the mean daily POD_0SPEC in each treatment. Solid trend lines indicate a significant regression ($p < 0.05$); dashed lines indicate that the trend was not significant.

Table 4.2. Accumulated flux (POD_YSPEC) at the onset of O_3-induced senescence, for 2015 treatments which exhibited significant accelerated senescence.

Cultivar	O_3 Treatment (2015)	POD_0SPEC at senescence onset (mmol m^{-2})	POD_6SPEC at senescence onset (mmol m^{-2})
Skyfall	LP	17.8	6.5
	MB	15.3	7.9
	MP	22.0	12.9
	HB	24.7	14.1
	HP	25.1	16.2
	VHB	22.9	14.4
	VHP	25.7	18.6
Mulika	VHP	30.1	20.6

4.4.5 Response of photosynthesis and g_{sto} over time and in elevated O_3

Figure 4.7 presents combined datasets for four leaf-level physiological parameters capable of short-term or 'instantaneous' change in response to environmental stimuli (A_{sat}, V_{cmax}, J_{max} and g_{sto}). Data has been combined across all three cultivar-year combinations, and the hue of each data point corresponds to the accumulated POD_0SPEC at the time of measurement (an equivalent figure indicating the accumulated POD_6SPEC at the time of measurement is presented in section 4.7.4 of the supporting information). The average physiological values for high and low O_3-treated plants within each time-bin are also shown on the plots. The average 'low' value represents the mean value for the lowest 2015 treatment (LB) and lowest 2016 treatment (LP2) combined. The average 'high' value represents the mean value for the highest 2015 treatment (VHP) and the highest 2016 treatment (VHP) combined. A decline in the photosynthetic parameters (A_{sat}, V_{cmax}, J_{max}) was observed across the growing season, and this decline was accelerated in high O_3. g_{sto} did not decline over time in low O_3, but did decline over the course of the season in high O_3.

The outcome of LMM analysis carried out on each combination of cultivar and year, and in each thermal time group, for the parameters A_{sat}, V_{cmax}, J_{max} and g_{sto}, is shown in Figure 4.8. A full statistical summary of this analysis is presented in Tables 4.8 – 4.11 in section 4.7.6 of the supporting information. Grey regions on plots denote the period following the observation of a significant negative effect of accumulated POD_0SPEC on flag leaf CCI. Across all cultivar-year combinations, no significant negative effects of accumulated POD_0SPEC on any of the instantaneous physiological parameters was observed before negative effects of accumulated POD_0SPEC on CCI were observed. A significant negative association of accumulated POD_0SPEC on the parameters V_{cmax} and J_{max} was not observed until the 5th thermal time bin (1568 – 1796 °C days).

Some evidence of heightened physiological performance in the early-season in high O_3 was observed across all combinations of cultivar and year, although the pattern was not consistent across the three combinations. A significant positive association between accumulated POD_0SPEC and physiology in either the first or second time-bin was observed i) for J_{max} in cv. Mulika in 2015; ii) for A_{sat} and g_{sto} in cv. Skyfall in 2015; and iii) for A_{sat} and V_{cmax} in cv. Skyfall in 2016.

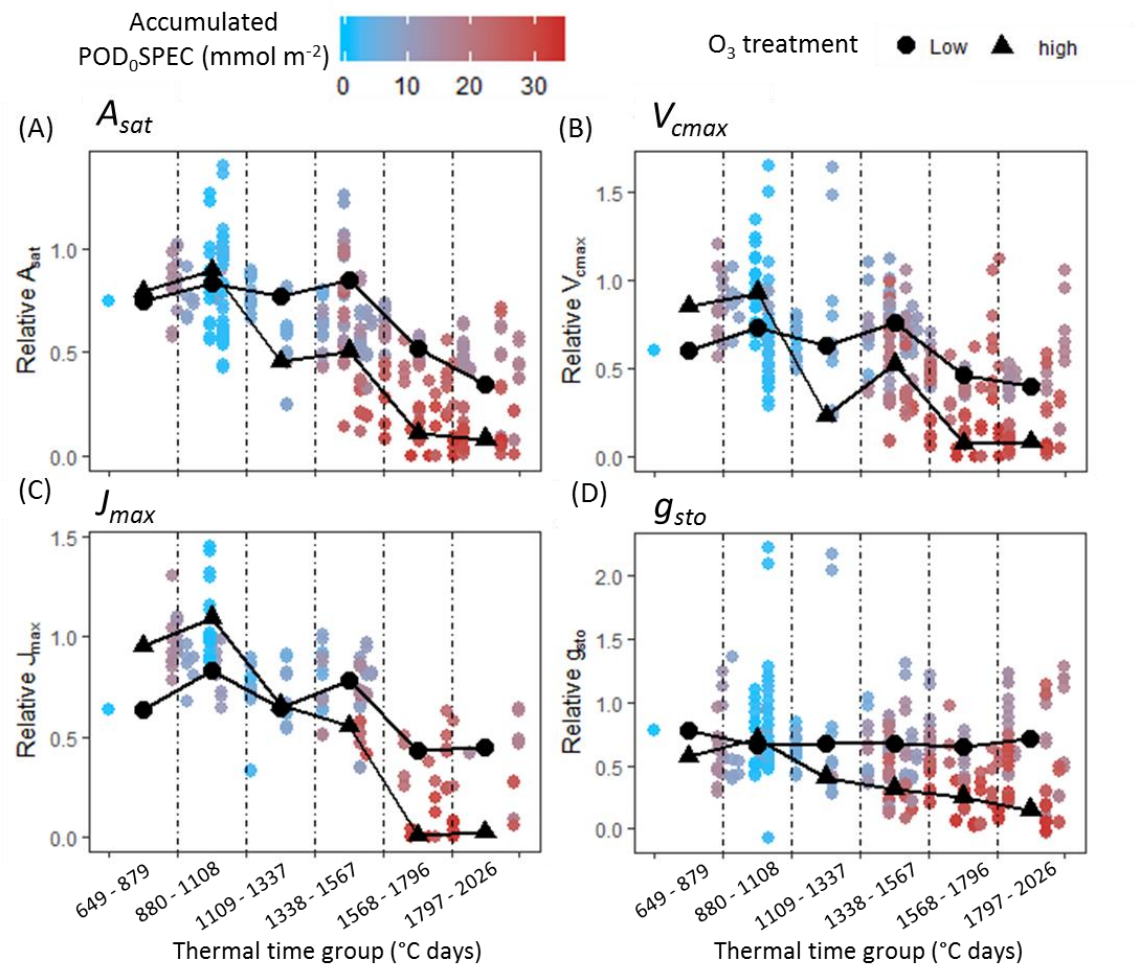

Figure 4.7. Flag leaf data for (A) A_{sat}, (B) V_{cmax}, (C) J_{max}, and (D) g_{sto}, combined across all cultivar-year combinations. The hue of each data point corresponds to the accumulated POD_0SPEC at the moment of measurement. Mean values of physiological parameters in low O_3-treated plants (averaged across 2015 LB and 2015 LP2 treatments) and high O_3-treated plants (averaged across 2015 VHP and 2016 VHP treatments) are shown as black data points on the plots.

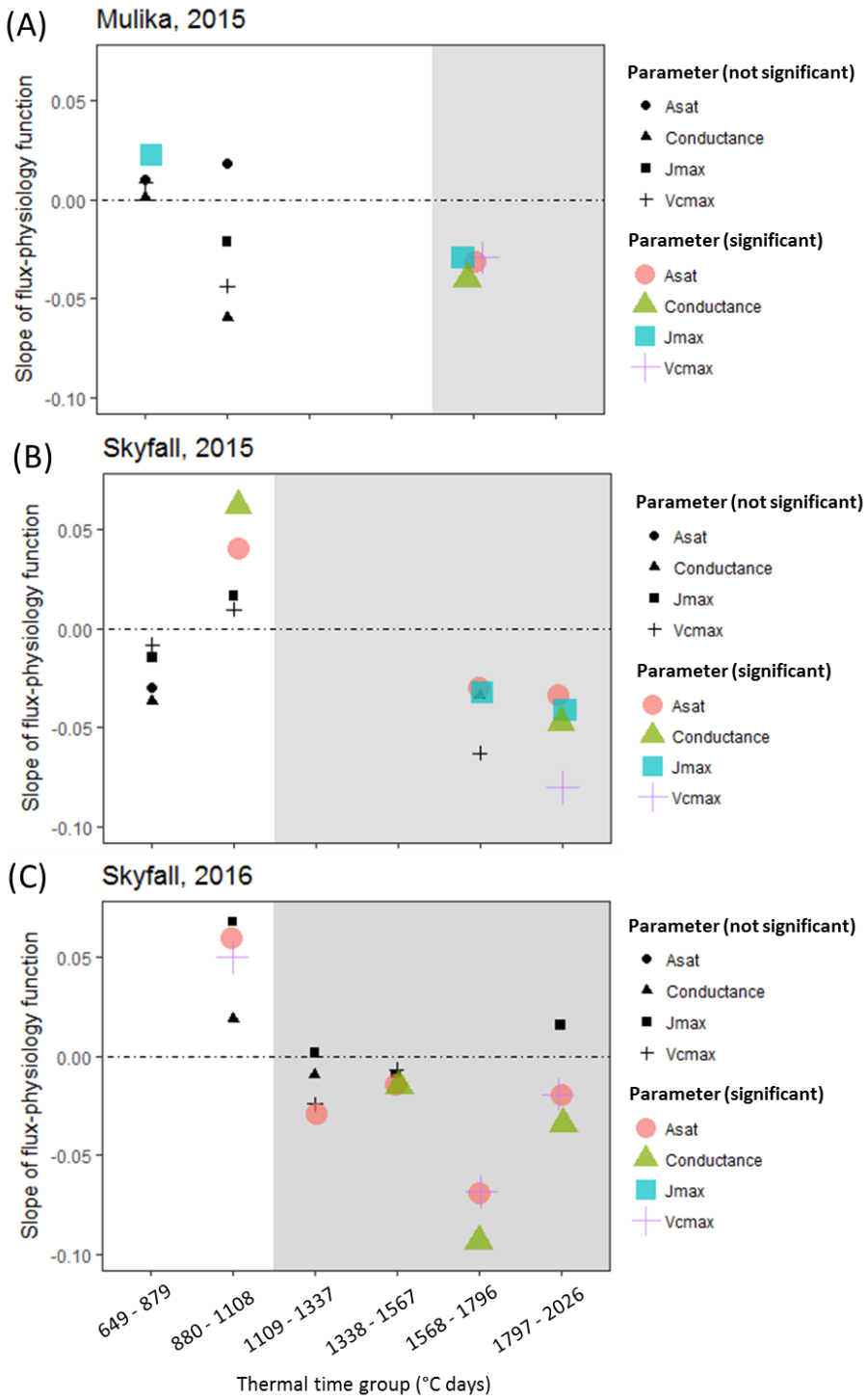

Figure 4.8. Plots showing the response of A_{sat}, V_{cmax}, J_{max}, and g_{sto} to O_3 flux. The y-axis represents the accumulated POD_0SPEC-physiology slope in the 'best' LMM model for each thermal time group. Positive slope indicates a positive effect of O_3 on the physiological variable; a negative slope indicates a negative effect. (A) cv. Mulika in 2015, (B) cv. Skyfall in 2015, (C) cv. Skyfall in 2016. Coloured symbols indicate a significant POD_0SPEC-physiology association; black symbols indicate no statistically significant physiological response. Grey regions on plots indicate the period following an observed significant effect of O_3 on flag leaf CCI.

4.4.6 Comparison of O_3 exposure metrics for predicting physiological response to O_3

For all measured physiological parameters (CCI, A_{sat}, V_{cmax}, J_{max}, g_{sto}) and for both cultivars, a flux-based metric of exposure was better at predicting physiological response of wheat to O_3, compared to the concentration-based metrics (24-hour mean and AOT40) (Table 4.3). For four out of the ten model sets created in this analysis, the accumulated POD_0SPEC (i.e. without a threshold for accumulation) produced the best model fit. For the other six model sets, the accumulated POD_0SPEC and POD_6SPEC metrics were equally good at predicting physiological response. The O_3 flux metric with no threshold for accumulation was therefore equal to, or better than, the O_3 flux metric with a detoxification threshold at predicting the physiological response to O_3.

The inclusion of an explanatory variable describing the profile of O_3 exposure in the 'best' model did not improve fit in nine out of the ten model sets created with the accumulated POD_0SPEC metric, and in all models created with the accumulated POD_6SPEC metric. Using O_3 flux as the metric of exposure therefore accounts for differences in the O_3 exposure resulting from peak-dominated treatments and those featuring a consistent background level, in the majority of cases.

Table 4.3. Summary of LMM analysis to determine whether accumulated POD_0SPEC, accumulated POD_6SPEC, 24-hour mean, or AOT40 represent the best predictor of physiology in the 5th thermal time-bin. The lowest AIC for each parameter and cultivar – indicating the best model – is highlighted in grey. The outcome of model selection to determine if the profile of O_3 exposure (i.e. peak versus background) was important in the flux-based models is also shown.

Parameter	Cultivar	AIC: POD_0SPEC	AIC: POD_6SPEC	AIC: AOT40	AIC: 24-hour mean	O_3 profile important in POD_0SPEC model?	O_3 profile important in POD_6SPEC model?
CCI	Mulika	-62.8	-60.5	-59.2	-58.3	No	No
	Skyfall	3.7	10.4	12.3	15.0	No	No
A_{sat}	Mulika	-0.5	1.3	4.1	3.2	No	No
	Skyfall	-82.9	-68.0	-48.1	-54.2	No	No
V_{cmax}	Mulika	6.1	6.9	9.9	9.0	No	No
	Skyfall	-63.0	-62.9	-34.6	-32.3	No	No
J_{max}	Mulika	-1.7	0.2	3.2	2.3	No	No
	Skyfall	6.3	7.3	9.2	9.5	Yes	No
g_{sto}	Mulika	13.4	14.8	17.3	16.5	No	No
	Skyfall	-19.1	-7.3	2.7	-1.6	No	No

4.5 Discussion

The first aim of the data analysis presented here was to assess whether published approaches for modelling O_3-induced senescence are able to account for inter-cultivar variation in response. Both cultivars exhibited accelerated senescence in response to O_3 exposure, but the pattern of response differed according to cultivar. In 2015, significant accelerated senescence was observed in seven O_3 treatments for Skyfall, but only in the highest treatment for Mulika, suggesting a higher level of O_3 tolerance in Mulika (Figure 4.5). This differential tolerance is also indicated by the earlier appearance of significant O_3 effects on leaf CCI across all treatments for Skyfall compared to Mulika. The completion of leaf senescence occurred progressively earlier – and hence, total leaf duration became progressively shorter - in both cultivars as average O_3 flux (mean daily POD_0SPEC) in the treatment increased (Figure 4.6B), according to a linear relationship. Completion of leaf senescence occurred at a similar thermal time in both cultivars (Mulika = 1841 °C days, Skyfall = 1867 °C days), meaning that the total senescence duration was longer for Skyfall. While O_3-induced senescence in Mulika was characterised by a sudden drop in leaf CCI towards the end of the season, Skyfall exhibited a more gradual O_3-induced decline in CCI.

The linear relationship between mean flux and total leaf duration observed in this study for both cultivars gives support to the senescence function of Ewert and Porter (2000), which assumes a linear decline in mature leaf lifespan as O_3 exposure increases. However, the differential senescence duration in the two cultivars suggests that a key assumption of the Ewert and Porter (2000) function – that leaf senescence will always comprise the final third of the mature leaf lifespan – may not hold true for all cultivars, and the duration of leaf senescence is also likely to vary with O_3 exposure. For example, in 2015 for cv. Skyfall, leaf senescence in the highest O_3 treatment comprised 76.7% of the total life of the flag leaf (flag leaf emergence = 877 °C days, leaf senescence onset = 1075 °C days, senescence completion = 1725 °C days). The inter-cultivar variation in senescence response observed in this study would therefore only be captured by the Ewert and Porter (2000) senescence function if the proportion of the leaf lifespan that comprises leaf senescence – represented by the parameter $t_{l,se}$ – can be calibrated for different cultivars. The results of this study suggest that in order to effectively model variation in the pattern of O_3-induced senescence, the timing of senescence onset, and the rate (or duration) of senescence, need to be able to be calibrated to experimental data. The DO_3SE O_3 senescence function published by Danielsson *et al.* (2003) theoretically fulfils these criteria, as the O_3 flux 'trigger' for senescence, and parameters describing the senescence rate and hence determining the timing of senescence completion, are already identified as requiring definition.

However, analysis in this paper highlights the degree of error associated with the approach adopted by Danielsson *et al.* (2003) for modelling the onset of O_3-induced senescence using a

threshold of accumulated flux. Following this approach, onset of senescence may occur at different points in time at different levels of mean exposure, but should occur at approximately the same value of accumulated flux. This method was designed in the absence of a known mechanism for induction of senescence by O_3, but could be interpreted mechanistically if accumulated O_3 flux is assumed to be proportional to increased respiratory effort integrated over the course of the season, which has been proposed as a potential trigger for O_3-induced senescence (Ewert and Porter, 2000). For Skyfall, across the five highest O_3 treatments in 2015, onset occurred across a POD_0SPEC range of 22.0-25.7 mmol m^{-2}. Given the limitations associated with the method applied in this study for defining senescence onset – arbitrarily defined as a 10% reduction in leaf CCI relative to the control treatment – as well as the inherent variation that exists between seedlings, this flux range can be considered relatively narrow. However, when all treatments which exhibited a significant O_3 effect on senescence are considered for Skyfall in 2015, the range of flux at senescence onset is considerably wider (17.8 – 25.7 mmol m^{-2} POD_0SPEC). These results provide an estimate of the degree of error likely to be associated with applying this type of approach in models, and suggest that accumulated respiratory effort as the trigger for O_3-induced senescence may be too simplistic as a mechanistic interpretation.

A second key objective of this study was to test the hypothesis that O_3 reduces photosynthetic rate in the short term by reducing carboxylation capacity of rubisco (V_{cmax}). The assumption that O_3 reduces V_{cmax} is central to the 'instantaneous' O_3 effect function proposed by Martin *et al.* (2000). A version of this function is also applied by Ewert and Porter (2000), where O_3 is assumed to reduce photosynthesis in a short-term and reversible way, in addition to and independent of the O_3 senescence effect. The analysis presented here of O_3 effects on physiological parameters during different thermal time segments of the growing season found that a significant negative effect of O_3 on photosynthesis and g_{sto} was only observed concurrent with O_3-induced leaf senescence (Figure 4.8). This result was consistent across all combinations of cultivar and year. For Skyfall in 2015 and 2016, significant negative effects of O_3 on A_{sat} were observed *before* a negative association between O_3 and V_{cmax}, suggesting that reduced carboxylation capacity is not responsible for the initial reduction in photosynthetic capacity observed in these experiments. There was therefore no evidence of an 'instantaneous' effect of O_3 on the photosynthetic mechanism occurring, in the period preceding leaf senescence.

These results contradict several studies which observed short-term reduction in photosynthetic rate in response to O_3 (Dann and Pell, 1989; Farage and Long, 1995; Farage *et al.*, 1991). One possible explanation for this contradiction is that instantaneous reduction of carboxylation capacity by O_3 may only be relevant at acute concentrations. The reduced carboxylation efficiency reported by Farage *et al.* (1991) was observed following 4-16 hours of exposure at unrealistically high O_3 concentrations of 200-400 ppb – considerably higher hourly

concentrations compared to those used in the experiments described in this study, which more closely mimic ambient conditions (maximum hourly O_3 exposure of 117 ppb). The results presented here therefore indicate that accelerated senescence is likely to be more important than short-term effects on photosynthesis for determining crop yield loss in most agricultural landscapes, where O_3 concentrations are typically moderate for the majority of the time with occasional peaks in concentration. Understanding and simulating the early senescence response to O_3 should therefore be the priority for O_3 experimentalists and modellers.

Alternatively, the results presented here could be explained by a differential response to O_3 in younger and older leaves. Bernacchi *et al.* (2006) and Morgan *et al.* (2004) observed in field experiments with soybean that O_3 effects on photosynthesis and g_{sto} were not apparent in new fully expanded leaves, and Reichenauer *et al.* (1998) saw similar results in three cultivars of wheat. Younger leaves may have a higher tolerance than older leaves to O_3, or alternatively the O_3 effect on photosynthesis may be associated with a cumulative build-up of O_3 damage in leaves. Either way, the age-dependency of O_3 effects is an important consideration in O_3 effects modelling. The function described by Ewert and Porter (2000) for modelling short-term effects of O_3 on photosynthesis allows for leaf age to influence the rate of overnight recovery from O_3 damage, but not the threshold for damage. The role of leaf age in determining O_3 flux thresholds would benefit from further investigation.

A surprising result from the data analysis is that O_3 had a significant positive effect on a number of physiological parameters early in the season. CCI, A_{sat}, V_{cmax} and g_{sto} all exhibited a positive association with O_3 exposure for one or more of the cultivar-year combinations, in either the first or second thermal time group (up to 32 days following beginning of exposure). Stimulation of photosynthesis and g_{sto} in wheat during the first few weeks of O_3 exposure was also observed by Mulholland *et al.* (1997b) in their open-top chamber experiment, although generally there are few reported cases of this phenomenon in crop species. Ozone-induced physiological stimulation could be an adaptive response associated with plant defence responses – for example, heightened g_{sto} and photosynthesis may enable the upregulation of antioxidant synthesis. Observations that yield can actually be stimulated at low O_3 exposure concentrations have also given rise to the theory that free radicals, at low concentrations, can act as growth promotors in plants (Wilkinson and Davies, 2010). An alternative hypothesis is that the observed early-season physiological boost in this study is related to disruption of stomatal control by O_3, as has been observed in some grassland species (Mills *et al.*, 2009; Wilkinson and Davies, 2009), leading to heightened g_{sto} and an associated boost in other physiological parameters. More experimental data is needed in order to establish if the early-season physiological boost induced by O_3 in this study is consistent across other plant species and environments.

The third aim of this study was to test whether O_3 flux would be a better predictor of physiological response than concentration-based metrics of O_3 exposure (AOT40 and 24-hour mean). Analysis showed that flux was superior at predicting the response to O_3 of five physiological variables (CCI, A_{sat}, V_{cmax}, J_{max}, g_{sto}) in regression models, for both cultivars (Table 4.3). Previous studies have reported that flux is better than AOT40 at predicting the spatial distribution of O_3 injury in a range of plant species (Mills *et al.*, 2011a), and at predicting wheat yield under O_3 exposure (Pleijel *et al.*, 2004), but few have compared the association between leaf-level physiology and different flux metrics. The results of this study align with general consensus in the O_3 research community that O_3 flux represents a more biologically relevant metric of O_3 exposure than ambient concentration (Ashmore, 2005; Fuhrer *et al.*, 1997; Mills *et al.*, 2011a; Paoletti and Manning, 2007), and indicate that O_3 flux should be the preferred metric of exposure in O_3 effect model functions. More surprising is the fact that the flux metric without an accumulation threshold – POD_0SPEC – was a better, or equal, predictor of physiological response of crops as compared to POD_6SPEC, which employs an accumulation threshold of six. POD_6SPEC produced the closest correlation between flux and relative yield of wheat in previous analysis testing varying flux accumulation thresholds (Pleijel *et al.*, 2007), and has been applied in several assessments of O_3 impacts in wheat (González-Fernández *et al.*, 2013; Tang *et al.*, 2013). More research is therefore needed to establish how much the capacity to detoxify O_3 varies between cultivars, and why the threshold flux required to induce leaf-level physiological changes appears to differ from the threshold required to reduce final yield.

The view that O_3 flux should be the metric of exposure applied in O_3 effect modelling is also supported by the fact that O_3 flux accounted for the different levels of exposure in treatments dominated by peaks in concentration, versus those characterised by a consistent background level, for the majority of physiological parameters tested in analysis presented here. Flux is therefore likely to perform well as a predictor of physiological response across large geographic areas encompassing heterogeneous profiles of O_3 exposure; and in different world regions which are currently experiencing divergent trends in the pattern of O_3 exposure (Lei *et al.*, 2012; Paoletti *et al.*, 2014; Xu *et al.*, 2008).

The limitations of this study need to be considered when interpreting and applying the results. Calculated values of O_3 flux were not verified by leaf-level measurements of gas flux through stomata. However, the decision to apply the multiplicative DO_3SE model in this study was based on the fact that fluxes produced by this model have previously been evaluated in several independent studies which have demonstrated the model's predictive capability (Büker *et al.*, 2007; Büker *et al.*, 2012; Emberson *et al.*, 2000c; Fares *et al.*, 2013; González-Fernández *et al.*, 2013; Pleijel *et al.*, 2002). A further limitation is that estimates of the onset of leaf senescence were based on leaf chlorophyll content, which would have represented both the chlorophyll loss resulting from leaf injury, as well as chlorophyll loss relating to senescence. In addition, the

analysis is based on only one crop species and two cultivars. As the variation in yield response to O_3 exhibited by different crops, and different cultivars within the same crop species, is well established (Mills *et al.*, 2007; Sawada and Kohno, 2009), caution must be used when extrapolating results presented here to other wheat cultivars and other crops. It should however be noted that the observation in this study that no O_3 effect on photosynthesis could be observed in young wheat leaves – indicating the senescence response is more important than direct effects on photosynthesis – is supported by previous work in other wheat cultivars (Reichenauer *et al.*, 1998), and by other experimental work in soybean (Bernacchi *et al.*, 2006; Morgan *et al.*, 2004). Considerations when applying the results presented in this study – particularly when attempting to up-scale modelled responses from the leaf to canopy level – include the fact that the response observed in the wheat flag leaf may differ from the responses of lower-canopy leaves, and O_3 exposure during early seedling and leaf development may also alter the sensitivity to O_3 observed in the flag leaf.

4.6 Conclusions

In conclusion, this study has shown that current approaches for modelling O_3 effects on leaf longevity and photosynthesis in crops have some limitations, and are not fully supported by the experimental data presented here. When integrated into crop yield models and applied in O_3 risk assessments under future emission and climate scenarios, these O_3 effect functions are therefore likely to result in a degree of error in the final yield estimates. Model functions representing O_3-induced senescence must allow for parameterisation of the timing of senescence onset, and rate of senescence, if inter-cultivar variation in response is to be accurately simulated. Further research aimed at understanding the mechanistic 'trigger' of O_3-induced senescence should be a priority, as this understanding may allow for the development of a more effective mechanism in models for inducing the senescence response. The results also suggest an age-dependency in the response of photosynthesis to O_3 which is not currently considered in modelling methods; and indicate that acceleration of senescence is more important than direct effects of O_3 on photosynthesis in determining final O_3-induced yield loss, at the surface O_3 concentrations that crops are likely to be exposed to on a day-to-day basis. Building functions that can accurately represent the O_3-induced senescence effect in crops should therefore be the priority for O_3 effect modellers.

4.7 Supporting information

4.7.1 Summary of DO_3SE model methodology and parameterisation used for calculating O_3 flux

DO_3SE estimates hourly stomatal conductance to O_3 (g_{sto_O3}, mmol O_3 m^{-2} PLA s^{-1}) using the following algorithm (Büker *et al.*, 2012; Emberson *et al.*, 2000b; Emberson *et al.*, 2000d),

which takes a species-specific maximum g_{sto} value (g_{max}), and modifies it by a series of factors relating to environmental variables:

$$g_{sto\_O3} = g_{max} * [\min(f_{phen}, f_{O3})] * f_{light} * \max\{f_{min}, (f_{temp} * f_{VPD} * f_{SWP})$$

where f_{phen}, f_{O3}, f_{light}, f_{temp}, f_{VPD} and f_{SWP} represent the influence of phenology, O_3, photosynthetically active radiation (PAR), air temperature, vapour pressure deficit (VPD) and soil water potential on g_{max}, respectively; and f_{min} represents the minimum g_{sto_O3}. A detailed description of how parameters relating to the different DO$_3$SE *f*-functions are derived can be found in CLRTAP (2017).

Stomatal flux of O_3 - F_{ST} (nmol m^{-2} PLA s^{-1}) - is calculated following the assumption that the concentration of O_3 at the top of the canopy represents a reasonable estimate of the concentration at the upper surface of the laminar layer of the flag leaf, using the following algorithm:

(1) $$F_{ST} = c(z_i) * g_{sto\_O3} * \frac{r_c}{r_b + r_c}$$

Where $c(z_i)$ is the concentration of O_3 at the top of the canopy of height i (m) , and r_c and r_b represent the leaf surface and quasi-laminar resistances, respectively. The derivation of r_c and r_b based on leaf dimension and wind speed are described in detail in CLRTAP (2017). Once hourly F_{ST} has been derived, the hourly F_{ST} is then accumulated over a species-specific accumulation period using the following equation:

(2) $$POD_Y SPEC = \sum[(F_{ST} - Y) * \left(\frac{3600}{10^6}\right)$$

Where POD$_Y$SPEC stands for the species-specific phytotoxic O_3 dose (mmol m^{-2} PLA), the term (3600/10^6) converts to hourly fluxes and to mmol m^{-2} PLA, and the value Y represents the threshold of flux above which negative O_3 effects may occur (i.e. the detoxification capacity). In this study the flux accumulation period was defined by the life of the flag leaf.

Model parameters used in the calculation of O_3 flux in this study are presented in Table 4.4. The same parameterisation was applied for both wheat cultivars and both years. The parameterisation follows that published for European wheat (CLRTAP, 2017; Grünhage *et al.*, 2012; Pleijel *et al.*, 2007), with the exception of the parameters f_{phen_e} and f_{phen_h} which were calibrated so that the period of flux accumulation aligned approximately with the observed life of the flag leaf in both experiments; and the two parameters which define the f_{O3} function (the flux at senescence onset, and the exponent of the senescence function), which were calibrated so that the end of flux accumulation in the highest O_3 treatments in 2015 and 2016 aligned approximately with observed date of leaf senescence in those treatments.

Table 4.4. Parameters applied in DO$_3$SE to derive the species-specific accumulated O$_3$ flux (POD$_0$SPEC and POD$_6$SPEC) for the 2015 and 2016 experiments.

Function	Parameter	Units	Parameter description	Parameter Value
g_{max}	g_{max}	mmol O_3 m^{-2} PLA s^{-1}	maximum rate of g_{sto_O3}	500
f_{min}	f_{min}	Fraction	Fraction of g_{max} at minimum g_{sto_O3}	0.01
f_{phen}	*Mid-anthesis*	DOY	Decimal growth stage 65*	174 (2015); 181 (2016)
	A_{start}	DOY	Beginning of flux accumulation/ flag leaf emergence	146 (2015); 158 (2016)
	A_{end}	DOY	End of flux accumulation/flag leaf senescence	207 (2015); 214 (2016)
	f_{phen_a}	Fraction	Proportional fall in g_{sto} between f_{phen_g} and f_{phen_h}	0.3
	f_{phen_b}	Fraction	Fraction of g_{max} that g_{sto_O3} takes at the beginning of flag leaf senescence	0.7
	f_{phen_e}	°C days	Temperature sum at A_{start}	- 490
	f_{phen_f}	°C days	Temperature sum at mid-anthesis	0
	f_{phen_g}	°C days	Temperature sum at end of maximum g_{sto_O3} following mid-anthesis	100
	f_{phen_h}	°C days	Temperature sum at start of flag leaf senescence	525
	f_{phen_i}	°C days	Temperature sum at A_{end}	795
f_{light}	*light_a*	constant	The rate of saturation of g_{sto} in response to PAR	0.0105
f_{temp}	T_{min}	°C	Temperature below T_{opt} where g_{sto} reaches f_{min}	12
	T_{opt}	°C	Optimum temperature for g_{sto}	26
	T_{max}	°C	Temperature above T_{opt} where g_{sto} reached f_{min}	40
f_{VPD}	VPD_{max}	kPa	Value where VPD begins to limit g_{sto}	1.2
	VPD_{min}	kPa	Value of VPD where f_{min} is reached	3.2
	ΣVPD_{crit}	kPa	Sum of hourly VPD values after sunrise above which afternoon stomatal reopening will not occur	8.0
f_{PAW}	PAW_t	%	Minimum non-limiting percentage of soil water	50

f_{SWP}	SWP_{max}	MPa	Maximum SWP below which g_{sto} will start to decline	N/A
	SWP_{min}	MPa	SWP at which g_{sto} reaches f_{min}	N/A
f_{O3}	POD_0SPEC/ POD_6SPEC	mmol m^{-2}	Threshold flux at which O_3-induced senescence begins	28
	exponent	constant	Rate of g_{sto} decline with increasing flux accumulation	25

4.7.2 Timelines for 2015 and 2016 experiments

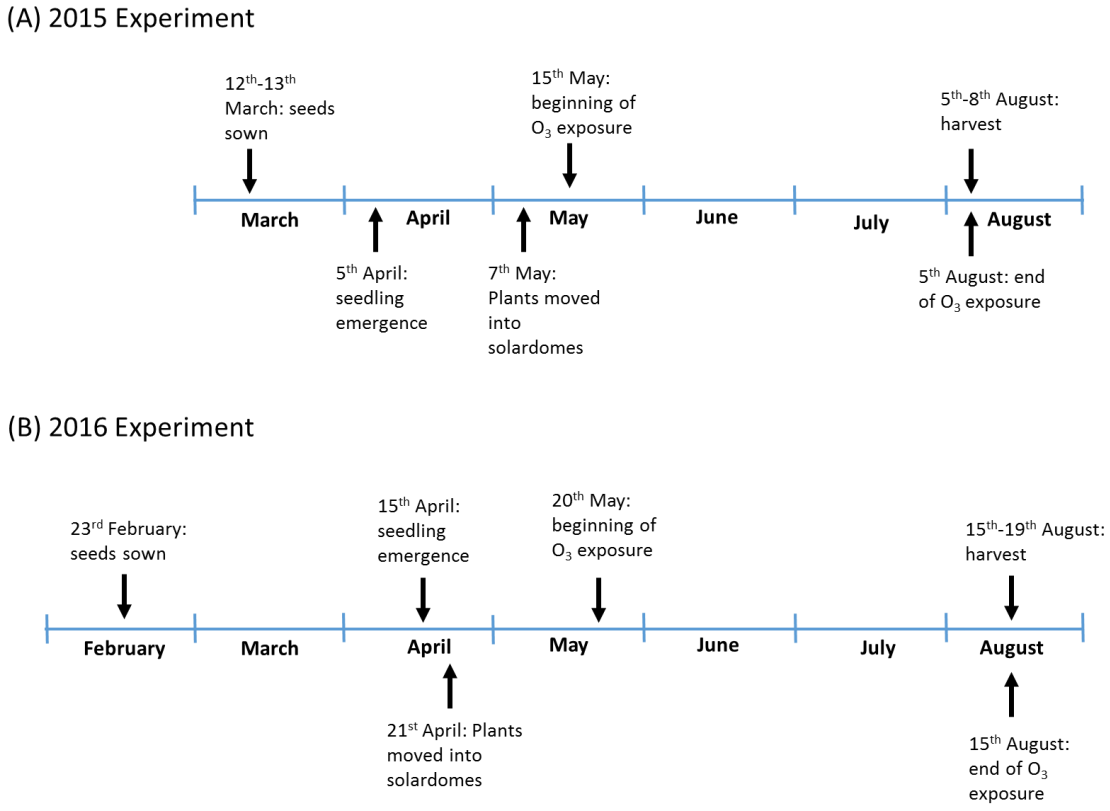

Figure 4.9. Timeline for sowing, seedling emergence, O_3 exposure and plant harvest for (A) the 2015 experiment, and (B) the 2016 experiment.

4.7.3. Comparison of chlorophyll content index (CCI) measurements in Skyfall made in 2015 and 2016

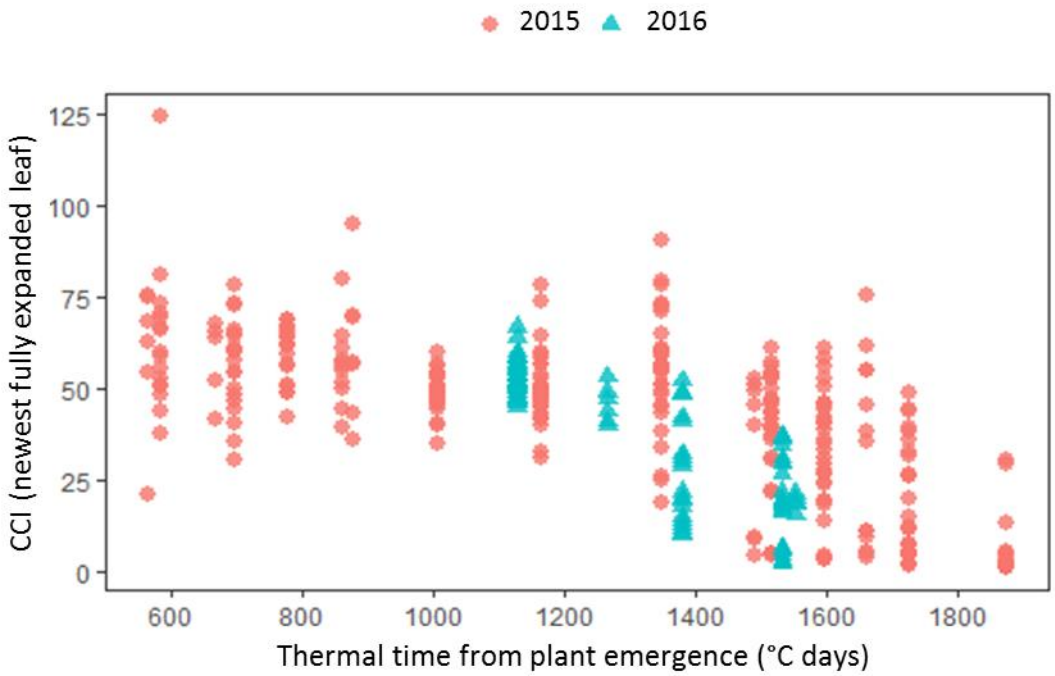

Figure 4.10. Chlorophyll content index (CCI) measurements made in the cultivar Skyfall, in 2015 (red circles) and 2016 (blue triangles). The 2016 observations align approximately with the 2015 observations recorded during the same thermal time period.

4.7.4 Physiological observations aligned with accumulated POD$_6$SPEC

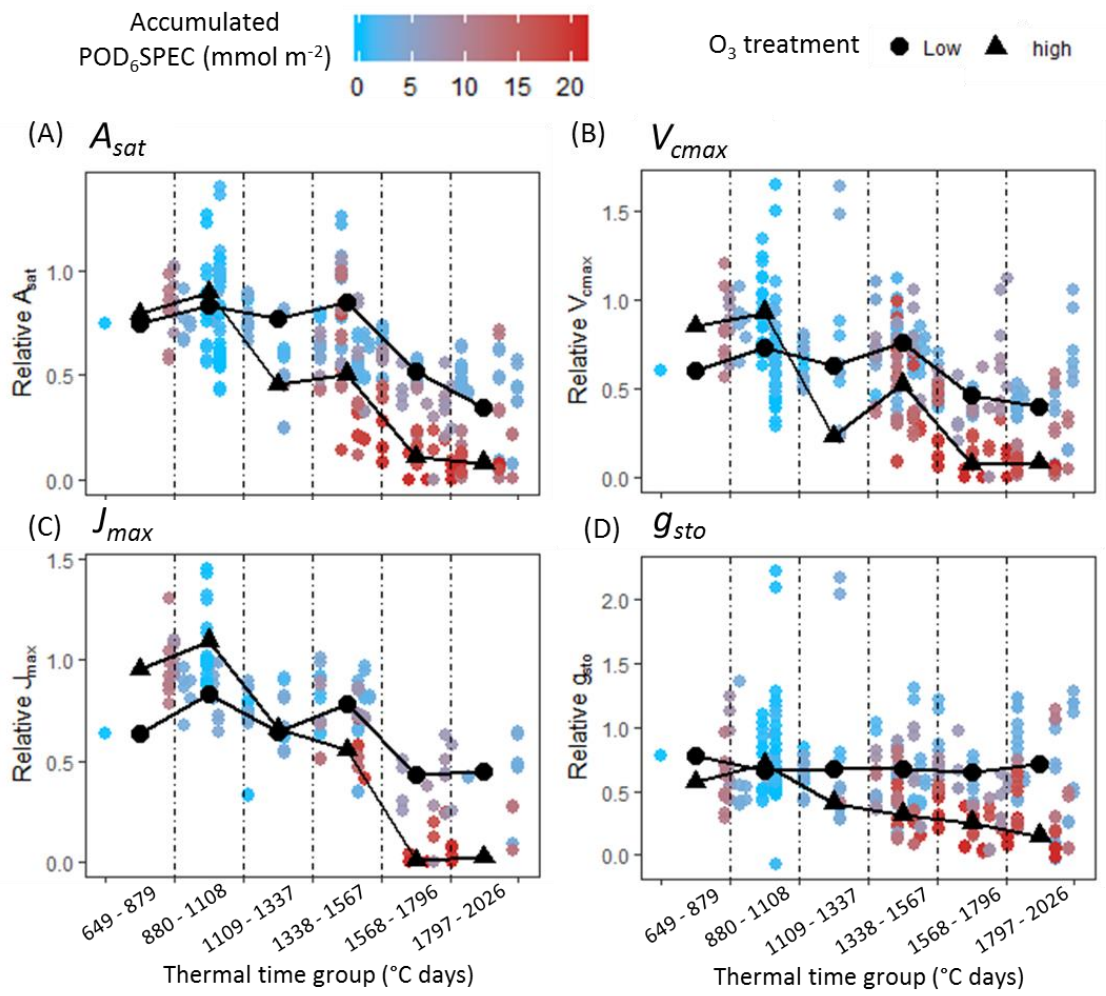

Figure 4.11. Flag leaf data for (A) A_{sat}, (B) V_{cmax}, (C) J_{max}, and (D) g_{sto}, combined across all cultivar-year combinations. The hue of each data point corresponds to the accumulated POD$_6$SPEC at the moment of measurement. Vertical lines on the plots indicate the divisions between thermal time groups. Mean values of physiological parameters in low O_3-treated plants (averaged across 2015 LB and 2015 LP2 treatments) and high O_3-treated plants (averaged across 2015 VHP and 2016 VHP treatments) are shown as black data points on the plots.

4.7.5 Equations used in the derivation of V_{cmax} using the one-point method

Table 4.5. Equations used to derive the Michaelis-Menten constant for CO_2 (K_C), the Michaelis-Menten constant for O_2 (K_O) and the CO_2 compensation point in the absence of mitochondrial respiration (Γ^*).

Parameter	Unit	Equation used in derivation
K_C	μmol mol^{-1}	$404.9 * \exp\left(\frac{79403(T_K - 298.15)}{298.15 * R * T_K}\right)$
K_O	mmol mol^{-1}	$278.4 * \exp\left(\frac{36380(T_K - 298.15)}{298.15 * R * T_K}\right)$
Γ^*	μmol mol^{-1}	$42.75 * \exp\left(\frac{37830(T_K - 298.15)}{298.15 * R * T_K}\right)$

T_K = leaf temperature in Kelvin; R = Universal gas constant, 8.314 J mol^{-1} K^{-1}

4.7.6 Statistical summary of LMM analysis on physiological parameters

Table 4.6. Outcome of LMM analysis investigating which O_3 treatments in 2015 and 2016 exhibited an early decline in leaf chlorophyll (CCI) relative to the control treatments.

Cultivar-year combination	Ozone treatment code	Accelerated senescence in treatment relative to control?**	Mean POD_0SPEC*thermal time interaction variable p-value
Mulika, 2015	LP	No	n.e.
	MB	No	n.e.
	MP	No	n.e.
	HB	No	n.e.
	HP	No	n.e.
	VHB	No	n.e.
	VHP	Yes	$p < 0.001$
Skyfall, 2015	LP	Yes	$p < 0.001$
	MB	Yes	$p < 0.0001$
	MP	Yes	$p < 0.0001$
	HB	Yes	$p < 0.0001$
	HP	Yes	$p < 0.0001$
	VHB	Yes	$p < 0.0001$
	VHP	Yes	$p < 0.0001$
Skyfall, 2016	LP1	No	n.e.
	MP	Yes	$p < 0.0001$
	HP	Yes	$p < 0.05$
	VHP	Yes	$p < 0.0001$

**** Control treatment was defined as the lowest treatment in terms of mean daily POD_0SPEC for each season (i.e. treatment LB in 2015, treatment LP2 in 2016).**
n.e. = no significant effect at $p < 0.05$.

Table 4.7. Statistics summarising the effect of accumulated POD_0SPEC on flag leaf chlorophyll (CCI) in the six thermal time groups.

Cultivar-year combination	Thermal time bin (°days)	Number of observations	POD_0SPEC variable p-value	Direction of effect
Mulika, 2015	649 – 879	44	n.e.	
	880 - 1108	18	n.e.	
	1109 - 1337	16	n.e.	
	1338 - 1567	34	n.e.	
	1568 - 1796	52	$p < 0.01$	- ve
	1797 - 2026	17	n.e.	
Skyfall, 2015	649 – 879	36	$p < 0.05$	+ ve
	880 - 1108	16	n.e.	
	1109 - 1337	16	$p < 0.05$	- ve
	1338 - 1567	38	$p < 0.05$	- ve
	1568 - 1796	38	$p < 0.001$	- ve
	1797 - 2026	16	n.e.	
Skyfall, 2016	649 – 879	0		
	880 - 1108	0		
	1109 - 1337	50	$p < 0.001$	- ve
	1338 - 1567	55	$p < 0.01$	- ve
	1568 - 1796	0		
	1797 - 2026	0		

n.e. = no significant effect at $p < 0.05$.

Table 4.8. Statistics summarising the effect of accumulated POD_0SPEC on flag leaf A_{sat}.

Cultivar-year combination	Thermal time bin (°days)	Number of observations	POD_0SPEC variable p-value	Direction of effect
Mulika, 2015	649 – 879	9	n.e.	
	880 - 1108	6	n.e.	
	1109 - 1337	0		
	1338 - 1567	0		
	1568 - 1796	16	$p < 0.05$	- ve
	1797 - 2026	0		
Skyfall, 2015	649 – 879	8	n.e.	
	880 - 1108	8	$p < 0.01$	+ ve
	1109 - 1337	0		
	1338 - 1567	0		
	1568 - 1796	7	$p < 0.05$	- ve
	1797 - 2026	8	$p < 0.001$	- ve
Skyfall, 2016	649 – 879	0		
	880 - 1108	52	$p < 0.001$	+ ve
	1109 - 1337	28	$p < 0.05$	- ve
	1338 - 1567	118	$p < 0.05$	- ve
	1568 - 1796	56	$p < 0.001$	
	1797 - 2026	66	$p < 0.001$	

n.e. = no significant effect at $p < 0.05$.

Table 4.9. Statistics summarising the effect of accumulated POD_0SPEC on flag leaf V_{cmax}.

Cultivar-year combination	Thermal time bin (°days)	Number of observations	POD_0SPEC variable p-value	Direction of effect
Mulika, 2015	649 – 879	9	n.e.	
	880 - 1108	6	n.e.	
	1109 - 1337	0		
	1338 - 1567	0		
	1568 - 1796	16	$p < 0.01$	- ve
	1797 - 2026	0		
Skyfall, 2015	649 – 879	8	n.e.	
	880 - 1108	8	n.e.	
	1109 - 1337	0		
	1338 - 1567	0		
	1568 - 1796	7	n.e.	
	1797 - 2026	8	$p < 0.001$	- ve
Skyfall, 2016	649 – 879	0		
	880 - 1108	54	$p < 0.001$	+ ve
	1109 - 1337	28	n.e.	
	1338 - 1567	118	n.e.	
	1568 - 1796	56	$p < 0.001$	- ve
	1797 - 2026	66	$p < 0.001$	- ve

n.e. = no significant effect at $p < 0.05$.

Table 4.10. Statistics summarising the effect of accumulated POD_0SPEC on flag leaf J_{max}.

Cultivar-year combination	Thermal time bin (°days)	Number of observations	POD_0SPEC variable p-value	Direction of effect
Mulika, 2015	649 – 879	9	$p < 0.05$	+ ve
	880 - 1108	6	n.e.	
	1109 - 1337	0		
	1338 - 1567	0		
	1568 - 1796	16	$p < 0.01$	- ve
	1797 - 2026	0		
Skyfall, 2015	649 – 879	8	n.e.	
	880 - 1108	8	n.e.	
	1109 - 1337	0		
	1338 - 1567	0		
	1568 - 1796	7	$p < 0.05$	- ve
	1797 - 2026	8	$p < 0.001$	- ve
Skyfall, 2016	649 – 879	0		
	880 - 1108	16	n.e.	
	1109 - 1337	28	n.e.	
	1338 - 1567	48	n.e.	
	1568 - 1796	0		
	1797 - 2026	14	n.e.	

n.e. = no significant effect at $p < 0.05$.

Table 4.11. Statistics summarising the effect of accumulated POD_0SPEC on flag leaf g_{sto}.

Cultivar-year combination	Thermal time bin (°days)	Number of observations	POD_0SPEC variable p-value	Direction of effect
Mulika, 2015	649 – 879	9	n.e.	
	880 - 1108	6	n.e.	
	1109 - 1337	0		
	1338 - 1567	0		
	1568 - 1796	15	$p < 0.05$	- ve
	1797 - 2026	0		
Skyfall, 2015	649 – 879	8	n.e.	
	880 - 1108	59	$p < 0.01$	+ ve
	1109 - 1337	28		
	1338 - 1567	116		
	1568 - 1796	63	n.e.	
	1797 - 2026	74	$p < 0.001$	- ve
Skyfall, 2016	649 – 879	8		
	880 - 1108	7	n.e.	
	1109 - 1337	0	n.e.	
	1338 - 1567	0	$p < 0.01$	- ve
	1568 - 1796	7	$p < 0.001$	- ve
	1797 - 2026	8	$p < 0.001$	- ve

n.e. = no significant effect at $p < 0.05$.

5. Synthesis

5.1 Summary of key research findings

This body of work has confirmed the substantial impact which exposure to chronic ozone (O_3) pollution can have on the yield of wheat and soybean, and underlines the O_3 threat to global food supply. It has made a novel contribution to understanding of temporal and geographical trends in O_3 sensitivity of cultivars; interactions between O_3 and drought; response of photosynthesis to O_3 exposure; and the efficacy of techniques for modelling O_3 effects. A summary of the key findings is given below.

5.1.1 Key findings from paper 1

The first piece of research conducted as part of this thesis was an analysis of published dose-response data for soybean. This analysis revealed a wide range in the O_3 sensitivity of soybean cultivars. At a concentration of 55 ppb 7-hour mean (14.37 ppm AOT40) – a level of surface O_3 that has been exceeded in South Asia, East Asia and North America within the last 20 years (Chakraborty *et al.*, 2015; Jaffe and Ray, 2007; Wang *et al.*, 2007) – estimated yield reduction of soybean cultivars varied from 13.3% in the most tolerant cultivar, to 37.9% in the most sensitive. When all data were pooled to produce a single dose-response function for soybean, a yield reduction of 17.2% was estimated at 55 ppb 7-hour mean, which aligns approximately with the yield reduction estimated by previously published dose-response functions at the same approximate exposure concentration (Mills et al, 2007 = 16.2%; Lesser et al, 1990 = 18.9%). Further analysis revealed that data from Chinese and Indian experiments exhibited higher sensitivity than data collected in the USA.

When the dose-response slope of each cultivar was plotted against the year of release to market, a significant negative association was observed, indicating that cultivar sensitivity to O_3 progressively increased between 1950 and 2000. Average yield reduction at 55 ppb 7-hour mean rose from 14.1% in 1960 to 19.3% in 2000 ($p = 0.0019$). Although it was not possible to analyse physiological trait data for different cultivars in this study, it can be hypothesised that this temporal trend may have been driven by plant breeding practises targeting high yield, and unintentionally, high stomatal conductance (g_{sto}). This hypothesis is supported by a previous study which found that the g_{sto} of soybean cultivars increases progressively with the year of release (Koester *et al.*, 2014), and the observation that O_3 sensitivity of wheat cultivars is associated with high g_{sto} (Biswas *et al.*, 2008). The analysis conducted in this thesis also found slightly higher soybean sensitivity in FACE (free air concentration enrichment) studies compared to OTC (open-top-chamber) studies, and found no significant difference in the dose-response slope exhibited by pot-grown and field-grown soybean.

5.1.2 Key findings from paper 2

The second piece of research conducted as part of this thesis was an investigation into O_3-drought interactions. The European wheat cultivar 'Mulika' was exposed for 12 weeks in solardomes to eight different O_3 exposure profiles, four of which were characterised by regular daily peaks in concentration, and four by a consistent background level. The sensitivity of wheat to O_3 was confirmed, with final yield in the highest O_3 treatment (55 ppb 24-hour mean) 33% lower than final yield in the lowest treatment (27 ppb 24-hour mean). However, comparison of the Mulika flux-yield relationship with that reported by CLRTAP (2017) for five different wheat cultivars revealed that Mulika is comparatively O_3-tolerant. One explanation for this relative tolerance could be the maximal g_{sto} (g_{max}) for Mulika (383 mmol m^{-2} s^{-1}), which is somewhat lower than the average g_{max} for wheat of 497 mmol O_3 m^{-2} s^{-1} (Grünhage *et al.*, 2012).

Two drought events – one applied early in the season during vegetative growth, and one late in the season during grain fill – also resulted in significant yield loss. On average, early drought plants exhibited a 14.1% reduction in final yield, and late drought plants a 13.8% reduction in final yield. Yield reduction in the two drought treatments arose *via* effects on different yield components. The drought event late in the season significantly reduced individual grain weight, but did not alter the number of wheat ears. Plants which experienced early drought stress exhibited reduced individual grain weight, as well as significantly fewer ears per plant. Interestingly, a compensatory response which resulted in an increase in the number of grains per wheat ear was observed in early drought plants.

DO_3SE modelling of O_3 uptake through stomata during the drought events revealed that the two droughts only had a relatively small effect on total O_3 uptake through stomata. The early drought event reduced total seasonal flux by 3.0%, while the late drought reduced total flux by only 0.3%. The difference in effect of the two drought events on O_3 flux can be explained by the fact that the late drought event was applied towards the end of the reproductive cycle, when plants typically exhibit a decline in photosynthetic activity and g_{sto} (an effect represented by the f_{phen} function in the multiplicative DO_3SE model) (Uddling and Pleijel, 2006). This hypothesis is supported by the soil moisture record, which showed slower soil drying – indicative of lower rates of transpiration – during the late drought event compared to the early drought.

Contrary to the findings of some previous studies, drought offered no significant protection against the effects of O_3. This is most likely due to the relatively small effect which the drought events had on total O_3 flux to flag leaves. While the drought treatments had little effect on the degree of O_3-induced yield reduction, the effect of drought itself on yield was severe. Negative effects of drought on yield therefore far outweighed the potential benefits of reduced O_3 uptake in this experiment. When the flux-response functions under different watering regimes were compared statistically, no significant difference in the slope of the functions was observed. This

indicates that no interaction between O_3 and drought was taking place that was not explained by changes in stomatal O_3 uptake. Ozone-drought interactions should therefore be fully accounted for by the current O_3 flux methodology.

5.1.3 Key findings from paper 3

The ability of published modelling approaches to simulate O_3 effects on wheat physiology was scrutinised in the final part of this thesis. Examination of leaf chlorophyll under different O_3 exposure regimes showed that two modern cultivars of European wheat – Mulika and Skyfall – both exhibited accelerated senescence under O_3 exposure. However, the response was cultivar-specific: Skyfall exhibited a senescence response much earlier in the season and experienced a gradual O_3-induced decline in leaf chlorophyll, while Mulika exhibited a sudden reduction in leaf chlorophyll content towards the end of the growing season. The results therefore indicate that the timing of senescence onset, and the rate of leaf senescence, need to be able to vary by species and cultivar in O_3 senescence model functions. The senescence function currently employed in the multiplicative version of the DO_3SE model theoretically fulfils these criteria, where onset of senescence is 'triggered' by a threshold value of accumulated O_3 flux, and the rate of senescence can be parameterised to empirical data. The flux 'trigger' approach to determining senescence onset is likely to be associated with a significant degree of error according to the analysis conducted as part of this study, which found that O_3 flux at senescence onset (POD_0SPEC – the phytotoxic ozone dose accumulated above no threshold) varied across a range of 17.8 – 25.7 mmol m^{-2} in the sensitive cultivar, Skyfall.

Analysis of the physiological response of wheat to O_3 over six time-periods within the growing season allowed the relative timing of different O_3 impacts on physiology to be investigated. Negative effects of O_3 on photosynthesis were only observed concurrent with O_3-induced leaf senescence and not before, and this result was consistent across all three combinations of cultivar and year. Ozone therefore did not impair photosynthesis in young flag leaves at the exposure concentrations applied in this study. This result is supported by a number of previous studies conducted in soybean and wheat, which found that O_3 effects on photosynthesis and g_{sto} were not apparent in new fully expanded leaves (Bernacchi *et al.*, 2006; Morgan *et al.*, 2004; Reichenauer *et al.*, 1998). Accelerated senescence is therefore likely to be the dominant O_3 effect influencing final yield in most agricultural environments, where O_3 concentrations are typically moderate with occasional peaks.

Finally, comparison of the ability of different metrics of O_3 exposure – some accumulated flux-based (POD_0SPEC, POD_6SPEC) and some concentration-based (AOT40, 24-hour mean) – to predict physiological response to O_3 found that flux-based metrics were superior at predicting response for all five physiological variables tested (CCI, A_{sat}, V_{cmax}, J_{max}, g_{sto}), in both cultivars. These results reinforce the view that O_3 flux should be the favoured metric of exposure for O_3

effect modelling. Interestingly, the analysis also found that POD_0SPEC – a metric of accumulated flux not employing a detoxification threshold – was equal or better at predicting physiological response of wheat to O_3 compared to POD_6SPEC, which employs a detoxification threshold of six. In the majority of the model sets created in the analysis, the flux-based O_3 metric was able to account for the difference in exposure resulting from peak-dominated treatments and those featuring a consistent background level. Stomatal O_3 flux is therefore likely to perform well as a predictor of physiological response across a wide range of geographic regions (i.e. rural and urban) where a diversity of O_3 exposure patterns can be expected.

5.2 Novelty and implications of key results

5.2.1. Evidence that soybean cultivars have become more sensitive to O_3 over time

The temporal and geographical trends in soybean cultivar sensitivity to O_3, observed in the analysis of soybean dose-response data, mirror results seen for other major food crops. For example, an association between the release date and O_3 sensitivity of wheat cultivars has been reported a number of times (Barnes *et al.*, 1990; Biswas *et al.*, 2008; Pleijel *et al.*, 2006; Velissariou *et al.*, 1992), and Emberson *et al.* (2009) observed higher sensitivity of Asian wheat and rice cultivars compared to North American cultivars, when pooled dose-response data was compared. However, the results presented in this study are the first clear evidence of these trends for soybean. These results add to the body of evidence which indicates that crop breeding practises have inadvertently selected for O_3 sensitivity, possibly as a result of selection of cultivars with a high g_{sto}. If this is indeed the case, this is a significant concern for farmers as well as those interested in securing global food security; crop varieties bred in 'clean air' regions may perform significantly worse if they are sold and grown in a region with significant surface O_3 pollution. Crop breeders and farmers need to be aware of the trade-off for stress tolerance that might be associated by a high yielding variety, and how selecting a particular plant physiological trait can lead to multiple outcomes – for example, targeting high water-use efficiency (e.g. by targeting low g_{sto}) could select for O_3 tolerance as well as drought tolerance.

5.2.2. The impact of experimental method and design on plant response to O_3

The marginally higher O_3 sensitivity observed for soybean exposed in FACE systems compared to OTC's, and the lack of an observed difference in sensitivity between soybean grown in pots and in the field, are important results as they contribute to the debate surrounding the impact of experimental methods on the plant O_3 response. It is generally assumed that fully open-air O_3 exposure experiments with field-grown plants are the most accurate representation of real agricultural environments, and therefore are the most reliable way of deriving quantitative yield predictions (Long *et al.*, 2005). The OTC 'chamber effect', where temperature is elevated and humidity and light intensity typically reduced, is well-established (Piikki *et al.*, 2008;

Whitehead *et al.*, 1995); one might therefore expect to see some degree of difference in response to O_3 in FACE systems compared to OTC's. The observation in this study of higher soybean sensitivity in FACE studies compared to OTC's is supported by the FACE study by Morgan *et al.* (2006), which reported a steeper dose-response relationship for soybean than reported in earlier chamber studies. Modellers attempting to predict future impacts of O_3 on food supply must therefore consider and be aware of the limitations associated with dose-response relationships based on chamber studies, and further FACE studies are clearly important. Interestingly, the analysis in this thesis found no significant difference between the dose-response slope of soybean plants grown in pots and those grown in the open field (Figure 2.7), despite the likelihood of restricted root growth in pot-grown plants. These results are supported by those of Feng and Kobayashi (2009), who also found no difference in O_3 response of pot and field-grown plants of six major food crops in their meta-analysis. While full field condition experiments are important for making quantitative harvest predictions, the results presented in this thesis indicate that pot and container studies – which can often operate at a smaller scale and on a cheaper budget - are a valid method for developing understanding of O_3 effects on plant physiology and yield, particularly in comparative studies. OTC studies also have the advantage of being able to reduce O_3 in the chamber below the current ambient level, thereby showing the benefits of reducing the current ambient concentration; FACE studies can only add O_3 to the ambient concentration.

5.2.3. Greater understanding of how drought and O_3 interact to influence yield

Following on from the analysis of existing dose-response data for soybean, the second piece of research conducted as part of this thesis resulted in new dose-response data being generated for European wheat. While the results from this experiment certainly don't resolve the question of how drought influences the response to O_3 – and *vice versa* - they do contribute some additional experimental data to the debate. The experimental results, combined with stomatal flux modelling, indicated that 10 days of watering withdrawal did result in a small reduction of total O_3 flux to the flag leaf, but the potential benefit of this O_3 exclusion was far outweighed by the yield reduction induced by drought stress. The ability of drought to protect against O_3 may therefore be dependent on a cost-benefit model, where drought has a positive net effect only if the benefits of reduced O_3 flux outweigh the drought-induced yield penalty. This understanding could potentially lead to an improvement in O_3-drought interaction modelling in O_3 risk assessments: while the effect of drought on O_3-induced yield reduction could be estimated *via* existing flux modelling methodology (CLRTAP, 2017), the corresponding drought impact on yield could be calculated using empirically derived relationships between water stress and yield. More experimental data may however be required to achieve this, as the degree of stress inflicted by drought is dependent on a host of different factors (e.g. ambient temperature, soil type, phenology, VPD, drought-adaptive cultivar traits).

The results of the O_3-drought exposure experiment also help to elucidate how phenological timing of drought stress influences final yield. Although these results are agronomic and don't directly relate to O_3 effects, they are relevant for modellers aiming to improve estimates of current and future yield, and provide some indication of how a lack of available water can differentially influence O_3 uptake at different stages of growth. Water withdrawal in the early-season and late-season had an almost equal impact on final yield in this experiment. Early drought resulted in fewer wheat ears, a reduced individual grain weight, and an increased number of grains per ear. Early drought also induced stomatal closure for several days, which would have reduced carbon assimilation during that time. Conversely, water withdrawal during grain fill only had a very small impact on g_{sto}, and slower soil drying was observed during this late-season water withdrawal, compared to water withdrawal in the early-season. The grain fill period can therefore be considered more sensitive to water stress than the vegetative stage, as equal yield loss was observed even though a less severe drought, with less rapid soil drying, occurred during the late-season. These results highlight the complexity associated with predicting the impact of water withdrawal on final yield, as the severity of the resulting drought, and the physiological impact of that drought, are both influenced by phenology.

5.2.4. Understanding the strengths and limitations of existing methods for modelling O3-induced early senescence

The final piece of research conducted as part of this thesis involved applying physiological data collected during experimentation, to test a number of O_3 effect modelling approaches. As part of this study, different methods for modelling O_3 senescence effects were directly compared in their ability to capture inter-cultivar differences in response – something which has not been done before and which is of direct relevance to modellers aiming to accurately simulate O_3 effects on yield. Both the timing of senescence onset, and the rate of O_3-induced senescence, were found to be necessary parameters for capturing inter-cultivar variation in response. The O_3 senescence function first published by Danielsson *et al.* (2003) and currently used in DO_3SE (CLRTAP, 2017) meets these criteria, while calibration of the leaf senescence duration parameter in the Ewert and Porter (2000) according to cultivar would allow this function to better capture inter-cultivar differences in response. However, the results from this study also indicate that a clearer understanding of the mechanisms involved in 'triggering' the early senescence response in models is required. In the Danielsson *et al.* (2003) O_3 senescence function, onset of senescence is triggered when a threshold of accumulated stomatal O_3 flux is reached, and this method can be interpreted mechanistically if accumulated flux is assumed to be proportional to increased respiratory effort integrated over the course of the season. Analysis presented in this thesis indicates that senescence onset in the cultivar Skyfall actually took place over a considerable range of O_3 flux (17.8 – 25.7 mmol m^{-2} POD_0SPEC). At higher levels of O_3 exposure, the method appears to work better, with a considerably narrower range of flux at

senescence onset observed in the five highest O_3 treatments (22.0 – 25.7 mmol m^{-2} POD_0SPEC). However, these results suggest that the view that O_3-induced senescence is triggered after a certain amount of accumulated O_3 damage, or total respiratory effort, is too simplistic. Other factors – for example, the total duration of O_3 exposure, or the phenological stage at the beginning of exposure – may also play a role in determining the timing of senescence onset. Research aimed at understanding the mechanistic basis of accelerated senescence could aid in the future development of an improved O_3 senescence function; and the results of this study indicate that the Danielsson *et al.* (2003) method represents the best current published method for modelling O_3-induced senescence, but is nevertheless likely to be associated with a certain degree of error.

5.2.5. Ozone-induced accelerated senescence is more important than direct effects on photosynthesis in determining final yield loss

The observation that photosynthetic impairment at high O_3 did not occur in the period preceding the onset of leaf senescence is relevant to the question of whether direct effects of O_3 on photosynthesis, or O_3-induced accelerated senescence, are more important in determining final yield loss. The fact that impaired photosynthetic capacity at high O_3 was only observed concurrent with leaf senescence raises the possibility that photosynthetic impairment was wholly driven by senescence processes in this experiment. Leaf senescence is a highly regulated process, characterised initially by increased expression of senescence-associated genes (SAGs) and decreased expression of genes related to photosynthesis, and later by the degradation of proteins and lipids, including photosynthetic pigments, to facilitate nutrient remobilisation (Lim *et al.*, 2007). The results presented in this thesis indicate that the early induction of leaf senescence processes by O_3 is more important than direct effects of O_3 on photosynthesis in determining final yield loss. The contradiction between these results and those reported by previous authors (Dann and Pell, 1989; Farage and Long, 1995; Farage *et al.*, 1991) may relate to the experimental setup and O_3 concentrations applied: the much-cited studies of Farage *et al.* (1991) and Farage and Long (1995) applied relatively high hourly O_3 concentrations (200-400 ppb), and 'instantaneous' impairment of photosynthesis may therefore only occur at acute concentrations. The results reported in this thesis also reveal an age-dependency in the response of the photosynthetic mechanism to O_3 exposure, which is supported by other experimental evidence (Bernacchi *et al.*, 2006; Morgan *et al.*, 2004; Reichenauer *et al.*, 1998), but is not currently accounted for in proposed methods for modelling O_3 effects on photosynthesis. Incorporating age-dependency into O_3-photosynthesis functions therefore represents a simple way to improve existing modelling methods, and may be an important consideration for estimates of whole canopy carbon assimilation.

5.2.6. Ozone flux is better than concentration at predicting physiological response to O_3

Finally, the finding that flux is a better predictor of O_3 effects on physiology compared to concentration-based metrics supports the results of previous studies that have found flux to be superior for predicting visible injury and yield loss (Mills *et al.*, 2011b; Pleijel *et al.*, 2004). However, this study is the first to compare flux and concentration-based metrics in their ability to predict photosynthetic capacity under O_3 exposure, and the first to test whether flux-based methods can account for differences in the pattern of O_3 exposure on physiological response. Ozone flux was able to account for the varying exposure resulting from peak-dominated exposure profiles, and profiles characterised by a consistent background concentration, in nine out of ten model sets created as part of this analysis. Modellers can therefore have confidence that O_3 flux will perform well as a predictor of plant response in O_3 risk assessment modelling applied across a diversity of landscape types (i.e. rural and urban) and world regions (i.e. North America and South Asia), which may have rather different diurnal and seasonal O_3 profiles.

5.3 Common themes

5.3.1. Which is better at predicting plant response – concentration or flux?

A number of common themes are explored across the different pieces of research presented in this thesis. One such theme is the contrast between concentration-based and flux based metrics of O_3 in their ability to predict response to O_3. An advantage of expressing O_3 exposure using stomatal flux is presented in the second research paper presented here: accumulated stomatal O_3 flux (POD_6SPEC) is found to fully account for the impact of co-occurring drought on final yield. Although the results of the O_3-drought exposure experiment showed that there was very little effect of drought on total O_3 uptake in this case – meaning that the concentration-based and flux-based dose-response function slopes were very similar (Figure 3.7) – under different environmental conditions and different patterns of water withdrawal (e.g. chronic drought), the total impact of drought on O_3 uptake could be greater. The fact that the POD_6SPEC metric can take into account the effects of co-occurring drought when calculating internal O_3 dose is therefore an important advantage, and advocates the use of flux-based metrics in studies where the combined effects of future climate and O_3 scenarios are being investigated. In the third research paper presented in this thesis, the ability of concentration-based and flux-based metrics of O_3 exposure to predict physiological response to O_3 was directly compared. For every measured physiological parameter (CCI, A_{sat}, V_{cmax}, J_{max}, g_{sto}) and for both cultivars, O_3 flux was a better predictor than concentration, and these results clearly promote the use of O_3 flux as a metric for summarising O_3 exposure – while recognising that the derivation of flux is more technically demanding, and requires more data than concentration-based methods. The same results also indicated that POD_0SPEC – not employing a threshold for accumulation – performed better than the POD_6SPEC at predicting physiology, even though the POD_6SPEC has

been shown in previous work to be the best predictor of wheat yield (Pleijel *et al.*, 2007). The POD_6SPEC also produced a greater r-squared and lower p-value than the POD_0SPEC in a regression of O_3 flux versus final yield carried out on the well-watered Mulika yield data from the O_3-drought exposure experiment (Figure 5.1). The results presented here therefore suggest that a lower dose of O_3 flux is required to induce physiological changes at the leaf level than is required to influence the final yield for the cultivar Mulika. This suggestion of a difference in sensitivity of physiology and yield to O_3 flux merits future work, as it raises the question as to what extent final yield is 'buffered' from fluctuations in leaf-level physiological activity.

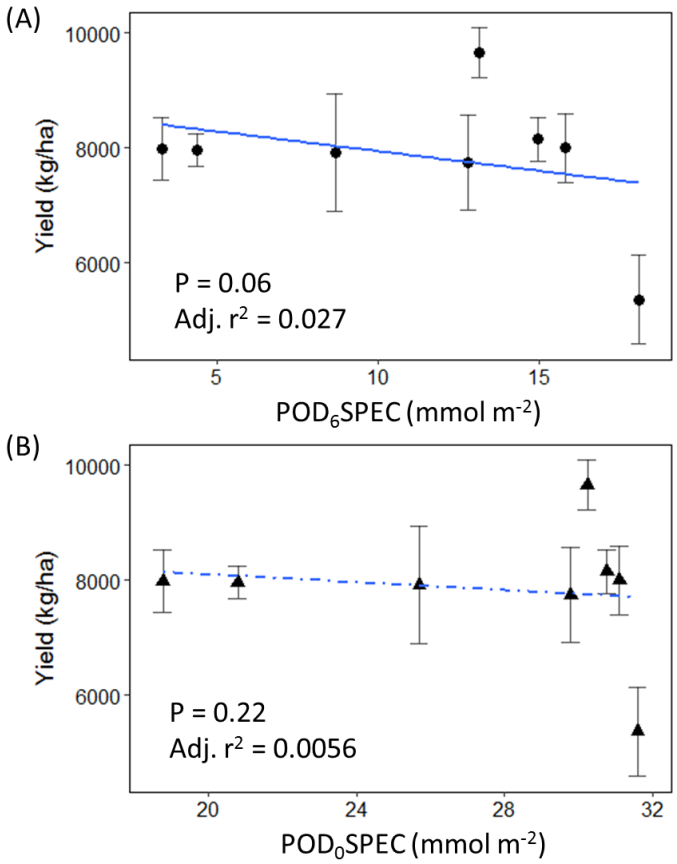

Figure 5.1. Linear regression of final yield for well-watered 'Mulika' plants from the 2015 O_3-drought exposure experiment (methods summarised in section 3.3), versus O_3 dose. (A) Final yield versus POD_6SPEC in each of the O_3 treatments. (B) Final yield versus POD_0SPEC in each of the O_3 treatments. Regression with POD_6SPEC produces a higher adjusted r-squared and lower p-value for the regression. Error bars represent plus and minus one standard error.

5.3.2. Stomatal conductance as a determinant of O_3 sensitivity

Another theme which cuts across the different research papers of this thesis is the variation in sensitivity to O_3 that exists between different crop cultivars, and the likely link between sensitivity and g_{sto}. In the first paper presented here, a substantial range in the degree of O_3-induced yield loss at a given concentration is estimated for different soybean cultivars (13.3 – 37.9% yield loss at 55 ppb 7-hour mean). In the same paper, soybean cultivar O_3 sensitivity is shown to be correlated both with the year of cultivar release (Figure 2.6) and geographical location (Figure 2.4). Both of these patterns in O_3 sensitivity could hypothetically be linked to g_{sto}, if the g_{sto} of cultivars has increased over time as a result of selective breeding practises (Koester *et al.*, 2014), and if climatic conditions favouring high humidity and high g_{sto} are predominant at the Asian experimental sites. Unfortunately, it was not possible to directly test these hypotheses using the data gathered for this thesis. However, results presented in the second paper align with the view that g_{sto} is a key driving factor underlying crop cultivar sensitivity, as the wheat cultivar 'Mulika' was found to be relatively tolerant to O_3 (Figure 3.8), and also has a lower-than-average maximal g_{sto} (Mulika g_{max} = 383 mmol m^{-2} s^{-1}, average g_{max} for wheat = 497 mmol m^{-2} s^{-1}) (Grünhage *et al.*, 2012). Results presented in the final research paper of this thesis are also consistent with the view that O_3 sensitivity of crop cultivars is closely linked to g_{sto}. Analysis of leaf chlorophyll data in this study indicates that Skyfall is more sensitive to O_3 than Mulika, as O_3-induced senescence effects occur much earlier in Skyfall; and analysis of g_{sto} observations indicates that Skyfall has a maximal g_{sto} that is higher than the cultivar average for wheat and substantially higher than that of Mulika (Skyfall g_{max} = 569 mmol m^{-2} s^{-1}).

5.3.3. How does the pattern of O_3 exposure influence the response?

The importance of the profile, or pattern, of O_3 exposure is another theme which is explored in both the second and third research papers presented in this thesis. In the O_3 exposure experiment which generated the data presented in these two papers, the O_3 treatments were paired so that four pairs of treatments produced approximately the same seasonal concentration of O_3 (24-hour mean), but applied O_3 in either a peak-dominated profile, or a profile characterised by a consistent background concentration (Figure 3.1). Final yield reduction in the cultivar 'Mulika' was greater in the high treatment dominated by peaks than in the equivalent high treatment with a more consistent background level, suggesting that exposure of wheat to peaks in concentration has a more severe effect than consistent exposure to a relatively high background concentration. However, statistical analysis of the association between final yield of Mulika and accumulated O_3 flux (POD_6SPEC) indicated that a linear relationship was the best fit to the data (Figure 3.7), and that exposure profile was not significant as an explanatory variable in the model (Table 3.3). In addition, in the third research paper of this thesis, the profile of O_3 exposure was not significant as an explanatory variable in the vast majority of model sets, when O_3 exposure was

expressed in terms of accumulated flux (Table 4.3). The results from these two papers therefore suggest that the more severe effect of peak profile exposure on plants can be explained by the fact that peaked profiles result in a higher total O_3 flux than the more stable background concentration profiles. Conversely, the 24-hour mean O_3 concentration does not capture the difference in O_3 exposure caused by a peak-dominated and consistent background profile. This result is important, as the profile of O_3 exposure in the real world is heterogenous, and agricultural regions – particularly those located close to urban areas – are likely to experience background O_3 exposure as well as occasional severe peaks in O_3 concentration (DEFRA, 2009; Royal Society, 2008). Risk assessment modelling methods applied to these areas therefore need to be able to adequately predict the response of crops to O_3 under various different exposure patterns. Different geographical regions will also differ in terms of the frequency of peak O_3 episodes: while Eastern Europe, the Middle East and East Asia are predicted to see an increase in the frequency of severe peaks of O_3 concentration by 2050 (Lei *et al.*, 2012), Western Europe and North America are likely to see a decline in frequency (Paoletti *et al.*, 2014).

5.4 Limitations and Future work

A key limitation of the soybean dose-response data analysis was the disproportionate representation of data from the USA, relative to data from Asia. A steeper dose-response slope was observed for data collected in India and China compared to data collected in the United States, but clear conclusions could not be drawn from this trend, as the Asian studies were far outnumbered by studies from the USA (three studies were from Asia while twenty-five were from the USA). Although it can be hypothesised that the higher sensitivity observed in Asian studies may result from plant physiological traits or the influence of climate, the possibility that the three cultivars tested in Asia were not representative, or that characteristics specific to the experimental sites (e.g. co-occurring pollutants) drove the observed response, cannot be ruled out. More experimental data, either gathered in Asia or for Asian cultivars, is therefore needed if O_3 effects in this region – where soybean is a significant food crop and export commodity (FAO, 2014; Hartman *et al.*, 2011) – are to be quantified. Currently, there is a concern that O_3 risk assessments of crop yields in Asia – which have typically used empirical dose-response functions based on European or North American experiments (Avnery *et al.*, 2011a, b; van Dingenen *et al.*, 2009; Wang and Mauzerall, 2004) – may have underestimated the scale of the problem in Asia. Research investigating O_3 effects on Asian cultivars, *in situ* in non-temperate climate zones, should therefore be a future priority for the O_3 effects research community.

The large amount of variation in O_3 sensitivity observed in the soybean cultivar dataset suggests that there is a large amount of scope for identification of plant traits associated with O_3 sensitivity through experimental work. It also suggests that substantial genetic diversity is available for efforts to breed O_3-tolerant soybean cultivars. The observed relationship between year of release and O_3 sensitivity was hypothesised as being driven by changes in g_{sto}, but it was

not possible to test this hypothesis in this analysis as insufficient physiological data were available for the soybean cultivars. This hypothesis could however be tested in future experimental work. Cultivars of varying release date could for example be exposed to O_3 at the same site and under the same experimental conditions, and final yield as well as physiological traits potentially associated with O_3 tolerance (e.g. g_{sto}, antioxidant content of leaves, plant hormone production, mesophyll structure) could be measured. A similar approach could be used to investigate the higher O_3 sensitivity of Asian soybean cultivars observed in this study: cultivars from different world regions, exposed to O_3 under identical environmental conditions at the same location, could be compared in their physiological and yield response to O_3 exposure. The identification in both wheat and soybean of physiological traits associated with O_3-tolerance, and identification of existing O_3-tolerant lines, would be of direct relevance to the crop cultivar breeding community.

The drought-O_3 interaction experiment which comprised the second study within this thesis allowed for comparison of early-season and late-season drought effects on O_3 uptake, but the capacity to use the results to quantitatively predict drought effects on yield is somewhat limited by the fact that plants were grown in containers. It is therefore likely that the structure, reach and density of the root system in the experiment was not an accurate representation of wheat crop root systems in real agricultural environments. As the potential for drought to protect against O_3 effects seems to be governed by a cost-benefit trade-off, understanding the difference in the 'cost' of drought experienced in pot-grown plants compared to field-grown plants is key to applying this cost-benefit model in real-world O_3 risk assessments. Ozone-drought experiment work conducted on field-grown plants, or a comparison of the physiological and yield response to drought in container-grown and field-grown plants, represents potential future experimental work that could develop or support the existing results.

As well as comparing the effect of container-grown versus field-grown plants, there is considerable additional scope for extension of the drought-interaction experimental work presented in this thesis. While the experimental results presented here have indicated how O_3 and a 10-day acute drought can interact, drought stress can manifest in a number of ways. For example, how would the results have differed if a chronic drought – consisting of long-term low water availability, rather than a short period of total water withdrawal – had been applied? In addition, withholding the same amount of water in the early and late season in the experiment presented in this thesis actually resulted in different degrees of drought due to the influence of plant phenology, so what would the outcome have been if exactly the same degree of water stress had been applied in the early and late season? Furthermore, periods of low soil moisture are often accompanied by high temperatures which drive an increase in atmospheric vapour pressure deficit (VPD). High VPD increases the atmospheric demand for water and is thought to limit g_{sto} to a greater extent that soil moisture deficit in some biomes (Novick *et al.*, 2016).

Investigation of how high VPD alongside soil moisture deficit influences stomatal behaviour, and hence O_3 uptake, would therefore be an interesting and novel future direction for this research.

There is also scope for extending the analysis of senescence and photosynthesis responses to O_3 conducted in this thesis. The results failed to observe 'instantaneous' impairment of photosynthesis in the early life of the wheat flag leaf at the experimental exposure concentrations, but instantaneous impairment of carboxylation capacity has been observed in previous experiments in wheat where higher O_3 concentrations were used (Farage and Long, 1995; Farage *et al.*, 1991). This suggests that there is a threshold O_3 concentration where direct effects of O_3 on the photosynthetic mechanism begin to occur, and experimental work involving photosynthetic measurements across a range of O_3 concentrations – perhaps spanning 100-200 ppb – could allow this threshold to be identified for wheat. Ozone concentrations in the range of 100-200 ppb have been observed in some areas of India and China in the last two decades (Beig *et al.*, 2007; Kumari *et al.*, 2013; Xu *et al.*, 2008), and surface O_3 concentrations in South and East Asia may continue to increase for several decades (IPCC, 2013a). Understanding O_3 effects on crop physiology within this concentration range is therefore highly relevant for efforts to estimate O_3 effects on current and future yield in these regions.

It would also be interesting to attempt to determine whether O_3 separately induces senescence and impairs photosynthesis in older leaves, or whether these actually represent the manifestation of one O_3-induced process: leaf senescence. Answering this question would require disentangling O_3 effects on photosynthesis from O_3-induced senescence effects, which could perhaps be achieved if photosynthetic capacity was measured at a high time resolution, alongside monitoring for senescence markers (e.g. upregulation of senescence-related genes). The 'one-point method' – successfully validated for wheat in the third research paper presented in this thesis – represents one method by which carboxylation capacity could be measured at a high temporal resolution.

References

Agarwal DK, Billore S, Sharma A, Dupare B, Srivastava S. 2013. Soybean: introduction, improvement, and utilization in India - problems and prospects. Agricultural Research **2**, 293-300.

AHDB. 2015. Wheat Growth Guide. Kenilworth, UK.

Ainsworth EA, Long SP. 2005. What have we learned from 15 years of free-air CO_2 enrichment (FACE)? A meta-analytic review of the responses of photosynthesis, canopy properties and plant production to rising CO_2. New Phytologist **165**, 351-372.

Ainsworth EA, Rogers A, Leakey ADB. 2008. Targets for crop biotechnology in a future high-CO_2 and high-O_3 world. Plant Physiology **147**, 13-19.

Ainsworth EA, Yendrek CR, Sitch S, Collins WJ, Emberson LD. 2012. The effects of tropospheric ozone on net primary productivity and implications for climate change. Annual Review of Plant Biology **63**, 637-661.

Alonso R, Elvira S, Castillo FJ, Gimeno BS. 2001. Interactive effects of ozone and drought stress on pigments and activities of antioxidative enzymes in *Pinus halepensis*. Plant, Cell & Environment **24**, 905-916.

Ariyaphanphitak W, Chidthaisong A, Sarobol E, Bashkin VN, Towprayoon S. 2005. Effects of elevated ozone concentrations on Thai Jasmine rice cultivars (*Oryza sativa* L.). Water Air and Soil Pollution **167**, 179-200.

Ashmore M. 2005. Assessing the future global impacts of ozone on vegetation. Plant, Cell & Environment **28**, 949-964.

Avnery S, Mauzerall DL, Liu JF, Horowitz LW. 2011a. Global crop yield reductions due to surface ozone exposure: 1. Year 2000 crop production losses and economic damage. Atmospheric Environment **45**, 2284-2296.

Avnery S, Mauzerall DL, Liu JF, Horowitz LW. 2011b. Global crop yield reductions due to surface ozone exposure: 2. Year 2030 potential crop production losses and economic damage under two scenarios of O_3 pollution. Atmospheric Environment **45**, 2297-2309.

Ball JT, Woodrow IE, Berry JA. 1987. A model predicting stomatal conductance and its contribution to the control of photosynthesis under different environmental conditions. Progress in Photosynthesis Research **4**, 221-224.

Barnes J, Velissariou D, Davison A, Holevas C. 1990. Comparative ozone sensitivity of old and modern Greek cultivars of spring wheat. New Phytologist **116**, 707-714.

Beig G, Gunthe S, Jadhav DB. 2007. Simultaneous measurements of ozone and its precursors on a diurnal scale at a semi urban site in India. Journal of Atmospheric Chemistry **57**, 239-253.

Beig G, Singh V. 2007. Trends in tropical tropospheric column ozone from satellite data and MOZART model. Geophysical Research Letters **34**, L17801.

Belsley DA, Kuh E, Welsch RE. 1980. Regression diagnostics: identifying influential data and sources of collinearity. Wiley, New York.

Bender J, Weigel HJ. 2011. Changes in atmospheric chemistry and crop health: A review. Agronomy for Sustainable Development **31**, 81-89.

Bergmann E, Bender J, Weigel HJ. 1999. Ozone threshold doses and exposure–response relationships for the development of ozone injury symptoms in wild plant species. New Phytologist **144**, 423-435.

Bernacchi C, Singsaas E, Pimentel C, Portis Jr A, Long S. 2001. Improved temperature response functions for models of Rubisco-limited photosynthesis. Plant, Cell & Environment **24**, 253-259.

Bernacchi CJ, Leakey ADB, Heady LE, *et al.* 2006. Hourly and seasonal variation in photosynthesis and stomatal conductance of soybean grown at future CO_2 and ozone concentrations for 3 years under fully open-air field conditions. Plant, Cell & Environment **29**, 2077-2090.

Betzelberger AM, Gillespie KM, McGrath JM, Koester RP, Nelson RL, Ainsworth EA. 2010. Effects of chronic elevated ozone concentration on antioxidant capacity, photosynthesis and seed yield of 10 soybean cultivars. Plant, Cell & Environment **33**, 1569-1581.

Betzelberger AM, Yendrek CR, Sun JD, Leisner CP, Nelson RL, Ort DR, Ainsworth EA. 2012. Ozone exposure response for U.S. soybean cultivars: linear reductions in photosynthetic potential, biomass, and yield. Plant Physiology **160**, 1827-1839.

Biswas DK, Jiang GM. 2011. Differential drought-induced modulation of ozone tolerance in winter wheat species. Journal of Experimental Botany **62**, 4153-4162.

Biswas DK, Xu H, Li YG, Sun JZ, Wang XZ, Han XG, Jiang GM. 2008. Genotypic differences in leaf biochemical, physiological and growth responses to ozone in 20 winter wheat cultivars released over the past 60 years. Global Change Biology **14**, 46-59.

Blum A. 1996. Crop responses to drought and the interpretation of adaptation. Plant Growth Regulation **20**, 135-148.

Booker F, Muntifering R, McGrath M, Burkey K, Decoteau D, Fiscus E, Manning W, Krupa S, Chappelka A, Grantz D. 2009. The ozone component of global change: potential effects on agricultural and horticultural plant yield, product quality and interactions with invasive species. Journal of Integrative Plant Biology **51**, 337-351.

Booker FL, Miller JE, Fiscus EL, Pursley WA, Stefanski LA. 2005. Comparative responses of container-versus ground-grown soybean to elevated carbon dioxide and ozone. Crop Science **45**, 883-895.

Boote KJ, Jones JW, White JW, Asseng S, Lizaso JI. 2013. Putting mechanisms into crop production models. Plant, Cell & Environment **36**, 1658-1672.

Bou Jaoudé M, Katerji N, Mastrorilli M, Rana G. 2008. Analysis of the ozone effect on soybean in the Mediterranean region: II. The consequences on growth, yield and water use efficiency. European Journal of Agronomy **28**, 519-525.

Bowler C, Vanmontagu M, Inze D. 1992. superoxide-dismutase and stress tolerance. Annual Review of Plant Physiology and Plant Molecular Biology **43**, 83-116.

Brasseur G, Muller, J., Tie, X., Horowitz, L. 2001. Tropospheric Ozone and Climate: Past, Present and Future. In: Matsuno T, Kida, H., (Ed.). Present and Future of Modeling Global Environmental Change: Toward Integrated Modeling. Terrapub.

Brosché M, Merilo EBE, Mayer F, Pechter P, Puzõrjova I, Brader G, Kangasjärvi J, Kollist H. 2010. Natural variation in ozone sensitivity among *Arabidopsis thaliana* accessions and its relation to stomatal conductance. Plant, Cell & Environment **33**, 914-925.

Büker P, Emberson LD, Ashmore MR, *et al.* 2007. Comparison of different stomatal conductance algorithms for ozone flux modelling. Environmental Pollution **146**, 726-735.

Büker P, Morrissey T, Briolat A, *et al.* 2012. DO_3SE modelling of soil moisture to determine ozone flux to forest trees. Atmospheric Chemistry and Physics **12**, 5537-5562.

Burkart S, Bender J, Tarkotta B, Faust S, Castagna A, Ranieri A, Weigel HJ. 2013. Effects of ozone on leaf senescence, photochemical efficiency and grain yield in two winter wheat cultivars. Journal of Agronomy and Crop Science **199**, 275-285.

Burkey KO, Wei CM, Eason G, Ghosh P, Fenner GP. 2000. Antioxidant metabolite levels in ozone-sensitive and tolerant genotypes of snap bean. Physiologia Plantarum **110**, 195-200.

Burnham K, Anderson D. 2002. Model Selection and Multimodel Inference. A Practical Information-Theoretic Approach. Springer-Verlag New York.

Butler LK, Tibbitts T. 1979. Variation in ozone sensitivity and symptom expression among cultivars of *Phaseolus vulgaris* (L). Journal of the American Society for Horticultural Science **104**, 208-210.

Calfapietra C, Fares S, Manes F, Morani A, Sgrigna G, Loreto F. 2013. Role of Biogenic Volatile Organic Compounds (BVOC) emitted by urban trees on ozone concentration in cities: A review. Environmental Pollution **183**, 71-80.

Castagna A, Ranieri A. 2009. Detoxification and repair process of ozone injury: From O_3 uptake to gene expression adjustment. Environmental Pollution **157**, 1461-1469.

Chakraborty T, Beig G, Dentener FJ, Wild O. 2015. Atmospheric transport of ozone between Southern and Eastern Asia. Science of the Total Environment **523**, 28-39.

Challinor AJ, Ewert F, Arnold S, Simelton E, Fraser E. 2009. Crops and climate change: progress, trends, and challenges in simulating impacts and informing adaptation. Journal of Experimental Botany **60**, 2775-2789.

Chappelka AH, Freer-Smith PH. 1995. Predisposition of trees by air pollutants to low temperatures and moisture stress. Environmental Pollution **87**, 105-117.

Chaves MM, Maroco JP, Pereira JS. 2003. Understanding plant responses to drought - from genes to the whole plant. Functional Plant Biology. **30**, 239-264.

Chernikova T, Robinson JM, Lee EH, Mulchi CL. 2000. Ozone tolerance and antioxidant enzyme activity in soybean cultivars. Photosynthesis Research **64**, 15-26.

Chuwah C, van Noije T, van Vuuren DP, Stehfest E, Hazeleger W. 2015. Global impacts of surface ozone changes on crop yields and land use. Atmospheric Environment **106**, 11-23.

CLRTAP. 2017. Mapping Critical Levels for Vegetation. Chapter 3 of manual on methodologies and criteria for modelling and mapping critical loads and levels and air pollution effects, risks and trends. www.icpmapping.org.

Conklin P, Barth C. 2004. Ascorbic acid, a familiar small molecule intertwined in the response of plants to ozone, pathogens, and the onset of senescence. Plant, Cell & Environment **27**, 959-970.

Cooper OR, Parrish D, Ziemke J, Balashov N, Cupeiro M, Galbally I, Gilge S, Horowitz L, Jensen N, Lamarque J-F. 2014. Global distribution and trends of tropospheric ozone: An observation-based review. Elementa: Science of the Anthropocene **2**, 29.

Cowan I, Farquhar G. 1977. Integration of activity in the higher plant. Cambridge University Press, Cambridge.

DAC. 2014. Agricultural statistics at a glance 2014. New Delhi.

Dai A. 2011. Drought under global warming: a review. Wiley Interdisciplinary Reviews: Climate Change **2**, 45-65.

Damour G, Simonneau T, Cochard H, Urban L. 2010. An overview of models of stomatal conductance at the leaf level. Plant, Cell & Environment **33**, 1419-1438.

Danielsson H, Karlsson GP, Karlsson PE, Pleijel HH. 2003. Ozone uptake modelling and flux-response relationships - an assessment of ozone-induced yield loss in spring wheat. Atmospheric Environment **37**, 475-485.

Dann MS, Pell EJ. 1989. Decline of activity and quantity of ribulose bisphosphate carboxylase/oxygenase and net photosynthesis in ozone-treated potato foliage. Plant Physiology **91**, 427-432.

De Kauwe MG, Lin Y-S, Wright IJ, *et al.* 2016. A test of the 'one-point method' for estimating maximum carboxylation capacity from field-measured, light-saturated photosynthesis. New Phytologist **210**, 1130-1144.

DEFRA. 2009. Air Quality Expert Group - Ozone in the United Kingdom. London, UK.

Derwent R, Kay P. 1988. Factors influencing the ground level distribution of ozone in Europe. Environmental Pollution **55**, 191-219.

Derwent R, Stevenson D, Doherty R, Collins W, Sanderson M. 2008. How is surface ozone in Europe linked to Asian and North American NOx emissions? Atmospheric Environment **42**, 7412-7422.

Derwent RG, Jenkin ME, Saunders SM, Pilling MJ, Simmonds PG, Passant NR, Dollard GJ, Dumitrean P, Kent A. 2003. Photochemical ozone formation in north west Europe and its control. Atmospheric Environment **37**, 1983-1991.

Dignon J, Hameed S. 1989. Global emissions of nitrogen and sulfur oxides from 1860 to 1980. JAPCA **39**, 180-186.

Eck HV. 1986. Effects of water deficits on yield, yield components, and water use efficiency of irrigated corn. Agronomy Journal **78**, 1035-1040.

Emberson L, Pleijel H, Ainsworth EA, *et al.* submitted. Ozone effects on crops and consideration in crop models. **European Journal of Agronomy**.

Emberson L, Simpson D, Tuovinen J, Ashmore M, Cambridge H. 2000a. Towards a model of ozone deposition and stomatal uptake over Europe. Research note (Norske meteorologiske institutt) **6**.

Emberson L, Simpson D, Tuovinen J, Ashmore M, Cambridge H. 2000b. Towards a model of ozone deposition and stomatal uptake over Europe. EMEP MSC-W Note **6**.

Emberson L, Wieser G, Ashmore M. 2000c. Modelling of stomatal conductance and ozone flux of Norway spruce: comparison with field data. Environmental Pollution **109**, 393-402.

Emberson LD, Ashmore MR, Cambridge HM, Simpson D, Tuovinen JP. 2000d. Modelling stomatal ozone flux across Europe. Environmental Pollution **109**, 403-413.

Emberson LD, Buker P, Ashmore MR, *et al.* 2009. A comparison of North American and Asian exposure-response data for ozone effects on crop yields. Atmospheric Environment **43**, 1945-1953.

Engardt M. 2008. Modelling of near-surface ozone over South Asia. Journal of Atmospheric Chemistry **59**, 61-80.

Estrada-Campuzano G, Slafer GA, Miralles DJ. 2012. Differences in yield, biomass and their components between triticale and wheat grown under contrasting water and nitrogen environments. Field Crops Research **128**, 167-179.

Ewert F, Porter JR. 2000. Ozone effects on wheat in relation to CO_2: modelling short-term and long-term responses of leaf photosynthesis and leaf duration. Global Change Biology **6**, 735-750.

Fagnano M, Maggio A, Fumagalli I. 2009. Crops' responses to ozone in Mediterranean environments. Environmental Pollution **157**, 1438-1444.

Falkenmark M. 2013. Growing water scarcity in agriculture: future challenge to global water security. Philosophical Transactions of the Royal Society A: Mathematical Physical and Engineering Sciences **371**, 20120410.

Fangmeier A, Bender J. 2002. Air pollutant combinations - Significance for future impact assessments on vegetation. Phyton: Horn **42**, 65-72.

Fangmeier A, Brockerhoff U, Grüters U, Jäger HJ. 1994a. Growth and yield responses of spring wheat (*Triticum aestivum* L. cv. Turbo) grown in open-top chambers to ozone and water stress. Environmental Pollution **83**, 317-325.

Fangmeier A, Brunschon S, Jager HJ. 1994b. Time-course of oxidant stress biomarkers in flag leaves of wheat exposed to ozone and drought stress. New Phytologist **126**, 63-69.

FAO. 2011. The state of the world's land and water resources for food and agriculture (SOLAW) - Managing systems at risk. Earthscan, London/Rome.

FAO. 2012. World Agriculture Towards 2030/2050: The 2012 Revision. ESA Working Paper No. 12-03. Rome.

FAO. 2014. FAOSTAT. FAO. Rome, Italy. http://faostat.fao.org/default.aspx

FAO. 2015. The State of Food Insecurity in the World 2015. Meeting the 2015 international hunger targets: taking stock of uneven progress. Rome.

Farage P, Long S. 1995. An in vivo analysis of photosynthesis during short-term O_3 exposure in three contrasting species. Photosynthesis Research **43**, 11-18.

Farage PK, Long SP, Lechner EG, Baker NR. 1991. The sequence of change within the photosynthetic apparatus of wheat following short-term exposure to ozone. Plant Physiology **95**, 529-535.

Fares S, Matteucci G, Scarascia Mugnozza G, Morani A, Calfapietra C, Salvatori E, Fusaro L, Manes F, Loreto F. 2013. Testing of models of stomatal ozone fluxes with field measurements in a mixed Mediterranean forest. Atmospheric Environment **67**, 242-251.

Farquhar GD, Caemmerer SV, Berry JA. 1980. A biochemical model of photosynthetic CO_2 assimilation in leaves of C3 species. Planta **149**, 78-90.

Feng Z, Kobayashi K. 2009. Assessing the impacts of current and future concentrations of surface ozone on crop yield with meta-analysis. Atmospheric Environment **43**, 1510-1519.

Feng Z, Kobayashi K, Ainsworth EA. 2008. Impact of elevated ozone concentration on growth, physiology, and yield of wheat (Triticum aestivum L.): a meta-analysis. Global Change Biology **14**, 2696-2708.

Feng Z, Pang J, Kobayashi K, Zhu J, Ort DR. 2011. Differential responses in two varieties of winter wheat to elevated ozone concentration under fully open-air field conditions. Global Change Biology **17**, 580-591.

Finlayson-Pitts BJ, Pitts JN. 1993. Atmospheric chemistry of tropospheric ozone formation - scientific and regulatory implications. Journal of the Air & Waste Management Association **43**, 1091-1100.

Finnan J, Burke J, Jones M. 1997. An evaluation of indices that describe the impact of ozone on the yield of spring wheat (*Triticum aestivum* L.). Atmospheric Environment **31**, 2685-2693.

Fiore AM, Naik V, Spracklen DV, *et al.* 2012. Global air quality and climate. Chemical Society Reviews **41**, 6663-6683.

Fiscus EL, Booker FL, Burkey KO. 2005. Crop responses to ozone: uptake, modes of action, carbon assimilation and partitioning. Plant Cell and Environment **28**, 997-1011.

Fiscus EL, Reid CD, Miller JE, Heagle AS. 1997. Elevated CO_2 reduces O_3 flux and O_3-induced yield losses in soybeans: Possible implications for elevated CO_2 studies. Journal of Experimental Botany **48**, 307-313.

Fox J, Weisberg S. 2011. An R companion to Applied Regression, Second Edition. Thousand Oaks CA: Sage.

Frei M. 2015. Breeding of ozone resistant rice: Relevance, approaches and challenges. Environmental Pollution **197**, 144-155.

Frei M, Tanaka JP, Chen CP, Wissuwa M. 2010. Mechanisms of ozone tolerance in rice: characterization of two QTLs affecting leaf bronzing by gene expression profiling and biochemical analyses. Journal of Experimental Botany **61**, 1405-1417.

Frei M, Tanaka JP, Wissuwa M. 2008. Genotypic variation in tolerance to elevated ozone in rice: dissection of distinct genetic factors linked to tolerance mechanisms. Journal of Experimental Botany **59**, 3741-3752.

Fuhrer J. 2009. Ozone risk for crops and pastures in present and future climates. Naturwissenschaften **96**, 173-194.

Fuhrer J, Egger A, Lehnherr B, Grandjean A, Tschannen W. 1989. Effects of ozone on the yield of spring wheat (*Triticum aestivum* L., cv. Albis) grown in open-top field chambers. Environmental Pollution **60**, 273-289.

Fuhrer J, Skarby L, Ashmore MR. 1997. Critical levels for ozone effects on vegetation in Europe. Environmental Pollution **97**, 91-106.

Galmés J, Aranjuelo I, Medrano H, Flexas J. 2013. Variation in Rubisco content and activity under variable climatic factors. Photosynthesis Research **117**, 73-90.

Gelang J, Pleijel H, Sild E, Danielsson H, Younis S, Selldén G. 2000. Rate and duration of grain filling in relation to flag leaf senescence and grain yield in spring wheat (*Triticum aestivum*) exposed to different concentrations of ozone. Physiologia Plantarum **110**, 366-375.

Gillespie KM, Xu FX, Richter KT, McGrath JM, Markelz RJC, Ort DR, Leakey ADB, Ainsworth EA. 2012. Greater antioxidant and respiratory metabolism in field-grown soybean exposed to elevated O_3 under both ambient and elevated CO_2. Plant Cell and Environment **35**, 169-184.

Glick RE, Schlagnhaufer CD, Arteca RN, Pell EJ. 1995. Ozone-induced ethylene emission accelerates the loss of ribulose-1,5-biphosphate carboxylase oxygenase and nuclear-encoded messenger-rnas in senescing potato leaves. Plant Physiology **109**, 891-898.

González-Fernández I, Bermejo V, Elvira S, De La Torre D, González A, Navarrete L, Sanz J, Calvete H, García-Gómez H, López A. 2013. Modelling ozone stomatal flux of wheat under mediterranean conditions. Atmospheric Environment **67**, 149-160.

Graham PH, Vance CP. 2003. Legumes: Importance and constraints to greater use. Plant Physiology **131**, 872-877.

Grandjean A, Fuhrer J. 1989. Growth and leaf senescence in spring wheat (*Triticum aestivum*) grown at different ozone concentrations in open-top field chambers. Physiologia Plantarum **77**, 389-394.

Granier C, Bessagnet B, Bond T, *et al.* 2011. Evolution of anthropogenic and biomass burning emissions of air pollutants at global and regional scales during the 1980–2010 period. Climatic Change **109**, 163-190.

Grantz DA, Farrar JF. 2000. Ozone inhibits phloem loading from a transport pool: compartmental efflux analysis in Pima cotton. Australian Journal of Plant Physiology **27**, 859-868.

Grünhage L, Pleijel H, Mills G, Bender J, Danielsson H, Lehmann Y, Castell J-F, Bethenod O. 2012. Updated stomatal flux and flux-effect models for wheat for quantifying effects of ozone on grain yield, grain mass and protein yield. Environmental Pollution **165**, 147-157.

Guidi L, Degl'Innocenti E, Soldatini GF. 2002. Assimilation of CO_2, enzyme activation and photosynthetic electron transport in bean leaves, as affected by high light and ozone. New Phytologist **156**, 377-388.

Hanson P, Samuelson L, Wullschleger S, Tabberer T, Edwards G. 1994. Seasonal patterns of light-saturated photosynthesis and leaf conductance for mature and seedling *Quercus rubra* L. foliage: differential sensitivity to ozone exposure. Tree Physiology **14**, 1351-1366.

Harmens H, Hayes F, Sharps K, Mills G, Calatayud V. 2017. Leaf traits and photosynthetic responses of *Betula pendula* saplings to a range of ground-level ozone concentrations at a range of nitrogen loads. Journal of Plant Physiology **211**, 42-52.

Harmens H, Mills G, Emberson LD, Ashmore MR. 2007. Implications of climate change for the stomatal flux of ozone: A case study for winter wheat. Environmental Pollution **146**, 763-770.

Hartman GL, West ED, Herman TK. 2011. Crops that feed the World 2. Soybean - worldwide production, use, and constraints caused by pathogens and pests. Food Security **3**, 5-17.

Hayes F, Wagg S, Mills G, Wilkinson S, Davies W. 2012. Ozone effects in a drier climate: implications for stomatal fluxes of reduced stomatal sensitivity to soil drying in a typical grassland species. Global Change Biology **18**, 948-959.

Hayes F, Williamson J, Mills G. 2015. Species-specific responses to ozone and drought in six deciduous trees. Water, Air, & Soil Pollution **226**, 156.

Heagle A. 1989. Ozone and crop yield. Annual Review of Phytopathology **27**, 397-423.

Heagle A, Flagler RB, Patterson RP, Lesser VM, Shafer SR, Heck WW. 1987. Injury and yield response of soybean to chronic doses of ozone and soil-moisture deficit. Crop Science **27**, 1016-1024.

Heagle A, Heck WW, Rawlings JO, Philbeck RB. 1983a. Effects of chronic doses of ozone and sulfur dioxide on injury and yield of soybeans in open-top field chambers. Crop Science **23**, 1184-1191.

Heagle A, Lesser VM, Rawlings JO, Heck WW, Philbeck RB. 1986. Response of soybeans to chronic doses of ozone applied as constant or proportional additions to ambient air. Phytopathology **76**, 6.

Heagle A, Letchworth M. 1982. Relationships among injury, growth, and yield responses of soybean cultivars exposed to ozone at different light intensities. Journal of Environmental Quality **11**, 690-694.

Heagle A, Letchworth MB, Mitchell CA. 1983b. Effects of growth medium and fertilizer rate on the yield response of soybeans exposed to chronic doses of ozone. Phytopathology **73**, 134-139.

Heagle A, Miller JE, Pursley WA. 1998. Influence of ozone stress on soybean response to carbon dioxide enrichment: III. Yield and seed quality. Crop Science **38**, 128-134.

Heagle A, Miller JE, Rawlings JO, Vozzo SF. 1991. Effect of growth stage on soybean response to chronic ozone exposure. Journal of Environmental Quality **20**, 562-570.

Heagle AS, Miller JE, Heck WW, Patterson RP. 1988. Injury and yield response of cotton to chronic doses of ozone and soil moisture deficit. Journal of Environmental Quality **17**, 627-635.

Heggestad H, Anderson EL, Gish TJ, Lee EH. 1988. Effects of ozone and soil-water deficit on roots and shoots of field-grown soybeans. Environmental Pollution **50**, 259-278.

Heggestad H, Gish T, Lee E, Bennett J, Douglass L. 1985. Interaction of soil moisture stress and ambient ozone on growth and yields of soybeans. Phytopathology **75**, 472-477.

Heggestad H, Lesser VM. 1990. Effects of ozone, sulfur dioxide, soil water deficit, and cultivar on yields of soybean. Journal of Environmental Quality **19**, 488-495.

Herridge DF, Peoples MB, Boddey RM. 2008. Global inputs of biological nitrogen fixation in agricultural systems. Plant and Soil **311**, 1-18.

Hewitt D, Mills G, Hayes F, Norris D, Coyle M, Wilkinson S, Davies W. 2015. N-fixation in legumes–An assessment of the potential threat posed by ozone pollution. Environmental Pollution, In press.

Hewitt DKL, Mills G, Hayes F, Davies W. 2016. The climate benefits of high-sugar grassland may be compromised by ozone pollution. Science of the Total Environment **565**, 95-104.

Hewitt DKL, Mills G, Hayes F, Wilkinson S, Davies W. 2014. Highlighting the threat from current and near-future ozone pollution to clover in pasture. Environmental Pollution **189**, 111-117.

Hollaway MJ, Arnold SR, Challinor AJ, Emberson LD. 2012. Intercontinental trans-boundary contributions to ozone-induced crop yield losses in the Northern Hemisphere. Biogeosciences **9**, 271-292.

Hough AM, Derwent RG. 1990. Changes in the global concentration of tropospheric ozone due to human activities. Nature **344**, 645-648.

Huot B, Yao J, Montgomery BL, He SY. 2014. Growth-defense tradeoffs in plants: a balancing act to optimize fitness. Molecular Plant **7**, 1267-1287.

ICAR. 2012. Recent Varieties and Hybrids of Annual Oilseeds Recommended for Different States. Directorate of Oilseeds Development, Himayatnager, Hyderabad.

IPCC. 2013a. Annex II: Climate System Scenario Tables. Cambridge University Press. Cambridge, UK, and New York, USA.

IPCC. 2013b. Summary for Policymakers. Cambridge University Press. Cambridge, UK and New York, USA.

IPCC. 2014a. Climate Change 2014: Synthesis Report. Contribution of Working Groups I, II and III to the Fifth Assessment Report of the Intergovernmnetal Panel on Climate Change (Core Writing Team, R.K. Pauchauri and L.A. Meyer (*Eds.*)]. Geneva, Switzerland.

IPCC. 2014b. Summary for policymakers. Cambridge University Press. Cambridge, UK and New York, USA.

Jaffe D, Price H, Parrish D, Goldstein A, Harris J. 2003. Increasing background ozone during spring on the west coast of North America. Geophysical Research Letters **30**, 1613.

Jaffe D, Ray J. 2007. Increase in surface ozone at rural sites in the western US. Atmospheric Environment **41**, 5452-5463.

Jäger HJ, Unsworth M, De Temmerman L, Mathy P. 1992. Effects of air pollution on agricultural crops in Europe: results of the European open-top chambers project. Air Pollution Research Report 46, Belgium.

Jamieson P, Brooking I, Semenov M, McMaster G, White J, Porter JR. 2007. Reconciling alternative models of phenological development in winter wheat. Field Crops Research **103**, 36-41.

Jarvis P. 1976. The interpretation of the variations in leaf water potential and stomatal conductance found in canopies in the field. Philosophical Transactions of the Royal Society of London B: Biological Sciences **273**, 593-610.

Jin J, Liu X, Wang G, Mi L, Shen Z, Chen X, Herbert SJ. 2010. Agronomic and physiological contributions to the yield improvement of soybean cultivars released from 1950 to 2006 in Northeast China. Field Crops Research **115**, 116-123.

Kangasjärvi J, Talvinen J, Utriainen M, Karjalainen R. 1994. Plant defence systems induced by ozone. Plant, Cell & Environment **17**, 783-794.

Karlsson P, Braun S, Broadmeadow M, *et al.* 2007. Risk assessments for forest trees: The performance of the ozone flux versus the AOT concepts. Environmental Pollution **146**, 608-616.

Karlsson PE, Klingberg J, Engardt M, Andersson C, Langner J, Karlsson GP, Pleijel H. 2017. Past, present and future concentrations of ground-level ozone and potential impacts on ecosystems and human health in northern Europe. Science of the Total Environment **576**, 22-35.

Karmakar PG, Bhatnagar PS. 1996. Genetic improvement of soybean varieties released in India from 1969 to 1993. Euphytica **90**, 95-103.

Khan S, Soja G. 2003. Yield responses of wheat to ozone exposure as modified by drought-induced differences in ozone uptake. Water, Air, and Soil Pollution **147**, 299-315.

Khemani L, Momin G, Rao P, Vijayakumar R, Safai P. 1995. Study of surface ozone behaviour at urban and forested sites in India. Atmospheric Environment **29**, 2021-2024.

Klingberg J, Engardt M, Uddling J, Karlsson PE, Pleijel H. 2011. Ozone risk for vegetation in the future climate of Europe based on stomatal ozone uptake calculations. Tellus A **63**, 174-187.

Koester RP, Skoneczka JA, Cary TR, Diers BW, Ainsworth EA. 2014. Historical gains in soybean (*Glycine max* Merr.) seed yield are driven by linear increases in light interception, energy conversion, and partitioning efficiencies. Journal of Experimental Botany **65**, 3311-3321.

Kohut RJ, Amundson RG, Laurence JA. 1986. Evaluation of growth and yield of soybean exposed to ozone in the field. Environmental Pollution Series A **41**, 219-234.

Kress LW, Miller JE. 1983. Impact of ozone on soybean yield. Journal of Environmental Quality **12**, 276-281.

Kress LW, Miller JE, Smith HJ, Rawlings JO. 1986. Impact of ozone and sulfur-dioxide on soybean yield. Environmental Pollution Series A **41**, 105-123.

Krupa S, McGrath MT, Andersen CP, Booker FL, Burkey KO, Chappelka AH, Chevone BI, Pell EJ, Zilinskas BA. 2001. Ambient ozone and plant health. Plant Disease **85**, 4-12.

Kumari S, Jayaraman G, Ghosh C. 2013. Analysis of long-term ozone trend over Delhi and its meteorological adjustment. International Journal of Environmental Science and Technology **10**, 1325-1336.

Kuznetsova A, Brockhoff PB, Christensen RHB. 2016. lmerTest: Tests in Linear Mixed Effects Models. R package version 2.0-33.

Lehnherr B, Grandjean A, Mächler F, Fuhrer J. 1987. The effect of ozone in ambient air on ribulosebisphosphate carboxylase/oxygenase activity decreases photosynthesis and grain yield in wheat. Journal of Plant Physiology **130**, 189-200.

Lehnherr B, Mächler F, Grandjean A, Fuhrer J. 1988. The regulation of photosynthesis in leaves of field-grown spring wheat (*Triticum aestivum* L., cv Albis) at different levels of ozone in ambient air. Plant Physiology **88**, 1115-1119.

Lei H, Wuebbles DJ, Liang X-Z. 2012. Projected risk of high ozone episodes in 2050. Atmospheric Environment **59**, 567-577.

Lesser VM, Rawlings JO, Spruill SE, Somerville MC. 1990. Ozone effects on agricultural crops - statistical methodologies and estimated dose-response relationships. Crop Science **30**, 148-155.

Leuning R. 1990. Modelling stomatal behaviour and and photosynthesis of *Eucalyptus grandis*. Functional Plant Biology **17**, 159-175.

Leuning R. 1995. A critical appraisal of a combined stomatal-photosynthesis model for C3 plants. Plant, Cell & Environment **18**, 339-355.

Licker R, Johnston M, Foley JA, Barford C, Kucharik CJ, Monfreda C, Ramankutty N. 2010. Mind the gap: how do climate and agricultural management explain the 'yield gap' of croplands around the world? Global Ecology and Biogeography **19**, 769-782.

Lim PO, Kim HJ, Nam HG. 2007. Leaf senescence. Annual Review of Plant Biology **58**, 115-136.

Liu G, Chunwu Y, Kezhang X, Zhian Z, Dayong L, Zhihai W, Zhanyu C. 2012. Development of yield and some photosynthetic characteristics during 82 years of genetic improvement of soybean genotypes in northeast China. Australian Journal of Crop Science **6**, 1416-1422.

Lombardozzi D, Sparks J, Bonan G, Levis S. 2012. Ozone exposure causes a decoupling of conductance and photosynthesis: implications for the Ball-Berry stomatal conductance model. Oecologia **169**, 651-659.

Long SP, Ainsworth EA, Leakey AD, Morgan PB. 2005. Global food insecurity. Treatment of major food crops with elevated carbon dioxide or ozone under large-scale fully open-air conditions suggests recent models may have overestimated future yields. Philosophical Transactions of the Royal Society B: Biological Sciences **360**, 2011-2020.

Long SP, Ainsworth EA, Leakey AD, Nösberger J, Ort DR. 2006. Food for thought: lower-than-expected crop yield stimulation with rising CO_2 concentrations. Science **312**, 1918-1921.

López-Castañeda C, Richards R. 1994. Variation in temperate cereals in rainfed environments III. Water use and water-use efficiency. Field Crops Research **39**, 85-98.

Loreto F, Velikova V. 2001. Isoprene produced by leaves protects the photosynthetic apparatus against ozone damage, quenches ozone products, and reduces lipid peroxidation of cellular membranes. Plant Physiology **127**, 1781-1787.

Maas R, Grennfelt P. 2016. Towards Cleaner Air. Scientific Assessment Report 2016. EMEP Steering Body and Working Group on Effects of the Convention on Long-Range Transboundary Air Pollution. Oslo, Norway.

Maas RJM. 2007. Review of the Gothenburg Protocol. Report of the Task Force on Integrated Assessment Modelling and the Centre for Integrated Assessment Modelling. Bilthoven, The Netherlands.

Martin MJ, Farage PK, Humphries SW, Long SP. 2000. Can the stomatal changes caused by acute ozone exposure be predicted by changes occurring in the mesophyll? A simplification for

models of vegetation response to the global increase in tropospheric elevated ozone episodes. Functional Plant Biology **27**, 211-219.

Mason CH, Perreault Jr WD. 1991. Collinearity, power, and interpretation of multiple regression analysis. Journal of marketing research **28**, 268-280.

Massman W. 1998. A review of the molecular diffusivities of H_2O, CO_2, CH_4, CO, O_3, SO_2, NH_3, N_2O, NO, and NO_2 in air, O_2 and N_2 near STP. Atmospheric Environment **32**, 1111-1127.

Massman W. 2004. Toward an ozone standard to protect vegetation based on effective dose: a review of deposition resistances and a possible metric. Atmospheric Environment **38**, 2323-2337.

Masuda T, Goldsmith PD. 2009. World soybean production: area harvested, yield, and long-term projections. International Food and Agribusiness Management Review **12**, 143-162.

Mateos-Aparicio I, Redondo-Cuenca A, Villanueva-Suárez M, Zapata-Revilla M. 2008. Soybean, a promising health source. Nutrición Hospitalaria **23**, 305.

Matyssek R, Le Thiec D, Löw M, Dizengremel P, Nunn A, Häberle K-H. 2006. Interactions between drought and O_3 stress in forest trees. Plant Biology **8**, 11-17.

McAinsh MR, Evans NH, Montgomery LT, North KA. 2002. Calcium signalling in stomatal responses to pollutants. New Phytologist **153**, 441-447.

Medlyn BE, Duursma RA, Eamus D, Ellsworth DS, Prentice IC, Barton CV, Crous KY, De Angelis P, Freeman M, Wingate L. 2011. Reconciling the optimal and empirical approaches to modelling stomatal conductance. Global Change Biology **17**, 2134-2144.

Meyer U, Köllner B, Willenbrink J, Krause GHM. 2000. Effects of different ozone exposure regimes on photosynthesis, assimilates and thousand grain weight in spring wheat. Agriculture, Ecosystems & Environment **78**, 49-55.

Miglietta F. 1989. Effect of photoperiod and temperature on leaf initiation rates in wheat (*Triticum* spp.). Field Crops Research **21**, 121-130.

Miladinović J, Vidić M, Đorđević V, Balešević-Tubić S. 2015. New trends in plant breeding - example of soybean. Genetika **47**, 131-142.

Miller J, Booker F, Fiscus E, Heagle A, Pursley W, Vozzo S, Heck W. 1994. Ultraviolet-B radiation and ozone effects on growth, yield, and photosynthesis of soybean. Journal of Environmental Quality **23**, 83-91.

Miller J, Heagle AS, Vozzo SF, Philbeck RB, Heck WW. 1989. Effects of ozone and water stress, seperately and in combination, on soybean yield. Journal of Environmental Quality **18**, 330-336.

Miller JD, Arteca RN, Pell EJ. 1999. Senescence-associated gene expression during ozone-induced leaf senescence in *Arabidopsis*. Plant Physiology **120**, 1015-1023.

Mills G, Buse A, Gimeno B, Bermejo V, Holland M, Emberson L, Pleijel H. 2007. A synthesis of AOT40-based response functions and critical levels of ozone for agricultural and horticultural crops. Atmospheric Environment **41**, 2630-2643.

Mills G, Harmens H. 2011. Ozone pollution: a hidden threat to food security. Convention on long-range transboundary air pollution. ICP Vegetation, Centre for Ecology and Hydrology, Bangor, UK.

Mills G, Hayes F, Simpson D, Emberson L, Norris D, Harmens H, Buker P. 2011a. Evidence of widespread effects of ozone on crops and (semi-)natural vegetation in Europe (1990-2006) in relation to AOT40-and flux-based risk maps. Global Change Biology **17**, 592-613.

Mills G, Hayes F, Wilkinson S, Davies WJ. 2009. Chronic exposure to increasing background ozone impairs stomatal functioning in grassland species. Global Change Biology **15**, 1522-1533.

Mills G, Pleijel H, Braun S, *et al.* 2011b. New stomatal flux-based critical levels for ozone effects on vegetation. Atmospheric Environment **45**, 5064-5068.

Mills G, Wagg S, Harmens H. 2013. Ozone pollution: impacts on ecosystem services and biodiversity. Centre for Ecology & Hydrology, Bangor, UK.

Mittal ML, Hess PG, Jain S, Arya B, Sharma C. 2007. Surface ozone in the Indian region. Atmospheric Environment **41**, 6572-6584.

Morgan PB, Ainsworth EA, Long SP. 2003. How does elevated ozone impact soybean? A meta-analysis of photosynthesis, growth and yield. Plant Cell and Environment **26**, 1317-1328.

Morgan PB, Bernacchi CJ, Ort DR, Long SP. 2004. An in vivo analysis of the effect of season-long open-air elevation of ozone to anticipated 2050 levels on photosynthesis in soybean. Plant Physiology **135**, 2348-2357.

Morgan PB, Mies TA, Bollero GA, Nelson RL, Long SP. 2006. Season-long elevation of ozone concentration to projected 2050 levels under fully open-air conditions substantially decreases the growth and production of soybean. New Phytologist **170**, 333-343.

Morrison MJ, Voldeng HD, Cober ER. 2000. Agronomic changes from 58 years of genetic improvement of short-season soybean cultivars in Canada. Agronomy Journal **92**, 780-784.

Mulchi C, Lee E, Tuthill K, Olinick EV. 1988. Influence of ozone stress on growth processes, yields and grain quality characteristics among soybean cultivars. Environmental Pollution **53**, 151-169.

Mulchi C, Rudorff B, Lee E, Rowland R, Pausch R. 1995. Morphological responses among crop species to full-season exposures to enhanced concentrations of atmospheric CO_2 and O_3. Water Air and Soil Pollution **85**, 1379-1386.

Mulholland B, Craigon J, Black C, Colls J, Atherton J, Landon G. 1997a. Effects of elevated carbon dioxide and ozone on the growth and yield of spring wheat (*Triticum aestivum* L.). Journal of Experimental Botany **48**, 113-122.

Mulholland B, Craigon J, Black C, Colls J, Atherton J, Landon G. 1997b. Impact of elevated atmospheric CO_2 and O_3 on gas exchange and chlorophyll content in spring wheat (*Triticum aestivum* L.). Journal of Experimental Botany **48**, 1853-1863.

Novick KA, Ficklin DL, Stoy PC, Williams CA, Bohrer G, Oishi AC, Papuga SA, Blanken PD, Noormets A, Sulman BN. 2016. The increasing importance of atmospheric demand for ecosystem water and carbon fluxes. Nature Climate Change **6**, 1023-1027.

O'brien RM. 2007. A caution regarding rules of thumb for variance inflation factors. Quality & Quantity **41**, 673-690.

Ojanperä K, Pätsikkä E, Yläranta T. 1998. Effects of low ozone exposure of spring wheat on net CO_2 uptake, Rubisco, leaf senescence and grain filling. New Phytologist **138**, 451-460.

Osborne SA, Mills G, Hayes F, Ainsworth EA, Büker P, Emberson L. 2016. Has the sensitivity of soybean cultivars to ozone pollution increased with time? An analysis of published dose–response data. Global Change Biology **22**, 3097-3111.

Pääkkönen E, Vahala J, Pohjola M, Holopainen T, Kärenlampi L. 1998. Physiological, stomatal and ultrastructural ozone responses in birch (*Betula pendula* Roth.) are modified by water stress. Plant, Cell & Environment **21**, 671-684.

Pang J, Kobayashi K, Zhu JG. 2009. Yield and photosynthetic characteristics of flag leaves in Chinese rice (*Oryza sativa* L.) varieties subjected to free-air release of ozone. Agriculture Ecosystems & Environment **132**, 203-211.

Panthee D. 2010. Varietal improvement in soybean. CABI, UK.

Paoletti E. 2005. Ozone slows stomatal response to light and leaf wounding in a Mediterranean evergreen broadleaf, *Arbutus unedo*. Environmental Pollution **134**, 439-445.

Paoletti E. 2007. Ozone impacts on forests. CAB Reviews: Perspectives in Agriculture, Veterinary Science, Nutrition and Natural Resources. **2**, 68.

Paoletti E, De Marco A, Beddows DC, Harrison RM, Manning WJ. 2014. Ozone levels in European and USA cities are increasing more than at rural sites, while peak values are decreasing. Environmental Pollution **192**, 295-299.

Paoletti E, De Marco A, Racalbuto S. 2007. Why should we calculate complex indices of ozone exposure? Results from Mediterranean background sites. Environmental Monitoring and Assessment **128**, 19-30.

Paoletti E, Manning WJ. 2007. Toward a biologically significant and usable standard for ozone that will also protect plants. Environmental Pollution **150**, 85-95.

Parrish D, Lamarque JF, Naik V, Horowitz L, Shindell D, Staehelin J, Derwent R, Cooper O, Tanimoto H, Volz-Thomas A. 2014. Long-term changes in lower tropospheric baseline ozone concentrations: Comparing chemistry-climate models and observations at northern midlatitudes. Journal of Geophysical Research: Atmospheres **119**, 5719-5736.

Parrish DD, Law KS, Staehelin J, *et al.* 2012. Long-term changes in lower tropospheric baseline ozone concentrations at northern mid-latitudes. Atmospheric Chemistry and Physics **12**, 11485-11504.

Parry ML, Rosenzweig C, Iglesias A, Livermore M, Fischer G. 2004. Effects of climate change on global food production under SRES emissions and socio-economic scenarios. Global Environmental Change - Human and Policy Dimensions **14**, 53-67.

Pedersen P, Lauer JG. 2004. Soybean growth and development in various management systems and planting dates. Crop Science **44**, 508-515.

Piikki K, De Temmerman L, Högy P, Pleijel H. 2008. The open-top chamber impact on vapour pressure deficit and its consequences for stomatal ozone uptake. Atmospheric Environment **42**, 6513-6522.

Pinheiro J, Bates D, DebRoy S, Sarkar D, Team RC. 2015. lme: linear and nonlinear mixed effects models.

Pleijel H, Danielsson H, Emberson L, Ashmore M, Mills G. 2007. Ozone risk assessment for agricultural crops in Europe: further development of stomatal flux and flux–response relationships for European wheat and potato. Atmospheric Environment **41**, 3022-3040.

Pleijel H, Danielsson H, Ojanpera K, De Temmerman L, Hogy P, Badiani M, Karlsson PE. 2004. Relationships between ozone exposure and yield loss in European wheat and potato - a comparison of concentration- and flux-based exposure indices. Atmospheric Environment **38**, 2259-2269.

Pleijel H, Danielsson H, Vandermeiren K, Blum C, Colls J, Ojanperä K. 2002. Stomatal conductance and ozone exposure in relation to potato tuber yield - results from the European CHIP programme. European Journal of Agronomy **17**, 303-317.

Pleijel H, Eriksen AB, Danielsson H, Bondesson N, Sellden G. 2006. Differential ozone sensitivity in an old and a modem Swedish wheat cultivar - grain yield and quality, leaf chlorophyll and stomatal conductance. Environmental and Experimental Botany **56**, 63-71.

Pleijel H, Ojanpera K, Danielsson H, Sild E, Gelang J, Wallin G. 1997. Effects of ozone on leaf senescence in spring wheat - possible consequences for grain yield. Phyton Austria **37**, 227-232.

Pradhan P, Fischer G, van Velthuizen H, Reusser DE, Kropp JP. 2015. Closing yield gaps: How sustainable can we be? Plos One **10**, e0129487.

Quarrie S, Kaminska A, Dodmani A, Gonzalez I, Gillespie C, Bilsborrow P, Barnes J. 2007. QTLs governing ozone impacts on wheat yield. Comparative Biochemistry and Physiology Part A: Molecular & Integrative Physiology **146**, S261.

R Core Team. 2016. R: A Language and Environment for Statistical Computing. Vienna, Austria: R Foundation for Statistical Computing.

Ramankutty N, Foley JA, Norman J, McSweeney K. 2002. The global distribution of cultivable lands: current patterns and sensitivity to possible climate change. Global Ecology and Biogeography **11**, 377-392.

Rao MV, Hale BA, Ormrod DP. 1995. Amelioration of ozone-induced oxidative damage in wheat plants grown under high carbon dioxide (role of antioxidant enzymes). Plant Physiology **109**, 421-432.

Rao MV, Paliyath G, Ormrod DP. 1996. Ultraviolet-B-and ozone-induced biochemical changes in antioxidant enzymes of *Arabidopsis thaliana*. Plant Physiology **110**, 125-136.

Ray DK, Mueller ND, West PC, Foley JA. 2013. Yield trends are insufficient to double global crop production by 2050. Plos One **8**, e66428.

Ray DK, Ramankutty N, Mueller ND, West PC, Foley JA. 2012. Recent patterns of crop yield growth and stagnation. Nature communications **3**, 1293.

Reddy AR, Rasineni GK, Raghavendra AS. 2010. The impact of global elevated CO_2 concentration on photosynthesis and plant productivity. Current Science **99**, 46-57.

Reddy G, Arteca R, Dai YR, Flores H, Negm F, Pell E. 1993. Changes in ethylene and polyamines in relation to mRNA levels of the large and small subunits of ribulose bisphosphate carboxylase/oxygenase in ozone-stressed potato foliage. Plant, Cell & Environment **16**, 819-826.

Reich PB. 1987. Quantifying plant response to ozone: a unifying theory. Tree Physiology **3**, 63-91.

Reich PB, Amundson RG. 1985. Ambient levels of ozone reduce net photosynthesis in tree and crop species. Science **230**, 566-570.

Reichenauer T, Goodman B, Kostecki P, Soja G. 1998. Ozone sensitivity in *Triticum durum* and *T. aestivum* with respect to leaf injury, photosynthetic activity and free radical content. Physiologia Plantarum **104**, 681-686.

Reid CD, Fiscus EL, Burkey KO. 1998. Combined effects of chronic ozone and elevated CO_2 on Rubisco activity and leaf components in soybean (*Glycine max*). Journal of Experimental Botany **49**, 1999-2011.

Reinert R, Weber D. 1980. Ozone and sulfur dioxide-induced changes in soybean growth. Phytopathology **70**, 914-916.

Reinert RA, Eason G. 2000. Genetic control of O_3 sensitivity in a cross between two cultivars of snap bean. Journal of the American Society for Horticultural Science **125**, 222-227.

Richards R, Rebetzke G, Condon A, Van Herwaarden A. 2002. Breeding opportunities for increasing the efficiency of water use and crop yield in temperate cereals. Crop Science **42**, 111-121.

Rincker K, Nelson R, Specht J, Sleper D, Cary T, Cianzio SR, Casteel S, Conley S, Chen P, Davis V. 2014. Genetic improvement of US soybean in maturity groups II, III, and IV. Crop Science **54**, 1419-1432.

Robinson JM, Britz SJ. 2000. Tolerance of a field grown soybean cultivar to elevated ozone level is concurrent with higher leaflet ascorbic acid level, higher ascorbate-dehydroascorbate redox status, and long term photosynthetic productivity. Photosynthesis Research **64**, 77-87.

Roche D. 2015. Stomatal conductance is essential for higher yield potential of C3 crops. Critical Reviews in Plant Sciences **34**, 429-453.

Rockström J, Williams J, Daily G, Noble A, Matthews N, Gordon L, Wetterstrand H, DeClerck F, Shah M, Steduto P. 2017. Sustainable intensification of agriculture for human prosperity and global sustainability. Ambio **46**, 4-17.

Royal Society. 2008. Ground-level ozone in the 21st century: future trends, impacts and policy implications. London, UK.

Rubel F, Kottek M. 2010. Observed and projected climate shifts 1901–2100 depicted by world maps of the Köppen-Geiger climate classification. Meteorologische Zeitschrift **19**, 135-141.

Saini HS, Westgate ME. 1999. Reproductive Development in Grain Crops during Drought. In: Donald LS, (Ed.). Advances in Agronomy, Vol. 68 Academic Press.

Saitanis C, Bari S, Burkey K, Stamatelopoulos D, Agathokleous E. 2014. Screening of Bangladeshi winter wheat (*Triticum aestivum* L.) cultivars for sensitivity to ozone. Environmental Science and Pollution Research **21**, 13560-13571.

Sanders GE, Clark AG, Colls JJ. 1991. The influence of open-top chambers on the growth and development of field bean. New Phytologist **117**, 439-447.

Sawada H, Kohno Y. 2009. Differential ozone sensitivity of rice cultivars as indicated by visible injury and grain yield. Plant Biology **11**, 70-75.

Sharkey TD, Bernacchi CJ, Farquhar GD, Singsaas EL. 2007. Fitting photosynthetic carbon dioxide response curves for C3 leaves. Plant, Cell & Environment **30**, 1035-1040.

Shiferaw B, Smale M, Braun H-J, Duveiller E, Reynolds M, Muricho G. 2013. Crops that feed the world 10. Past successes and future challenges to the role played by wheat in global food security. Food Security **5**, 291-317.

Silva RA, West JJ, Zhang YQ, *et al.* 2013. Global premature mortality due to anthropogenic outdoor air pollution and the contribution of past climate change. Environmental Research Letters **8**, 11.

Simpson D, Benedictow A, Berge H, Bergström R, Emberson LD, Fagerli H, Flechard CR, Hayman GD, Gauss M, Jonson JE. 2012. The EMEP MSC-W chemical transport model–technical description. Atmospheric Chemistry and Physics **12**, 7825-7865.

Sinclair TR, Messina CD, Beatty A, Samples M. 2010. Assessment across the United States of the benefits of altered soybean drought traits. Agronomy Journal **102**, 475-482.

Singh. 2006. Success of soybean in India: the early challenges and pioneer promoters. Asian Agri-History **10**, 41-47.

Singh E, Tiwari S, Agrawal M. 2010. Variability in antioxidant and metabolite levels, growth and yield of two soybean varieties: An assessment of anticipated yield losses under projected elevation of ozone. Agriculture Ecosystems & Environment **135**, 168-177.

Singh S, Agrawal SB. 2011. Cultivar-specific response of soybean (*Glycine max* L.) to ambient and elevated concentrations of ozone under open top chambers. Water Air and Soil Pollution **217**, 283-302.

Slafer GA, Rawson HM. 1995. Photoperiod × temperature interactions in contrasting wheat genotypes: Time to heading and final leaf number. Field Crops Research **44**, 73-83.

Smart CM. 1994. Gene expression during leaf senescence. New Phytologist **126**, 419-448.

Smith AC, Koper N, Francis CM, Fahrig L. 2009. Confronting collinearity: comparing methods for disentangling the effects of habitat loss and fragmentation. Landscape Ecology **24**, 1271-1285.

Solberg S, Hov Ø, Søvde A, Isaksen I, Coddeville P, De Backer H, Forster C, Orsolini Y, Uhse K. 2008. European surface ozone in the extreme summer 2003. Journal of Geophysical Research: Atmospheres **113**.

Specht JE, Williams JH. 1984. Contribution of genetic technology to soybean productivity - Retrospect and prospect. pp 49-74 in: Fehr W.R. (Ed.). Genetic contributions to yield gains of five major crop plants. Crop Science Society of America Special Publication 7. Madison, USA.

Staehelin J, Thudium J, Buehler R, Volzthomas A, Graber W. 1994. Trends in surface ozone concentrations at Arosa (Switzerland). Atmospheric Environment **28**, 75-87.

Stevenson DS, Dentener FJ, Schultz MG, *et al.* 2006. Multimodel ensemble simulations of present-day and near-future tropospheric ozone. Journal of Geophysical Research - Atmospheres **111**, D08301.

Symonds MR, Moussalli A. 2011. A brief guide to model selection, multimodel inference and model averaging in behavioural ecology using Akaike's information criterion. Behavioral Ecology and Sociobiology **65**, 13-21.

Tai APK, Martin MV, Heald CL. 2014. Threat to future global food security from climate change and ozone air pollution. Nature Climate Change **4**, 817-821.

Tang H, Takigawa M, Liu G, Zhu J, Kobayashi K. 2013. A projection of ozone-induced wheat production loss in China and India for the years 2000 and 2020 with exposure-based and flux-based approaches. Global Change Biology **19**, 2739-2752.

Temple PJ. 1986. Stomatal conductance and transpirational responses of field-grown cotton to ozone. Plant, Cell & Environment **9**, 315-321.

Thomas D, Eamus D, Bell D. 1999. Optimization theory of stomatal behaviour I. A critical evaluation of five methods of calculation. Journal of Experimental Botany **50**, 385-392.

Tingey DT, Blum U. 1973. Effects of ozone on soybean nodules. Journal of Environmental Quality **2**, 341-342.

Tottman DR. 1987. The decimal code for the growth stages of cereals, with illustrations. Annals of Applied Biology **110**, 441-454.

Troiano J, Colavito L, Heller L, HcCune DC, Jacobson Js. 1983. Effects of acidity of simulated rain and its joint action with ambient ozone on measures of biomass and yield in soybean. Environmental and Experimental Botany **23**, 113-119.

Tubiello FN, Amthor JS, Boote KJ, Donatelli M, Easterling W, Fischer G, Gifford RM, Howden M, Reilly J, Rosenzweig C. 2007. Crop response to elevated CO_2 and world food supply: a comment on "Food for Thought…" by Long et al., Science 312: 1918–1921, 2006. European Journal of Agronomy **26**, 215-223.

Tuzet A, Perrier A, Leuning R. 2003. A coupled model of stomatal conductance, photosynthesis and transpiration. Plant, Cell & Environment **26**, 1097-1116.

Uddling J, Gunthardt-Goerg MS, Matyssek R, Oksanen E, Pleijel H, Sellden G, Karlsson PE. 2004. Biomass reduction of juvenile birch is more strongly related to stomatal uptake of ozone than to indices based on external exposure. Atmospheric Environment **38**, 4709-4719.

Uddling J, Pleijel H. 2006. Changes in stomatal conductance and net photosynthesis during phenological development in spring wheat: implications for gas exchange modelling. International Journal of Biometeorology **51**, 37-48.

USDA. 2015. Germplasm Resources Information Network. National Germplasm Resources Laboratory, Beltsville, Maryland. Available: http://www.ars-grin.gov/cgi-bin/npgs/html/site_holding.pl?SOY.

van Aardenne JA, Dentener FJ, Olivier JGJ, Goldewijk C, Lelieveld J. 2001. A 1 degrees x 1 degrees resolution data set of historical anthropogenic trace gas emissions for the period 1890-1990. Global Biogeochemical Cycles **15**, 909-928.

van Dingenen R, Dentener FJ, Raes F, Krol MC, Emberson L, Cofala J. 2009. The global impact of ozone on agricultural crop yields under current and future air quality legislation. Atmospheric Environment **43**, 604-618.

van Vuuren DP, Edmonds J, Kainuma M, *et al.* 2011. The representative concentration pathways: an overview. Climatic Change **109**, 5.

Velissariou D, Barnes JD, Davison AW. 1992. Has inadvertent selection by plant breeders affected the O_3 sensitivity of modern greek cultivars of spring wheat? Agriculture Ecosystems and Environment **38**, 79-89.

Vingarzan R. 2004. A review of surface ozone background levels and trends. Atmospheric Environment **38**, 3431-3442.

Volz A, Kley D. 1988. Evaluation of the Montsouris series of ozone measurements made in the 19th Century. Nature **332**, 240-242.

Wada Y, Bierkens MF. 2014. Sustainability of global water use: past reconstruction and future projections. Environmental Research Letters **9**, 104003.

Wang, Manning, Feng, Zhu. 2007. Ground-level ozone in China: Distribution and effects on crop yields. Environmental Pollution **147**, 394-400.

Wang, Mauzerall DL. 2004. Characterizing distributions of surface ozone and its impact on grain production in China, Japan and South Korea: 1990 and 2020. Atmospheric Environment **38**, 4383-4402.

Webb R. 1972. Use of the boundary line in the analysis of biological data. Journal of Horticultural Science **47**, 309-319.

Weigel HJ, Bender J. 2012. Ground-level ozone - A risk for crops and food security? Gesunde Pflanzen **64**, 79-87.

Wesely M, Cook D, Williams R. 1981. Field measurement of small ozone fluxes to snow, wet bare soil, and lake water. Boundary-Layer Meteorology **20**, 459-471.

West PC, Gerber JS, Engstrom PM, *et al.* 2014. Leverage points for improving global food security and the environment. Science **345**, 325-328.

White DA, Beadle CL, Sands PJ, Worledge D, Honeysett JL. 1999. Quantifying the effect of cumulative water stress on stomatal conductance of *Eucalyptus globulus* and *Eucalyptus nitens*: a phenomenological approach. Functional Plant Biology **26**, 17-27.

White JW, Hoogenboom G, Kimball BA, Wall GW. 2011. Methodologies for simulating impacts of climate change on crop production. Field Crops Research **124**, 357-368.

Whitehead D, Hogan K, Rogers G, Byers J, Hunt J, McSeveny T, Hollinger D, Dungan R, Earl W, Bourke M. 1995. Performance of large open-top chambers for long-term field investigations of tree response to elevated carbon dioxide concentration. Journal of Biogeography **22**, 307-313.

Wilkinson S, Davies WJ. 2009. Ozone suppresses soil drying and abscisic acid (ABA)-induced stomatal closure via an ethylene-dependent mechanism. Plant Cell and Environment **32**, 949-959.

Wilkinson S, Davies WJ. 2010. Drought, ozone, ABA and ethylene: new insights from cell to plant to community. Plant Cell and Environment **33**, 510-525.

Wilkinson S, Mills G, Illidge R, Davies WJ. 2012. How is ozone pollution reducing our food supply? Journal of Experimental Botany **63**, 527-536.

Wittig VE, Ainsworth EA, Long SP. 2007. To what extent do current and projected increases in surface ozone affect photosynthesis and stomatal conductance of trees? A meta-analytic review of the last 3 decades of experiments. Plant, Cell & Environment **30**, 1150-1162.

Xu X, Lin W, Wang T, Yan P, Tang J, Meng Z, Wang Y. 2008. Long-term trend of surface ozone at a regional background station in eastern China 1991–2006: enhanced variability. Atmospheric Chemistry and Physics **8**, 2595-2607.

Yoshida S. 1972. Physiological aspects of grain yield. Annual Review of Plant Physiology **23**, 437-462.

Yu Q, Zhang Y, Liu Y, Shi P. 2004. Simulation of the stomatal conductance of winter wheat in response to light, temperature and CO_2 changes. Annals of Botany **93**, 435-441.

Zabel F, Putzenlechner B, Mauser W. 2014. Global agricultural land resources – a high resolution suitability evaluation and its perspectives until 2100 under climate change conditions. Plos One **9**, e107522.

Zhang Q, Streets DG, He K, *et al.* 2007. NOx emission trends for China, 1995–2004: The view from the ground and the view from space. Journal of Geophysical Research: Atmospheres **112**.

Zhang WW, Wang GG, Liu XB, Feng ZZ. 2014. Effects of elevated O_3 exposure on seed yield, N concentration and photosynthesis of nine soybean cultivars (*Glycine max* (L.) Merr.) in Northeast China. Plant Science **226**, 172-181.

Zhao T, Cao Y, Wang Y, Dai Z, Liu Y, Liu B. 2012. Effects of ozone stress on root morphology and reactive oxygen species metabolism in soybean roots. Soybean Science **1**, 013.